DISS. ETH NO.: 16011

Structural and Signalling Functions of Sarcomeric Proteins

A dissertation submitted to the
SWISS FEDERAL INSTITUTE OF TECHNOLOGY ZURICH

for the degree of
Doctor of Natural Sciences

Presented by
STEPHAN LANGE
Dipl. biol., Humboldt University Berlin

born 28.10.1975

citizen of
Berlin, Germany

accepted with the recommendation of
Prof. Jean-Claude Perriard, examiner (ETH Zürich)
Prof. Mathias Gautel, co-examiner (King's College London)
Prof. Edgar Stüssi, co-examiner (ETH Zürich)
Dr. Jachen Denoth, co-examiner (ETH Zürich)

2005

1. Zusammenfassung

Das Sarkomer ist die kleinste Einheit des kontrahierenden Apparats der quergestreiften Muskulatur und besteht mehrheitlich aus Struktur-, Signal- und Gerüstproteinen. Es wird aus drei unterschiedlichen Filamentsystemen, sowie Proteinen, die mit diesen parakristallinen Proteinkomplexen assoziieren, gebildet. Die regulierte Interaktion von zweien dieser Filamentsysteme, den Myosinfilamenten sowie den Aktinfilamenten, bildet die mechanische Grundlage für die Muskelkontraktion. Das dritte Filamentsystem besteht aus dem Protein Titin. Titin (auch als Connectin bekannt) erfüllt verschiedenste Aufgaben während des Zusammenbaus, der Funktion und der Erhaltung der quergestreiften Muskulatur. Die Z-Scheibe, sowie die M-Bande sind zwei strukturelle Multiproteinkomplexe welche die Integrität des Sarkomers gewährleisten. Sie quervernetzen die verschiedenen Filamentsysteme im Zentrum, sowie am Ende des Sarkomers. Im Gegensatz zur intensiv untersuchten Z-Scheibe ist über die Struktur und Signalfunktion der M-Bande vergleichbar wenig bekannt. Fokussierend auf die Suche nach Interaktionspartnern für das Strukturprotein Myomesin, sowie den M-Banden Abschnitt des gigantischen Muskelproteins Titin, welche Hauptkomponenten des M-Band Proteinkomplexes sind, untersuchten wir die strukturellen, gerüstbildenden und signaltransduzierenden Eigenschaften dieser Proteine.

Myomesin ist ein essentieller struktureller Bestandteil der sarkomerischen M-Bande. Das Protein ist modular aus Blöcken von Immunoglobulin- und Fibronektindomänen zusammengesetzt. Seine singuläre Kopfdomäne bindet an die Myosinfilamente, wohingegen der zentrale Block aus Fibronektindomänen mit der Muskelisoform der Kreatin Kinase, sowie der M4 Domäne von Titin interagiert. Wir untersuchten die Funktion von Myomesin mittels der Suche nach unbekannten Interaktionspartnern mit Hilfe des Hefe-Doppel-Hybrid Systems. Einer der prominentesten Bindungspartner war Myomesin selbst, welches über Domäne 13 des Proteins ein antiparalleles Dimer auszubilden vermag. Zur genaueren Untersuchung der molekularen Eigenschaften der Bindungsstelle bestimmten wir die Kristallstruktur der C-terminalen Myomesindomänen 12 und 13 und zeigten mit Hilfe von Mutagenesestudien die Funktion von Aminosäuren auf, die eine Schlüsselfunktion bei der Ausbildung der antiparallelen β-Faltblatt Interaktionsfläche ausüben. Die neuen und bereits publizierten molekularen Bindungspartner von Myomesin wurden in neues dreidimensionales Modell der M-Banden Struktur integriert.

Neben der Dimerisierung wurde Myomesin auch als Substratprotein für die posttranslationale Modifizierung durch Sumo identifiziert. So interagiert Myomesin direkt mit den Proteinen Ubc9, PIAS1 und Sumo, welche wichtige enzymatische Schritte im Sumoylierungsprozess katalysieren. Alle bekannten und neu identifizierten Interaktionspartner von Myomesin, wie zum Beispiel MIQ, wurden in einer neu zusammengestellten Interaktionskarte für Myomesin vereint und zeigen die vielfältigen Bindungspartner dieses strukturellen M-Bandenbestandteils.

Das herzspezifische Protein DRAL hat neben seiner Lokalisation in der M-Bande einen zweiten sarkomerischen Bindungsort, die I-Bande des Sarkomers. Die Suche nach Interaktionspartnern

identifizierte die herzspezifische N2B Region, sowie die is2 M-Bandenregion von Titin als Bindungsstellen für DRAL. Eine genauere Untersuchung der weiteren Interaktionspartner, wie die Muskelisoform der Kreatin Kinase und deren intrazelluläre Lokalisation zeigten, daß DRAL und verwandte Proteine der FHL-Proteinfamilie als Adaptoren fungieren können die Protein-Protein Interaktionen über ihre spezialisierte LIM-Domänenstruktur vermitteln.

Mit Hilfe des Tiermodells der homozygoten DRAL-Knockout Maus, sowie der Kreuzung mit einer konditionellen herzspezifischen β-Catenin Knockout Maus untersuchten wir den Einfluß von DRAL auf verschiedene Signaltransduktionswege, wie den Androgen Rezeptor-, sowie den Wnt-mediierten Signalweg. Die nur in DRAL Knockout Herzzellen beobachtete Hypertrophiereaktion nach Stimulierung des Androgen Rezeptors ist möglicherweise verbunden mit einer kürzlich entdeckten Titin Mutation in einer japanischen Familie, welche mit dem Ausbruch einer Form der hypertrophen Kardiomyopathie assoziiert wurde.

Titin erfüllt nicht nur wichtige Funktionen in der Myofibrillogenese, sondern ist über seine C-terminale Kinasedomäne auch in muskelspezifische Signaltransduktionswege eingebunden. Obgleich Telethonin frühzeitig als eines der Hauptsubstrate der Titin Kinase identifiziert wurde, blieb die genaue Zusammensetzung der Titin Kinase Signalkaskade unklar. Mit Hilfe verschiedener Doppel-Hybrid Systeme und Protein-Lokalisationsstudien in Neonatalen Ratten Kardiomyocyten wurde ein muskelspezifischer Komplex bestehend aus den Proteinen NBR1, p62 und Murf2 identifiziert, welcher die mechanisch modulierte Titin Kinase Aktivität an eine veränderte Sumo-abhängige transkriptionelle Funktionalität des Serum Response Factors (SRF) koppelt.

Über das Studium und die Charakterisierung verschiedener Struktur-, Signal- und Gerüstproteine der sarkomerischen M-Bande konnten wir zeigen, daß die M-Bande nicht nur eine rein strukturelle Gerüstfunktion innerhalb des Sarkomers ausübt, sondern daß es sich hier um einen sehr viel dynamischeren Proteinkomplex handelt, der Bindungsstellen für eine Vielzahl von Proteinen anbietet und verschiedenste Signaltransduktionswege zu beeinflussen vermag.

2. Summary

The sarcomere is the minimal building block of the force generating apparatus of striated muscle cells and is mainly formed of structural, signalling and scaffolding proteins. Three different filament systems as well as proteins that associate with these paracrystalline protein complexes are thought to constitute the sarcomere. The regulated interaction of two of these filament systems, namely thick filaments, assembled of the myosin proteins, and the thin filaments, made up of actin filaments and associated proteins is the driving force behind the controlled muscular contraction (Cooke, 2004). The third filament system is composed of the giant protein titin. The titin protein (also known as connectin) serves many different purposes in the development, function and maintenance of any striated muscle type. Two structural multi-protein complexes, the M-band and the Z-disc, cross-link the three filament systems at the centre as well as the ends of the sarcomere, respectively. Whereas the Z-disc structure and function is widely investigated, comparatively little is known about the structural and signalling functions of the sarcomeric M-band. Concentrating on the three different M-band proteins myomesin, DRAL (FHL2) as well as the kinase domain of the giant protein titin, this study investigates their structural, scaffolding and signalling functions mainly via their respective interaction partners and relates them to the overall function of the M-band proteosome and signalsome.

Myomesin is an essential structural component of the sarcomeric M-band expressed in every type of striated muscle investigated so far. It is modularly composed of immunoglobulin-like and fibronectin-type III domains. A unique domain at the N-terminus anchors myosin, while the central Fn-domains interact with titin domain M4 as well as the muscle isoform of creatine kinase (MMCK). We investigated the function of myomesin via a screen for new interaction partners. This revealed a strong interaction with myomesin itself. Using various biochemical and cellbiological assays we were able to demonstrate that the antiparallel dimerisation of myomesin is mediated by the C-terminal immunoglobulin-like domain 13 of the protein. The crystal structure of myomesin domains 12 and 13 as well as mutational analysis based on this structure revealed the underlying molecular mechanisms leading to the formation of the antiparallel β-sheet binding interface and its function. The new and already published interactions are integrated into a three-dimensional model of the sarcomeric M-band on a molecular basis.

Besides the dimerisation, myomesin was also revealed to be a target for the posttranslational modification with the small ubiquitin-like modifier Sumo. Myomesin interacts directly with the key enzymes of the sumoylation machinery Ubc9 and PIAS1 as well as with the modifier Sumo itself. In conjunction with the other newly identified and characterised binding partners of myomesin, like MIQ, an interaction map on a molecular basis of myomesin is proposed, displaying the versatile binding partners of this structural M-band component.

The heart-specific four and a half-LIM domain protein DRAL (FHL2) was shown to have a dual localisation pattern in the I-band as well as the M-band of the sarcomere. The search for interaction partners of DRAL identified two binding sites within the titin protein, namely the N2B-region of cardiac

titin as well as the is2 M-band region of the giant muscle protein. Further analysis of putative interaction partners, like MMCK and their subcellular localisation revealed that the family of the FHL proteins acts as sarcomeric adaptor proteins, mediating protein-protein interactions via their domain structure composed of LIM domains.

Using mice, which are null for the DRAL allele as well as crossbreeding these with mice carrying a conditional heart-specific knockout for β-catenin, we investigated the association and influence of DRAL on several signalling pathways, like the androgen receptor (AR) or the Wnt/β-catenin signalling pathway. The observed hypertrophic response in DRAL -/- cardiomyocytes after stimulation of the AR-signalling pathway may be connected to a mutation in the DRAL binding site of human titin, which was recently linked to the onset of a form of hypertrophic cardiomyopathy (HCM).

The major protein involved in signalling via the sarcomeric M-band is thought to be the kinase domain of titin. Although telethonin was early identified as a major substrate, signalling via titin kinase as well as the identity of the proteins involved in the signalling cascade remained elusive. Using yeast two-hybrid screens and localisation studies in neonatal rat cardiomyocytes (NRCs) we identified a muscle-specific signalling complex consisting of the proteins NBR1, p62 and Murf2, which subsequently link the mechano-activated titin kinase to an altered transcriptional activity via the serum response factor (SRF), utilising the posttranslational Sumo modification pathway.

Studying several structural, adaptor and signalling components of the sarcomeric M-band, we were able to demonstrate that the M-band is not a mere static scaffold, but a highly dynamic structure, offering binding sites for a multitude of proteins and integrating as well as modulating a number of myofibrillar signalling cascades.

3. Table of Contents

4. Used abbreviations

AK	adenylate kinase	ANF	atrial natriuretic factor
Androstan	5α-androstan-17β-ol-3-one	Ankrd2	ankyrin repeat domain protein 2
AR	androgen receptor	ARE	androgen responsive element
BSA	bovine serum albumine		
CaM	calmodulin	CFP/eCFP	cyan fluorescent protein
Cos	African green monkey kidney cells	Cy2	cyanine
Cy3	indocarbocyanine	Cy5	indodicarbocyanine
Da	Dalton	DCM	dilated cardiomyopathy
DHT	dihydro-testosterone	DNA/cDNA	(complementory) deoxyribonucleic acid
dNTPs	deoxynucleoside triphophate	DRAL	downregulated rhabdosarcoma LIM protein
DTT	dithiothreitol	Dvl	dishevelled
eColi	Escherichia coli	EDTA	ethylene diamine tetraacetic acid
EGTA	ethylene glycol-bis[β-aminoethyl ether] N,N,N',N' tetraacetic acid	EH	embryonic heart
EMBL	European Molecular Biology Laboratory	EMT	endothelial-mesenchymal transdifferentiation
ER	oestrogen receptor	EtOH	ethanol
FATZ	γ-filamin/ABP-L, α-Actinin and telethonin binding protein of the Z-disc	FITC	fluorescein isothiocyanate
FHL	four and a half LIM domain	Fn	fibronectin-type III
Foxo	forkhead box class O	FRET	fluorescence energy resonance transfer
gal	galactosidase	GFP/eGFP	green fluorescent protein
glc	glucose	GST	glutathione S-transferase
HA	hemagglutinine protein epitope	HCM	hypertrophic cardiomyopathy
HEPES	2-[4-(2-hydroxyethyl)-1-piperazinyl]-ethansulfone acid	HSP	heat shock protein
Ig	immunoglobulin-like	IPTG	isopropyl β-D-thiogalactopyranoside
is	insertion sequence		
LB	luria-bertani	LIM	lin-11, isl-1, mec-3
Luminol	5-amino-2,3,-dihydro 1,4 phtalazine-dione, sodium salt		
MCS	multiple cloning site	MD	muscular dystrophy
MHC	myosin heavy chain	minK	minimal potassium channel protein
MIQ	M-band interacting glutamine-rich	MMCK	muscle isoform of creatine kinase
MLC	myosin light chain	MLP	muscle LIM protein
MOPS	3-[N-morpholino]ethanesulfonic acid	Murf	muscle RING finger protein
My	myomesin	MyBP-C	myosin binding protein-C
NBR	next to BRAC1	NMCs	neonatal mouse cardiomyocytes
N-RAP	nebulin related anchoring protein	NRCs	neonatal rat cardiomyocytes
PAGE	polyacrylamide gel electrophoresis	PB1	phox and bem1
PBS	phosphate buffered saline	PCR/ RT-PCR	(reverse transcriptase) polymerase chain reaction
pers. comm..	personal communication	PEST	proline, glutamate, serine, threonine
PFA	paraform aldehyde	PFK	phosphofructokinase
PIAS1	protein inhibitor of activates STAT1	PIPES	piperazine-1,4bis(2 ethanesulfonic acid)
PKA/PKC/ PKD	protein kinase A/C/D	PLZF	promyelocytic leukimia zinc finger protein
RACE	rapid amplification of cDNA ends		
SDS	sodium dodecyl sulphate	SMPX	small muscle protein X
SRE	serum responsive element	SRF	serum response factor
Sumo	small ubiquitin related modifier		
TCF/LEF	T cell factor / lymphoid enhancer factor	TEMED	N,N,N',N'-tetramethylethylenediamine
TK	titin kinase	TRIZMA	tris[hydroxymethyl] aminomethane
UBA	ubiquitin associated	Ubc	ubiquitin conjugating enzyme
us	unique sequence		
VEGF	vascular endothelial growth factor	VSD	ventricular septum defect
wt	wildtype		
X-gal	5-bromo-4chloro-3-indolyl-β-D-galactopyranoside		
YFP/eYFP	yellow fluorescent protein		
Zf	zinc finger		

5. Introduction

5.1. Muscle morphology and ultrastructure

Striated muscle cells developed the ability to generate mechanical force via an elaborate mechanism that involves the regulated and directed interaction of a complex network of proteins and protein filaments. Two different types of striated muscle cells, the skeletal and cardiac muscles are responsible for the generation of mechanical force and the maintenance of the blood-circulation, respectively (see figure 1 panel A and B). Although cardiac and skeletal muscles display ultra-structurally many similarities, their myofibrillar development is quite different. Whereas the heart is formed of single cells (cardiomyocytes; figure 1 panel B), which are connected structurally and conductivity-wise via specialised cell-cell contacts (the intercalated discs; see figure 3), skeletal cells are derived from the fusion of many myoblasts, which undergo myofibrillar differentiation to form elongated single muscle fibres (figure 1 panel A).

5.1.1. Structural proteins of the sarcomere

The sarcomere is the minimal building block of the force generating apparatus within all kinds of striated muscle cells. It is a complex protein network, mainly formed of structural, signalling and scaffolding proteins, which is interconnected with the cytoskeleton of the cell. Three different filament systems as well as proteins that associate with these protein complexes are thought to assemble the

Figure 1. From the muscle to the sarcomere.
A. & B. Two types of cross-striated muscle cells found in vertebrates.
A. Skeletal muscle cells form the biggest group of cross-striated muscle cells. They originate from single cells, called myoblasts, which fuse during differentiation to form multinucleated myotubes. Single myotubes are packed together into bundles of myofibres. Sorrounding the force generating apparatus is a membranous web-like structure formed by the sarcoplasmic reticulum.
B. The second type of cross-striated muscle cells are the heart cells, also known as cardiomyocytes. Although very similar in the composition of the force generating apparatus, the heart consists of single cells connected via specialised cell-cell contacts, the so called intercalated discs.
C. The sarcomere is the basic unit of the force generating apparatus within each type of cross-striated muscle cells. It appears in electron micrographs as electron dense filaments, cross-connected in several areas via cross-bridging structures.
D. Schematic presentation of the sarcomeric multi-protein complex. Three different filament systems, the thick filaments of the myosin molecules, the thin filament system assembled of multimeric G-actin proteins and the elastic filament system composed of the giant protein titin as well as associated proteins are shown. Two cross-bridging structures, the Z-discs at the end of the sarcomere as well as the M-band in the centre cross-connect the three filament systems. Proteins like titin and obscurin anchor the sarcomere to membranes.
Scheme adapted by Prof. M. Gautel.

Figure 1. From the muscle to the sarcomere

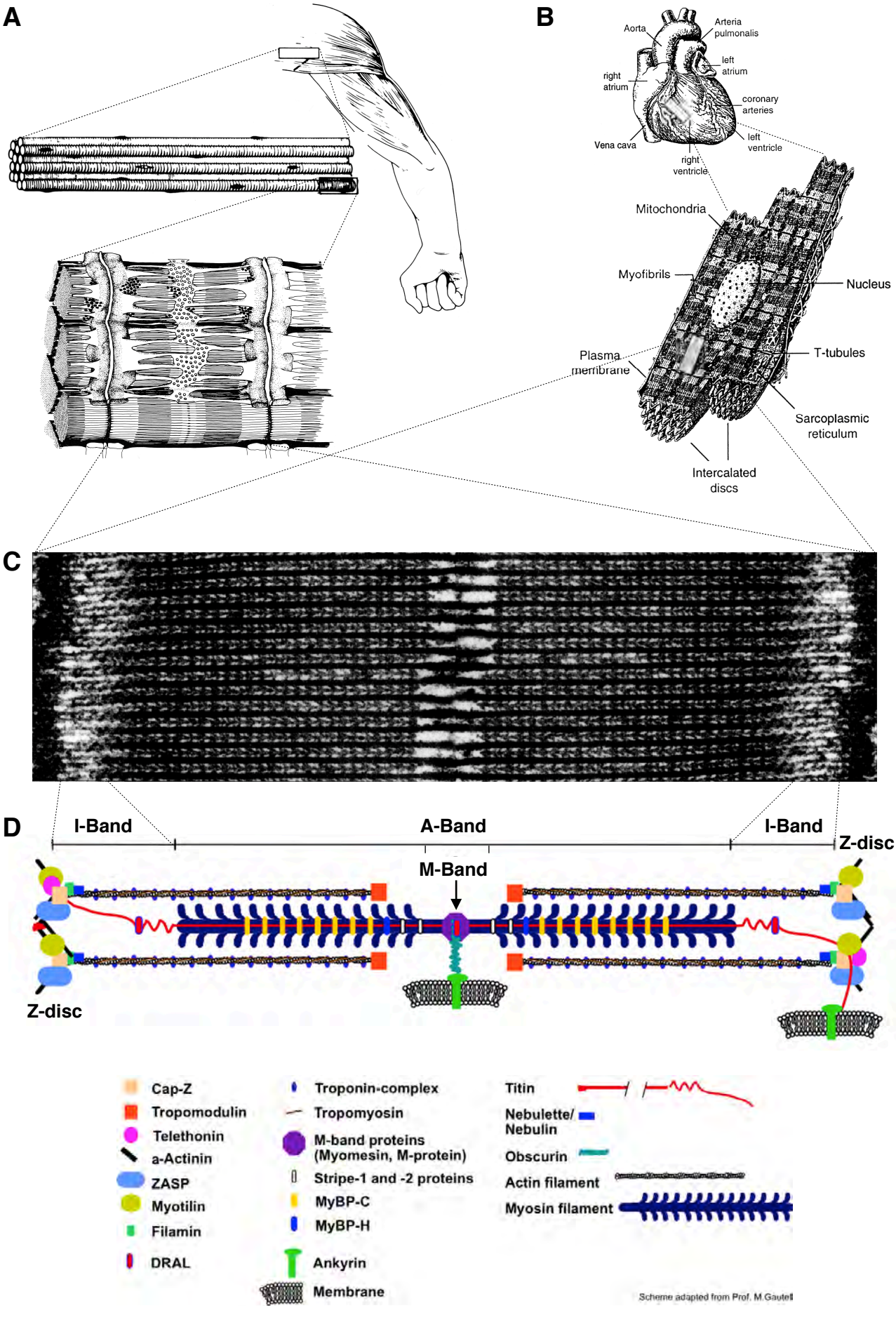

sarcomere (see figure 1 panel D). The regulated interaction of two of these filament systems, namely thick filaments, assembled of the myosin protein, and the thin filaments, made up of actin filaments and associated proteins is the driving force behind the controlled muscular contraction (Cooke, 2004).

Myosin

Sarcomeric myosin is a large homodimeric protein complex consisting of six polypeptide chains, two heavy chains of about 200 kilo Dalton (kDa) and four light chains with a molecular weight of about 20kDa. The heavy chain (MHC, myosin heavy chain) can be further structurally subdivided into a C-terminal α-helix domain, transmitting cohesion of the two monomers via hydrophobic interactions of the helices in a coiled-coil structre and the globular N-terminal motor-domain, acting as a molecular motor using chemical energy via hydrolysis of ATP and converting it via a conformational change into mechanical work. The motor domain contains, despite the catalytic centre, which controls the hydrolysis of ATP, also a binding site for polymerised actin, enabling the transmission of the generated force onto the sarcomere and the cytoskeleton. The C-terminal part of MHC harbours binding sites for titin and proteins like myomesin, M-protein and myosin binding protein-C (MyBP-C).

Actin

Actin, the major protein of the microfilament system is expressed in six isoforms of about 42kDa in eukaryotic cells, all showing a highly conserved sequence homology, suggesting an important role throughout various cellular processes (Vandekerckhove and Weber, 1984). In the myofibrils, actin is in conjunction with other proteins, e.g. the tropomyosin-troponin complex, organised to the thin filament system. The interaction of actin filaments with myosin heads leads to the earlier mentioned muscle contraction.

Titin (connectin)

The third filament system is composed of the giant protein titin. The titin protein (also known as connectin) serves many different purposes in the development, function and maintenance of any striated muscle type. With its size of about 3-3.5 mega Daltons and a slack length of about 1μm, which enables the protein to anchor its N-terminus in the Z-disc and the C-terminus in the M-band of the sarcomere (Labeit and Kolmerer, 1995), it is not only considered the biggest protein in the vertebrate striated muscle, but also one of the most abundant (Au, 2004; Maruyama, 1997; Tskhovrebova and Trinick, 2003). Despite its somewhat simple modular domain architecture, assembled mainly of clusters of immunoglobulin-like (Ig) and fibronectin-type III (Fn) domains which are interspersed with unique sequences, it offers a multitude of spatially distinct binding sites for the major structural components of the sarcomere, like α-actinin, actin, myomesin and M-protein, myosin binding protein-C (MyBP-C or C-Protein) as well as myosin and for associated proteins with scaffolding and signalling functions, like the FHL domain protein family, the Murf proteins or calpain. The single kinase domain of

titin, located close to the C-terminus of the protein, is implicated in the regulation of sarcomeric development, myofibrillar assembly and sarcomeric remodelling (Amodeo et al., 2001; Mayans et al., 1998) and may serve as an integrative link between various signalling pathways and mechanical strain (Grater et al., 2005) to alter the cellular response (e.g. change in protein expression pattern) via a hitherto unknown muscle-specific signalling cascade.

Table 1 summarises novel and published mutations of the titin molecule, associated with the generation of several myopathies.

The myomesin protein family

Myomesin (skelemin, MYOM1), M-protein (MYOM2) as well as the recently discovered miamesin (MYOM3) are members of the myomesin protein family. Myomesin, a myosin and titin binding protein of about 190kDa is an essential structural component of the sarcomeric M-band (see figure 2) and expressed in all kinds of cross-striated muscles investigated so far. It was suggested that myomesin links myosin- and titin-filaments and is involved in the maintenance of the sarcomeric lattice (Obermann et al., 1997). Myomesin exists in two splice variants the “normal” myomesin protein of about 190kDa with a unique head domain, two clusters of 2 N-terminal and 5 C-terminal Ig-domains and a central cluster of 5 Fn domains as well as the EH isoform (EH-myomesin, skelemin; (Agarkova et al., 2000; Bantle et al., 1996; Steiner et al., 1999)), which displays the presence of an additional unstructured domain between Fn domains 6 and 7 of the protein. EH-myomesin expression was found to be regulated in a developmentally and tissue specific expression pattern (Agarkova et al., 2004). Besides its interaction with light meromyosin (LMM) and titin domain M4, myomesin was shown to associate with Fn-domains 7 and 8 to the muscle isoform of creatine kinase (MMCK; (Hornemann et al., 2003)).

The other characterised structural M-band component of the myomesin protein family is M-protein. The identical domain pattern of M-protein and myomesin as well as the presence of comparable interaction sites with other M-band components, like myosin, titin and MMCK within M-protein indicate that both proteins evolved from a common ancestor. The alignment of the Ig- and Fn-domains of several sarcomeric proteins substantiate the homology between these two M-band proteins (Kenny et al., 1999). Although myomesin and M-protein may fulfil comparable functions, M-protein displays a tissue specific expression pattern, being restricted to fast-twitch fibres and the adult heart as well as the absence of an alternative splice-isoform.

Miamesin was recently identified as the third member of the myomesin protein family (Agarkova et al. pers. comm. and unpublished results). Its identical domain layout with myomesin and M-protein indicate as in the case for M-protein a comparable functional role for this protein. Investigations for the tissue specific and developmental regulation of miamesin expression are currently underway and might shed light into the modulation of the sarcomeric M-band structure.

α-actinin

The protein α-actinin is a antiparallel homodimer with a subunit molecular mass of about 94-103 kDa. Its main function is the formation of cross-bridges between neighbouring actin and titin filaments and to provide the tetragonal lattice of the Z-disc as its major structural component. Furthermore, α-actinin links actin to a number of integral membrane proteins, i.e. the cadherins and catenins (Knudsen et al., 1995; Nieset et al., 1997). The association of α-actinin to several signalling molecules and adaptor molecules like the muscle LIM Protein (MLP, CRP3; (Gehmlich et al., 2004; Louis et al., 1997)) or the α-actinin associated LIM-protein (ALP; (Xia et al., 1997)) suggest a role of α-actinin beyond its structural function.

Myosin binding protein-C (MyBP-C, C-Protein)

Myosin binding protein-C belongs like myomesin and titin to the class of giant sarcomeric proteins characterised by its modular Ig- and Fn-domain composition (Bennett et al., 1999). Three isoforms are found within cross-striated muscle cells: slow skeletal (also known as X-Protein), fast skeletal and cardiac MyBP-C. The C-terminus of MyBP-C was reported to bind to light meromyosin (LMM) and to titin, while the N-terminus is interacting with the S2 region of myosin. There are also indications that MyBP-C domains C5 and C8 may permit the formation of MyBP-C homodimers (Moolman-Smook et al., 2002). Besides its structural role to cross-link myosin and titin in the A-band of the sarcomere, MyBP-C was also suggested to be involved in the regulation of thick-filament assembly. Several mutations in MyBP-C have been linked to the onset of cardiomyopathies (Bonne et al., 1995).

5.1.2. Non structural proteins associated with the sarcomere

In addition to the sarcomeric proteins, which serve more structural roles like myomesin, α-actinin and titin, a multitude of partially muscle-specific proteins are involved in the maintenance and modulation of the myofibrils, in muscle-specific-signalling pathways as well as the linkage of the sarcomeric filament systems to cytoskeletal filament systems, like the intermediate filaments as well as to the plasma membrane.

5.1.2.1. Z-disk associated proteins

An essential structural component of the sarcomere is the multi-protein complex known as the Z-disc. Apart from its structural components α-actinin, titin and filamentous actin, a multitude of proteins utilise the structural Z-disc scaffold as myofibrillar anchorage point and interaction platform. The Z-disc proteome includes adaptor proteins like the muscle LIM Protein (MLP, CRP3), ZASP (Cypher, Oracle) or ALP, which are reported to bind directly to α-actinin, nebulin or nebulette which interact and modulate the actin-filament, as well as the giant protein obscurin and telethonin (T-cap), which are associated with Z-disc domains of titin (for a review see: (Au, 2004; Tskhovrebova and Trinick, 2003)).

Other proteins with partially unknown sarcomeric interaction partners are also associated with the Z-disc, e.g. proteins of the calsarcin family, myotilin, myopalladin, myopodin, calcineurin or the intermediate filament protein desmin (for a review see (Faulkner et al., 2001)).

Telethonin (T-cap)

Telethonin (or T-cap) was initially identified as a binding partner for the N-terminal titin domains Z1/Z2 (Gregorio et al., 1998; Mues et al., 1998) and was later found to be a major phosphorylation substrate for the kinase domain of titin (Mayans et al., 1998). Telethoin was further shown to interact with the muscle LIM protein (MLP) via the central part of the protein as well as to act as a binding partner for the integral membrane proteins minK and small ankyrin and the Z-disc associated protein FATZ (Faulkner et al., 2000; Furukawa et al., 2001; Kojic et al., 2004). Several telethonin mutations implicated in the generation of various myopathies have been described (see table 1).

Muscle LIM protein (MLP, CRP3)

MLP (CRP3) belongs to the family of the LIM domain proteins and is composed of two tandemly arranged LIM and glycine-rich modules. Apart from its interaction with telethonin, α-actinin, zyxin β-spectrin and N-RAP (Nebulin related anchoring protein), MLP was found to play a major role in cardiac development, since ablation of the MLP gene in mice results in the onset of dilated cardiomyopathy (DCM) with a disorganised contractile apparatus and defects in costameres as well as the intercalated disc region (Arber et al., 1994; Arber et al., 1997; Ehler et al., 2001; Louis et al., 1997).

In addition to its contribution to the mechanical integrity of the muscle via its compartmentalisation in the sarcomere and the region of the intercalated disc (Knoll et al., 2002), MLP was also implicated in the sarcomeric-nuclear communication (Mohapatra et al., 2003). Various mutations in MLP associated with the development of muscular diseases have been described in the litreature and can be found in table 1.

5.1.2.2. I-band associated proteins

Apart from the scaffold related functions of titin in the Z-disc and in the M-band of the sarcomere, titin exhibits in the I-band of the muscle the function of a molecular spring, maintaining the overlap of the thin and thick filament systems. The domain architecture of I-band titin is characterised by clusters of Ig-domains, interspersed with large unique sequence insertions and is altered in a tissue specific manner via subjection to a considerable variety of splicing events. One of the unique peptide sequences, the PEVK region, displays with its rich content in proline, glutamate, valine and lysine residues qualities of an intrinsically unstructured peptide and may function as one of the major elastic spring elements in titin. Two other unique peptide regions with no obvious domain structure interspersed with several Ig-domains are the N2A-region as well as the cardiac specific N2B-region.

Characterised protein-protein interactions in this region include the Calcium modulated binding of nebulin to the PEVK-region (Gutierrez-Cruz et al., 2001; Ma and Wang, 2002), the cardiac specific association of actin filaments to the PEVK and the N2B-region (Kulke et al., 2001; Yamasaki et al., 2001) as well as the interactions of MARP, myopalladin and calpain-3 to the N2A-region of titin (Kinbara et al., 1997; Miller et al., 2003). The four and a half LIM protein DRAL (also called FHL2, Slim3) was recently identified as a protein displaying a dual sarcomeric localisation pattern: in the I-band and M-band of the sarcomere (see Results part and (Lange et al., 2002) and references therein).

DRAL

DRAL (also known as FHL2 or Slim3) is a heart-specific member of the four and a half LIM (FHL) domain protein family, which was initially found to be downregulated in a rhabdosarcoma cell line (Chan et al., 1998; Scholl et al., 2000). The multitude of interaction partners (see below) for DRAL and the other members of this protein family like the ubiquitously expressed FHL1, indicate that FHL proteins act as adaptor proteins, mediating protein-protein binding through their modular composition of LIM domains (Schmeichel and Beckerle, 1994). Table 1 lists published single nucleotide polymorphisms (SNPs) of DRAL and FHL1.

5.1.2.3. A-band associated proteins

A-band titin interacts with myosin binding protein-C (MyBP-C), AMP-deaminase as well as the tail region of myosin. The domain layout of titin exhibits the occurrence of super-repeats in this region, identical clusters of fibronectin and immunoglobulin-like domains. Because it is thought that the 11 domain super-repeats in C-zone titin correspond to the electron dense 43nm repeats of MyBP-C in negatively stained electron micrographs, they may harbour binding sites for A-band myosin and MyBP-C. In fact, myosin binding protein-C was found to interact with the first Ig-domain within each of these super-repeats (Freiburg and Gautel, 1996).

5.1.2.4. M-band associated proteins

The M-band is thought to be the structural counterpart of the Z-disc in the middle of the sarcomere. Proteins of the myomesin protein family act as cross-bridges, linking the thick and the elastic filament system. Besides their structural functions, myosin, myomesin, M-protein as well as titin offer binding sites for a multitude of proteins with various functions, ranging from enzymes like the muscle isoform of creatine kinase (MMCK), which contribute to the regulation of the energy metabolism to proteins serving as adaptors to mediate protein-protein interactions, like DRAL (see earlier).

MMCK

Like DRAL, the muscle isoform of creatine kinase (MMCK) exhibits also a dual sarcomeric localisation pattern with binding sites in the M-band as well as in the I-band of the sarcomere. MMCK is an enzyme of the energy metabolism, catalysing the reaction of ADP and phospho-creatine to creatine and ATP. In addition to its interaction with proteins of the myomesin family (Hornemann et al., 2003), MMCK was also shown to bind to DRAL (this work). Single nucleotide polymorphisms found in this protein are shown in table 1.

Table 1 – published and novel missense mutations in muscle proteins associated with the development of muscular diseases.

Overview over a selection of published and unpublished missense mutation in sarcomeric and non-sarcomeric proteins associated with the onset of hypertrophic cardiomyopathy (HCM), dilated cardiomyopathy (DCM) or muscular dystrophies (MD) as well as published single nucleotide polymorphisms (SNPs) with unknown biological effect (see http://www.ncbi.nlm.nih.gov/projects/SNP).

Protein	Mutation (position in bp or amino acid residues)	Phenotypical effect	Reference
Titin			
Z-disc	V54M (telethonin binding site)	DCM	(Hein and Schaper, 2002)
	R740L (α-actinin binding site)	HCM	Matsumoto & Kimura unpubl.
	A743V (α-actinin binding site)	DCM	(Hein and Schaper, 2002)
	W930R (IgZ4)	DCM	(Gerull et al., 2002)
I-band	mdm (N2A-region mouse titin; Calpain3A binding site; deletion of 83 aa res.)	MD (MD myositis)	(Garvey et al., 2002)
	S3799Y (N2B-region; DRAL binding site)	HCM	(Itoh-Satoh et al., 2002)
	Q4053x (N2B-region; premature stop)	DCM	
	R4084Q (N2B-region)	?	
	T4215P (N2B-region)	?	
	S4465N (N2B-region)	DCM	
	L-x (N2B-region zebrafish titin; pik^{m171})	no sarcomeres	(Xu et al., 2002)
	TGYVI-SLAMx, 2bp insertion & premature stop (exon 326; 43,628; AT insertion aa residues 14544-14548)	DCM	(Gerull et al., 2002)
A-band	T-I (exon A45; 233,784; ACT>ATT)	TMD (tibial MD)	(Hackman et al., 2002)
	S-G (exon A149; 274,193; AGT>GGT)	TMD	
	V-I (exon A166; 283,464; GTT>ATT)	TMD	
M-band	R-W (titin kinase aa 279; CGG>TGG)	MD	B.Udd et al. unpublished
	R25618Q (exon Mex1; is2 DRAL binding site)	DCM	Matsumoto & Kimura unpubl.
	EVTW-VKEK, 11bp exchange (exon Mex6; 293,268-293,280)	TMD	(Hackman et al., 2002)
	L-P (exon Mex6; 293,357; CTG-CCG)	TMD	
Telethonin			
	E13del (titin binding site)	DCM	Knöll et al. unpublished
	36LLPAx (del. of nucleotides G108, G109 in Tel. cds causes frameshift)	MD (limb-girdle)	(Moreira et al., 2000)
	Q53x (titin binding site)	MD (limb-girdle)	
	R87Q (titin & MLP binding site)	DCM	(Knoll et al., 2002)
	E132Q	DCM	(Hayashi et al., 2004)
	T137I	HCM	
	R153H	HCM	

continuation of table 1.

MLP			
	W4R (telethonin interaction site) L44P (MyoD binding site) SG54/55RE (MyoD binding site) C58G (MyoD, α-actinin & N-RAP binding site) K69R (α-actinin & N-RAP binding site) A77T (α-actinin & N-RAP binding site)	DCM HCM HCM HCM DCM ?	(Knoll et al., 2002) (Geier et al., 2003) (Gehmlich et al., 2004) (Mohapatra et al., 2003) rs746207
Myomesin			
	V22L (domain 1) P181S (domain 1) T215M (domain 1) A341G (domain 1) E600V (domain Fn3) I960T (domain Fn7) V1134G (domain Ig9) E1249K (domain Ig10) D1408N (domain Ig11) M1453T (domain Ig11)	? ? ? ? ? ? ? ? ? ?	rs1791085 rs1962519 rs2230166 rs11664-7 rs9807556 rs1071600 (Scavello et al., 2005) rs7229433 rs3765623 rs9966837 / rs16944397
M-protein			
	S869N (domain Fn5) L1022F (domain Ig10) T1294P (domain Ig12)	? ? ?	rs968381 rs2280896 rs10086990
DRAL			
	M167K (altering 3' exon splice consensus site) G232D	? ?	rs112758 rs1803518
FHL1			
	C34R R51L H69T (affects folding of LIM domain 1)	? ? ?	rs11557265 rs11557264 rs11557267
MMCK			
	V72M E83G L127V T166M G243A	? ? ? ? ?	rs1803285 rs11559024/rs17875651 rs17875653 rs17357122 rs17875625

5.1.3. Ultrastructure of the M-band

Historically the M-band is defined from its appearance in negatively stained electron micrographs of cross-striated muscle cells as a 100nm wide dark zone with a series of electron dense lines situated in the centre of the sarcomere. Depending on fibre type a total of nine lines can be identified starting from the central M1 line and extending to the M9 line at the edge of the bare zone (see figure 2 panel A). The major lines were defined as the central M1 line in the middle of the M-band, the flanking M4 and M4' lines, located approximately 22nm apart from the M1 line, and the flanking outer lines M6 and M6'

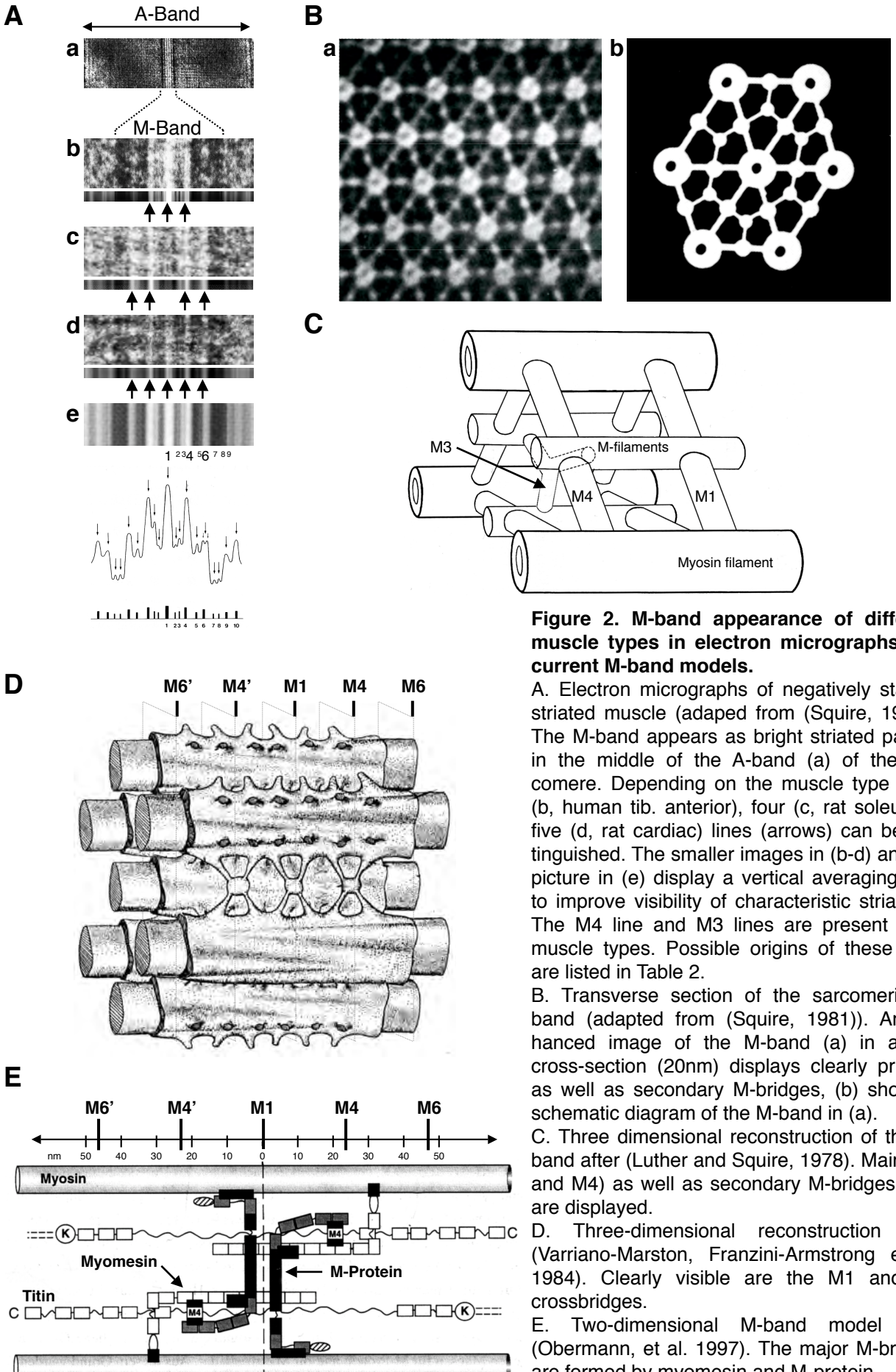

Figure 2. M-band appearance of different muscle types in electron micrographs and current M-band models.

A. Electron micrographs of negatively stained striated muscle (adaped from (Squire, 1981)). The M-band appears as bright striated pattern in the middle of the A-band (a) of the sarcomere. Depending on the muscle type three (b, human tib. anterior), four (c, rat soleus) or five (d, rat cardiac) lines (arrows) can be distinguished. The smaller images in (b-d) and the picture in (e) display a vertical averaging filter to improve visibility of characteristic striations. The M4 line and M3 lines are present in all muscle types. Possible origins of these lines are listed in Table 2.

B. Transverse section of the sarcomeric M-band (adapted from (Squire, 1981)). An enhanced image of the M-band (a) in a thin cross-section (20nm) displays clearly primary as well as secondary M-bridges, (b) shows a schematic diagram of the M-band in (a).

C. Three dimensional reconstruction of the M-band after (Luther and Squire, 1978). Main (M1 and M4) as well as secondary M-bridges (M3) are displayed.

D. Three-dimensional reconstruction after (Varriano-Marston, Franzini-Armstrong et al. 1984). Clearly visible are the M1 and M4 crossbridges.

E. Two-dimensional M-band model after (Obermann, et al. 1997). The major M-bridges are formed by myomesin and M-protein.

further towards the edge of the M-band region (for a review see: (Squire, 1981)). A summary of the fibre type specific appearance of the different M-lines can be found in table 2.

The results of the electron micrographic studies were interpreted in early structural models of the sarcomeric M-band (see figure 2 compilation of early models) like the model of Squire and Luther, the model by Strehler et al. (Strehler et al., 1983) or the model of Varriano-Marston and coworkers (Luther and Squire, 1978; Luther and Crowther, 1984; Varriano-Marston et al., 1984).

While all authors agree on the basic hexagonal lattice of the thick filament, there are different views on the type of the secondary cross-bridging structures and their origin. The model of Luther favours the presence of additional M-filaments that run in parallel to the myosin filaments and orthogonal primary and secondary cross-bridges linking the thick filaments, with the primary bridges representing the major M-lines (see figure 2 panels B and C). The reconstruction by Varrion-Marston lacks interdigital parallel M-filaments and presents the thick filaments connected by a network of lateral cross-bridges (figure 2 panel D). More recently, the arrangement of titin, myomesin, myosin and M-protein was studied using immunoelectron microscopy and epitope-specific antibodies, and another two-dimensional model was proposed (figure 2 panel E). In this model, the M1 line was implied to be based on M-protein oriented in a perpendicular like fashion and thereby connecting the thick-filaments and titin, whereas the M4 and M4' lines are based on myomesin (Obermann et al., 1996).

Table 2 – Fibre type specificity of M-line appearance in negatively stained EM-micrographs.

Fibre type-specific distribution of M-lines found in different types of vertebrate muscle. The positions noted are measured from the central M1 line in the middle of the sarcomeric M-band. Correlations of fibre type, contraction speed and Z-disc width are noted in the right column of the table (Squire, 1981).

Line No.	Distance from M1 line (nm)	Possible Origin	Fibre type	M-band pattern	Z-band width
M1	-	M-bridge	Skeletal		
M2	9.6±1.2	Rod	II A	5 lines	Thick
M3	15.1±0.1	n.d.	II B	3 lines (no M6 line)	Thin
M4	22.0±0.5	M-bridge	Skeletal and heart	4 lines (no M1 line)	Thick
M5	34.0±1.1	Rod			
M6	43.7±0.6	M-bridge	Cardiac	5 lines	Thick
M7	54.4±1.1	Rod	n.d.	4+1 lines	Thick
M8	60.8±1.0	Rod	n.d.	4 lines (no M1 line)	
M9	69.2±1.2	Rod (?)	n.d.		
P1	81.0±1.8	myosin head			

Later, the structure of the sarcomeric M-band was studied using biochemical methods, e.g. dot blot overlay assays and co-purification and co-sedimentation assays. Obermann and coworkers identified the myosin binding site within the unique head domain of myomesin and the titin M4 binding site within the first three domains of the central fibronectin-cluster in myomesin (Obermann et al., 1997). Further studies revealed a M-protein binding site within domains 3 to 8 of myomesin (see Dissertation Dr. F. Steiner 1997, Georg-August Universität Göttingen).

5.1.4. Cell-cell and cell-matrix contact proteins – structural and signalling functions

The cytoskeletal anchorage of the myofibrils to membranes and to adjacent cells requires special contact sites, which form in cardiomyocytes so called intercalated disc structures (see figure 3). These multi-protein complexes are formed by several specialised subgroups of junctions that ensure mechanical coupling as well as intercellular communication. Three different types of junctions are distinguishable: desmosomes that anchor intermediate filaments, adherens junctions that anchor myofibrils and gap junctions, composed of connexin proteins that serve for ion transport and allow a

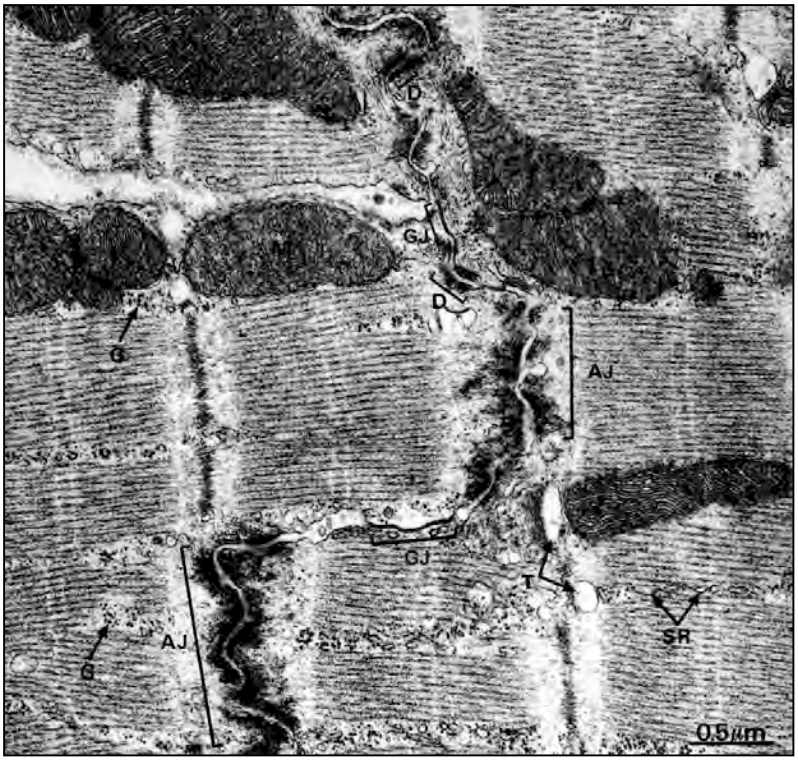

Figure 3. Electron micrograph of an intercalated disc in cardiac tissue.
Shown are cardiomyocytes and their specialised cell-cell contacts. For further explanation see (Wheater et al., 1996). Abbrevations: AJ – adherens junctions, D – desmosomes, G – glycogen granules, GJ – gap junctions, SR – sarcoplasmatic reticulum, M – mitochondria, T – T-Tubules. (EM x 31000)

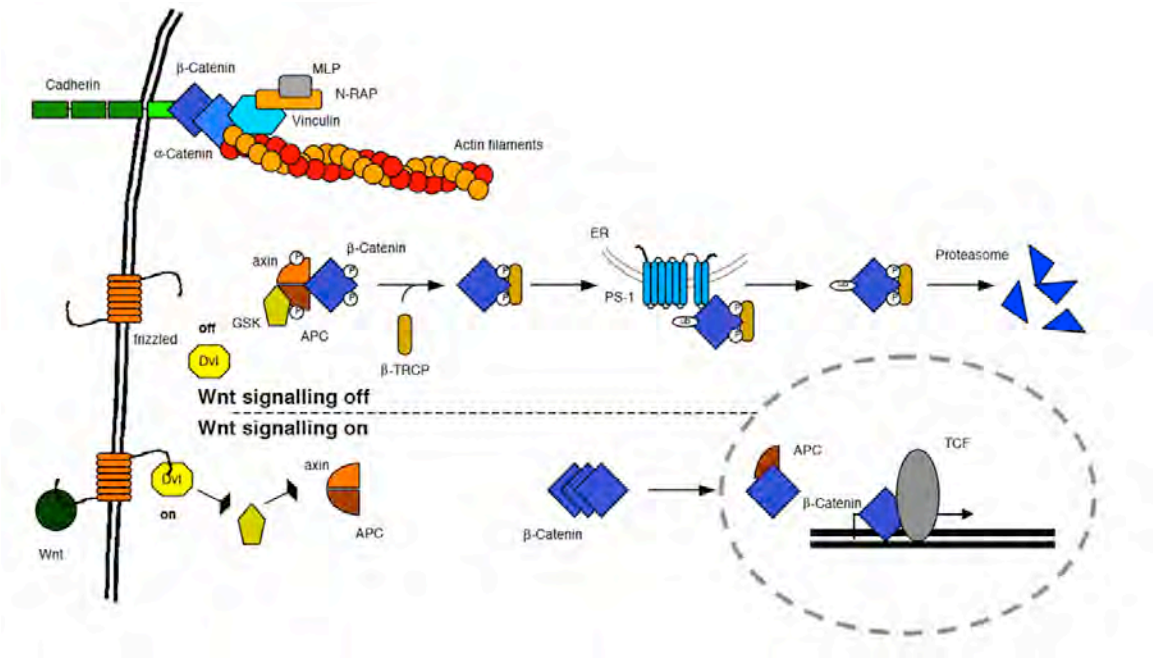

Figure 4. Model of the role of β-catenin in cell adhesion and the Wnt signaling pathway.
Abbreviations: APC – adenomatous polyposis coli tumour suppressor protein; Dvl – dishevelled; ER – endoplasmatic reticulum membrane; GSK – glycogen synthase kinase 3 β; MLP – muscle LIM protein; N-RAP – nebulin related anchoring protein; P – Phosphorylation; PS-1 – Presenilin 1; β–TRCP – β–transducing repeats containing protein; TCF – T cell specific transcription factor 1; ub – ubiquitin. For more details see (De Strooper and Annaert, 2001; Miller and Moon, 1996) and references therein.

synchronised beating of the heart.

The large family of the cadherins plays a major role in cell-cell adhesion and can be divided into four subgroups: classical cadherins, desmosomal cadherins, protocadherins as well as atypical cadherins. All subgroups share structural homologies; they are transmembrane glycoproteins, interacting via bound calcium together in a zipper like structure. Most cadherins are type I transmembrane proteins localised in adherens junctions in the region of the intercalated disc and linked to the cytoskeleton by cytoplasmic proteins like the catenin protein family.

β-catenin is a linker protein mediating contact of cadherins to actin within a complex of proteins in between. The 92kDa protein offers binding sites for proteins like classical cadherins or α-catenin. In addition to its localisation at cell-cell contacts, β-catenin plays also a role in the canonical Wnt-signalling pathway in analogy to the role of its Drosophila melanogaster homologue armadillo in the wingless pathway (see figure 4). At the moment the significance of signaling via β-catenin is still investigated in the case of cardiomyopathies. However, since the mechanical stress that is caused in the course of cardiomyopathy might also affect the cell-cell contacts, an additional potential signaling role for β-catenin is of general interest.

In addition to cell-cell contacts, cell-matrix contacts, called costameres, are localised at the lateral side of cross-striated muscle cells and connect the myofibrils laterally to the membrane via a vinculin-

integrin interaction. The integrins make contact to extracellular matrix components like laminin that surround the muscle cells.

Several examples of cardiac diseases were found, i.e. dilated and hypertrophic cardiomyopathies cohering with irregular and abnormal expression and localisation pattern of cytoskeletal and sarcomeric proteins (for a review see (Towbin and Bowles, 2000)).

5.1.5. Modulation of protein functions

Many proteins undergo posttranslational modification during their maturation or downstream of a signal pathway. These protein modifications can dramatically alter the function as well as the subcellular localisation of the protein. Common protein modifications are phosphorylation by protein kinases, glycosylation, ribosylation, acetylation, nitrosylation, carbamoylation, methylation, farnesylation, palmitylation and myristoylation, sulfation as well as the group of ubiquitin and ubiquitin-like modifications.

The Sumoylation pathway

Sumo, short for small ubiquitin related modifier, is a member of the ubiquitin-like protein family. It is thought to regulate a multitude of cellular functions modifying a broad variety of target proteins. The

Figure 5. The sumoylation pathway and involved proteins.
A. Schematic representation of the enzymatic steps in the sumoylation of a designated substrate protein. The Sumo-propeptide is converted into the active Sumo peptide and anchored to the E1 enzyme, consisting of the proteins Uba2 and Aos1. Sumo is transferred to Ubc9 (ubiquitin carrier enzyme; E2-enzyme) and with the assistance of an E3-enzyme (e.g. PIAS1) covalently linked to the lysine residue of a substrate. The covalently linked Sumo peptide is easily cleaved off the substrate by specialised SUSPs (Sumo1 specific protease) and can be reused for another round of the sumoylation pathway. See also (Kim et al., 2002; Melchior, 2000) and references therein.
B. Protein alignment and phylogenetic tree of the four different Sumo-protein family members. The phylogenetic tree reveals the close relationship between Sumo and ubiquitin. Sumo-2, Sumo-3 and Sumo-4 form a separate cluster, whereas Sumo-1 is closer related to ubiquitin. Sumo-2 and Sumo-4 are almost identical. The sequence alignment reveals further that Sumo-1 lacks a critical lysine residue, present in Sumo-2/-4 and Sumo-3. This VKTE motif in Sumo-2/-4 and Sumo-3 is thought to enable the establishment of poly Sumo-chains.
C. Crystal structure of Sumo (b) and ubiquitin (c) as well as electrostatic surface presentation of both modifiers (a: Sumo, d: ubiquitin). The more pronounced basic amino acid composition in Sumo is thought to be important for specificity (see blue colour of the Sumo surface representation).
D. Schematic presentation of the domain and protein motif search as well as reported interaction partners for PIAS1. The identified regions and characterised binding partners as well as proposed functions are indicated in the scheme. The underlined area indicates the protein-part contained in the initial yeast-two hybrid clone (see myomesin domain 9-13 yeast-two hybrid). The dotted line indicates the putative minimal binding site of myomesin, as identified in a forced yeast-two hybrid assay.

Figure 5. Sumoylation pathway and involved proteins.

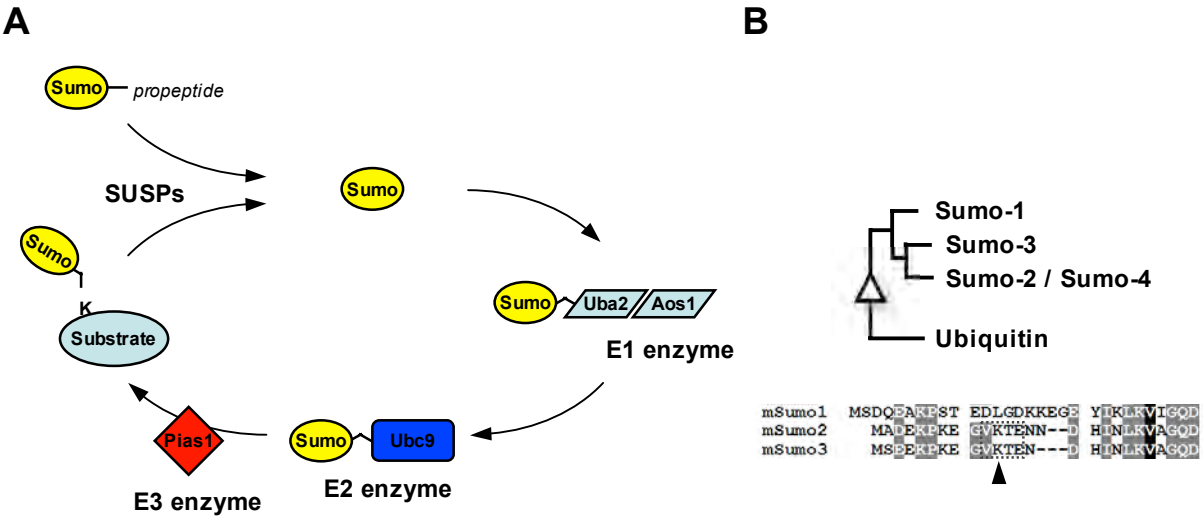

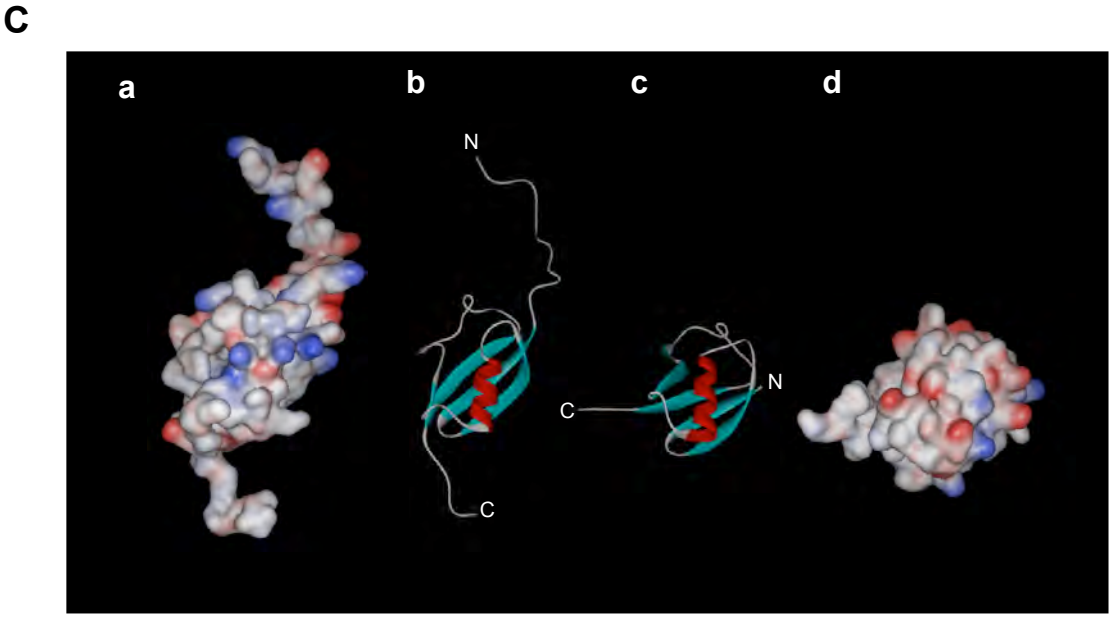

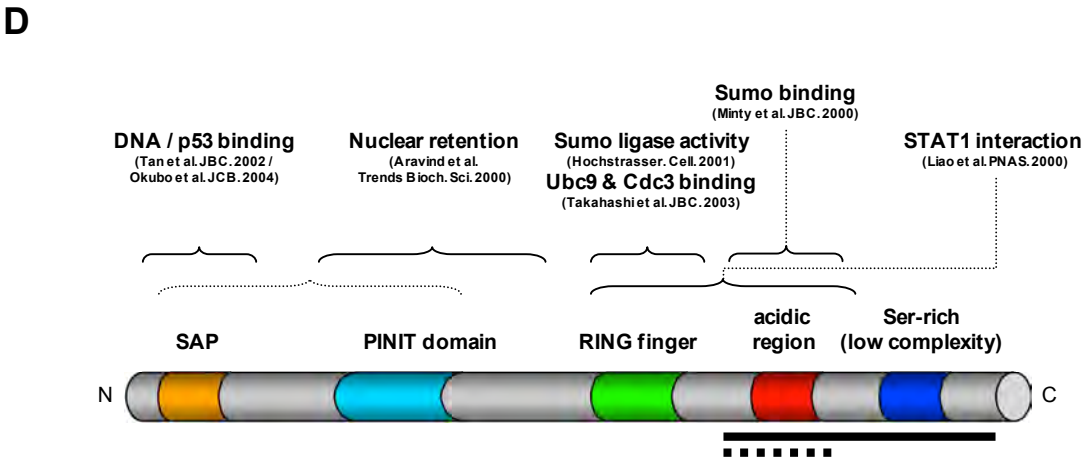

mechanism of the conjugation of the Sumo protein to a target is analogous to the ubiquitination of a protein. Three enzymatic steps are involved in this process (see figure 5 panel A). The E1 heterodimeric coenzyme complex of Aos1 and Uba2 processes the Sumo precursor and formes a covalent thioester bond between Sumo and the Uba2 subunit. The E2 Sumo-conjugating enzyme Ubc9 is thought to be responsible for the target recognition and the conjugation of the Sumo modifier to its target protein. The third enzymatic step is carried out by the family of the E3 ligases. Although sumoylation occurs *in vitro* also in the absence of the E3 enzyme, the rate of the reaction as well as the amount of sumoylated target proteins is largely increased in presence of the E3 ligase. The protein family of the Sumo E3 ligases consists up to date of the PIAS protein family, the vertebrate specific Ranbp2/Nup358 protein and the polycomb group protein Pc2. Although several domains within the E3 enzymes were implied in Sumo binding as well as the interaction with Ubc9, they are not common to all E3 ligases. The PIAS protein family consists of five different domains and peptide motifs (see figure 5 panel D). The N-terminal SAP motif (SAF-A/B, Acinus, PIAS) with the signature sequence VxELx(12)GxKxxL was suggested to mediate the binding of DNA and to nuclear scaffold/matrix attachment regions (SARs/MARs). The central PINIT motif or LxxLL motifs are thought to play a role in the nuclear localisation of the PIAS proteins (Duval et al., 2003). The SP-RING domain of the PIAS proteins is a classical ubiquitin RING finger motif with the consensus sequence $Cx_2Cx_{(9-39)}Cx_{(1-3)}Hx_{(2-3)}C/Hx_2C/x_{(4-48)}Cx_2C$ through which a pair of zinc ions is coordinated by cysteine and histidine residues. The functional role of the RING domain was suggested in the binding of Ubc9, the E2 enzyme of the sumoylation pathway. Interestingly, all E3 enzymes are target proteins for the Sumo modification itself. However, some mutations or truncations of the RING domain, leading to the loss of the coordinating zinc ion only slightly perturb the binding of Ubc9 to PIAS, and do not completely abolish the interaction (Kotaja et al., 2002; Takahashi et al., 2003). A region C-terminal to the RING domain was implied in retaining the Ubc9 binding activity.

A region for the binding of the Sumo protein itself was suggested to be located at the C-terminus of the PIAS proteins. This highly conserved region consists of the consensus motif hhxSxS/Taaa, where h is a hydrophobic residue, x represents any amino acid and a is an acidic residue. The presence of several acidic residues termed this region acidic region. Mutation of either the serine residues or the acidic residues in this motif to alanine was shown to abolish the interaction of Sumo to PIAS in yeast two-hybrid assays (Minty et al., 2000).

Four different Sumo proteins are described in the literature up to date, namely Sumo1, Sumo2, Sumo3 and Sumo4 (Guo et al., 2004), although the progress in the sequencing of the human as well as other genomes suggests that this protein family might consist of even more closely related proteins. Figure 5 panel B shows the phylogenetic tree of ubiquitin and the four Sumo proteins. Sumo1 is the closest relative to ubiquitin of the Sumo proteins. The Sumo proteins Sumo2 and Sumo4 as well as Sumo3 form a separate subgroup because of their high homology. One characteristic feature of the Sumo1 protein is the lack of a crucial lysine residue, responsible for the formation of poly-ubiquitin as well as poly-Sumo chains (see arrowhead in figure 5 panel B). A comparison of the available crystal and NMR structures shows that despite the typical ubiquitin fold, the electrostatic surface charges in

the Sumo protein are somewhat more positive due to exposed lysine residues compared to a more negative surface charge in the case of ubiquitin (see figure 5 panel C.a and panel C.d). These differences might account for the different characteristics and interaction partners for Sumo as well as ubiquitin. The major functional difference between sumoylation and ubiquitination however, is reflected in the fate of the modified target proteins. Whereas poly-ubiquitination serves as one of the major signals for the degradation of proteins, sumoylation alters drastically the function and subcellular localisation of the target protein. The variety of functional changes of sumoylated proteins range from nuclear exclusion (e.g. SRF, see below), to the accumulation of proteins into the nucleus (e.g. several steroid receptors like the androgen receptor (Poukka et al., 1999)), into PML bodies within the nucleus or to a decreased susceptibility for ubiquitin-mediated protein degradation (Bies et al., 2002).

5.2. Aim of this work

The major goal of this doctoral thesis was to investigate the sarcomeric M-band with respect to its structural and scaffolding functions as well as its role as a muscle-specific modulator to integrate and alter several signalling pathways. To elucidate the function of the M-band in these aspects, the three prominent M-band proteins myomesin, titin and DRAL were studied in greater detail via the search and the characterisation of newly identified interaction partners.

6. Results

6.1. The M-band component myomesin

The 190kDa protein myomesin is one of the major structural component of the sarcomeric M-band. It provides a link between the thick and elastic filament systems by providing binding sites for myosin in the unique head domain of myomesin and for the titin M4 Ig-domain within in the first 3 fibronectin-type III domains 4 to 6 of myomesin (Obermann et al., 1997; Obermann et al., 1995). Apart from these structural components of the sarcomere, myomesin domains 7 and 8 also bind to the muscle isoform of creatine kinase (MMCK; (Hornemann et al., 2003)).

Developmentally, myomesin is expressed early in all kinds of cross-striated muscle cells, but gets later integrated into the sarcomere compared to Z-disc components (e.g. Z-disc domains of titin as well as α-actinin) along with the titin M-band domains (Ehler et al., 1999). Two splice isoforms of myomesin are described, myomesin as well as EH-myomesin (formerly known also as skelemin), which contains an additional domain between the fibronectin domains 6 and 7 (Agarkova et al., 2000; Bantle et al., 1996; Steiner et al., 1999).

To reveal further binding partners for myomesin, two yeast-two hybrid screens were established. One covering the highly conserved C-terminal set of immunoglobulin-like domains (domains 9-13), which show a high degree of conservation during evolution, and the second screen for the N-terminal and central part of the protein, covering domains 2 to 8 of myomesin.

6.1.1. Myomesin domain 9-13 yeast two-hybrid screen

The yeast two-hybrid system, originally developed by Fields and Song (Fields and Song, 1989) is a powerful high throughput method to screen for novel protein interaction partners in an *in vivo* system.

The system takes advantage of a property often found in transcriptional coactivators. These coactivators consist of two domains, namely a DNA-binding domain, which binds to a specific DNA sequence followed by an activation domain, which is responsible for the activation of the transcriptional activity. The two domains can be expressed independently and reconstitute their transcriptional activity when brought into close proximity.

To facilitate this system for the screening of unknown interaction partners, the protein of interest is genetically fused with the DNA binding domain and cloned into a selectable vector. A library containing cDNAs is fused to the activation domain and also cloned into a vector with a selection marker.

If the protein of interest is interacting with a target protein encoded by a library plasmid, transcriptional activity is reconstituted and a screening for this interaction is possible by growth

selection on selective media lacking essential amino acids and the detection of a reporter gene, e.g. β-galactosidase.

For the following yeast two-hybrid screen, the C-terminal cluster of immunoglobulin-like domains 9-13 of the murine myomesin was subcloned to the pLex-MGkan vector, to form a C-terminal fusion protein with the LexA DNA-binding domain (=bait). After co-transformation with an adult human cardiac cDNA library in pACT-2 (Clontech; =prey), the yeast transformants were assayed for growth on selection plates lacking the amino acids histidine, leucine as well as tryptophane, and for β-galactosidase activity. 1x10*7 transformants were screened, resulting in 250 clones that grew on selective media and were positive for β-galactosidase activity in a filter assay.

Library plasmids from positive clones were isolated, analysed for insert length, grouped into identical clones according to Nco I and Hae III digestion patterns of the insert and subsequently sequenced.

To confirm the interactions, the bait plasmid and selected library plasmids of putative interacting proteins were cotransformed into the yeast L40 strain and assayed again.

Table 3 shows an overview of the putative interactors identified in the yeast two-hybrid screen.

Table 3 – Overview of myomesin domain 9-13 yeast two-hybrid screen interacting proteins.

BLAST search results using the insert sequences of positive clones recovered from the LexA-mMy9-13 screen. The insert length was determined by PCR with pACT2.fwd and pACT2.rev primers.
For selected clones (printed in bold) the interaction strength is shown using liquid β-galactosidase assay (ONPG as substrate [(Miller, 1972; Miller, 1992)]; values correspond to β-galactosidase units). Abbreviation: n.d. = not determined.

clone No.	Acc. Number	BLAST result	insert length (kb)	liquid β-Gal assay	anno-tations
5	NM_003869	Carboxylesterase 2	2	n.d.	
13, 19, 108, 140, 141	**BC004429**	**ubiquitin-conjugating enzyme E2I (homologous to yeast Ubc9)**	**1.5**	**337.2±4.9**	**complete coding sequence**
20	BC020794	serologically defined colon cancer antigen 1	1	n.d.	
21, 41, 39	XM_063046; NM_001003399	LOC122282; DKFZp451A211 protein; (MIQ)	4	n.d.	
22	AJ132592	mRNA for zinc finger protein 3,1kb (GZP1)	2	n.d.	
27, 60, 147	NM_006006; AF060568	zinc finger protein 145; promyelocytic leukemia zinc finger protein (PLZF) gene,	1.5-1.8	n.d.	
43	NM_001100	α 1 skeletal muscle actin	1.7	n.d.	
74	XM_087067	UDP-glucose pyrophosphorylase 2 (UGP2),	1.5	n.d.	
36, 88, 122, 137, 139, 160, 190, 242	**NM_003803**	**Myomesin 1 (MYOM1)**	**1.4-2.4**	**46.7±1.7**	**various clones encoding domains 9-13**
93, 115	XM_084376; AJ133768; AJ133767	LIM domain binding 3 (LDB3); ZASP protein variant 2; ZASP protein variant 3	3	n.d.	
109	NM_006308	Heat shock 27kD protein 3 (HSPB3)	1	n.d.	false positive
124	HSCRTRGN	Creatine transporter gene	1.5	n.d.	
129	XM_165547	Neuropilin 1 (NRP1)	1.5	n.d.	
163	**XM_083920**	**Protein Inhibitor of Activated STAT, 1 (PIAS1)**	**1.2**	**17.0±0.5**	**encoding for the C-terminal part of the protein**

The analysed clones can be divided into five main groups: sarcomeric and cytoskeletal proteins, zinc finger containing proteins, proteins of the posttranslational sumoylation machinery, cytoplasmic proteins and enzymes as well as proteins with unknown functions.

6.1.1.1. Sarcomeric and cytoskeletal proteins

Out of the initial 250 clones, a large number of clones were found to encode for the C-terminal part of myomesin itself, suggesting that the protein may form dimers.

No clones were found that would encode for any of the other known M-band components like M-protein, titin, myosin, DRAL or the muscle isoform of creatin kinase (MMCK).

Apart from myomesin, α-1 skeletal actin was the only other sarcomeric/cytoskeletal protein identified in the screen. α-skeletal actin is the main component of the thin filament system, which is located in the Z-disc, the I-band and the A-band, but absent from the M-band of the sarcomere. The spatial separation of filamentous actin and myomesin in the sarcomere indicates that an interaction of the C-terminal part of myomesin with α-sarcomeric actin seems very unlikely. Further investigations into the interaction of myomesin with sarcomeric proteins focussed therefore on the putative dimerisation of myomesin (see below).

6.1.1.2. Zinc finger proteins

The yeast two-hybrid screen identified 3 different zinc-finger proteins as putative interaction partners, namely zinc finger protein 3.1kb (GZP1; Acc. No: AJ132592), the promyelocytic leukaemia zinc finger protein (PLZF; Acc. No: AF060568) and the LIM domain binding 3 protein (LDB3/ZASP; Acc. No: XM_084376).

Zinc finger-containing proteins have been reported as common false-positive interactors in yeast two-hybrid screens [for further reference see: http://www.fccc.edu/research/labs/golemis]. To assess these clones as putative interaction partners of myomesin, the inserts of the recovered library plasmids containing parts of the coding regions of these proteins were subcloned to either eGFP- or HA-tagged eukaryotic expression vectors (pEGFP or pHA; see later) and transfected into cultures of neonatal rat cardiomyocytes (NRCs). The subcellular localisation of the proteins was studied in comparison to the localisation of the M-band epitope M8 of titin.

Figure 6 shows an overview of the different subcellular localisations of the zinc-finger proteins in comparison to the titin M8 M-band epitope.

Although some of the constructs show a weak association to the sarcomeric M-band, their overall localisation was either mainly diffusely cytoplasmic, like in the case for PLZF, or more Z-disc associated, like in the case for LDB3 / ZASP.

LBD3 (ZASP) was earlier described to be an α-actinin interacting protein (Faulkner et al., 1999; Klaavuniemi et al., 2004), making it an unlikely candidate for an interaction with the M-band component myomesin.

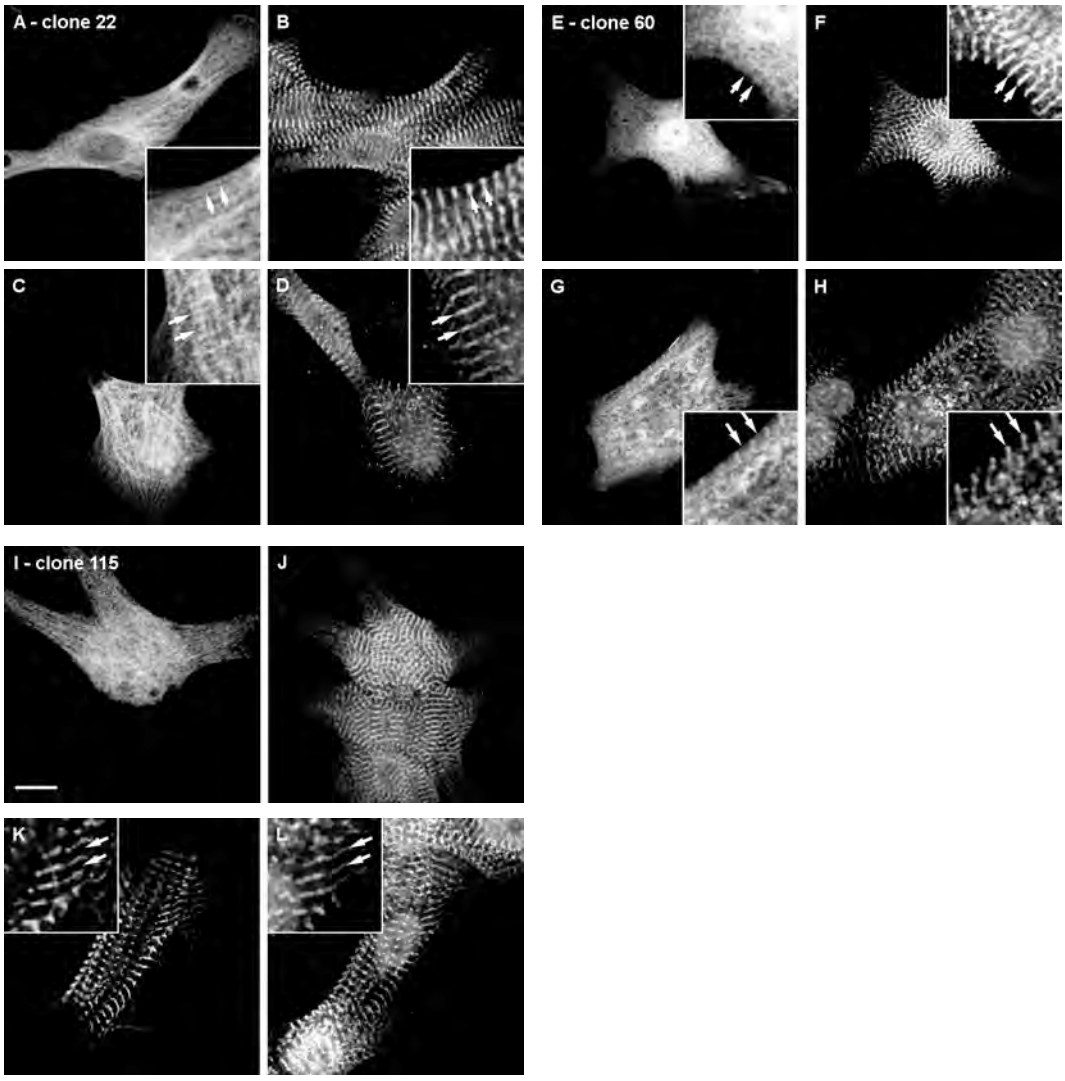

Figure 6. Subcellular localisation of transfected epitope tagged yeast two-hybrid clones.
HA- (A, E, I) or GFP- tagged (C, G, K) GZIP1 (A-D), PLZF (E-H) as well as LBD3/ZASP (I-L) were transfected into neonatal rat cardiomyocytes and counterstained with an antibody recognising the M8 epitope of titin. Whereas GZIP1 and PLZF showed consistent localisation to the sarcomeric Z-disc as well as the M-band (arrow in blowups), LBD3/ZASP was either diffuse cytoplasmic (I) or localised exclusively to the Z-disc of the sarcomere (K).
Scalebar = 10µm

The protein GZP1 was found to be a transcriptional coactivator, binding to GC-rich sequences and sharing sequence homologies with another zinc finger protein ZBP-89, which was shown to regulate the gene activity of enzymes like β-enolase (Lisowsky et al., 1999). β-enolase (see also later) is an enzyme of the energy metabolism catalysing the interconversion of 2-phosphoglycerate and phosphoenolpyruvate. Cytoplasmic β-enolase was partially localised in muscle tissues to the region of the sarcomeric M-band (Arrio-Dupont et al., 1997), most likely via a comparable mechanism like the earlier described DRAL targeting of enzymes of metabolic pathways to the sarcomeric M-band and I-band (see below; (Lange et al., 2002)).

However, the observation that GZP1 is able to activate the expression of the HIS3 reporter gene even in the absence of the GAL4 domain points toward a false positive interaction with myomesin (Lisowsky et al., 1999). Furthermore, the localisation of this protein in transfected cultures of neonatal rat cardiomyocytes is a mainly diffuse. Only a fraction of this protein was localised to the sarcomeric M-band as well as Z-disk (see figure 6).

Several clones encoding for the promyelocytic leukemia zinc finger protein (PLZF) were identified during the yeast two-hybrid screen. The PLZF protein was described earlier as a binding partner of another zinc-finger protein, namely DRAL/FHL2 (McLoughlin et al., 2002). Localisation of PLZF in transfected NRCs shows a mostly diffuse cytoplasmic localisation (see figure 6). Some fractions of the protein can be found in the sarcomere (Z-disc and M-band) as well as in the nucleus, where PLZF is thought to function as an transcriptional repressor for genes like myc, involved in tumor repression ((McConnell et al., 2003); for a review see (Lin et al., 2001)). Furthermore, the transcriptional activity of PLZF is regulated by conjugation of Sumo1, a ubiquitin-like posttranslational protein-modification which will be described later in this chapter [(Kang et al., 2003)].

In summary, the identified zinc-finger proteins are either unlikely interactors with myomesin or false-positive clones. PLZF seems to be the only candidate, which may be a putative binding partner to the C-terminal domains of myomesin. But since the sarcomeric binding partner DRAL may explain the sarcomeric localisation of this protein, no further emphasis was laid on experiments supporting the interaction of myomesin and PLZF.

6.1.1.3. Proteins of the sumoylation machinery

Two putative interactors for the C-terminal part of myomesin encode for proteins which are enzymes of a ubiquitin-like posttranslational modification machinery – the sumoylation pathway (see figure 5; for a review see (Schmidt and Muller, 2003)).

The ubiquitin conjugating enzyme E21 (homologous to the yeast protein Ubc9) was, beside myomesin itself, the most abundant clone in the yeast two-hybrid screen, making it a promising candidate for a relevant protein-protein interaction with myomesin. Furthermore, it was shown that most interactors with Ubc9 are also substrates for the sumoylation pathway (Melchior, 2000), indicating a new posttranslational modification of myomesin.

PIAS1 (Protein Inhibitor of STAT1) was first implicated in the transcriptional regulation of the JAK/STAT pathway. STATs comprise a family of cytoplasmic proteins, which act as transcription

factors and become activated via tyrosine phosphorylation (Y701) by the Janus-family of tyrosine-kinases in response to cytokine stimulation (Liao et al., 2000). Activated STAT proteins dimerise through a reciprocal Src homology domain in the C-terminus of the protein and translocate to the nucleus. Binding of PIAS1 protein to the activated STAT1 dimer specifically inhibits the transcriptional activity of these transcription factors. However, recent data showed that PIAS1, which harbours a RING domain in its C-terminal part, serves also as an E3-enzyme in the sumoylation pathway. E3-enzymes of the sumoylation machinery are, in contrast to the ubiquitinylation pathway, not essential for transferring the Sumo protein to its substrate, but may serve as mere enhancers of this reaction (for a review see: (Melchior, 2000)).

The fact that an E2- as well as an E3-enzyme of the sumoylation pathway are potential binding partners of myomesin indicates that myomesin may be indeed a substrate for this posttranslational modification. The binding of these proteins and the potential modification of myomesin were therefore investigated in more detail (see below).

6.1.1.4. Cytoplasmic proteins and enzymes

The M-band is known to harbour binding sites for enzymes of metabolic pathways, like β-enolase, the muscle isoform of creatine kinase (MMCK), phosphofructokinase (PFK) or adenylate kinase (AK). Some of these enzymes interact directly with scaffold proteins of the sarcomere, like in the case of MMCK and myomesin (Hornemann et al., 2003). For other enzymes a third protein mediates the compartmentalisation to the sarcomere, as in the case of PFK and AK. DRAL (or FHL2), a protein of the LIM only protein family, was indicated to play a role as a mediator of interaction, harbouring on one hand a binding site for the sarcomeric protein titin and offering on the other hand a binding site for enzymes like AK, PFK as well as MMCK (see below; (Lange et al., 2002)).

Hence, it was not surprising to find additional enzymes/proteins as potential binding partners for the C-terminal part of myomesin. Among the identified clones were the carboxylesterase 2, the UDP-glucose pyrophosphorylase 2 and the creatine transporter.

Other cytoplasmic proteins identified in the yeast two-hybrid as potential binding partners include the serologically defined colon cancer antigen 1 (SDCCAG1), the 27kDa heat shock protein 3 (HSPB3) and the neuropilin 1 protein (NPN1 or NRP1).

Carboxylesterase 2 is an enzyme which was originally found in human intestine and liver. It exhibits a broad substrate specificity including different drug ester substrates such as heroin and cocaine (Pindel et al., 1997). Although there are some reports suggesting an influence of overdoses of heroin on skeletal and cardiac muscle leading to myopathies (Melandri et al., 1996; Pena et al., 1993), there seems to be no obvious link to myomesin or the structure of the sarcomeric M-band.

The UDP-glucose pyrophosphorylase 2 is the key enzyme in the synthesis of glycogen. Apparently the presence of UDP-Glc pyrophosphorylase seems to enable the enzyme PFK to use the additional phosphate source pyrophosphate (PPi) to catalyse its reaction (Kruger and Dennis, 1985). The compartmentalisation of PFK and UDP-Glc pyrophosphorylase into close proximity within the M-band

could probably enhance the enzyme activity of PFK and the efficiency of overall metabolic substrate flow.

Another protein associated with energy metabolism is the creatine transporter. Mainly localised to the mitochondrial membrane it serves as a creatine/phosphocreatine shuttle. Stainings of adult rat cardiomyocytes and skeletal muscle samples revealed a strong colocalisation of the creatine transporter to the mitochondria as well as the sarcolemma of the cell, whereas no apparent sarcomeric localisation could be observed (Walzel et al., 2002a); (Walzel et al., 2002b).

Heat shock proteins play a vital role in the cellular stress response. In heart muscle, they were implied in myocardial recovery and protection after cardioplegic arrest. Two different heat-shock proteins were identified among the myomesin 9-13 and myomesin 2-8 (see below) yeast two-hybrid screens. HSP27 was identified as potential interaction partner for the C-terminal part of myomesin. Recently it was shown that HSP27 is expressed in hearts and gets only modestly upregulated after a heat-shock application. Confocal laser scanning microscopy revealed that HSP27 localises into the sarcomere (Leger et al., 2000). To confirm the interaction of myomesin domains 9-13 with the HSP27 the isolated pACT2 construct was subjected to a bait-dependency test and growth was assayed on selective media. No clones could be found on selective media lacking the amino acids histidine, leucine and tryptophane, whereas the transformed yeast grew on selective media lacking only the amino acids leucine and tryptophane (data not shown). This finding indicates that although the bait and prey plasmids were present, both proteins were not interacting, identifying HSP27 as a false positive clone.

Neuropilin 1 is a membrane protein, which is involved in vascular development, angiogenesis and organisation as well as exhibiting a function as a nerve growth guiding signal. The protein is a receptor for the vascular endothelial growth factor 165 (VEGF165) and acts as a coreceptor that enhances VEGF165 function through tyrosine kinase VEGF receptor 2. Although the depletion or the overexpression of neuropilin 1 in transgenic animals results in severe vascular defects and heart malformations, an interaction with the C-terminal Ig-domains of the sarcomeric protein myomesin and the membrane protein neuropilin 1 seemed to be unlikely and this putative interactor was not further investigated (Kawasaki et al., 1999; Yamada et al., 2001).

6.1.1.5. Proteins of unknown function

One of the most abundant clones found in the myomesin 9-13 yeast two-hybrid screening was LOC122282 (DKFZp451A211). The cDNA clones encode for the C-terminus of an uncharacterized protein. The clone was subjected to a bait dependency test to validate the interaction and transformed yeast were assayed for growth on yeast selective media (as described above). Transformed yeast grew on selective media lacking the amino acids leucine and tryptophane as well as histidine, indicating a robust interaction.

The interaction of myomesin with the uncharacterised protein LOC122282 was studied therefore in more detail (see below).

6.1.2. The dimerisation of myomesin

Myomesin appears to be the major structural component of the sarcomeric M-band. Historically, the structure of the sarcomeric M-band was studied using electron micrographs of transverse or longitudinal sections of skeletal muscle. In negatively stained longitudinal sections, the M-band is visible in a fibre type specific fashion as a series of parallel white lines (see figure 2). Early models of the M-band structure compiled information gained in the observation of electron micrographs of cross-striated muscle cells (see figure 2 panel C and D). Later on biochemical interaction data supported the structural cross-linking function of members of the myomesin protein family influencing the current structural M-band model (figure 2 panel E).

The finding of our yeast-two hybrid screen that the conserved C-terminus of myomesin shows a strong interaction with itself implicates therefore a tremendous impact on the way of how the sarcomeric M-band is assembled and serves its function. In the following paragraphs, the dimerisation of myomesin is analysed and further characterized with an emphasis on creating a new three-dimensional model of the sarcomeric M-band.

6.1.2.1. Yeast two-hybrid data and identification of the minimal binding site

The majority of the clones found in the yeast-two hybrid screen with myomesin domains 9 to 13 encoded the C-terminal part of myomesin itself, suggesting that the protein may form homodimers.

To identify the domain important for mediating this interaction, we established serial deletion constructs of myomesin and tested their interaction in a forced yeast-two hybrid (see table 4). Constructs containing domain 13 of myomesin were positive, whereas constructs lacking domain 13 showed no growth on selective media. These results imply that the C-terminal Ig-domain 13 is both required and sufficient for myomesin dimer formation.

Table 4 – Yeast two-hybrid analysis of myomesin dimer formation – serial deletion constructs

Forced yeast two-hybrid analysis with serial deletion constructs of myomesin. Yeast cells were transformed with the indicated bait and prey plasmids and growth on selective media lacking the amino acids histidine, leucine and tryptophane was assayed (as described earlier). Growth and strength of interaction are shown. (n.d. = not determined)

Transformed yeast two-hybrid constructs						
	My9-13	My11-13	My11-12	My12-13	My12	My13
My9-13	+++	+++	n.d.	n.d.	n.d.	+++
My11-13	+++	n.d.	n.d.	n.d.	n.d.	n.d.
My11-12	n.d.	-	-	-	-	-
My12-13	n.d.	-	-	+++	-	+++
My12	n.d.	-	-	-	-	-
My13	n.d.	-	-	+++	-	+++

6.1.2.2. Biochemical analysis of the myomesin dimerisation

To confirm the interaction found in the yeast two-hybrid assays and to validate domain 13 as the major dimerisation site, the binding of myomesin was further analysed in several biochemical assays, like GST-pulldown experiments and co-immunoprecipitation assays. Crosslinking experiments with epitope-tagged serial deletion constructs were used to determine the size of the myomesin complexes and to confirm the formation of dimeric or other multimeric complexes.

Figure 7 shows the characterisation of the myomesin interaction using a co-immunoprecipitation assay (A) and a GST-pulldown experiment (B) using various fragments of recombinantly tagged myomesin. The results indicate that the major myomesin interaction site for the dimerisation is located in the C-terminal Ig-domains of myomesin and confirms the results obtained by forced yeast two-hybrid analysis (see earlier). Neither the central fibronectin domains 5-8 of myomesin (figure 7.A row C) nor the Ig-domains 9-10 (figure 7.B) showed an interaction either with YFP-tagged myomesin domains 11-13 (figure 7.A) or with YFP-tagged myomesin domains 9-13. These results were further validated by a far western blot assay using multiple myomesin deletion constructs (see figure 7.C). Only constructs containing domain 13 of myomesin were able to bind T7-tagged recombinantly expressed myomesin domains 11-13 (see figure 7.C overlay panel). In the absence of domain 13 no or only a very weak interaction could be observed.

Finally, crosslinking experiments with lysates of transfected cells expressing T7-tagged myomesin constructs were used to determine the state of the interaction (see figure 7.D). Only constructs containing domain 13 showed bands corresponding to the size of a dimer in the presence of the

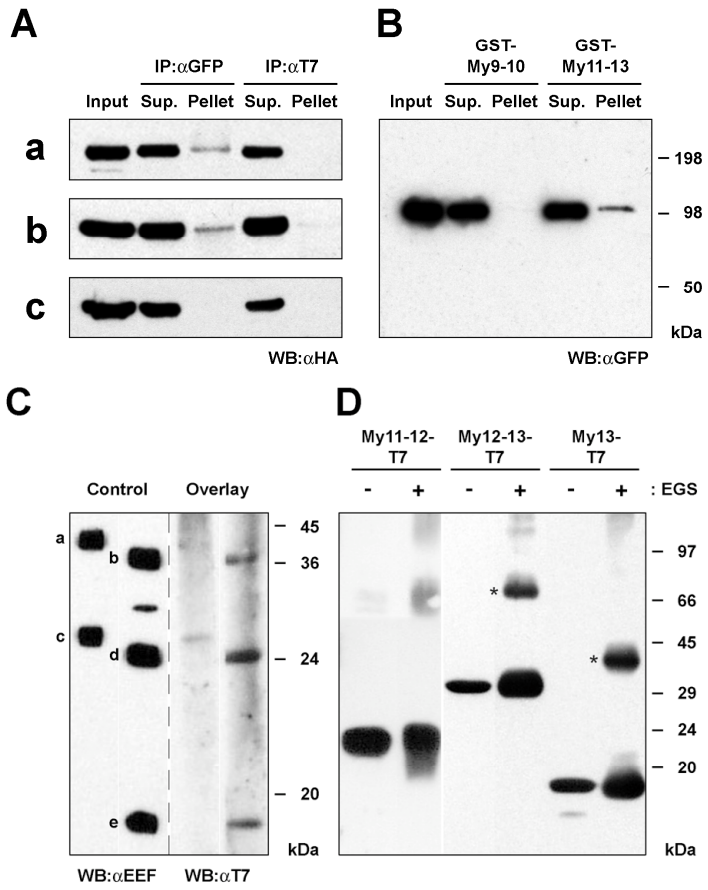

Figure 7. Biochemical characterisation of myomesin interaction.
A Co-immunoprecipitation. Cos cells were co-transfected with My9-13-HA (row a), My11-13-HA (row b) or My5-8-HA (row c) together with YFP-tagged My11-13. Lysates were immunoprecipitatedwith an anti GFP-antibody, followed by immunoblotting with an antibody against the HA-tag. My11-13 is co-precipitated with My9-13 and My11-13, but not with the central myomesin domains (My5-8). No co-precipitation is seen with an unrelated antibody against the T7 tag.
B GST pull-down assay. Cos cells were transfected with YFPMy9-13 and lysates were incubated with purified GST-My9-10 or GST-My11-13. Complexes were precipitated using glutathione-agarose beads and detected using anti-GFP antibody. YFP-My9-13 was precipitated with GST-My11-13, but not with GST-My9-10, which lacks the interacting domain 13.
C Far western blot assay. Bacterially expressed EEF-tagged myomesin fragments My9-11 (a), My11-13 (b), My11-12 (c), My12-13 (d) and My13 (e) were separated by SDS-PAGE, blotted onto nitrocellulose membrane and overlayed with T7 tagged recombinantly expressed My11-13. EEF-tagged proteins were detected by immunoblotting using an antibody specific against the EEF tag (overlay panel), wile bound protein was detected by a T7 antibody (overlay panel). Overlayed My11-13-T7 bound strong to My11-13-EEF, My12-13-EEF and My13-EEF and interacted much more weakly with My11-12-EEF. No binding could be observed for My9-11-EEF.
D Crosslinking assay. Cells were transfected with T7 tagged myomesin fragments My11-12-T7, My12-13-T7 and My13-T7 and lysates were incubated in the presence (+) or absence (-) of the chemical crosslinker EGS. Monomers and dimers (marked with an asterisk) were detected with an antibody specific for the T7 tag. Only constructs containing myomesin domain 13 were able to form a complex corresponding to the size of a dimer (see bands marked with an asterisk). The formation of higher complexes like trimers, tetramers or hexamers was not observed.
The far western blot assay and the crosslinking experiments were performed by Mirko Himmel and Katrin Hayess in the group of Prof. D.O. Fürst.

chemical cross-linker EGS (see bands marked with an asterisk in figure 7.D). Neither trimeric, tetrameric, hexameric nor the formation of any other multimeric complexes could be observed, indicating that the interaction mediated by myomesin domain 13 enables myomesin to form dimeric complexes.

6.1.2.3. Subcellular localisation of myomesin domains 9-13

Is the interaction of myomesin with itself sufficient to target myomesin *in vivo* to the sarcomeric M-band? Previous studies indicated that the N-terminus of myomesin was sufficient to mediate M-band targeting (Auerbach et al., 1999). However, only a chicken construct comprising domains 9-14 of myomesin was used to demonstrate largely cytoplasmic and only a marginal myofibrillar localisation of the epitope tagged construct. Conclusions derived from the *in vivo* localisation experiments of chicken myomesin in neonatal rat cardiomyocytes might be influenced by the presence of the additional unstructured C-terminal H-domain of myomesin, which is absent in the rodent as well as human protein. To assess the possibility of a so far unidentified *in vivo* M-band targeting site, we subcloned the C-terminal human myomesin domains 9-13 into an eukaryotic expression vector fused in frame with the green fluorescent protein (GFP). The construct was transfected into neonatal rat cardiomyocytes. Cells were subsequently fixed and stained with antibodies recognising the Z-disc protein α-actinin as a sarcomeric marker. Figure 8 shows the subcellular localisation of the GFP tagged myomesin 9-13 protein. Although an association of the fusion protein to myofibrils, namely to the Z-disc as well as to a lesser extent to the M-band of the sarcomere was observed, the exclusive targeting to the M-band, as described for tagged chicken myomesin domain 2 could not be detected (Auerbach et al., 1999). This result indicates that although domain 13 confers the ability to form

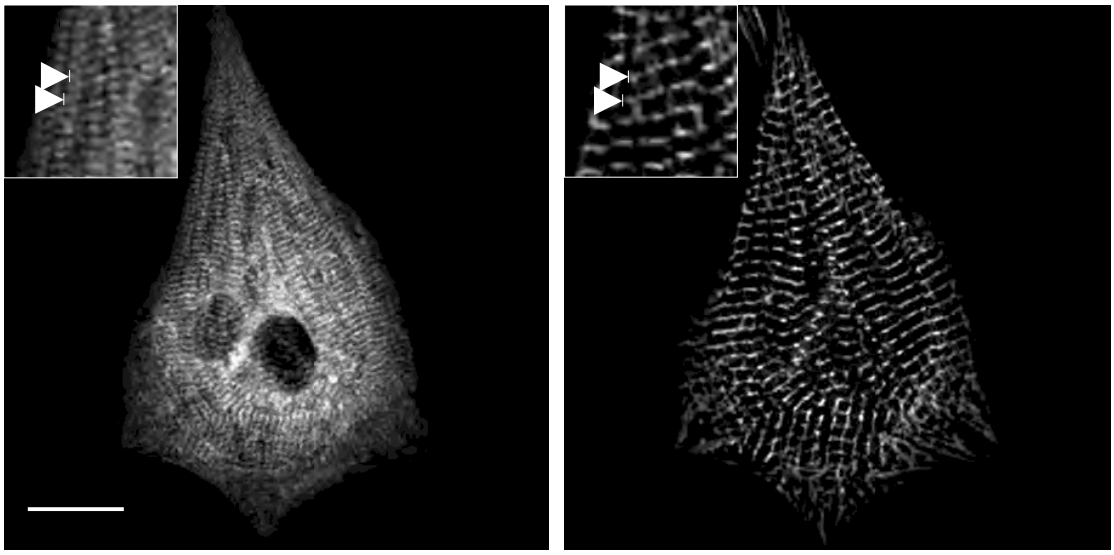

Figure 8. *In vivo* targeting of GFP-tagged myomesin domain 9-13 constructs
Confocal images of transfected neonatal rat cardiomyocytes. GFP-tagged human myomesin domains 9-13 (a) were transfected into neonatal rat cardiomyocytes and counterstained with an antibody against an epitope for the Z-disc protein α-actinin (b). The GFP-fusion construct targeted to the M-band as well as to the Z-disc of the sarcomere (arrows). Scalebar = 10um

myomesin dimers, the exclusive localisation of the protein to the M-band of the sarcomere seems to be the sum of several interactions. A concerted binding, first of the N-terminus of the protein, presumably to myosin and titin and secondly to another myomesin protein via the C-terminal domain 13 might be the prerequisite for correct M-band targeting and function of the protein.

6.1.2.4. Orientation of the myomesin dimers

To investigate, whether myomesin dimerisation occurs preferentially in parallel or antiparallel orientation, the technique of FRET (fluorescence resonance energy transfer) and a recently described technique, the protein complementation assay (PCA) were used. FRET occurs when two fluorophores with overlapping emission and absorbance spectra are brought together in close proximity. In the case of myomesin Cos-1 cells were transiently transfected with myomesin 11-13 constructs tagged either N- or C-terminally with cyan (CFP) or yellow fluorescent protein (YFP). Two different approaches were used to determine FRET occurrence and FRET efficiency. The first approach is based on the sensitised emission method, observing the FRET signal directly in the laser-scanning microscope upon excitation of the donor. The second method is based on the increase of donor fluorescence upon bleaching of the acceptor fluorophore (also called acceptor photobleaching technique) and gives additional information about the FRET efficiency (for a review and introduction into the methods see: (Berney and Danuser, 2003)).

PCA (or protein complementation assay) is a new method utilising the ability of a truncated protein or domain to reconstitute its function upon complementation with the missing parts of the protein. The parts are expressed independently and when brought into close proximity, the protein is folded correctly and the protein function is reconstituted. In the case of myomesin, the green fluorescent protein (GFP) was split into a N-terminal and a C-terminal part (hence the name split-GFP method; (Fang and Kerppola, 2004)) and fused either to the N- or the C-terminus of myomesin domain 13. Like in the FRET-based method the differential tagged myomesin domains were co-expressed in Cos cells.

For a parallel interaction, only N-terminally tagged (or C-terminally tagged, respectively) myomesin fusion proteins should lead to a strong FRET or fluorescent signal within the cotransfected cells. For an antiparallel binding of myomesin, fusion proteins tagged N- and C-terminally with the fluorescent proteins CFP and YFP for FRET or the N-terminus and the C-terminus of split-GFP should lead to a strong FRET or a reconstituted intrinsic fluorescence signal, respectively.

Figure 9 shows the results of the FRET and the split-GFP experiments. Using the sensitised emission method, no signal in the FRET channels could be observed, when both fluorescent proteins where situated at the C-terminus of myomesin (figure 9 panel A; combination of FRET pairs My11-13-CFP and My11-13-YFP). Only for the case of the cotransfection of My11-13-CFP and YFP-My11-13, combining C- as well as N-terminally tagged myomesin, FRET could be observed (figure 9 panel B (d)). This suggests that the dimeric interaction occurs in an antiparallel fashion, bringing the N- and C-terminally fused fluorescent proteins within the range of the Förster radius and enabling FRET to happen. To quantify these observations, the acceptor photobleaching method was used, where again a higher FRET efficiency was observed for the antiparallel interaction (see figure 9 panel C).

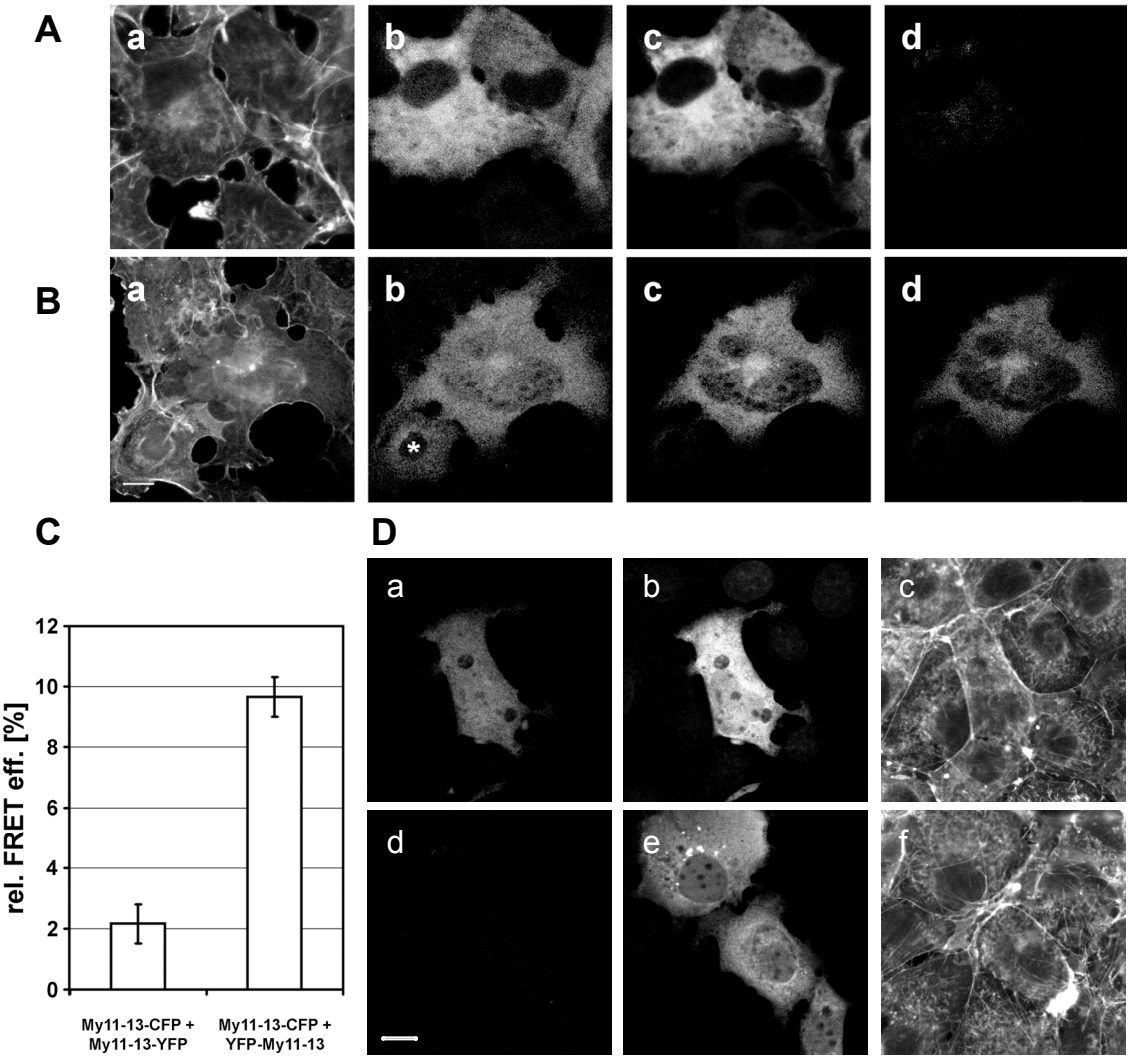

Figure 9. Orientation of the myomesin dimers.

A & B. FRET experiments of myomesin by the sensitized emission method. Cos cells were co-transfected with My11-13-CFP and My11-13-YFP (row A) or My11-13-CFP and YFP-My11-13 (row B). Panel a shows counterstain of F-actin with Alexa633 phalloidin, panel b the signal in the CFP channel, panel c the signal in the YFP channel and panel d the signal in the FRET channel (CFP excitation, YFP detection). No signal can be detected in the FRET channel with C-terminal tagging of the myomesin constructs, while the combination of N- and C-terminal tagging yields a signal due to FRET. This suggests an antiparallel interaction of myomesin constructs. The cell marked with an asterisk in row B is a single transfected cell for My11-13-CFP and serves as a control for bleedthrough.

C. Quantification of FRET efficiency using the acceptor bleaching method. Cos cells transiently co-transfected with My11-13-CFP and My11-13-YFP result in 2.2%, while those co-transfected with My11-13-CFP and YFP-My11-13 result in 9.6% FRET efficiency. The low yield can be explained by saturation due to CFP–CFP and YFP–YFP interactions or due to incomplete photobleaching (Berney et al. 2003), respectively.

D. Protein complememtation assay utilising the split-GFP system for myomesin domain 13. Cos cells were transiently transfected with myomesin domain 13 fused either N- as well as C-terminally to the split-GFP halves (a-c) or myomesin domain 13 fused only N-terminally to the different split-GFP halves (d-f). Reconstituted intrinstic GFP fluorescence (a, d) could be observed only in the case of the antiparallel myomesin dimerisation, whereas cells containing the GFP fusion (as determined by using the GFP-antibody; b, e) showed no reconstitution of intrinsic GFP fluorescence in the antiparallel case. Cells were counterstained with Alexa633 phalloidin (c, f). Scalebar = 10µm.

These results were confirmed using the split-GFP system (see earlier) and reducing myomesin to its minimal dimerisation site, immunoglobulin-like domain 13 (see figure 9 panel D). Again only for the case of an antiparallel interaction the reconstitution of intrinsic fluorescence could be observed, whereas in the parallel case transfected cells showed no intrinsic fluorescence for GFP.

In conclusion, the FRET experiments as well as the split-GFP system used to determine the orientation of the myomesin dimers point towards an antiparallel interaction mediated by a binding site in domain 13 of the protein.

6.1.2.5. Crystal structure of the myomesin dimer

Data from the yeast two-hybrid screen, the biochemical analysis and the FRET and split-GFP system indicate that myomesin dimerises via its last C-terminal immunoglobulin like domain in an antiparallel fashion. How exactly is this interaction mediated and which amino acid residues are involved in generating the interaction interface? To address this question we established in collaboration with the group of Prof. Matthias Willmans and Dr. Nikos Pinotsis at the DESY EMBL outstation in Hamburg bacterial expression constructs covering domains 12 to 13 of myomesin in order to determine the crystal structure of these domains in the dimeric complex.

Figure 10 shows the expression and purification as well as the crystals obtained from purified His-tagged myomesin domains 12-13 under various conditions (data from Nikos Pinotsis). The refraction pattern of the crystals was recorded and the crystal structure of the two myomesin domains was solved. Figure 10, panel C shows different presentations of the crystal structure of the myomesin domains 12 and 13. Most notably is that the structure confirms the antiparallel dimerisation of myomesin via its C-terminal domain. Domains 12 and 13 of myomesin display the typical folding pattern of immunoglobulin-like domains. Domain 12 as well as the dimerisation domain 13 of myomesin consist of 7 β-sheets (A-G) and a short α helix between the β-sheets E and F. Surprisingly, the linker between the two immunoglobulin-like domains folds into an α-helix, rather then a flexible and unstructured linker observed in other available crystal structures of immunoglobulin-like or fibronectin-type III domains of e.g. titin (see protein structure 1QR4 on the protein data bank; or crystal structure of titin domains Z1Z2 without telethonin, pers. comm. with Prof. Willmanns).

The following two paragraphs will focus on the amino acid residues responsible for the formation of the binding interface as well as on the putative role of the domain linker. Cross-species protein alignments of myomesin, M-protein and the recently discovered miamesin (pers. comm. Dr. Irina Agarkova; also known as myomesin family member 3) as well as mutation of key amino acids and their functional analysis on the formation of the myomesin dimer might give insights into the functional role of some of the amino acid residues.

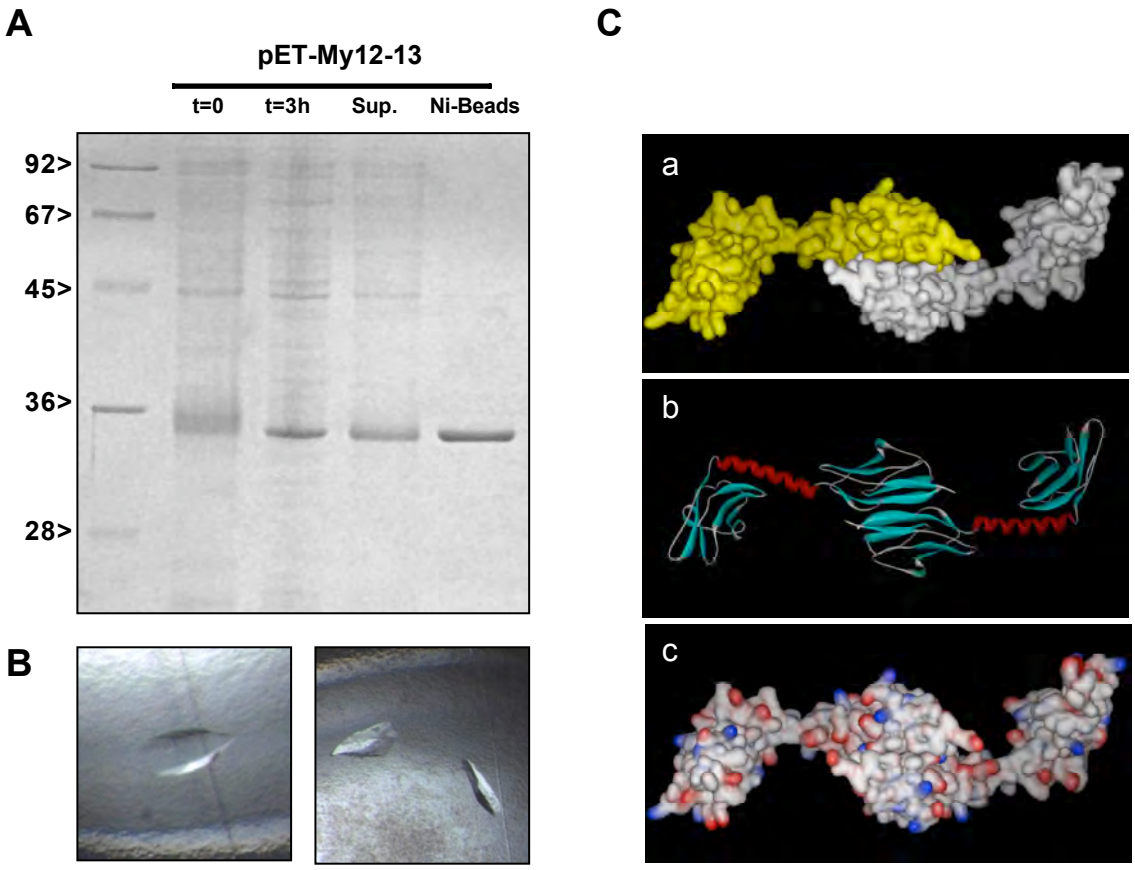

Figure 10. Heterologous expression, purification and crystallisation of myomesin domains 12-13.
A. Expression and purification of His-tagged human myomesin domains 12-13. The image showes a typical Coomassie-stained gel of the expression and purification of the bacterially expressed construct. The size of the protein corresponds with 34kDa to the calculated mass of myomesin domains 12-13 of about 32kDa. The protein was soluble and easily bound to Ni-NTA beads.
B. Typical crystals obtained in various crystalisation conditions. The experiment was carried out by Dr. Nikos Pinotsis at the DESY EMBL outstation in Hamburg, Germany.
C. Panel a gives an overview about the orientation of the myomesin dimers in the crystal structure. The surfaces of the monomers are depicted in white and yellow, respectively and show clearly that the dimer is assembled in an antiparallel fashion. Panel b highlights the secondary structure of myomesin domains 12 and 13. The domains 12 and 13 show the typical folding-pattern of an immunoglobulin-like domain and consist mainly of beta-sheets (coloured in blue), whereas the linker has the secondary structure of an alpha-helix (coloured in red). The surface view in panel d depicts the electrostatic charges from exposed amino acid side chains.

Characteristic residues of the binding interface

Yeast two-hybrid data and the biochemical analysis of the interaction via cross-linking indicated that the dimerisation of myomesin is mediated via the C-terminal immunoglobulin-like domain 13 of the protein. FRET data and the use of the split-GFP system showed that this interaction seems to occur preferentially in an antiparallel fashion. However, only the crystal structure of the dimerisation domain of myomesin, obtained in collaboration with Dr. Nikos Pinotsis from the group of Prof. Wilmanns, enabled us to investigate the principle underlying the formation of the binding interface and the functional role of some of the amino acid residues. The antiparallel-binding interface of the immunoglobulin-like domain 13 displays some characteristic features. Figure 11 shows the two binding interfaces and the involved amino acid residues. β-sheets 13B and 13C as well as residues of the adjacent turns contribute to the creation of the binding interface generated by two antiparallel interacting β-sheets. The interaction itself is largely mediated by a network of hydrogen bonds between the amino acid backbones, but also via salt-bridges of two key amino-acid side-chains, K1588 and D1580.

The larger binding interface 1 is formed by two antiparallel oriented β-strands 13B of each

Figure 11. The binding interface of myomesin domain 13.
A, D, F. Crystal structure images of myomesin dimerisation domain 13.
A. Binding interface 1 with amino acid residues contributing to the interaction of the two antiparallel myomesin Ig-domains. Whereas most of the interactions are created by the backbone via hydrogen bonds forming two antiparallel β-sheets, only aspartate 1580 and lysine 1588 display a saltbridge side-chain interaction.
B. Schematic presentation of the interacting amino-acid residues of binding interface 1. The colour of the residues corresponds to the secondary protein structure observed in the crystal structure.
C. Alignment of human, mouse and chicken myomesin with human and mouse M-protein and human miamesin (MYOM3). All residues contributing to the establishment of the two binding interfaces are conserved within the myomesin protein family as well as throughout evolution. The binding interfaces as well as the type of interaction are depicted. b: for hydrogen bond via backbone and s: for salt-bridge via amino-acid side-chain interactions.
D. Binding interface 2 and amino acid residues contributing to the formation of the dimer interaction. All interactions in binding interface 2 are mediated by hydrogen bonds of the peptide backbone. Only asparagine 1591 establishes a side-chain interaction with the backbone of threonine 1593. Note that asparagine 1591 seems not to be conserved in miamesin.
E. Schematic representation of binding interface 2. All amino-acid interactions as well as the secondary structure of the residues are shown.
F. Respresentation of the salt-bride interaction of residues aspartate 1580 with lysine 1588. One of the domains is shown in its electrostatic surface representation, whereas the other domain is displayed in ribbon-view. The aspartate and lysine residues forming a salt-bridge interaction via the side-chains are depicted.
G. Pulldown-assay of YFP-tagged wildtype myomesin domains 11-13 or 12-13 using His-tagged myomesin domains 12-13 wildtype, R1571P mutant, D1580K mutant or K1588D mutant. All mutants showed diminished (D1580K) or abolished interaction (R1571P, K1588D) with the wildtype protein. Fluorescent protein-tagged myomesin strongly bound to His-tagged domains 12-13 of wildtype myomesin.

Figure 11. The binding interface of myomesin domain 13.

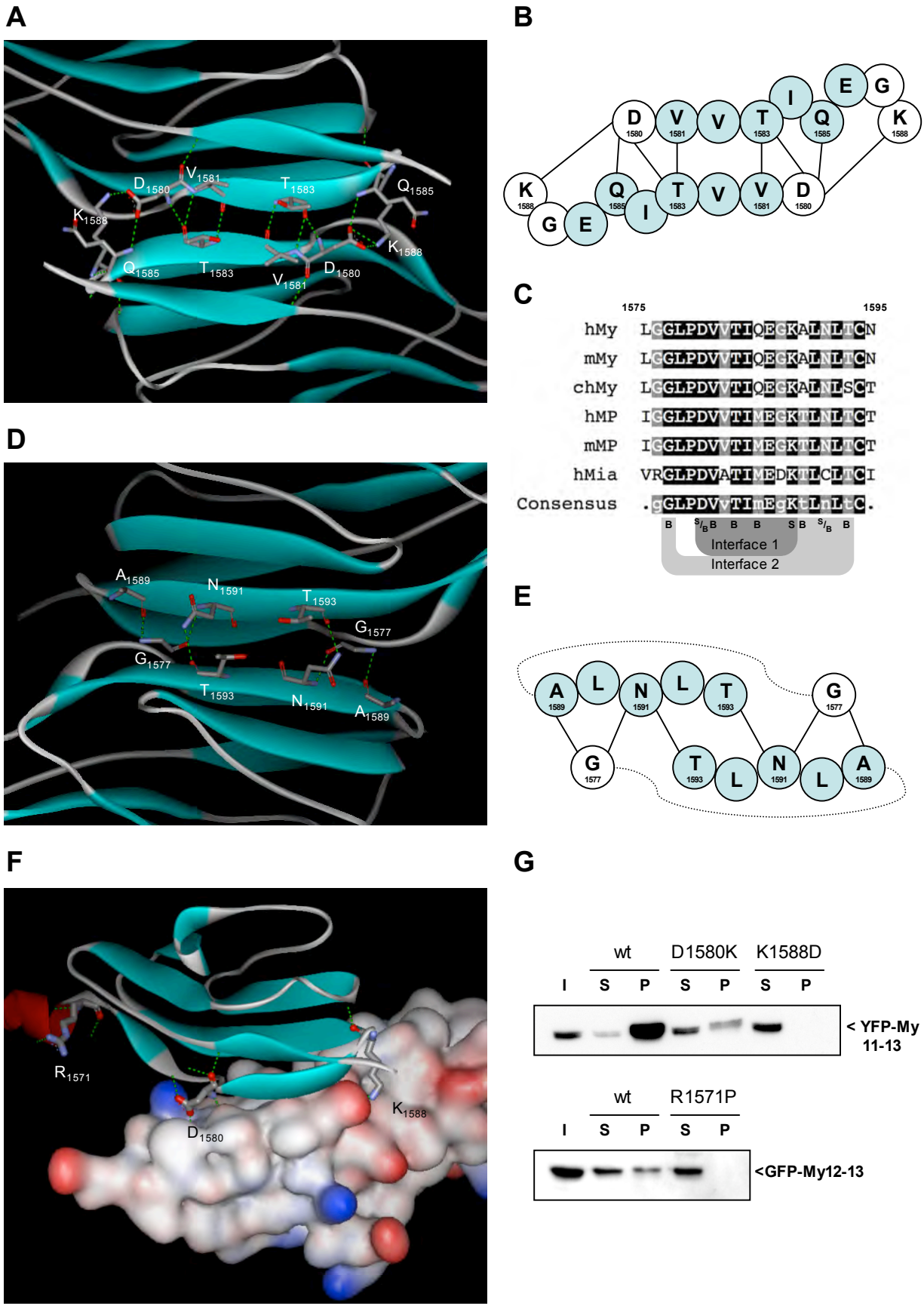

monomer, respectively. Hydrogen bonding occurs between the carboxyl-groups and the amino-groups in the peptide backbone utilising residues D1580, V1581, T1583 and Q1585. Furthermore, electrostatic forces between the negatively charged sidechains of the aspartate D1580 and the positively charged side-chain of the lysine residue K1588 generate a stabilising salt-bridge, which contributes largely to interaction mediated by this interface (see figure 11 panel F).

The smaller interface 2 is as well formed by two antiparallel interacting β-strands, building a network of hydrogen bonds which consists of the amino-acids A1589, N1591, T1539, which reside in β strand 13C as well as G1577 in the adjacent turn. Most of these interactions are formed by the peptide backbone. Only the hydrogen bond between N1591 and T1593 is mediated by the sidechain of the asparagine residue.

Another interesting feature of the β-strands 13B and 13C can be found in the nature of the amino acids contributing either to the intermolecular interaction or to the intramolecular β-sheet formation. All the amino acid residues contributing to the intramolecular β-sheet formation within domain 13 are hydrophobic in nature, like valine (V1582), leucine (L1590, L1592) or isoleucine (I1584), whereas the residues contributing to the binding interface of domain 13 are more hydrophilic in nature, like amino acid residues T1583, Q1585, N1591 or T1593.

Cross species alignment of myomesin as well as an alignment of the M-band proteins myomesin, M-protein as well as the putative third member of the myomesin family, miamesin (myomesin family member 3) reveals a strong conservation of most of the amino acids contributing to the binding interface (see figure 11 panel C). This finding indicates that the ability of myomesin to form antiparallel dimers via its C-terminal immunoglobulin-like domain might not be an exclusive feature of myomesin alone, but instead seems to be a conserved feature of all myomesin family members (see also M-protein section).

Because of the different nature of the bonding between the amino acids D1580 and K1588 compared to the hydrogen network between all other residues in the interaction interface we speculated that these amino acids were key residues in the mediation of the dimerisation. The introduction of a point mutation, which mutates either D1580K or K1588D, and the subsequent functional analysis of the dimer formation in a co-immunoprecipitation assay, showed that the interaction was strongly abolished in these mutants (see figure 11 panel G). The D1580K mutant was further tested in a yeast two-hybrid assay to confirm the biochemical *in vitro* result *in vivo*. Table 4 shows the forced two hybrid-assay of myomesin domains 9-13 wildtye (wt) or the D1580K mutant with the empty bait vector, myomesin domain 13 or the ubiquitin conjugating enzyme 9. As indicated by the biochemical interaction assay using this mutant, no interaction could be detected between the wildtype domain 13 and the mutant myomesin 9-13 D1580K. Surprisingly, the interaction between myomesin and Ubc9, which also resides in domain 13 (see below) was affected by this mutation as well, as seen by the abolished growth of transformed yeast on selective media lacking the amino-acids histidine, leucine and tryptophane. This indicates that the interaction interface with Ubc9 might be generated by the myomesin dimer rather than a monomeric myomesin domain 13.

Table 4 – Yeast two-hybrid analysis of myomesin dimer formation – dimer mutants

Forced yeast two-hybrid analysis with the D1580K dimerisation mutant of myomesin. Yeast cells were transformed with the indicated bait and prey plasmids and growth on selective media lacking the amino acids histidine, leucine and tryptophane was assayed (as described earlier). Growth and strength of interaction are shown.

Transformed yeast two-hybrid constructs			
	pAct2	pAct2-My13.wt	pAct2-Ubc9
LexA-My9-13.wt	-	++	+++
LexA-My9-13.K1588D	-	-	-

The linker between domains 12 and 13 of myomesin

The second intriguing observation of the myomesin crystal structure was the structure of the domain linker between the immunoglobulin like domains 12 and 13 of myomesin. In contrast to other published interdomain-linkers, like the linker between the fibronectin domains of the extracellular matrix protein tenascin (see crystal structure 1QR4; (Bisig et al., 1999)) or the linker between the titin immunoglobulin like domains Z1 and Z2 (unpublished results from Dr. Nikos Pinotsis and Prof. M. Willmans), which show a rather flexible arrangement of the domains because of an unstructured interdomain linker, the myomesin linker folds into the secondary structure of an α-helix which is furthermore anchored in a rigid position via sidechain interactions to domain 13 as well as to domain 12. These interactions seem to stabilize the two immunoglobulin-like domains in a preferred spatial position to each other, which indicates an important structural function for this linker.

Figure 12 shows the crystal structure of the linker and backbone as well as sidechain interactions of the peptide chain contributing to the formation of the secondary structure of the α-helix as well as to the positioning of the immunoglobulin like domains (see panel A, C and D). A cross species alignment as well as an alignment of the M-band proteins myomesin, M-protein as well as miamesin (myomesin family member 3) demonstrates that the interdomain linker is highly conserved between all M-band protein family members as well as during evolution. Besides the rigidity gained by the secondary structure of an α-helix, the linker provides via amino acid side-chain interactions anchorage points for myomesin domains 12 as well as 13. For domain 12 of myomesin the interaction is mediated by the three amino acid residues tyrosine 1551, alanine 1554 and lysine 1562 on the linker, which interact with proline 1523, serine 1470 as well as glutamate 1520 in the immunoglobulin like domain, respectively (see figure 12 panels A and D). The positioning of the myomesin domain 13 is mediated by the alanine 1567, glutamate 1566, asparagine 1570 residues on the linker and the arginines 1571 and 1573 as well as the aspartate 1599 and asparagine 1650 amino acid residues (see figure 12 panels C and D). Interestingly, the interactions of the linker with domain 13 are not only mediated by the amino acid side-chain (as for most interactions towards domain 12), but also by the peptide

Figure 12. The myomesin domains 12 and 13 interdomain linker.

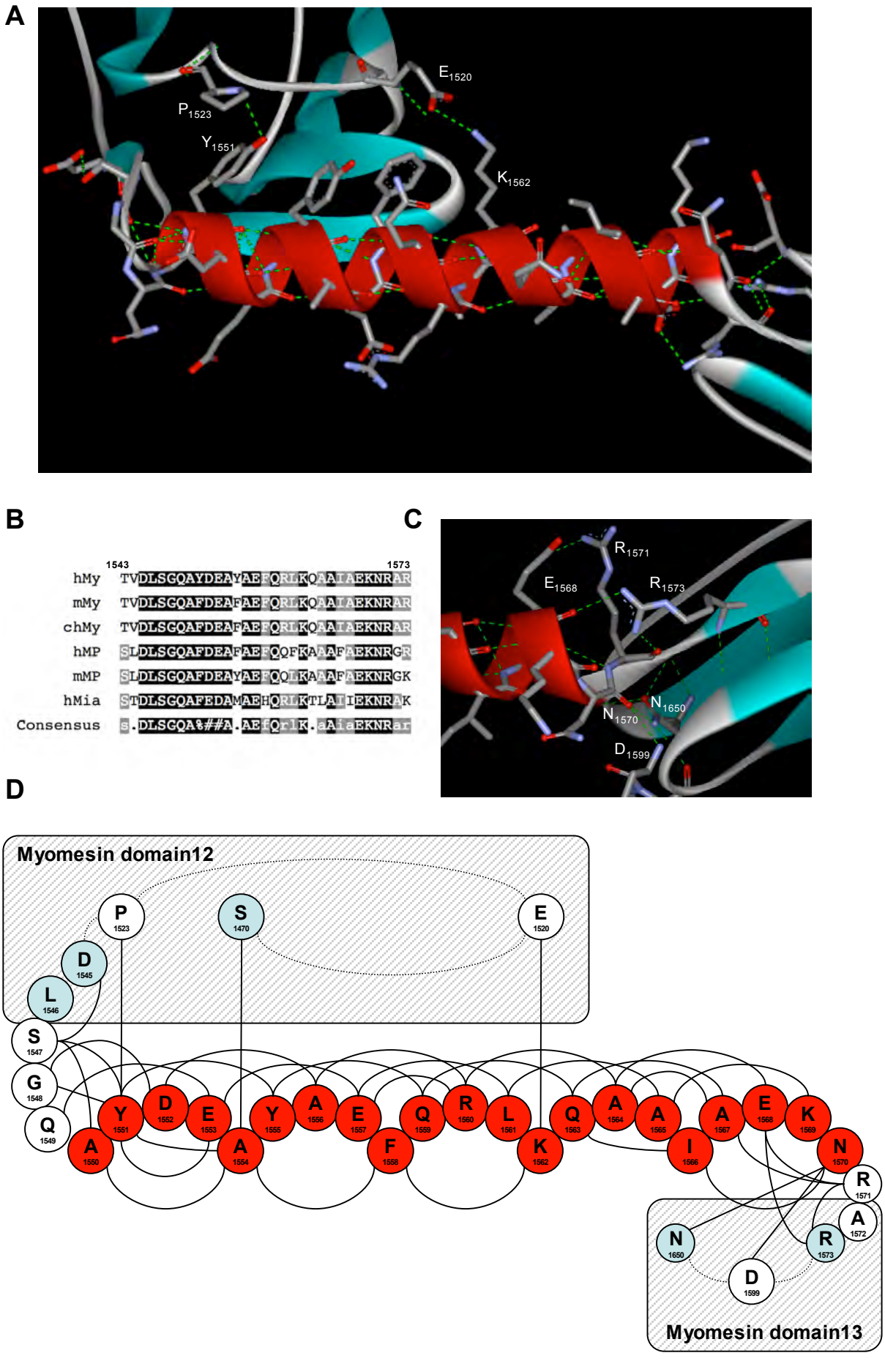

Figure 12. The myomesin domains 12 and 13 interdomain linker.
A. Crystal structure of the domain-linker between Ig-domains 12 and 13. The linker displays an α-helical secondary structure, positioning, via side-chain and backbone interactions, domains 12 and 13 of myomesin in an almost vertical orientation to each other. Two of the side-chain interactions stabilizing domain 12: tyrosine 1551 (on the linker) is interacting with proline 1523 (Ig-domain 12) and lysine 1562 (on the linker) is interacting with glutamate 1520 (Ig-domain 12). The third interaction is hidden behind the α-helix and not depicted: alanine 1554 (linker) interacts with serine 1470 (Ig-domain 12). Note also the three different aromatic residues tyrosine 1551, tyrosine 1555 and Phenylalanine 1558 are located on the same side of the α-helix.
B. Alignment of the inter-domain-linker of human, mouse and chicken myomesin with human and mouse M-protein and human miamesin. The sequence alignment of the linker displays a high degree of homology within the myomesin protein family and is also very conserved throughout evolution, suggesting an important structural function.
C. Crystal structure of the residues in domain 13 responsible for the anchorage and positioning of the α-helix. Backbone as well as side-chain interactions mediate the anchorage and positioning of the α-helix relative to domain 13 of myomesin. Note arginine 1571 which has been mutated into proline for the biochemical interaction assay in figure 11.
D. Schematical presentation of the side-chain and backbone interactions stabilising the α-helix and mediating the binding and positioning of myomesin domains 12 and 13. The colour of the residues indicates the secondary structure seen in the crystal.

backbone, which might indicate a more rigid and stable positioning of the linker towards myomesin domain 13 compared to domain 12.

To investigate the functional role of the linker, we established a myomesin mutant, which introduces a proline at the position of the arginine 1571. This mutation should abolish on one hand the side-chain interactions mediated by the arginine 1571 towards the aspartate 1568 and serve on the other hand as a helix breaker, destabilising the spatial positioning of the linker towards domain 13. The effect of this mutation was again tested biochemically with a co-immunoprecipitation assay using wildtype myomesin domains 11 -13 (see figure 11 panel G). As shown before for the dimer mutants D1580K and K1588D, the mutation of the arginine 1571 to a proline results in the abolishment of the interaction, indicating an important structural role of the interdomain linker in the stabilisation of the two myomesin domains in a rigid position to each other or the accessibility of the binding interface. This may contribute to the stability of the myomesin dimer interaction.

In summary, we identified the ability of myomesin to interact with itself. Crosslinking experiments as well as yeast two-hybrid data with myomesin truncations indicate that the last immunoglobulin-like domain 13 of the protein mediates its dimerisation. FRET as well as protein complementation experiments using fluorescent proteins showed a dimerisation of myomesin in an antiparallel fashion. The myomesin crystal structure explains at the atomic level the ability of myomesin domain 13 to form antiparallel dimers. The interaction is mediated by the peptide backbone as well as key amino acid side-chains, like aspartate 1580 and lysine 1588, leading to the formation of an antiparalllel β-sheet interface between the myomesin monomers. The interdomain linker was unexpectedly found to play a

pivotal structural role in the formation and stabilisation of the dimer. Functional mutants based on the crystal structure, interfering either with the binding interface or the folding and spatial positioning of the domain linker showed an abolishment of the dimer interaction.

The cross species alignment of myomesin as well as the alignment of the three family members of the myomesin family myomesin, M-protein and miamesin showed that the amino acid residues important for generating the binding interface as well as the interdomain linker were preserved during evolution and within the myomesin protein family. This in turn indicates that the ability to form dimers may be common to all members of this protein family (see also later).

Combining all biochemical interaction data and results obtained from electron micrographs of M-bands of different muscles, model-interpretations of electron density maps as well as current two-dimensional models of the sarcomeric M-bands, it should be possible to propose a new three-dimensional model (see below in the Discussion).

6.1.3. Crosstalk with the sumoylation pathway

Two of the putative interaction partners identified in the yeast two-hybrid screen of myomesin domains 9-13 were the Protein Inhibitor of STAT 1 (PIAS1) and the ubiquitin Conjugating Enzyme 9 (Ubc9). Both proteins are essential key-players in a posttranslational protein modification machinery, the sumoylation pathway (see earlier; for a review see: (Kim et al., 2002; Melchior, 2000)).

The putative interaction of myomesin with two components of the sumoylation machinery suggests that myomesin might be a target protein for Sumo or that myomesin may act as a scaffold protein, binding the E2 and the E3 enzyme and enabling a close vicinity to the designated target protein.

6.1.3.1. Interaction of myomesin with components of the Sumo pathway

The initial clones identified in the yeast two-hybrid consisted of the full-length coding sequence for Ubc9 and the C-terminal part of PIAS1 (PIAS1ac; residues 416-651), encoding for the acidic region and the C-terminal tail of the protein.

To identify the minimal binding site for these proteins within the C-terminus of the myomesin protein, a forced yeast two-hybrid assay was carried out with several myomesin truncation constructs. Since the proteins are involved in the Sumo modification pathway the Sumo proteins Sumo1 and Sumo3 were included in this assay. Table 5 shows the growth of the transformed yeast on selective media as described earlier.

The truncation mutants show that the minimal binding site for Ubc9 is located in the last C-terminal immunoglobulin like domain of myomesin. This finding is surprising, since this domain was found to be responsible for the myomesin dimer formation. In addition, the interaction of Ubc9 and myomesin domain 13 is probably not competing with the dimerisation ability. On the contrary, the establishment of a myomesin dimer might be a necessity for the formation of a binding interface for Ubc9, since the dimer mutant myomesin 9-13 D1580K showed, besides the abolishment of the dimer interaction, also no binding to Ubc9 (see table 4).

Table 5 – Yeast two-hybrid analysis of the interaction of myomesin with components of the sumoylation pathway

Forced yeast two-hybrid analysis with the truncation constructs of myomesin domains 9 to 13 and Sumo1, Sumo3, Ubc9 as well as full-length PIAS1 and the original C-terminal PIAS1 clone (PIAS1ac). Yeast cells were transformed with the indicated bait and prey plasmids and growth on selective media lacking the amino acids histidine, leucine and tryptophane was assayed (as described earlier). Growth and strength of interaction are shown. No growth could be detected for yeast transformed with pLex-Sumo1 (x). Abbreviation: n.d. = not determined.

Transformed yeast two-hybrid constructs				
	pLex-Sumo1	pLex-Sumo3	pLex-Ubc9	pLex-PIAS1
pAct2	x	-	-	-
pAct2-My9-13	x	n.d.	+++	+
pAct2-My9	x	n.d.	n.d.	+++
pAct2-My9-10	x	n.d.	n.d.	+
pAct2-My9-12	x	n.d.	-	n.d.
pAct2-My10	x	n.d.	n.d.	-
pAct2-My10-13	x	+	n.d.	n.d.
pAct2-My11-12	x	+	-	-
pAct2-My12-13	x	-	+++	-
pAct2-My13	x	n.d.	+++	-

The E3 enzyme PIAS1 was submapped to interact with myomesin domain 9. Using truncation mutants, the interaction of myomesin to PIAS1 was mapped to the peptide fragment encoding for the acidic region of the protein (see table 6 and dotted line in figure 5 panel D).

The yeast two-hybrid analysis of the interaction of the Sumo protein with myomesin was somewhat more intriguing. The transformation of the mouse Sumo1 bait plasmid into the L40 yeast strain resulted in a complete growth retardation. Only the transformation of the highly homologous mouse Sumo3 bait plasmid gave rise to viable yeast colonies. The forced yeast two-hybrid with Sumo3 indicated that the yeast were only able to grow on selective growth medium, when myomesin domain 11 was present in the prey construct (see table 5). Knowing the nature of the sumoylation, this result might either indicate a common protein-protein interaction or a covalent linkage of myomesin domain 11 with the Sumo protein utilising the endogenous E1 and E2 enzymes of the yeast to catalyse this reaction.

Table 6 – Yeast two-hybrid analysis – submapping of the myomesin binding site within PIAS1

Forced yeast two-hybrid analysis with PIAS1 truncation mutants with myomesin. Yeast cells were transformed with the indicated bait and prey plasmids and growth on selective media lacking the amino acids histidine, leucine and tryptophane was assayed (as described earlier). Growth and strength of interaction are shown.

Transformed yeast two-hybrid constructs		
	pLex	pLex-My9-13
pAct2	-	-
pAct2-PIAS1	-	+
pAct2-PIAS1ΔC (1-415)	-	-
pAct2-PIAS1ac (416-651)	-	+
pAct2-PIAS1ΔN (476-651)	-	-

GST pulldown assays with truncated myomesin constructs were used to validate the interaction of Ubc9 (the E2 enzyme) as well as of PIAS1 (the E3 enzyme) with the different myomesin domains. Figure 13 panel A shows the biochemical analysis of the interaction of PIAS1 with the myomesin domains 9-10. Only GST-myomesin domains 9-10 were able to interact with PIAS1, whereas GST alone was unable to retain bound PIAS1 in the pellet fraction. Panel B of figure 13 depicts the interaction of myomesin domains 11-13 with GFP tagged Ubc9, confirming a binding site for the E2 enzyme in the C-terminal part of the protein.

However, these result where obtained with cellular extracts and might not reflect the correct state of these interactions. Especially in the case of PIAS1 a direct binding to myomesin might be mimicked by an interaction of PIAS1 with endogenous Ubc9, which in turn interacts with myomesin, or by an interaction of PIAS1 with a Sumo protein bound to myomesin. Since the myomesin interaction site of PIAS1 was mapped to the acidic region of the E3 enzyme, which also mediates the interaction of PIAS1 to Sumo1, this possibility cannot be excluded. An assay for direct interaction of PIAS1 with myomesin in a cell-free environment using recombinantly expressed PIAS1 and myomesin was not possible, since the heterologous expression and purification of PIAS1 in E. coli turned out to be extremely difficult (data not shown). However, the yeast data indicate by mapping all three binding partners Sumo, Ubc9 as well as PIAS1 to different domains of myomesin that a direct interaction of these components with myomesin might occur.

In order to effectively modify target proteins, the enzymes of the sumoylation machinery have to get into close spatial vicinity. Figure 13 panel C shows cryo-sections of adult mouse ventricle stained with antibodies against PIAS1 (a), Ubc9 (b) as well as myomesin (c). Although PIAS1 and Ubc9 show a mainly diffuse localisation throughout the muscle cell, a subpopulation of the proteins is targeted to the M-band of the sarcomere as determined by the myomesin counterstaining (arrows). However, the localisation of PIAS1 and Ubc9 turned out to be more versatile than this. In neonatal rat

Figure 13. Myomesin and components of the sumoylation machinery.

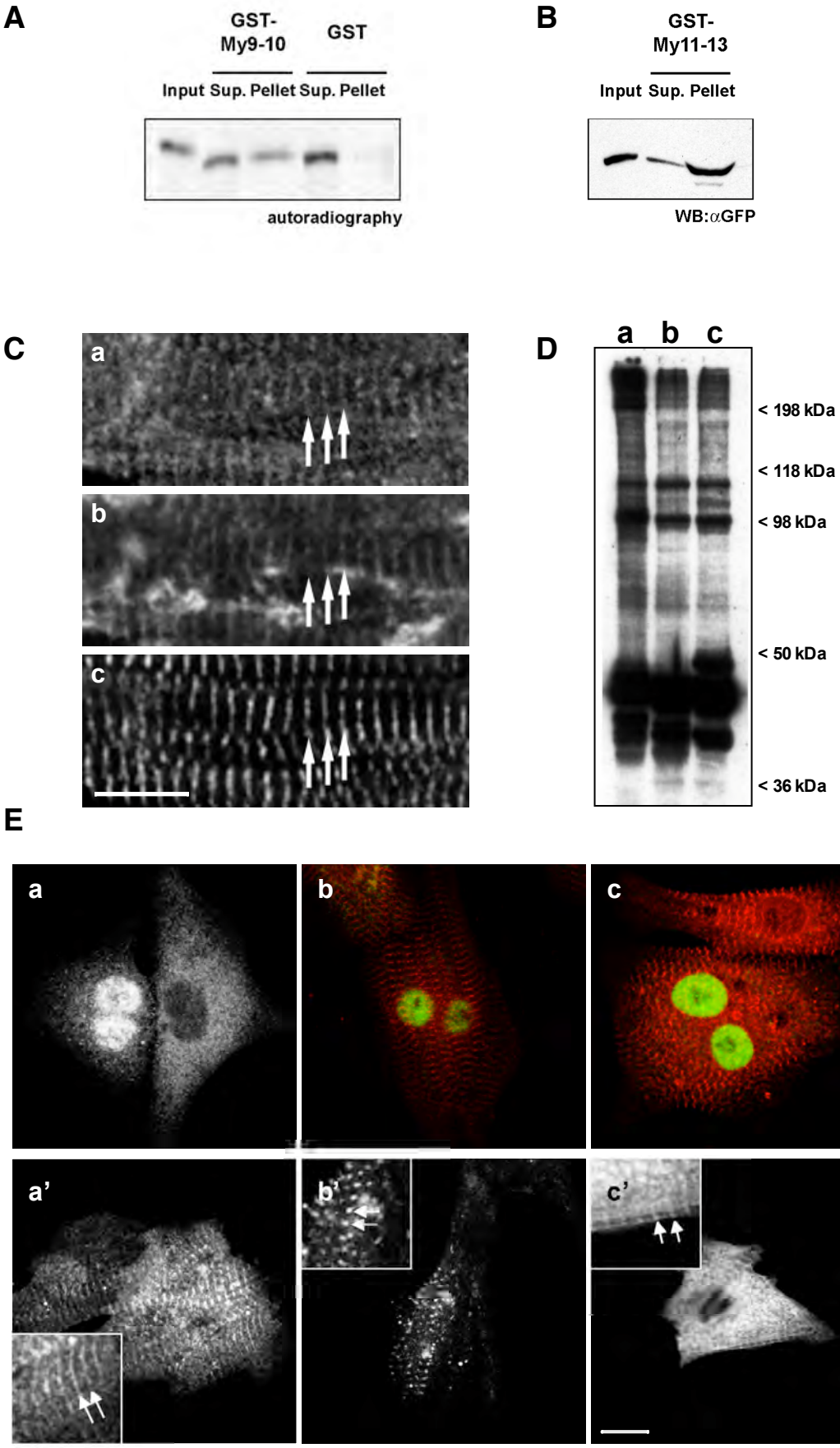

Figure 13. Myomesin and components of the Sumo machinery.
A. Pulldown experiment characterising the interaction of myomesin and PIAS1. ^{35}S-Methionine labeled PIAS1 was incubated with GST-My9-10 and GST alone. Whereas GST-tagged myomesin domains 9-10 were able to retain bound PIAS1 in the pellet fraction after washing, no binding of PIAS1 with GST alone could be observed, suggesting that the interaction of PIAS1 with myomesin is mediated by Ig-domains 9-10 of myomesin.
B. Pulldown experiment confirming the interaction of Ubc9 and myomesin. GFP-labelled Ubc9 was incubated with GST-labeled myomesin domains 11-13. Whereas GST alone was not able to retain bound GFP-labeled Ubc9 (data not shown), Ubc9 was identified in the pellet fraction of GST-myomesin domains 11-13. This suggests that the binding of Ubc9 to myomesin is mediated by the C-terminus of the protein.
C. Subcellular localisation of endogenous PIAS1, Ubc9 and myomesin in frozen sections of adult mouse hearts. Methanol fixed semi-thin cross-sections of adult heart ventricle of mouse showed a colocalisation of PIAS1 (a), Ubc9 (b) and myomesin (c) at the region of the sarcomeric M-band. Sometimes PIAS1 and Ubc9 were localised to the region of the sarcomeric A-band, resembling the subcellular localisation of myosin heavy chain (data not shown).
D. Immunoblot analysis of whole cell lysates of Sumo transfected neonatal rat cardiomyocytes (NRCs). GFP-tagged Sumo1 (a), Sumo2 (b) and Sumo3 (c) were transiently transfected into NRCs and whole cell lysates were blotted onto nitrocellulose after SDS-PAGE analysis. Sumoylated proteins as well as SDS-stable protein complexes with Sumo were identified using a GFP-antibody. The Sumo-monomers migrate at a molecula weight of about 46 kDa, whereas covalently modified Sumo substrates migrate at higher molecular weights. Besides a cluster of modified protein at around 100 kDa, most likely to represent the major Sumo substrate RanGAP1, a cluster of GFP-positive bands could be identified above 200kDa, suggesting the presence of a multitude of Sumo-targets with high molecular weight.
E. Heterogeneous subcellular Sumo localisation. GFP-tagged Sumo1 (a, a'), Sumo2 (b, b') and Sumo3 (c, c') were transiently transfected into NRCs. Immunocytological counterstaining with an antibody specific for myomesin (red in the overlay) indicated that despite the nuclear localisation of Sumo proteins in some cells, Sumo could also be found at the region of the Z-disc (arrow) and at the sarcomeric M-band (see inserts in a', b' and c'). Scalebars in C and E = 10μm.

cardiomyocytes both proteins localised to the region of the A-band, resembling a MyBP-C or myosin heavy chain / myosin light chain subcellular localisation (data not shown). Overexpression of epitope tagged PIAS1 as well as Ubc9 protein leads mainly to a targeting to cytoplasmic vesicles and partially to the nuclear speckles, indicating an abnormal protein targeting due to the uncontrolled overexpression of the proteins. It might be interesting to note that endogenous PIAS1 seldomly localised to nuclear PML bodies in cardiomyocytes, where it was reported to localise in the litreature in other cell types.

The target specificity and subcellular localisation of the three different main Sumo proteins: Sumo1, Sumo2 and Sumo3 turned out to be as diverse as the localisation of PIAS1 and Ubc9. Dependent on the cellular state, epitope-tagged Sumo proteins can be found either exclusively in the nucleus of the cell, diffuse in the cytoplasma or targeted to the Z-disc (see arrows in the blowups of the figure, respectively) as well as to a lesser extent to the M-band of the sarcomere (see figure 13 panel E).

An analysis of the different cellular targets of the sumoylation pathway revealed a multitude of different proteins, which can be subjected to a posttranslational modification via the three investigated

Sumos. Figure 13 panel D shows a SDS-PAGE and subsequent immunoblot analysis of whole cell extracts of neonatal rat cardiomyocytes transfected with GFP-tagged Sumo1 (a), Sumo2 (b) as well as Sumo3 (c). The free GFP-tagged Sumo monomers (the unprocessed propeptide as well as the processed free monomer) are detectable at around 42kDa. Several intensely stained bands are seen at around 100kDa, most likely originating from the major cellular target for sumoylation, RanGAP1 (Melchior, 2000). Another set of bands can be detected above 200kDa indicating several high molecular weight proteins, which have been modified by Sumo.

In summary, the small ubiquitin related modifier Sumo as well as the components of the sumoylation machinery Ubc9 and PIAS1 take on various functions in muscle cells, suggested by the multitude of sumoylated proteins observed in SDS-samples of Sumo-transfected neonatal rat cardiomyocytes and by the diverse subcellular localisation of these proteins. The cell stage-dependent compartmentalisation of Sumo, PIAS1 and Ubc9 indicates a regulation of the substrate specificity of intracellular Sumo targets. The occasional M-band localisation of Ubc9 and PIAS1 indicates further the possibility of a posttranslational modification of myomesin with Sumo.

6.1.3.2. *In vitro* sumoylation of myomesin

The interaction of myomesin with the two major components of the posttranslational sumoylation machinery indicates either that myomesin might be a target protein for this modification or that myomesin serves as a scaffold, bringing the E2 and E3 enzymes in close spatial proximity to their designated target proteins. Although all of the components of the Sumo pathway show a cell state-dependent and generally very diverse subcellular localisation, colocalisation of myomesin and the putative binding partners Ubc9 as well as PIAS1 could be observed in cryo-sections of adult mouse ventricle.

Sumoylation of myomesin

Recent studies indicated the presence of a conserved sumoylation motif within target proteins modified by Sumo. The newly identified consensus motif PsiKxD/E, where Psi represents a large hydrophobic amino acid, K defines the lysine residue to which Sumo is covalently attached via a thiolester bond, x represents any amino acid and D/E is either of the negatively charged amino acids glutamate or aspartate, was shown to be conserved in all sumoylated target proteins identified to date (Rodriguez et al., 2001). Figure 14 panel A gives an overview over all putative sumoylation motifs within the different domains of myomesin and aligns the human, mouse, chicken and zebrafish sequences to identify the preservation of this peptide motif during evolution. Out of the nine motifs identified, six were located in the C-terminal immunoglobulin domain-cluster of myomesin (domains 9-13), whereas only one could be found in the N-terminal part of the protein (domain 2). Only two of the putative Sumo sites were preserved in all of the analysed myomesin proteins, namely the peptide sequence LKDD/E around lysine 1197 in domain 11 of myomesin and the peptide sequence L/IKNE covering the lysine residue 1589 in domain 13 of the protein. Interestingly, the domains containing

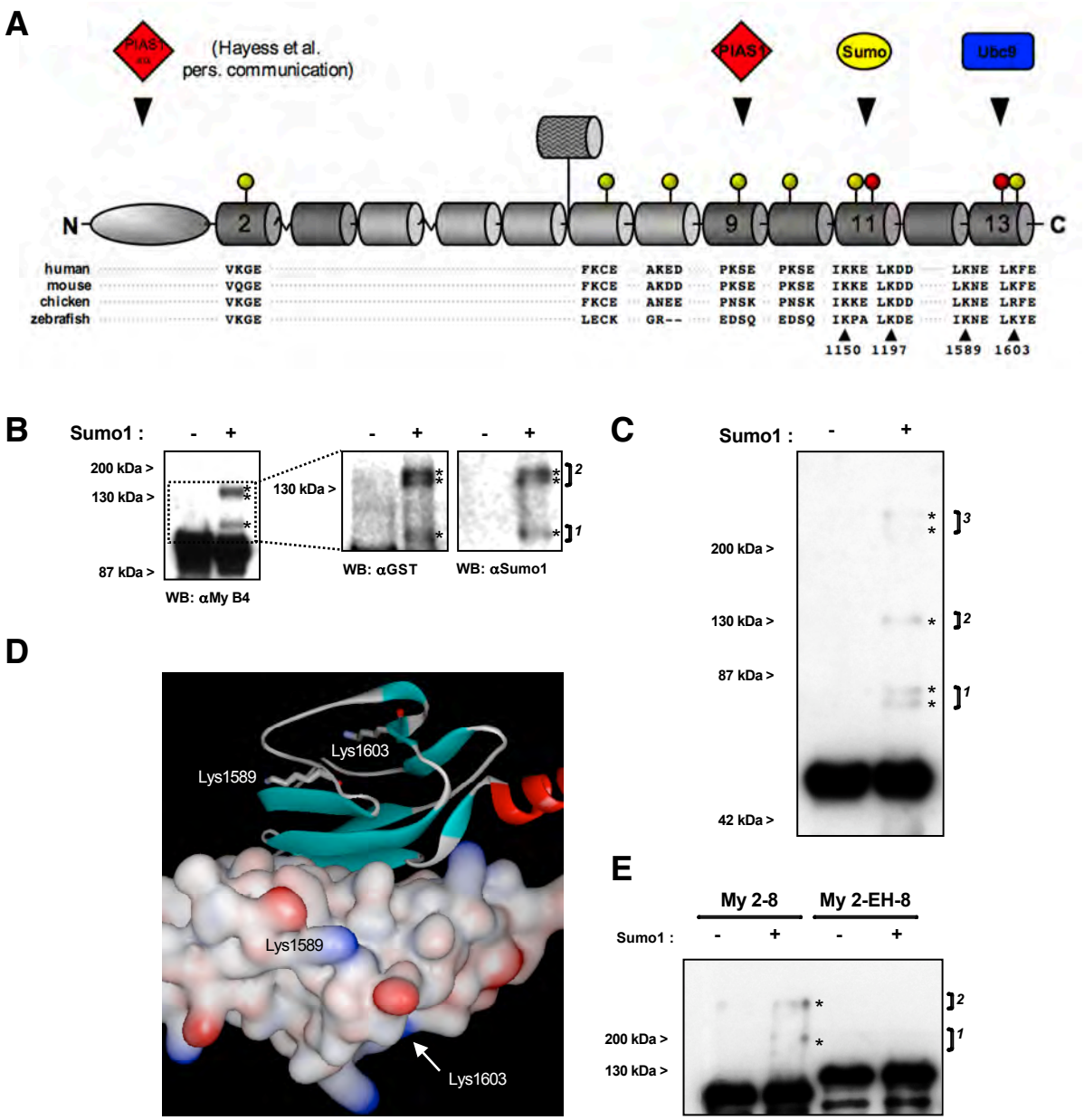

Figure 14. Sumoylation of myomesin.

A. Primary sequence analysis of myomesin for conserved sumoylation motifs. Schematic presentation of the myomesin domain pattern and mapped minimal binding sites of Ubc9, PIAS1, PIAS1xα (data from K. Hayess) and Sumo. Putative sumoylation sites are indicated by yellow and red circles in the schematic domain pattern. The protein sequence alignment of human, mouse, chicken and zebrafish myomesin indicates the presence of two highly conserved classical sumoylation motifs in domains 11 and 13 of myomesin (lysines 1197 and 1589; represented by red circles) and a number of not very well conserved Sumo-motifs (yellow circles). Interestingly, the number of putative Sumo-sites is higher in the C-terminal part of the protein (domains 9-13), whereas the N-terminal part (domains 1-8) contains only three putative and not very conserved classical Sumo-sites.

B. In vitro sumoylation assay using GST-tagged human myomesin domains 9-13. Immunoblot assay of sumoylated GST-myomesin (+) and not sumoylated control (-) using an antibody specific for myomesin, GST and Sumo1. Three different bands (asterisks) with higher molecular weight are identified in the sumoylated protein sample, reactive to myomesin, GST as well as Sumo1 antibodies, indicating that myomesin is a substrate for sumoylation and may be modified at three different sites.

Figure legend continues on the following page.

these motifs coincide with the identified putative binding sites for Sumo (domain 11) as well as Ubc9 (domain 13; see earlier). The identification of as many as nine putative sumoylation motifs within myomesin indicated that myomesin itself might be a target for sumoylation. In order to verify this hypothesis, an *in vitro* sumoylation assay was used. This assay utilises the bacterially expressed and purified components Uba2/Aos1(E1 enzyme), Ubc9 (E2 enzyme) as well as a "processed" Sumo protein (activated Sumo protein without the propeptide) to modify bacterially expressed and purified target proteins in a cell free environment. The modification of the protein is reflected in the change of the molecular weight of the protein due to its covalent linkage to a Sumo protein and visible in a SDS-PAGE/immunoblot analysis. Figure 14 panel B shows the posttranslational modification of GST-tagged myomesin domains 9-13 by Sumo1 in a typical *in vitro* sumoylation experiment. Three bands reactive to antibodies recognising the GST tag, the domain 11 of myomesin (B4) and the Sumo1 protein were detectable in an immunoblot analysis in the protein sample containing the Sumo protein, indicating a covalent modification of the C-terminal part of myomesin. The three different bands can be grouped into two clusters. The first cluster consisting of a band at around 115kDa is probably single modified myomesin, since the difference between the unmodified myomesin (which runs around 95kDa) and this modified myomesin reflects the molecular weight difference of one Sumo protein (approximately 18-20kDa). The second cluster consists of two distinguishable bands, which can be found at around approximately 140 and 145kDa. These two bands might originate from double or triple modified

Figure 14. Sumoylation of myomesin. (continued from previous page)
C. *In vitro* sumoylation assay of myomesin Ig-domains 12-13. Immunoblot analysis of Sumo1 modified GST-tagged myomesin domains 12-13 (+) and not sumoylated control (-) using a GST antibody. The truncated myomesin protein showed a comparable band pattern as myomesin domains 9-13, suggesting the presence of the Sumo-sites within domains 12-13 of the protein. A major difference however, was observed in the band-pattern: cluster 1 contains two detectable bands and cluster 2 only one; in comparison to myomesin domains 9-13 where cluster 1 contained one band and cluster 2 two to three bands. GST-tagged myomesin domains 12-13 showed also the presence of the third cluster of bands, suggesting again the presence of an SDS-stable complex of myomesin, Sumo1 and at least one of the Sumo-Enzymes (see figure 5 panel A).
D. Presentation of the crystal structure of the dimer of myomesin domains 13. Electrostatic surface presentation and ribbon presentation of domain 13 showing that both putative target lysine residues (1589 and 1603) are surface exposed and accessible to Sumo modification. The dimerisation interface is not likely to be influenced by the modification of myomesin via Sumo.
E. *In vitro* sumoylation of myomesin domains 2-8 and the EH isoform of myomesin domains 2-EH-8. Immunoblots of GST-tagged myomesin Ig-domains 2-8 and the EH isoform of myomesin Ig-domains 2-8 subjected to an *in vitro* sumoylation assay (+) or not sumoylated control (-). Detection of the GST-protein using an antibody against GST indicated that the EH isoform of myomesin domains 2-8 showed a strong reduction in the sumoylation efficiency compared to myomesin domains 2-8. Two cluster of bands could be identified for sumoylated myomesin domais 2-8, suggesting the presence of at least two Sumo sites in the C-terminal part of the protein.
If not mentioned otherwise, bands of higher molecular weight are marked for clarity reasons with an asterisk in all panels in this figure and figure 15.

myomesin protein. The fact that the migration distances between the first and the second cluster and the distance between the two bands within the second cluster do not match the 18-20kDa molecular weight difference of a Sumo protein might be explained by the unusual branched protein structure of sumoylated proteins rather than the regular serial peptide chain. The resulting three different bands with higher molecular weight compared to the unmodified myomesin protein suggests further that myomesin may harbour up to three different peptide motifs prone to sumoylation.

As depicted in figure 14 panel A, myomesin contains 4 conserved sumoylation sites within domains 11 and 13 of the protein. To narrow down the amount of putative sumoylation sites and to identify, whether myomesin can be also sumoylated in the absence of the sumo binding site situated in domain 11 of the protein (see earlier), a truncation construct was established, covering only Ig-domains 12 and 13 of myomesin. Figure 14 panel C depicts that this truncation mutant shows a comparable band-pattern as the myomesin 9-13 constructs, namely three clusters of modified bands. The first cluster, which runs around 75-80kDa consists of two distinguishable bands and might reflect single Sumo-modified myomesin at two different sites or single and double-modified protein. The second cluster consists of one band, which migrates at approximately 130kDa and might reflect a myomesin modified with two- to three Sumo proteins. The third cluster of two identifiable bands migrates again above 200kDa. Since the analysis of the primary structure of the myomesin protein identified only two conserved sumoylation motifs in domains 12-13 and the crystal structure of these two domains is available, we investigated whether the lysine residues are surface exposed or whether they are buried or involved in the formation of the myomesin dimer. Figure 14 panel D indicates that these two lysine residues are indeed surface-exposed and not covered by the dimer interaction interface and are hence available for the formation of a thiolester bond towards the Sumo protein.

Dr. Katrin Hayess in the lab of Prof. D.O. Fürst discovered myomesin as a putative target for sumoylation in an independent yeast two-hybrid screen using the head domain of myomesin as bait. Pias1 xα was identified as a putative interaction partner for the head domain. Although there are only three putative sumoylation sites present in the N-terminal and central part of myomesin located in domains 2, 7 and 8, which are not highly conserved during evolution, the *in vitro* sumoylation assay of myomesin domains 2-8 showed the appearance of two high molecular weight products. However, when we used the EH splice variant of myomesin and subjected the purified protein containing this additional domain to an *in vitro* sumoylation assay, the amount of Sumo-modified protein was reduced to a non-detectable level (see figure 14 panel E). This result indicates that two potential sumoylation sites are also located in the N-terminal part of the myomesin protein and that the modification of myomesin via Sumo might be altered in an isoform-dependent way.

No influence of myomesin point mutations on the sumoylation efficiency

To identify the lysine residues which might be responsible for the formation of the thiolester-bond to Sumo, the following myomesin mutants were generated: K1150A, K1197A, K1589R and K1603R as well as the double mutants K1150/1197A and K1589/1603R (see also figure 14 panel A). All mutants along with the wildtype form of myomesin were subjected to an *in vitro* sumoylation assay (as

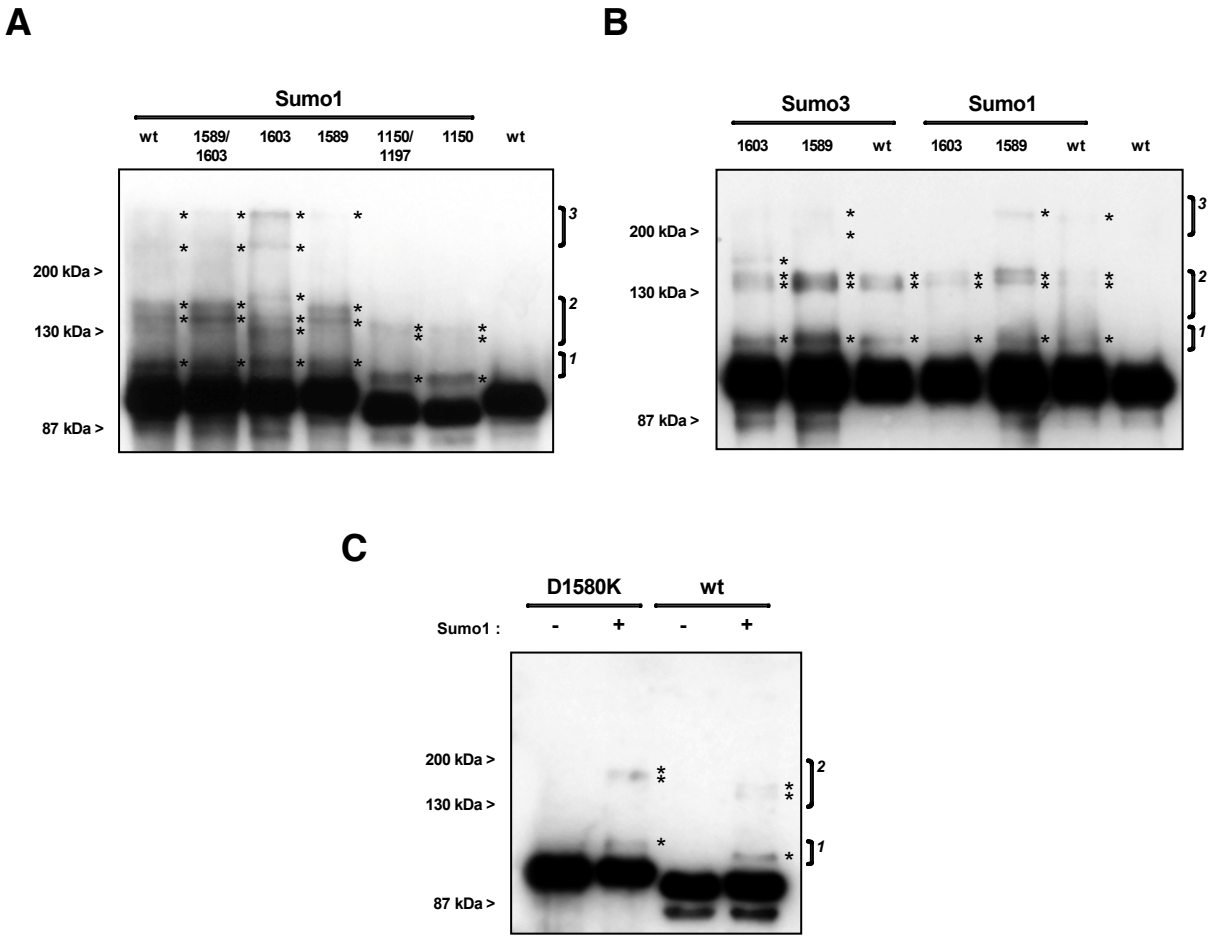

Figure 15. Effects of single residue mutants on the sumoylation of myomesin.
The nomenclature of band patterns is the same as in Figure 14.
A. In vitro sumoylation assay comparing the sumoylation efficiency and modification pattern of wildtype and myomesin mutants. Low percentage SDS-PAGE analysis followed by immunoblotting using a GST antibody identified three different clusters of bands: one band around 100kDa, a set of two to three bands around 130 to 150 kDa and a set of bands above 200kDa. All visible bands are marked with an asterisk. The first and second cluster of bands corresponds to Sumo modified myomesin proteins, whereas the third cluster may represent a SDS-stable complex of myomesin, Sumo and proteins of the sumoylation machinery. No apparent differences could be identified comparing the banding pattern of wildtype and mutant myomesin domains 9-13. Only the mutation of residues K1150A and K1197A of myomesin resulted in the disappearance of the third cluster of bands, most likely due to incomplete transfer of proteins onto the nitrocellulose or a low abundance of the complex and detection limits. Myomesin mutant K1603R showed an additional band in the second cluster, which was not always consistent (compare with panel B). The overall lower molecular weight of the myomesin K1150A and K1150/1197A mutants might be explained due to a changed overall charge of the protein.
B. Comparison of myomesin in vitro sumoylation using Sumo1 and Sumo3. Immunoblot analysis of in vitro-sumoylated myomesin domains 9-13 wildtype and K1589R as well as K1603R mutants using a GST-antibody. No major changes in the banding pattern of myomesin could be observed between Sumo1 and Sumo3. Only the myomesin K1603R mutant showed the appearance of an additional band in Sumo3 modified samples. The third cluster of bands showed as well differences between Sumo1 or Sumo3 modified wildtype, K1589R and K1603R mutants.
C. In vitro sumoylation assay of myomesin domains 9-13 wildtype and the dimerisation-deficiant mutant D1580K. GST-tagged wildtype as well as D1580K myomesin domains 9-13 were subjected to an in vitro sumoylation assay (+) and subsequently blotted alongside a non-sumoylated control (-) onto nitrocellulose membrane. Detection of the GST-tagged proteins using an antibody specific for GST showed no apparent differences between the wildtype and the D1580K dimerisation mutant as judged by the comparable band pattern.

described earlier) and the sumoylation was analysed using a low percentage SDS-gel as well as immunoblot analysis (see figure 15 panel A). Three different clusters of sumoylated bands could be identified. The first cluster contained the single modified protein migrating at around 115kDa (as described above). The second cluster consisted again of two bands, which run around 140 to 145kDa. Due to the low percentage of the gels a third cluster of bands reactive to the GST antibody could sometimes be identified at around 300 to 500kDa. This cluster of bands might represent a SDS-stable complex of myomesin, Sumo and the E2 enzyme, as observed for other ubiquitin and ubiquitin-like proteins (Luders et al., 2003). However, no apparent differences between the wildtype and the single or double mutants were visible upon sumoylation. The third cluster of bands could not be found in the case of the K1150A and K1150/1197A mutant, but this result might be explainable due to the low amount of protein represented by these bands and due to limitations in the detection sensitivity. Another difference was found for the K1603R mutant, which showed the presence of a third band in the second cluster and a general shift of the other two bands within this cluster. The reasons for these shifts are unclear, since this mutant showed comparable results to the wildtype in another sumoylation assay (compare K1603R mutant in figure 15 panel A and panel B).

Figure 15 panel B shows an experiment, which investigates possible differences in the sumoylation pattern of myomesin upon the use of Sumo3 rather than Sumo1. Sumo3 modified myomesin 9-13 showed also up to three different clusters of high molecular weight bands. The first cluster was present in all studied myomesin proteins (wildtype, K1589R and K1603R) modified with Sumo1 or Sumo3 and migrated at approximately the same molecular weight in the gel. The second cluster showed only a difference in the myomesin K1603R mutant upon modification with Sumo3 by the appearance of an additional band at approximately 150kDa. The third cluster of bands at around 300 to 500kDa was present in the Sumo1 modified wildtype and K1589R as well as in the Sumo3 modified K1589R mutant and absent in all other samples. This might again be due to limitations in the detection sensitivity.

Earlier the myomesin dimer mutant D1580K was found to show an impaired binding of myomesin to Ubc9 in a forced yeast two-hybrid experiment (see Table 4). Figure 15 panel C shows an experiment that investigates, whether this impaired binding of the E2 enzyme Ubc9 might be somehow reflected in a change in the sumoylation band-pattern. Apart from a slight shift of the myomesin D1580K mutant compared to the wildtype, which might be explained by the change in the overall charge of the protein, no differences in either the amount of the sumoylated protein nor the band-pattern could be observed.

In summary, we identified two proteins responsible for the posttranslational modification with the small ubiquitin-like modifier Sumo as potential interaction partners for the C-terminal part of myomesin, namely Ubc9 as well as PIAS1. Forced yeast two-hybrid analysis of myomesin truncation constructs as prey and Ubc9, PIAS1 as well as Sumo3 as bait identified domain 9 of myomesin as the minimal binding site for PIAS1, domain 11 of myomesin as an interaction partner for Sumo3 and the dimerisation domain 13 of myomesin as a binding site for Ubc9. Among the very variable and cell state-dependent localisations of Ubc9 and PIAS1, cryo-sections of adult mouse heart ventricle showed

a partial colocalisation of these enzymes with myomesin. Furthermore, upon transfection of tagged constructs into neonatal rat cardiomyocytes the three different Sumo proteins Sumo1, Sumo2 and Sumo3 could be also partially observed in the M-band of the sarcomere. The *in vivo* localisation data indicate that myomesin might be a target protein for this posttranslational modification machinery.

Primary structure analysis of the myomesin protein identified up to nine conserved sumoylation motifs, mainly present in the C-terminus of the protein. *In vitro* sumoylation assays indicated further that myomesin is indeed a target for sumoylation. Although none of the mutants showed a clear deficiency either in the sumoylation efficiency or the band-pattern, a myomesin isoform specific difference in the modification efficiency was observed upon the presence of the EH domain of myomesin.

6.1.4. Interaction of myomesin with the uncharacterised clone 21/39 (MIQ)

One of the most abundant proteins found in the yeast two-hybrid screen as a potential interaction partner for myomesin domains 9-13 was identified as an uncharacterised protein. Several independent clones were identified, coding for partially overlapping regions of this protein (see Table 3). A database search revealed that ESTs for this protein were grouped in the Unigene cluster Hs.181704 Homo sapiens DKFZp451A211. All clones identified coded for the C-terminal 542 or 267 amino acids of the protein. Although it was possible to extend the coding sequence up to 720 amino acid residues by using the DNA sequence from the EST BX647655 derived from human skeletal muscle, it remains unclear whether this clone represents the full-length mRNA. The cDNA sources for ESTs grouped into the Unigene entry for this protein originate from a broad variety of tissue samples, indicating an ubiquitous expression profile. Alignment with human proteins showed that the closest relative with 21% identities is the mucin 1 precursor splice variant A (accession number: A35175), a protein associated with the development and metastasis of cancer in different tissues. Alignment with ESTs from other species show even for sequences derived from mammalian mRNA an identity of only up to 40% for the alignment with the rat γ-aminobutyric acid A receptor (Accession number: NP_075579) or up to 38% for the alignment with the mouse gene cp2.2 (accession number: 1111288A). Figure 16 panel A gives an overview of the most important human ESTs and the clones analysed from the yeast two-hybrid screen. It shows furthermore a primary structure analysis as well as a secondary structure prediction of the peptide sequence.

The intriguing characteristic of the primary protein structure is the appearance of several internal peptide repeats in the N-terminal part of the known protein sequence. The biggest of these repeats with the consensus sequence GWEQTQIETQRQTQKGAQERAWEQGR/WEQ appears twice, the smallest with the sequence QAQXQXQXXXQ (where X is any amino acid) can be found seven times and the peptide sequence and the motif (QA)QKGAQ(ERA(RERA)) can be found 14 times in the amino acid sequence of this protein. This repetitive region is further characterised by the very frequent appearance of the amino acid glutamine (Q), which accounts for 30% of all amino acids in this region of the protein. The secondary structure prediction for this repetitive region indicates a completely α-helical folding. The very C-terminal part of this protein is characterised by a glycine-rich region of 73 amino acids with an overall glycine content of 26% and a smaller proline-rich subregion of 34 amino acids with a proline content of 26%. The secondary structure prediction for this C-terminal part of the protein indicates the formation of a globular domain formed by these two peptide regions.

An analysis of the clones indicated furthermore, that the binding of this protein to myomesin might be mediated by the globular C-terminus of this protein, rather than by the helical N-terminal region.

Searching for known domain patterns and motifs within the protein sequence using the SMART interface (www.smart.embl-heidelberg.de; (Letunic et al., 2004; Schultz et al., 1998)) revealed only a number of low complexity regions, but no known domains or peptide motifs. The identified regions of

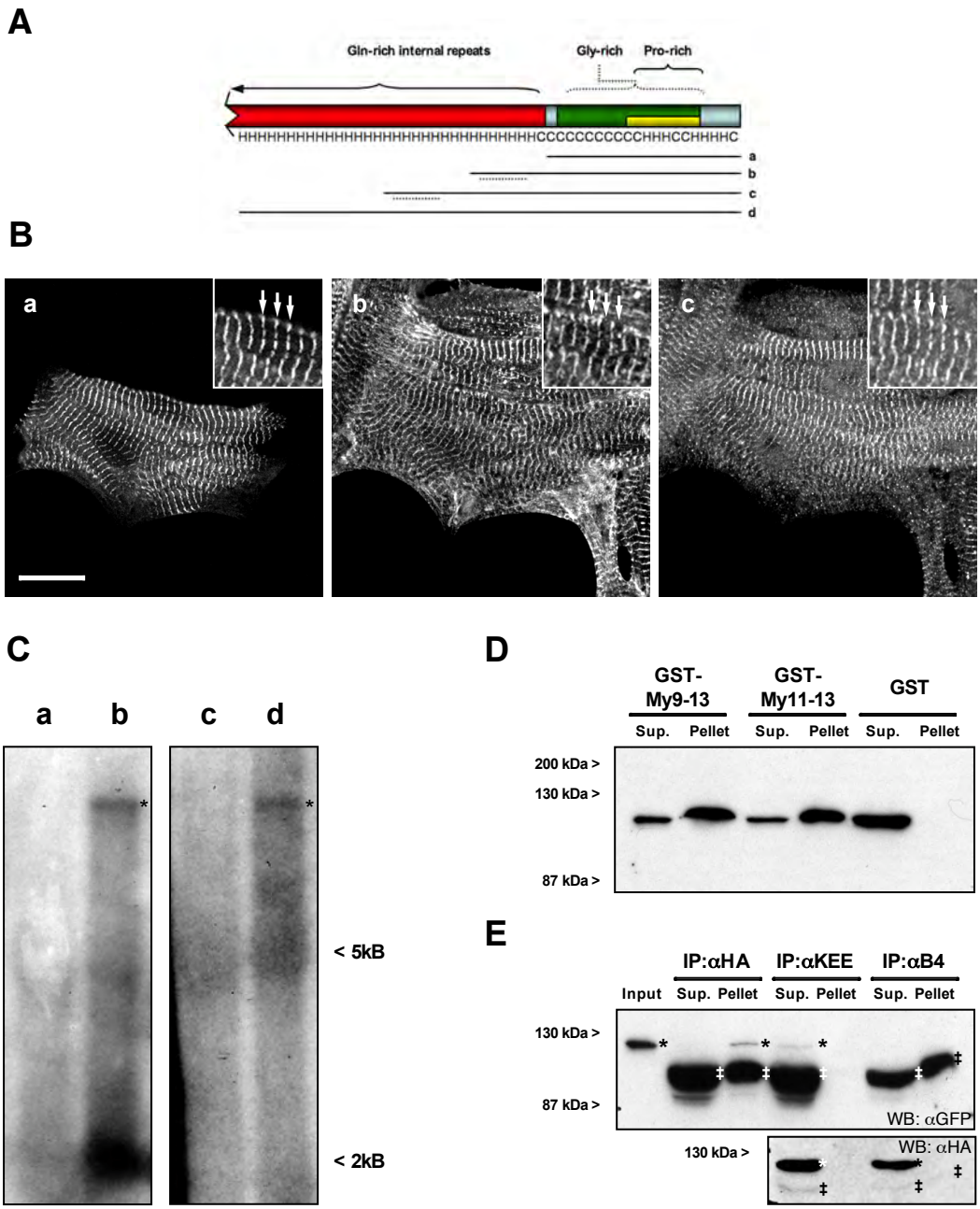

Figure 16. Interaction of myomesin with MIQ (clone 21/39).

A. Schematic representation of the MIQ domain and protein motif layout. Domain layout and secondary structure prediction as well as known ESTs and clones identified in the yeast two-hybrid screen are shown. Accession numbers of identified ESTs: IMAGE clone 4524214 (a) and BX647655 (d). Alignment of clones 21 (b) and clone 39 (c) to the EST clones. Dotted lines indicate regions used for Northern probe generation.

B. Subcellular localisation of MIQ in transiently transfected neonatal rat cardiomyocytes. GFP-tagged MIQ (a) localises to the sarcomeric M-band (arrows) as judged by α-actinin (b) and myomesin (c) counterstain.

C. Northern blot analysis of mouse (a, c) and human (b, d) total cardiac RNA samples. Two different radioactive labelled probes were used in the assay. Probe 21, derived from PCR of clone 21 and probe 39, derived from PCR of clone 39 respectively. (see also dotted lines in A). A band corresponding to about 8kb in size (asterisk) was found in human cardiac RNA.

D. GST-pulldown assay of GFP-labelled MIQ. GST fusion proteins of myomesin domains 9-13 and 11-13 are able to interact with GFP-HA-MIQ, whereas GST alone shows no binding to MIQ.

E. Interaction of MIQ with myomesin domain 11. GFP-tagged myomesin domains 9-13 (‡) coimmunoprecipitated with GFP-HA-tagged MIQ (*) using the HA antibody. Immunoprecipitation with an antibody specific for domain 11 of myomesin (B4) abolished the interaction of myomesin with MIQ (see bottom panel). Immunoprecipitation with an unrelated antibody showed neither unspecific binding for MIQ nor for myomesin domains 9-13.

low complexity are in general characterised as sequences of homo-polymeric runs and other biased amino acid compositions and cover in this case the regions of the peptide repeats. The following chapter analyses the protein encoded by clones 21/39 as well as the putative interaction with myomesin on a cellbiological, genetical as well as biochemical level and provides insights into the functions of this uncharacterised protein.

6.1.4.1. Characterisation of clone 21/39 (MIQ)

Since the protein encoded by clones 21 and 39 of the myomesin domain 9-13 yeast two-hybrid showed no obvious domain structure, and apart from the N-terminal glutamine-rich repeats and the C-terminal glycine and proline-rich regions no other distinguishing features, we tried to assess the subcellular localisation of this protein by subcloning the original yeast two-hybrid clones into the eukaryotic expression vectors pEGFP-C2 to investigate its potential role in M-band function. Neonatal rat cardiomyocytes were transfected with GFP-tagged coding sequence from clone 21 or 39 and stained with antibodies against α-actinin as well as myomesin B4 to reveal the localisation of the GFP-tagged fusion proteins within the sarcomere. Figure 16 panel B shows the subcellular localisation of GFP-tagged clone39 at the region of the sarcomeric M-band (see arrows in blowups). The truncated version of this protein encoded by clone21 showed a comparable localisation also restricted to the M-band of the sarcomere (data not shown), indicating that the minimal binding site for myomesin, which is putatively responsible for the targeting of this protein to the M-band, resides in the C-terminal part of the protein. Only in the case of an overexpression of this fusion protein the localisation pattern changed and the GFP tagged clone21 or clone39 could be observed in the M-band as well as to a lesser extent in the Z-disc of the sarcomere (data not shown).

The intriguing highly repetitive primary structure of the glutamine-rich region as well as the feature that this novel protein is localising almost exclusively to the sarcomeric M-band lead us to name the protein MIQ (an abbrevation for M-band Interacting glutamine rich Protein).

Data derived from the analysis of the sequence data and the alignment with the human genomic sequence indicated that the gene coding for MIQ is located on chromosome 13 in the cytogenetic region 13q34. A Genscan search using about 10Mb of genomic sequence data surrounding the region identified a possible mRNA of about 10kb in size (genes.mit.edu/GENSCAN.html; Burge et al. pp127-163 in (Salzberg, 1998)). Other mRNAs coding for closely related proteins were recently identified using also several gene prediction methods on genomic DNA sequences of canis familiaris (wolves; accession number: XM_534194) and of pan troglodytes (chimpanzees; accession number: XP_522732). A CD-search (www.ncbi.nlm.nih.gov; (Marchler-Bauer and Bryant, 2004)) using conserved peptide sequences of known domains revealed that the N-terminus contained an ADP-ribosylglycohydrolase domain and the C-terminus encoded for a TCB domain (domain in Tre-2, BUB2P, and Cdc16p) as well as a GTPase activating protein domain (COG5210). A blast search for proteins that comprise also an N-terminal ADP-ribosylglycohydrolase domain as well as the C-terminal TBC and GTPase activating protein domain came up with another closely related protein, the rat

LRRGT00052 protein (accession number: AY383707), indicating the possibility that all proteins might be part of a larger protein family.

Since the full-length coding sequence of the uncharacterised protein MIQ, which is partially encoded by clones 21 and 39, was predicted to be about 10kb in size, we performed a Nothern blot assay to determine the size of the mRNA in heart muscle of human and mouse (see figure 16 panel C). Two different probes were used that were derived either from a 308bp sequence in clone 21 or a 236bp sequence in clone 39 of the glutamine-rich region of the protein (see figure 16 panel A dotted lines). Both probes detected a band in the region of 8kb in the total human heart mRNA sample (figure 16 panel C, lanes b and d), whereas no band was found in the total heart mRNA derived from mouse (lanes a and c of the same figure). No other bands were visible in the human sample, indicating the absence of putative splice variants. The fact that no band could be observed in the mouse samples indicates that either the hybridisation conditions were too stringent to perform a cross-species hybridisation, or that the region chosen for hybridisation of the probe is poorly conserved during evolution. The fact that no murine sequence was found during blast searches for homologue proteins and ESTs emphasise the probability of a poorly conserved region of the protein. All clones identified in the yeast two-hybrid contained inserts of only about 4kb including the characteristic 3' poly-A tail of processed mRNAs. This fact and the information that the full-length mRNA is about 8kb in size, as concluded from Northern blot analysis, indicate that a further 4kb of the 5' sequence of the mRNA are still unknown.

A method to clone the unknown 5' sequence of any mRNA is the 5'RACE (or rapid amplification of cDNA ends) assay. This method is based on a RT-PCR reaction using a gene-specific primer and the subsequent addition of a poly T-tag on the 3' end of the newly synthesised cDNA using the terminal deoxynucleutidyl transferase enzyme, allowing the performance of a nested PCR using a mixture of gene specific and adaptor primers and the following ligation of a PCR product to a cloning vector. Although different gene-specific primers were used and the conditions for several reactions were altered during the protocol, no clones were derived encoding for the unknown 5'end of the MIQ mRNA (data not shown). Possible reasons for the failure of the 5'RACE-method to provide the unknown 5'end of the mRNA might be explained with the nature of the glutamine-rich region. With highly repetitive stretches of identical DNA sequences a correct hybridisation of primers and partially synthesised DNA strands seems very unlikely.

6.1.4.2. Interaction of myomesin with clone 21/39 (MIQ)

The minimal binding site for myomesin within the protein sequence of MIQ is probably located in the glycine and proline-rich region of the C-terminal part of the protein. This assumption is based on the sequence comparison of clone 21 and clone 39. Which domain of myomesin mediates binding to this protein and is it possible to validate this binding with biochemical interaction assays?

Two different protein binding assay were used to confirm this interaction biochemically as well as to assess information about the location of the minimal binding site for MIQ in myomesin. Figure 16 panel D shows the result of a GST-pulldown assay using recombinant GST tagged myomesin domains 9-13

as well as a truncation construct comprising domains 11-13 of myomesin. The GFP-HA-tagged fusion protein of clone21/39 bound strongly to both GST-tagged myomesin proteins (domains 9-13 as well as domains 11-13), whereas GST alone did not bind. The pullldown assay indicated a binding site which resides somewhere within domains 11 to 13 of myomesin. The second assay was a co-immunoprecipitation using the cell lysate of transiently co-transfected Cos-1 cells (see figure 16 panel E). A construct encoding for GFP-tagged myomesin domains 9-13 was co-transfected with GFP and HA double-tagged MIQ (clone39). In the first approach, the MIQ GFP-HA-fusion protein was immunoprecipitated using the HA tag. The second lysate sample was immunoprecipitated using an antibody specific for the mT-tag as a control for unspecific binding. The last sample was subjected to an immunoprecipitation with the myomesin B4 antibody, specific for domain 11 of myomesin (Obermann et al., 1996). Whereas HA-precipitated GFP-HA-MIQ was able to retain GFP-tagged myomesin in the pellet fraction, the KEE antibody showed neither an effective precipitation of the GFP-HA tagged MIQ protein nor an interaction with the GFP-tagged myomesin construct. As a surprise came the finding that the myomesin B4 antibody against domain 11 of myomesin was not able to effectively co-immunoprecipitate GFP-HA-tagged clone39 although the fusion protein was present in the lysate (see lower blot) and the immunoprecipitation worked (revealed by the GFP positive band in the pellet fraction of the upper blot in figure 16 panel E). This indicates that myomesin domain 11 is the minimal binding site for the MIQ-protein encoded by clones 21 and 39 and that the binding of the myomesin B4 antibody is highly competitive with this interaction.

6.1.4.3. Search for interaction partners of the novel protein clone 21/39 (MIQ)

The biochemical characterisation of MIQ indicated a strong binding site for the M-band protein myomesin in the C-terminal glycine- and proline-rich region of the protein. The minimal binding site for MIQ in myomesin was mapped to myomesin domain 11 as determined by competitive binding of the myomesin specific B4 antibody as well as myomesin truncation constructs. This interaction might be responsible for the strong M-band localisation of tagged MIQ protein in transfected neonatal rat cardiomyocytes.

Another method to reveal more about the cellular functions of a protein is to search for binding partners. Hence, we established a yeast two-hybrid screen by subcloning the cDNA for MIQ into the pLexA vector and subsequent cotransformation of yeast with the bait vector and a cDNA heart library (prey). Positive clones were selected by growth on selective media lacking the amino-acids histidine, leucine and tryptophane (as described above). The pGAD-10 prey plasmid (see later) was isolated from positive colonies and cDNA inserts were sequenced subsequently. Table 7 gives an overview over the putative binding partners for MIQ (clone39).

Table 7 – Yeast two-hybrid screen on a heart cDNA library using MIQ as bait

Search for novel interaction partners of the MIQ protein (clone39) using the yeast two-hybrid screen method. Yeast cells were transformed with the LexA-MIQ bait plasmid and cDNA library derived from heart mRNA cloned into the pGAD10 prey plasmid and growth on selective media lacking the amino acids histidine, leucine and tryptophane was assayed (as described earlier). BLAST search results using the insert sequences of positive clones recovered from the LexA-MIQ screen are shown. The insert length was determined by PCR with pACT2.fwd and pACT2.rev primers (see later).

clone No.	Acc. Number	BLAST result	insert length (kb)	annotations
1, 3, 4, 6, 7, 8, 10, 12, 15, 20, 23, 27, 40, 41	MYOM1	Myomesin	various, up to 2.5kb	coding region from domain 11 onwards
32	HSMYOLC2	ventricular Myosin light chain 2 mRNA	0.9kb	C-terminal half of the protein
49	NM_000257	Myosin, heavy polypeptide 7, cardiac muscle	0.9kb	C-terminal part of the protein; M-band region

The majority of the clones found in the MIQ yeast two-hybrid encoded for myomesin. Since the interaction of MIQ with myomesin has already been characterised (see earlier) this served as a good positive control that the yeast two-hybrid screen has worked and the bait plasmid was indeed expressing the MIQ protein (clone39) fused to the LexA DNA binding domain. However, an analysis of the myomesin clones indicated that myomesin only interacted when domain 11 was present in the cDNA of the prey plasmid. This result again confirmed the biochemical data obtained from the analysis of the binding of MIQ to myomesin.

Apart from a number of false positive clones encoding for mitochondrial DNA (data not shown), only two other putative interaction partners could be identified in the yeast two-hybrid. Both clones encode for proteins of the sarcomeric thick filament system. The first clone was identified as ventricular myosin light chain 2, which is a regulatory subunit of the thick filament protein myosin and is located in the A-band of the muscle. The second clone encoded for the M-band region of the cardiac isoform 7 of myosin.

The two isolated clones for myosin light chain as well as for myosin heavy chain were tested again for interaction with MIQ in a bait dependency test (forced yeast two-hybrid assay). Only myosin light chain showed a weak interaction, whereas the myosin heavy chain was unable to interact with MIQ, as seen by the absence of yeast clones on selective media.

MIQ interaction with myosin light chain 2 (MLC2)

The myosin light chain protein is the regulatory subunit of the myosin protein. Its function can be modified upon phosphorylation by the myosin light chain kinase (MLCK) as well as by binding of Calcium ions. Via its close association with myosin heads it can regulate the myosin ATPase activity as well as the assembly of the thick filaments in general ((Sachdev et al., 2003); for a review see: (Schiaffino and Reggiani, 1996)). The protein itself is composed of three EF-hand domains, residing at the positions 28 to 56, 97 to 125 as well as 133 to 165 of the 165-residue protein. EF-hands are the major domains responsible for the complexion of calcium ions. The typical EF-hand motif consists of a twelve amino acid residue loop that is flanked on both sides by an α-helix composed of again twelve amino acids. The residues responsible for the complexion of the calcium ion are in positions 1, 3, 5, 7, 9 and an invariant aspartate or glutamate on position 12 (Finn and Forsen, 1995).

The clone identified in the MIQ yeast two-hybrid screen encoded only for the C-terminal 79 residues of the MLC2 protein, indicating that the interaction of MLC2 may be mediated in a Calcium dependent way via the two EF-hand domains residing in this part of the protein.

Within the sarcomere, MLC2 localises like all muscle-specific myosin light chains to the A-band (Auerbach et al., 1997). The fact that GFP-tagged MIQ in transfected neonatal rat cardiomyocytes localises almost exclusively to the sarcomeric M-band, but never to the A-band region of the sarcomere, indicates that the interaction of MLC2 with MIQ might either be very transient or that MLC2 represents a false positive yeast two-hybrid interaction. The slow growth of the yeast in the forced yeast two-hybrid assay of MIQ with MLC2 as well as the slow reaction observed during the β-galactosidase filter lift-off assay (data not shown) points to the conclusion that the interaction might be very transient in nature.

Interaction of MIQ with the cardiac myosin heavy chain

The myosin protein is the major protein of the thick filament system (for a review see: (Cooke, 2004)). Myosin consists of a globular head domain in the N-terminus of the protein and a C-terminal tail domain. The Myosin head consists of three functional parts: an N-terminal myosin SH3-like domain, the ATPase domain, which is the molecular motor domain of myosin as well as an IQ domain responsible for the interaction with Calcium binding proteins, like the myosin light chains (MLC). The tail region of myosin allows assembly of higher order complexes. This function of the tail originates in the ability to form coiled-coil interactions and provides the structural backbone of the myosin molecule. The region of the tail domain of myomesin (also called light meromyosin) also harbours the binding sites for the M-band components myomesin as well as M-protein, which were mapped to the residues 1506 to 1674 in the case of myomesin or to the residues 1512 to 1673 of light meromyosin, respectively (LMM; (Obermann et al., 1997; Obermann et al., 1995; Obermann et al., 1998)).

The clone encoding for the cardiac isoform of myosin heavy chain identified in the yeast two-hybrid screen comprised only of the C-terminal 352 amino acids of this protein, indicating that the binding site for MIQ might be located in the M-band region of myosin.

However, a forced yeast-two hybrid using MIQ as bait as well as the isolated myosin heavy chain clone failed to give raise to colonies able to grow on selective yeast media. Further analysis of the original plasmid sample obtained from the screen indicated the presence of a mixed prey-plasmid population within the original clone (data not shown). Attempts to identify another putative interactor failed, since the second isolated prey-plasmid contained no insert.

In summary, the to date uncharacterised protein MIQ was identified as a new binding partner for myomesin. The clones identified encode probably for the C-terminal half of a protein, whose full-length mRNA in human heart is about 8kb in size. No obvious domains could be identified using the protein sequence encoded by two clones found in the yeast two-hybrid screen. However, the C-terminal glycine- and proline-rich region is the most likely the minimal binding site for myomesin. The N-terminus of the analysed protein fragment encoded for a glutamine rich region with a number of repetitive elements. BLAST search and genetic analysis of human and other genomes indicated the presence of a novel gene in chromosome 13 (location 13q34), which encodes in its 3' sequence the characterised region of this protein. Attempts to clone the missing 5' sequence of this mRNA via 5' RACE using human heart RNA failed.

Transfections of neonatal rat cardiomyocytes using GFP tagged MIQ constructs showed that MIQ targets almost exclusively to sarcomeric M-bands, indicating a strong interaction with a structural element of the sarcomere in the M-line. The biochemical analysis of the interaction of MIQ with myomesin revealed that domain 11 harbours the binding interface with MIQ, since myomesin B4 antibody effectively competes for the binding to the M-band protein. The search for further binding partners of MIQ indicated that two components of the thick filament system, namely the regulatory myosin light chain (MLC2) as well as the M-band region of the cardiac myosin heavy chain (MHC7) are putative interaction partners. Whereas a forced yeast two-hybrid assay verified MLC2 as putative transient binding partner for MIQ, MHC failed to be confirmed. Further analysis of these interaction partners as well as the generation of MIQ specific antibodies might clarify the functions and significance of this protein, as well as of the interactions to myomesin and other structural components of the sarcomere.

6.1.5. Myomesin domain 2-8 yeast two-hybrid screen

After successfully identifying several new interaction partners for the C-terminal immunoglobulin-like domains 9-13 of myomesin, we attempted to search also for novel interaction partners for the N-terminal immunoglobulin-like domain cluster (domains 2 and 3) as well as the central fibronectin-type III domain cluster (domains 4 to 8) of myomesin.

Obermann et al. as well as Hornemann et al. (Hornemann et al., 2003; Obermann et al., 1997; Obermann et al., 1995; Obermann et al., 1998) identified several binding partners, interacting with domains included in this region of myomesin. Myomesin domains 3 to 8 are thought to harbour a binding site for M-protein domains 7 and 8 and the central region of myomesin (domains 4 to 6) seem to comprise an interaction site for titin domain M4. Myomesin is, like DRAL (see below), also interacting with enzymes of the energy metabolism. The muscle isoform of Creatin kinase (MMCK) was reported to interact with the last two fibronectin-type III domains (domain 7 and 8) of myomesin. MMCK plays an important part in the regulation and stability of the intracellular energy metabolism by replenishing ATP from phosphocreatine (Wallimann et al., 1992). Besides a cytoplasmic pool of this enzyme, some MMCK is compartmentalised to the sarcomere via three different interaction partners: DRAL (see below; (Lange et al., 2002)), myomesin and M-protein (Hornemann et al., 2003).

However, no interaction partners for the first cluster of myomesin immunoglobulin-like domains are described in the litreature, although localisation data of GFP-tagged myomesin truncation constructs suggest that myomesin domain 2 may harbour a M-band targeting site (Auerbach et al., 1999). This M-band targeting by domain 2 is most likely due to an interaction with another M-band component. Attempts to search for an interaction partner using domain 2 alone or the cluster of domains 2 to 3 as a bait in a yeast two-hybrid screen failed, due to autoactivation and growth on selective media also in the absence of the prey plasmid (pers. comm. with Dr. D. Auerbach).

To avoid these problems and minimise the risk of autoactivation, the bait plasmid used in this yeast two-hybrid screen was designed to comprise of the human myomesin domains 2 to 8.

A total number of $1.8*10^7$ clones were screened, which gave rise to about 106 positive large to middle sized clones that grew on selective media lacking the amino-acids histidine, leucine and tryptophane and were positive in the β-galactosidase filter lift-off assay. Table 8 comprises an overview over the result of the yeast two-hybrid screen.

Table 8 – Yeast two-hybrid screen on a heart cDNA library using myomesin domains 2-8 as bait

Search for novel interaction partners of human myomesin domains 2-8 using the yeast two-hybrid screen method. Yeast cells were transformed with the LexA-hMy2-8 bait plasmid and a cDNA library derived from heart mRNA cloned into the pAct2 prey plasmid and growth on selective media lacking the amino acids histidine, leucine and tryptophane was assayed (as described earlier). BLAST search results using the insert sequences of positive clones recovered from the LexA-hMy2-8 screen are shown. The insert length was determined by PCR with pACT2.fwd and pACT2.rev primers (see later).

clone No.	Acc. Number	BLAST result	insert length (kb)	annotations
1.1	XM_051091, AB017814	KIAA1040 protein, mRNA for SF20 protein	3kb	C-terminal half of the coding sequence
1.2, 3-9, 10-16, 18-28, 35, 36	**NM_001824**	**muscle isoform of creatine kinase**	**1.8kb**	**full-length coding sequence**
32	AF151075, NM_016497	HSPC241, mitochondrial ribosomal protein L51	0.9kb	full-length coding sequence
50	NM_005346	heat shock protein 70kDa	2.5kb	C-terminal part of the protein, starts after ATP binding site in protein

About 90% of the analysed colonies encoded for the muscle isoform of creatine kinase (MMCK). MMCK has been shown recently to interact with myomesin domains 7 to 8 as well as with domains 6 to 8 of M-protein (Hornemann et al., 2003). Interestingly, a strong pH dependence of this interaction was observed with higher Kd values for a more acidic pH. The sequence analysis of the inserts revealed that all clones identified encoded for the full-length coding sequence of MMCK. This observation is supported by reports showing that four lysine residues, crucial for the mediation of the interaction with myomesin reside in the N-terminal part of MMCK, namely K8, K24, K104 as well as K115 (Stolz and Wallimann, 1998).

Since the interaction of myomesin with MMCK was recently already studied thoroughly, no further emphasis was laid on the biochemical analysis of this binding partner.

All other putative binding partners were subjected to a forced yeast two-hybrid analysis (as described earlier). None of the co-transformed clones gave rise to yeast that grew on selective media. This suggests that all other identified putative binding partners for the N-terminal and central part of myomesin, are probably false positive interactions. In fact, in the case of clone 1 of the yeast two-hybrid screen a mixed population of two different prey plasmids was present in the original DNA sample extracted from the yeast clone. One plasmid encoding for the SF20 protein (clone 1.1) turned

out to be a false positive. However, the original yeast clone derived its initial ability to survive the selection process by the presence of another prey plasmid (clone1.2), encoding for MMCK.

In summary we confirmed that the central part of myomesin mediates the interaction of myomesin with the muscle isoform of creatine kinase (MMCK). No other binding partners for this region of the protein could be identified in the yeast two-hybrid screen. The initial three other putative interacting proteins turned out to be false positive clones, most likely due to the presence of a mixed population of prey plasmids within the selected yeast clones as demonstrated for clone 1. The overwhelming majority of clones positive for MMCK might on the one hand reflect the *in vivo* situation, where MMCK is reported to be an abundant mRNA message in heart cells (Trask and Billadello, 1990). On the other hand, this abundance of the MMCK message might mask other interactors, which have a lower copy number and hence are fewer represented in the used heart cDNA library. No interaction could be found which might explain the sarcomeric M-band targeting of domain 2 of myomesin. This might be due to the fact that a hetero-dimeric complex of the M-band parts of myosin and titin mediates the targeting of this domain. Since the yeast two-hybrid system was initially developed to search for direct protein-protein interactions an interaction involving a trimeric complex of myomesin, titin and myosin cannot be observed. The use of a yeast tri-hybrid system as well as the truncation of the bait constructs for the MMCK binding domains 7 and 8 of myomesin might facilitate the future search for novel binding partners of the N-terminal part of the protein.

6.2. The four and a half LIM-domain protein DRAL

Protein-protein interactions play a pivotal role in many biological processes. Domains which are thought to act primarily as mediators of protein-protein interactions are the LIM domains (Schmeichel and Beckerle, 1994). A growing family of LIM only domain proteins possess four and a half LIM domains, hence the name FHL protein family (four and a half LIM). Members of this family are the FHL1 (SLIM1, KyoT) protein as well as splice variants (e.g. KyoT2; (Taniguchi et al., 1998)), FHL2 (DRAL, SLIM3), FHL3 (SLIM2), FHL4, FHL5, the ACT protein and ARA55/hic5 (for a review see: (Kadrmas and Beckerle, 2004; Mistry et al., 2004)). Although the FHL1 protein shows an ubiquitous expression in a variety of tissues, one characteristic feature of all other protein family members is their tissue and developmental stage specific expression pattern. Because of their domain structure, they were implicated in the mediation of a broad variety of protein-protein interactions.

DRAL (FHL2) is a four and a half LIM domain protein that was specifically identified as being downregulated in a rhabdosarcoma cell line (hence the name DRAL, for downregulated rhabdosarcoma LIM protein) and was subsequently shown to be highly expressed in the heart (Chan et al., 1998; Scholl et al., 2000). In primary cultures of neonatal rat cardiomyocytes, DRAL shows a cross-striated localisation pattern with a weaker staining of the M-band and a more prominent, broader localisation around the region of the Z-disc. In order to identify potential interaction partners for DRAL, a yeast two-hybrid screen was performed in collaboration with Dr. Patricia McLoughlin that resulted in the identification of the M-band insertion sequence 2 (is2) of titin, the muscle isoform of creatine kinase (MMCK) and the promyelocytic leukaemia zinc finger protein (PLZF) protein.

The following paragraphs investigate the sarcomeric localisation and targeting of the DRAL protein in cross-striated muscle cells by immunocytochemical and biochemical methods and places an emphasis on the putative crosstalk of DRAL with various muscle signalling pathways.

6.2.1. Expression and localisation pattern of DRAL

DRAL was first cloned from a fetal cardiac muscle library (Morgan and Madgwick, 1996) and was later found in several northern blot analysis to have a tissue specific expression pattern in the heart, testis and ovary and lung as well as to a lower extent in placenta, uterus, stomach and skeletal muscles (Chan et al., 1998; Scholl et al., 2000).

In order to investigate the expression level of DRAL at the protein level, immunoblot analysis of cardiac as well as fast- (tibialis anterior) and slow-twitch (soleus) muscle samples using a polyclonal antibody directed against DRAL/FHL2 were performed. Contradictory to the published Northern blot results, no DRAL expression was detected in fast- or slow-twitch skeletal muscles. However, a strong signal around 34kDa was apparent in mouse cardiac muscle samples, which corresponds well with the calculated molecular weight of the protein (see figure 17 panel A). We also analysed the developmental expression pattern of DRAL in cardiac muscle from early embryonic stages to

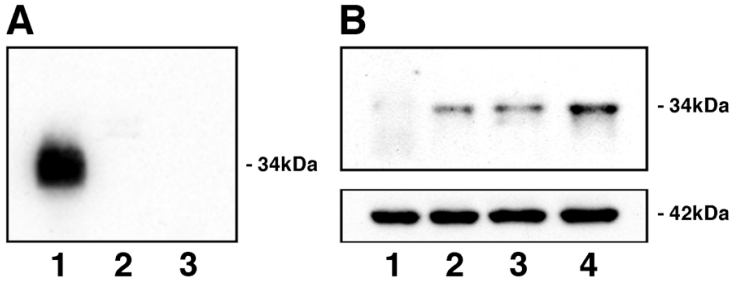

Figure 17. Expression pattern of DRAL in cardiac and skeletal muscle.
A. DRAL is expressed only in cardiac muscle (ventricle, lane 1), but is absent in samples of either fast-twitch skeletal muscle (tibialis anterior, lane 2) or slow-twitch skeletal muscle (soleus, lane 3) of adult mice. The band of around 34kDa corresponds to the calculated molecular weight of the DRAL protein.
B. DRAL expression is developmentally regulated in fetal mouse hearts. Immunoblots of whole heart samples of E12.5 (lane 1), E16.5 (lane 2), E18.5 (lane 3) and P0 (lane 4) reacted with a polyclonal rabbit anti DRAL antibody and show that DRAL is expressed in cardiomyocytes during late embryonic development (upper panel). Equal amounts of heart muscle tissue were loaded, as judged by the expression of α-cardiac actin (bottom panel)

adulthood (see figure 17 panel B). Very weak expression of DRAL was first detected at the embryonic stage E12.5 and increased up to postnatal stage P0. The same immunoblot was reprobed with an antibody specific for α-cardiac actin to demonstrate that the increase in DRAL expression level is not due to differences in the number of differentiated cardiomyocytes in the extracts. Whereas α-cardiac actin expression levels remained unchanged, DRAL was found to be highly upregulated during late embryonic development. Interestingly, two other family members of the four and a half LIM domain family FHL4 and ACT as well as a putative interaction partner of DRAL, namely MMCK are also developmentally upregulated (Carlsson et al., 1990; Fimia et al., 2000).

Thus, results from earlier reports were confirmed, which showed significant expression of DRAL only in heart, but not in any other type of cross-striated muscle. In addition, DRAL is expressed comparatively late during fetal heart development, at a time when contracting myofibrils have already been formed, and is only upregulated significantly during postnatal muscle development.

Initial studies have shown that ectopically expressed DRAL as well as endogenous DRAL is localised in a cross-striated pattern at two distinct sites in sarcomeres. DRAL localises in broad striations around the Z-disc and in fainter stripes at the M-band region (Scholl et al., 2000). In order to precisely pinpoint the region near the sarcomeric Z-disc where DRAL is bound, double labeling experiments with antibodies directed against different Z-disc and I-band epitopes of the giant protein titin were performed. The epitopes recognised by the antibodies are the T12 epitope, located at the outer edge of the Z-disc region of titin, the N2B, N2A as well as the 9D10 epitope, located in the I-band region of titin (see figure 18 panel A). The signal of DRAL was compared with the signals of the different titin epitopes observed in myofibrils of different states of contraction (see figure 18 panel B). In relaxed sarcomeres, DRAL was consistently found as a narrow doublet flanking the Z-disc and in

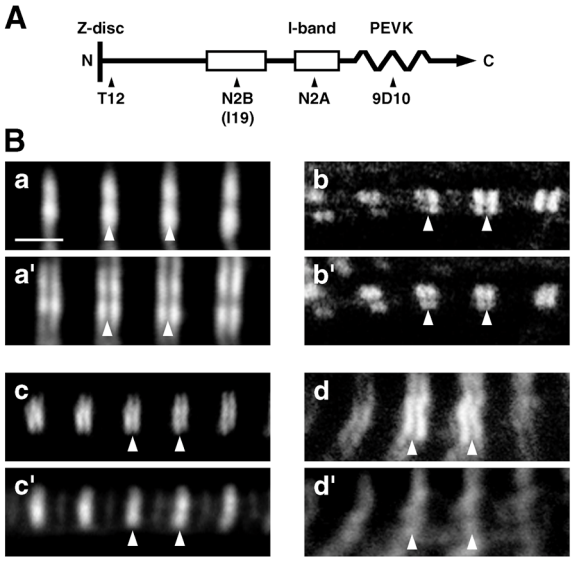

Figure 18. Co-localisation of DRAL with the N2B-region of titin.
A. Schematic representation of antibody epitopes in correspondence to the Z-disc and I-band domain layout of cardiac titin.
B. Mapping of the DRAL targeting location in the sarcomeric I-band. Cardiac myofibrils from papillary muscle (a, b, c) or neonatal rat cardiomyocytes (d) were stained with an antibody directed against DRAL (a', b', c', d'), together with antibodies directed against the N-terminus of titin (T12 epitope, a), the N2B-region (I19 epitope, b), the N2A-region (c) and against the PEVK region (9D10 epitope, d). DRAL colocalises with the N2B-region, but not with any other of the investigated regions of titin. Arrowheads indicate the center of the Z-disc. Bar = 2um.

very faint striations at the M-band (figure 18 panel B, c'). In contrast the titin T12 epitope marking the outer edges of the sarcomeric Z-disc could not be resolved into a doublet. Comparison of DRAL localisation with three other epitopes of titin showed that DRAL colocalised with the N2B-region of titin independently of the state of the muscle contraction, whereas the titin N2B as well as the PEVK region (recognised by the 9D10 antibody) were always located further towards the M-band of the sarcomere compared with DRAL. These results suggested that DRAL is bound at or very near the N2B-region of cardiac titin.

6.2.2. Identification of DRAL binding partners by yeast two-hybrid assay

The sarcomeric localisation of DRAL around the sarcomeric Z-disc and at the M-band cannot be explained by any of its interaction partners that have been identified so far. For this reason, a yeast two-hybrid screen (see also above) was carried out in order to identify sarcomeric interaction partners that might explain the targeting of DRAL to these two distinct sites within the sarcomere. Full-length human DRAL was used to screen an adult human cardiac cDNA library. Out of $1*10^7$ primary transformants, 200 clones were isolated that grew on selective media and were positive in a β-galactosidase assay (see table 9). Of these, one clone encoded for the titin is2 region located in the

M-band of the sarcomere (Labeit and Kolmerer, 1995) and five clones comprised the entire open reading frame of the muscle isoform of creatine kinase (MMCK; (Ordahl et al., 1984; Wallimann et al., 1992)).

Table 9 – Yeast two hybrid screen results – putative interaction partners of DRAL

BLAST results of positive clones recovered in the yeast two-hybrid screen using human DRAL as bait and a human cardiac library as prey (carried out by Dr. P. McLoughlin from the University of Zurich). Shown is a selection of positive clones. For the complete list of clones please refer to PD Dr. Beat Schäfer at the University children's Hospital in Zurich.

putative binding partner	number of clones
PLZF	1
MMCK	5
titin is2 region	1
SERCA	1
phospholamban	1
myosin binding protein-C3	1
myosin heavy chain 7	1
CARP (cardiac Ankyrin repeat protein)	1
myomesin	1
α-tropomyosin	1
myosin light chains (various isoforms)	5
muscle pyruvate kinase	1
PRELP	2
EMMPRIN	1

The interaction of DRAL with the is2 region of titin and with MMCK was subsequently tested in a bait dependency test (forced yeast two-hybrid) and gave rise to clones that grew on selective media, indicating a robust interaction.

No clones were isolated in the yeast two-hybrid screen that could explain the localisation of DRAL to the I-band of the sarcomere. Although the localisation pattern of MMCK displays also a dual targeting of this enzyme to the sarcomeric I-band as well as to the sarcomeric M-band, the intensity of the MMCK staining at these two sites did not resemble the observed DRAL localisation. MMCK has been found to stain the region of the sarcomeric M-band to a much greater extent than DRAL, whereas its I-band localisation displays a somewhat weaker staining compared to DRAL. Since DRAL colocalised exactly with the N2B-region of titin, we reasoned that it might be bound to this part of titin. The direct interaction of DRAL with titin N2B was investigated in a forced yeast two-hybrid assay. The entire N2B-region of titin interacts strongly and specifically with DRAL (see table 10).

In summary, the yeast two-hybrid data demonstrate an interaction of DRAL with the is2 and N2B-regions of titin, and with the metabolic enzyme MMCK. The previously observed sarcomeric dual-localisation pattern of DRAL in muscle fibres may originate from the targeting of DRAL to these two distinct regions in the titin protein.

Table 10 – Forced yeast two-hybrid analysis – interaction partners of DRAL

Yeast two-hybrid screen results using human DRAL as bait and a human cardiac library as prey (in collaboration with Dr. P. McLoughlin from the University of Zurich) as well as a forced yeast two-hybrid analysis of the interaction of DRAL with the N2B-region of human cardiac titin (in collaboration with Dr. D. Auerbach, Dualsystems AG, Switzerland). Yeast cells were transformed with the indicated bait and prey plasmids and growth on selective media lacking the amino acids histidine, leucine and tryptophane was assayed (as described earlier). Growth and strength of interaction are shown for the forced yeast two-hybrid assay.

Transformed yeast two-hybrid constructs		
	pLexA	pLexA-DRAL
Gal4AD-N2B	-	+++
Gal4AD	-	-

6.2.3. Cell biological and biochemical analysis of the DRAL interactions with titin

6.2.3.1. DRAL interacts with the N2B and the is2 region of cardiac titin

Three different proteins identified in the yeast two-hybrid screen or in the forced yeast-two hybrid analysis have been identified as putative binding partners of DRAL: the muscle isoform of the creatine kinase (MMCK) as well as two distinct regions in the giant protein titin. The titin M-band region is2 was found in the yeast two-hybrid screen. The I-band N2B-region of cardiac titin, which was previously identified via colocalisation studies using different titin epitopes and DRAL on stretched muscle fibres as well as in a forced yeast two-hybrid analysis.

These putative interaction partners for DRAL were confirmed and further analysed by transfection experiments using neonatal rat cardiomyocytes as well as with biochemical protein-protein interaction assays, like the GST-pulldown method or the co-immunoprecipitation.

Primary cultures of neonatal rat cardiomyocytes were cotransfected with constructs encoding FLAG tagged DRAL in combination with GFP-tagged titin is2 or titin N2B segments. In cotransfected cardiomyocytes, an identical localisation pattern for DRAL as well as the cotransfected I-band and M-band regions of titin was found: a doublet flanking the Z-disc in addition to a weaker striation at the M-band of the sarcomere (see figure 19). The finding that exogenously expressed N2B was also

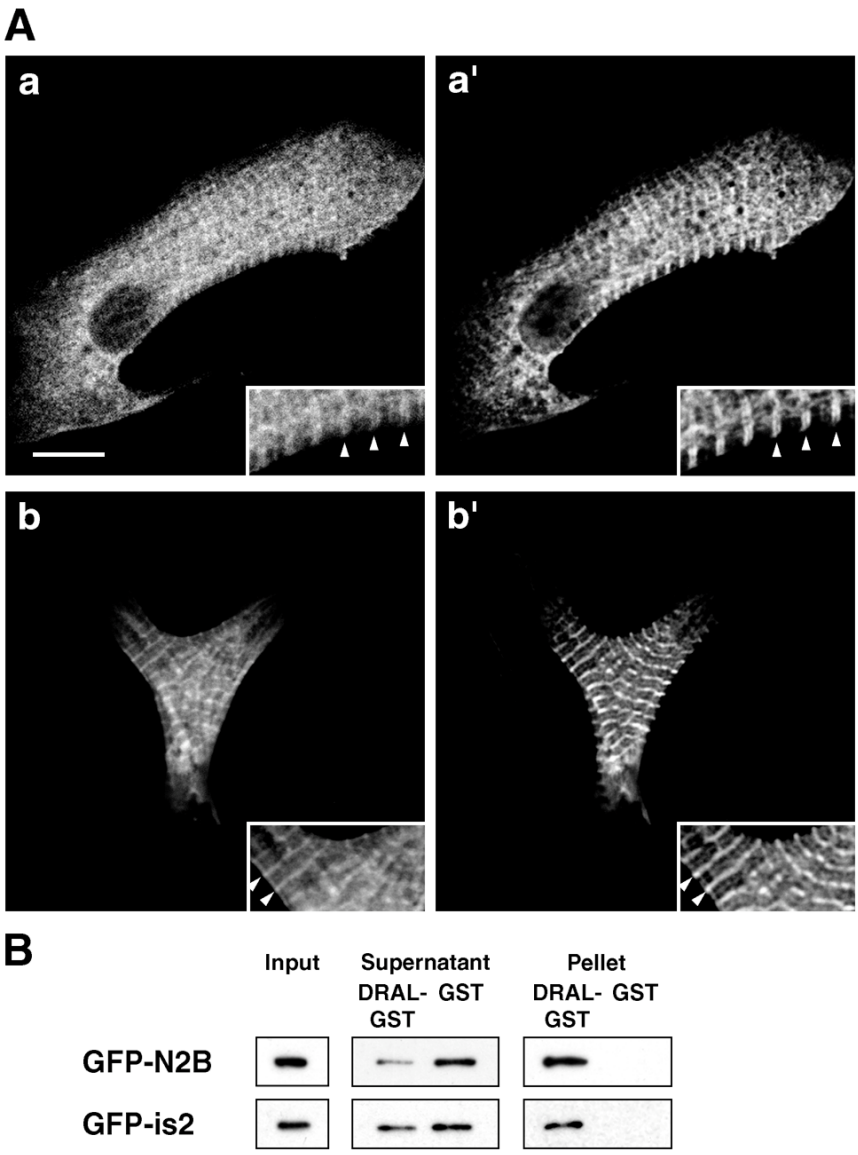

Figure 19. Confirmation of the interaction between DRAL and the domains N2B and is2 of cardiac titin by colocalisation and GST-pulldown assays.
A. Transient cotransfection assays of neonatal rat cardiomyocytes. GFP-N2B (a) and DRAL-FLAG (a') or GFP-is2 (b) and DRAL-FLAG (b') are localised in a similar pattern in transiently transfected NRC, with a broad doublet flanking the Z-disc (arrowheads) and a weaker striation at the M-band. Scalebar = 10µm.
B. Pulldown assay: GFP-N2B and GFP-is2 interact with DRAL-GST, but not with GST alone. Proteins in the input, the supernatant and pellet fractions were detected by immunoblotting using a GFP antibody.

localised at the M-band, whereas the is2 region was also found in a doublet flanking the Z-disc strongly suggests that these fragments are targeted to the sites by means of their interaction with DRAL (figure 19 panel A). These results were biochemically confirmed using a GST-pulldown experiment utilising a recombinantly expressed fusion protein of GST and DRAL and exogenously expressed GFP-tagged titin is2 as well as titin N2B-region (figure 19 panel B). As a control, GST alone was incubated with the cell lysates containing the GFP-tagged is2 region as well as the GFP-tagged N2B-region of cardiac titin. The specific interaction of the titin fragments with the GST-DRAL fusion protein, but the lack of binding to GST alone confirmed the observed colocalisation experiments in transfected neonatal rat cardiomyocytes and suggests that DRAL might be targeted to these sites in the sarcomere by a direct interaction with the N2B and the is2 regions of titin, respectively.

The N2B-region of titin contains a N-terminal and C-terminal block of immunoglobulin-like domains interrupted by the occurrence of two unique sequences us2 and us3 (figure 20 panel A). In order to determine the minimal binding site for DRAL, several deletion constructs were established and assayed with GST-pulldown and co-immunoprecipitation experiments for the interaction with DRAL (figure 20 panel B and D). GFP-N2BΔ1, which lacks the complete set of the C-terminal immunoglobulin-like domains as well as GFPN2BΔ2, which in addition is also C-terminally truncated for half of the large unique sequence 3, were still capable of binding to DRAL. However, further deletion of the unique sequence 3 by 270 amino acids (GFP-N2BΔ3) and a construct encoding only for the C-terminal Immunoglobulin like domains of this titin fragment (GFP-N2BΔ4) completely abolished the interaction of DRAL and N2B. These results suggest that a central 270 amino acid fragment located within the unique sequence 3 of the N2B-region mediates the interaction of DRAL with this I-band part of titin. To investigate this putative binding site more closely, we created an additional construct, GFP-N2BΔ5, which comprises amino acids 3750 to 4019 of cardiac titin. This minimal binding fragment displays upon cotransfection in neonatal rat cardiomyocytes almost an indistinguishable localisation pattern compared to DRAL and the full-length N2B-region of titin (figure 20 panel C). Additional proof for a direct interaction between DRAL and the 270 amino acid fragment of the unique sequence 3 of cardiac titin was provided by assaying Cos cells that were transiently transfected with DRAL-FLAG and GFP-N2BΔ5. Following immunoprecipitation with an anti-FLAG antibody, GFP-N2BΔ5 could be detected in the pellet fraction by immunoblot using anti GFP-antibodies, confirming the stable interaction of these proteins *in vivo* (figure 20 panel D).

In summary, the colocalisation and biochemical protein-protein interaction experiments confirm the direct interaction of DRAL with two distinct protein domains in the giant protein titin. These results strongly suggest that the observed characteristic dual localisation pattern of DRAL within myofibrils originates from the direct targeting of DRAL to the N2B as well as the is2 fragment within the titin protein.

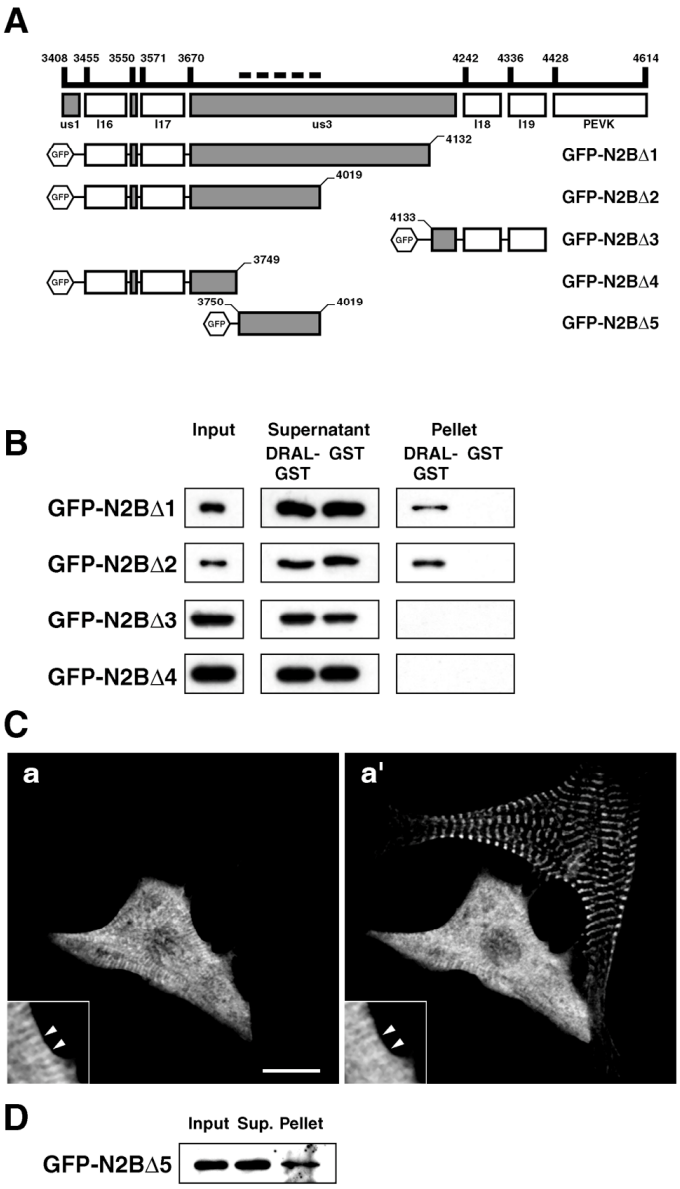

Figure 20. Mapping of the DRAL-binding site in the N2B region of cardiac titin.
Five different GFP tagged deletion constructs of the N2B region were assayed for their interaction with DRAL in pulldown assays.
A. Schematic representation of the employed constructs used. The amino-acid notation refers to the human cardiac N2B titin splice variant (Accession number: X90568).
B. Investigation of the interaction between different deletion constructs of the N2B region and DRAL by a GST-pulldown assay. Only constructs that contain the residues 3749 to 4019 of the unique sequence 3 are able to bind to DRAL-GST. The putative DRAL-binding site is indicated by a dashed line in the schematic drawing of the titin N2B region.
C. The putative DRAL-binding site alone shows proper targeting to the sarcomere, as shown in NRC double-transfection experiments using GFP-N2BΔ5 (a) and DRAL-FLAG (a'). Arrowheads in the insets indicate the region of the Z-disc. Scalebar = 10µm.
D. Co-immunoprecipitation of GFP-N2BΔ5 and DRAL-FLAG. Cos cells were cotransfected with GFP-N2BΔ5 and DRAL-FLAG, immunoprecipitation was carried out with a monoclonal anti-FLAG antibody followed by immunoblotting with a peroxidase-conjugated polyclonal rabbit anti GFP antibody.

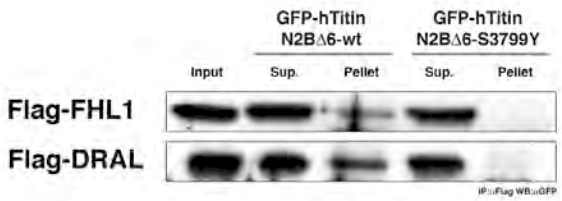

Figure 21. DRAL and FHL1 associate to wildtype, but not to the S3799Y mutant of the cardiac titin N2B-region.
Co-immunoprecipitation of Flag-tagged DRAL and FHL1 with GFP tagged human cardiac titin N2B. Cos-cells were cotransfected with GFP-N2BΔ6 wildtype or S3799Y mutant and either Flag-tagged DRAL or Flag-tagged FHL1. Co-immunoprecipitation was carried out with a monoclonal anti-Flag antibody, followed by immunoblotting and detection of the GFP-fusion protein with an antibody specific for GFP.
Whereas DRAL or FHL1 show a strong association to the wildtype titin N2B-region, the mutation of serine 3799 to tyrosine largely abolishes the interaction of the FHL proteins.

6.2.3.2. A mutation in the N2B-region abolishes DRAL and FHL-1 interaction

The functions of the giant protein titin are thought to range from its role as a key regulator for sarcomeric assembly, the preservation of sarcomeric alignment to the maintenance of the sarcomere (Au, 2004; Maruyama, 1997; Tskhovrebova and Trinick, 2003). The protein stretches from the Z-disk to the M-band (Labeit and Kolmerer, 1995), providing spatially distinct binding sites for a multitude of proteins and thereby acting in a sarcomeric-ruler function. The ligands for titin include proteins involved in the structural assembly of the sarcomere, like α-actinin, the proteins of the myomesin-family, myosin and filamentous actin as well as scaffolding and adaptor proteins like the proteins of the FHL-domain protein family, Calpain, the Murf proteins, NBR1 or telethonin (see below). Via its C-terminal kinase domain, titin is thought to be involved in a muscle-specific signalling cascade (see below), modulating actively differentiation and muscle-specific development as well as sarcomeric maintenance (Mayans et al., 1998).

Recent publications indicate that several mutations in the titin protein are linked to the development of several myopathy-forms (Gerull et al., 2002; Hackman et al., 2002; Hein and Schaper, 2002; Itoh-Satoh et al., 2002), like the development of dilated cardiomyopathy (DCM), hypertrophic cardiomyopathy (HCM) or the tibial muscular dystrophy (TMD). One mutation, which is located at the DRAL-binding site within the titin N2B-region is the replacement of serine 3799 with a tyrosine residue and is thought to be the cause of a hypertrophic cardiomoypathy (HCM) phenotype in human patients (Itoh-Satoh et al., 2002). To investigate, whether this mutation influences the association with DRAL or another member of the FHL protein family, the ubiquitously expressed FHL-1, we established a co-immunoprecipitation experiment, comparing DRAL and FHL-1 affinity to the wildtype as well as to the S3799Y mutation of the cardiac N2B-region of titin. Figure 21 clearly displays that the mutation of serine to tyrosine at position 3799 of cardiac titin largely abolishes the interaction to DRAL or FHL1, indicating that DRAL mediated anchorage of non-sarcomeric binding partners to the sarcomere (see below) may be largely disturbed in these patients.

In summary, the S3799Y HCM disease mutation in human patients is associated with a disturbed binding of FHL protein family members to the N2B-region of cardiac titin. The largely abolished interaction of DRAL or FHL-1 with the mutated titin suggests that FHL mediated binding of other interaction partners to the sarcomere may be reduced. DRAL mediates anchorage of metabolic enzymes to the sarcomere and the influence of DRAL on signalling pathways e.g. the steroid receptor as well as the Wnt-signalling pathway (see below) may be altered in humans carrying this titin mutation, which leads ultimately to the outbreak of hypertrophic cardiomyopathy.

6.2.4. Interaction of DRAL with metabolic enzymes

The metabolic enzyme MMCK was identified five times in the yeast two-hybrid screen. MMCK is a predominantly cytoplasmatic enzyme with a fraction of the enzyme targeted to two distinct sites in the sarcomere: near the M-band as well as in a doublet surrounding the Z-disc (Schafer and Perriard, 1988; Wallimann et al., 1992; Wegmann et al., 1992). In order to investigate the putative interaction of MMCK with DRAL, we studied the subcellular localisation of FLAG-tagged DRAL as well as GFP-tagged MMCK in cotransfected neonatal rat cardiomyocytes. Both proteins were found in a doublet flanking the Z-disc and at the sarcomeric M-band (see figure 22 panel A), indicating that DRAL might target MMCK to these two distinct sites within the sarcomere. However, while there was less DRAL present at the M-band compared to the I-band of the sarcomere, MMCK showed an almost identical signal intensity at both sites. This suggested that the interaction of MMCK with the M-band might not be exclusively mediated by DRAL, but that this enzyme contains also a binding site for another M-band component of the sarcomere. In an earlier chapter, it was shown that myomesin as well as M-protein are also binding partners of MMCK (see also: (Hornemann et al., 2003)). The occurrence of three different binding partners for MMCK in the region of the sarcomeric M-band might explain the increased targeting rate of this enzyme to the M-band of the sarcomere.

Two other metabolic enzymes, the adenylate kinase (AK) and the phosphofructokinase (PFK), are also found in the M-band and, depending on buffer conditions used for fixation, in the I-band as well (Dolken et al., 1975; Kraft et al., 2000). We therefore asked, whether those proteins may owe their localisation in the sarcomere to an interaction with DRAL, too. Two different approaches were used to confirm the putative targeting of these two enzymes to the sarcomere via an interaction with DRAL: a co-transfection experiment focussing on the subcellular localisation of AK and PFK in comparison with DRAL as well as a biochemical protein-protein interaction experiments using recombinant GST-DRAL.

Adenylate kinase as well as phophofructokinase were found in a doublet flanking the Z-disc and in a single stripe at the M-band (figure 22 panel A). Superposition showed that both proteins colocalised with DRAL. Thus, MMCK, AK as well as PFK are all located at the same sarcomeric sites flanking the Z-disc and the M-band together with DRAL.

To investigate wether the colocalisation of the three metabolic enzymes is due to their direct interaction with DRAL, we performed *in vitro* pulldown assays (as described earlier). GST-DRAL was

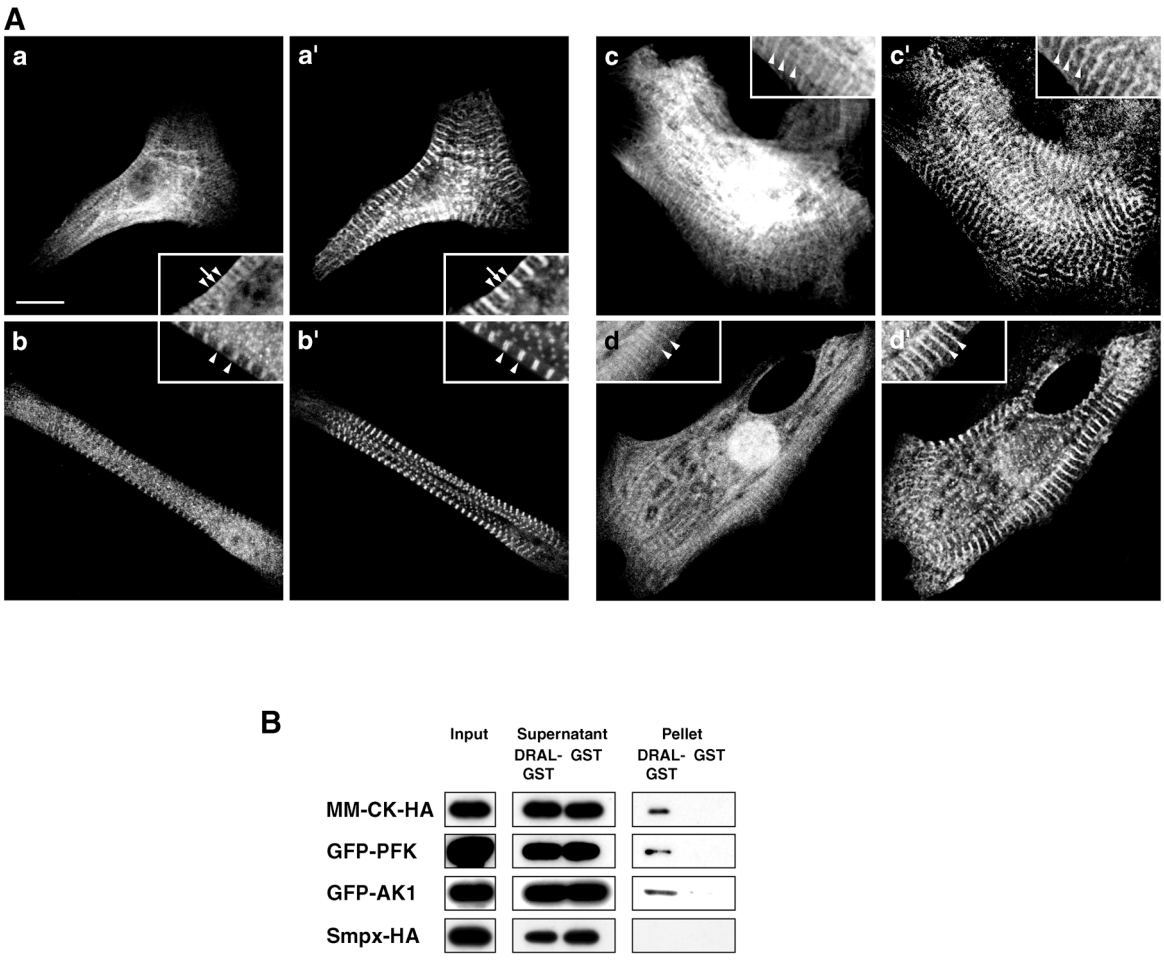

Figure 22. DRAL interacts with several enzymes of the energy metabolism.
A.Transient transfection assays of GFP-tagged MMCK (a), phosphofructokinase (b), adenylate kinase (c), the small muscle protein SMPX (d) as well as DRAL-FLAG (a', b', c', d') in neonatal rat cardiomyocytes. MMCK, PFK, AK and SMPX colocalise with DRAL in a broad striation flanking the Z-disc (arrowhead in insets) as well as in a fainter striation at the region of the sarcomeric M-band (arrows in the insets). Scalebar = 10µm.
B. Interaction of metabolic enzymes with DRAL in pulldown assays using DRAL-GST or GST. Only GFP-MMCK, GFP-PFK as well as GFP-AK were retained in the pellet fraction of GST-DRAL after washing, whereas GST alone showed no bands reactive to the GFP-antibody, indicating the specificity of the interaction. SMPX was unable to bind to GST as well as to DRAL-GST in the pulldown assay.
Abbrevations: AK: adenylate kinase; PFK: phosphofructokinase; MMCK: muscle isoform of creatine kinase; SMPX: small muscle protein X (also known as Csl).

incubated with lysates of Cos1 cells expressing GFP-tagged MMCK, AK as well as PFK. As a control to monitor any unspecific binding, GST alone was used. As shown in figure 22 panel B, all three enzymes interacted with GST-DRAL, but not with GST, confirming an interaction of DRAL with MMCK, AK as well as PFK. A recently identified protein showing a similar subcellular localisation in cross striated muscle cells is SMPX (Csl; (Kemp et al., 2001; Palmer et al., 2001)), which interacted neither with GST-DRAL nor with GST alone, confirming the specificity of the pulldown assay. These results suggest that in cardiomyocytes the three metabolic enzymes MMCK, AK and PFK are targeted to their two distinct sites in the I-band as well as in the M-band of the sarcomere by their interaction with DRAL. In contrast to the interactions between DRAL and titin, attempts to co-immunoprecipitate the metabolic enzymes with DRAL were not successful (data not shown). The failure to detect the interaction of DRAL and the metabolic enzymes may indicate that their association is transient in nature and may serve as a means for dynamic compartmentalisation rather than a strict immobilisation to the sarcomere. The recently published results of an affinity chromatography approach, identifying cellular binding partners of FHL2 via MALDI-TOF analysis suggested further that this linker function of DRAL to target enzymes to the sarcomere may indeed not only apply for MMCK, AK and PFK but may also be important for other enzymes (El Mourabit et al., 2004). Eight enzymes involved in different enzymatic steps of the glycolysis alone were identified in this approach (among them phophoglycerate kinase 1, fructose-bisphosphate aldolase A and phosphoglycerate mutase) and another putative candidate for an interaction with DRAL was identified in the initial yeast two-hybrid, namely the muscle pyruvate kinase strongly supporting the theory of a “universal” linker function of the DRAL protein, mediating the sarcomeric targeting of several enzymes to the sarcomere.

6.2.5. Interaction of DRAL with other LIM proteins

LIM domains are supposed to mediate protein-protein interactions (Schmeichel and Beckerle, 1994). Recently it was shown via FRET experiments and in a forced yeast two-hybrid that DRAL and FHL3 associate to form heterodimers (Li et al., 2001). Since an analysis of the primary protein structure revealed that all FHL proteins show a high degree of homology, we investigated whether DRAL may also form heterodimers with other members of the four and a half LIM domain protein family.

To study, whether the interaction of FHL3 with DRAL could be confirmed and furthermore, to investigate the possible interaction of DRAL with the ubiquitously expressed FHL1, epitope tagged DRAL and either FHL1 or FHL3 (a kind gift of Ju Chen, University of San Diego) were cotransfected in cultures of neonatal rat cardiomyocytes. DRAL as well as the other two FHL proteins colocalised exactly in two striations flanking the Z-disc as well as to a lesser extent in the M-band of the sarcomere (figure 23 panel A). The indistinguishable subcellular localisation of FHL1 or FHL3 in comparison to DRAL strongly indicates a comparable dual-binding pattern to the I-band as well as to

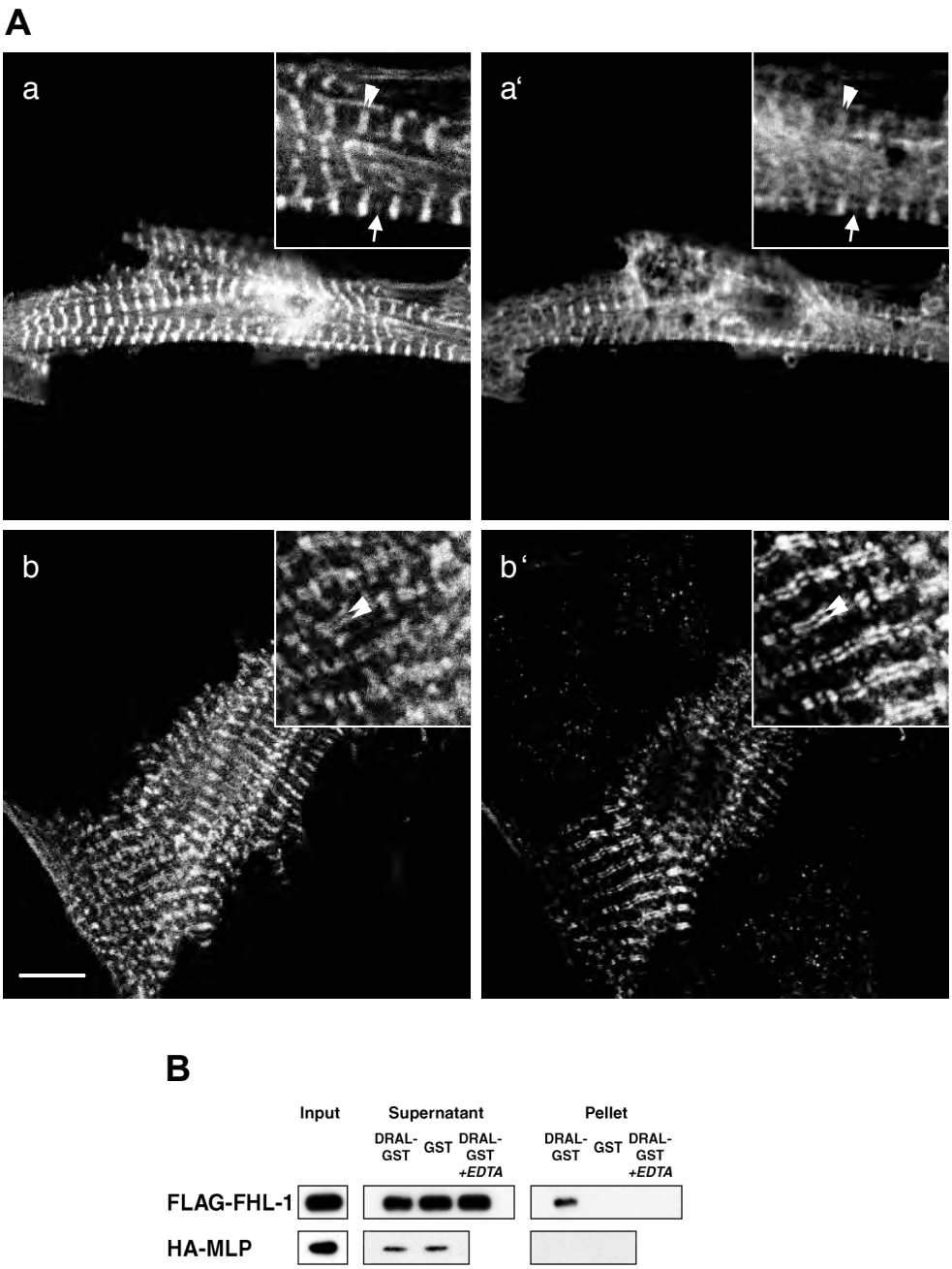

Figure 23. DRAL interacts with other LIM proteins of the FHL protein family.
A.Transient cotransfection of FLAG-tagged FHL1 (a') and FHL3 (b') together with GFP-tagged DRAL (a, b). Arrowheads indicate the double striation at the region of the sarcomeric I-band, arrows indicate the weaker striation at the M-band of the sarcomere. Scalebar = 10µm.
B. DRAL interacts with the four and a half LIM domain protein FHL1 but not with the muscle LIM protein (MLP). FLAG-tagged FHL1 interacts with DRAL-GST, but not with GST alone. The interaction with DRAL-GST is abolished in the presence of 10mM EDTA during incubation and washing. HA-MLP interacts neither with DRAL-GST or GST, indicating the specificity of the interaction of DRAL with FHL1.

the M-band of the sarcomere as well as an interaction among these proteins via the formation of heterodimers.

To demonstrate the binding of DRAL with FHL1 biochemically, a GST-pulldown assay was established. As shown in figure 23 panel B, FHL1 bound to GST-DRAL but not to GST alone. The interaction of FHL1 and GST-DRAL was also strongly abolished in the presence of EDTA during incubation. Since EDTA complexes polyvalent cations, it removes the Zn^{2+}-ions coordinated by the histidine and cysteine residues of the LIM protein, eventually leading to the destruction of the secondary and tertiary structure of the LIM protein. Thus, the proper conformation of the LIM domain is needed for the interaction of DRAL with FHL1 and the formation of heterodimers.

To exclude any non-specific interactions between LIM domains, we also tested an unrelated LIM protein, the muscle LIM protein (MLP), for binding to DRAL. MLP is expressed in the heart but shows a different subcellular targeting pattern compared with DRAL (Arber et al., 1994; Arber et al., 1997), making a direct interaction of the two proteins extremely unlikely. For this reason, MLP serves as a good control to assess non-specific interactions between LIM domains. As expected, MLP interacted neither with GST-DRAL nor with GST alone (see figure 23 panel B).

In summary, DRAL is able to form heterodimers with other members of the FHL protein family, like the ubiquitously expressed FHL1 or FHL3. This indicates further that the function of DRAL as a scaffolding protein, mediating protein-protein interactions with a various number of proteins and targeting of these proteins to the sarcomere, might be dependent on the formation of DRAL homo- or heterodimers. Furthermore, the loss of the interaction of DRAL and FHL1 in the presence of the strong chelator EDTA shows that the binding between the FHL proteins is dependent on the proper folding of the LIM domains and is not mediated by the non-specific attraction of the LIM domains to each other. The strikingly comparable subcellular targeting of FHL1 as well as FHL3 might indicate a certain functional redundancy among the members of the FHL protein family. Interestingly, mice with a targeted deletion for the FHL2 protein show no severe phenotype and only develop weak signs of hypertrophy upon β-adrenergic stimulation (Chu et al., 2000; Kong et al., 2001), again suggesting redundancy among the members of this protein family.

6.2.6. Crosstalk of DRAL with the Wnt and androgen receptor signalling pathways

6.2.6.1. Interactions of DRAL with β-catenin and plakoglobin

β-catenin, a protein involved in linking actin filaments to cadherins in adherence junctions as well as a major component of the Wnt signalling pathway was recently identified in a yeast two-hybrid screen as an interaction partner of DRAL (Martin et al., 2002). This interaction was confirmed by cellular colocalisation, immunoprecipitation and GST pulldown assays. Furthermore, DRAL represses

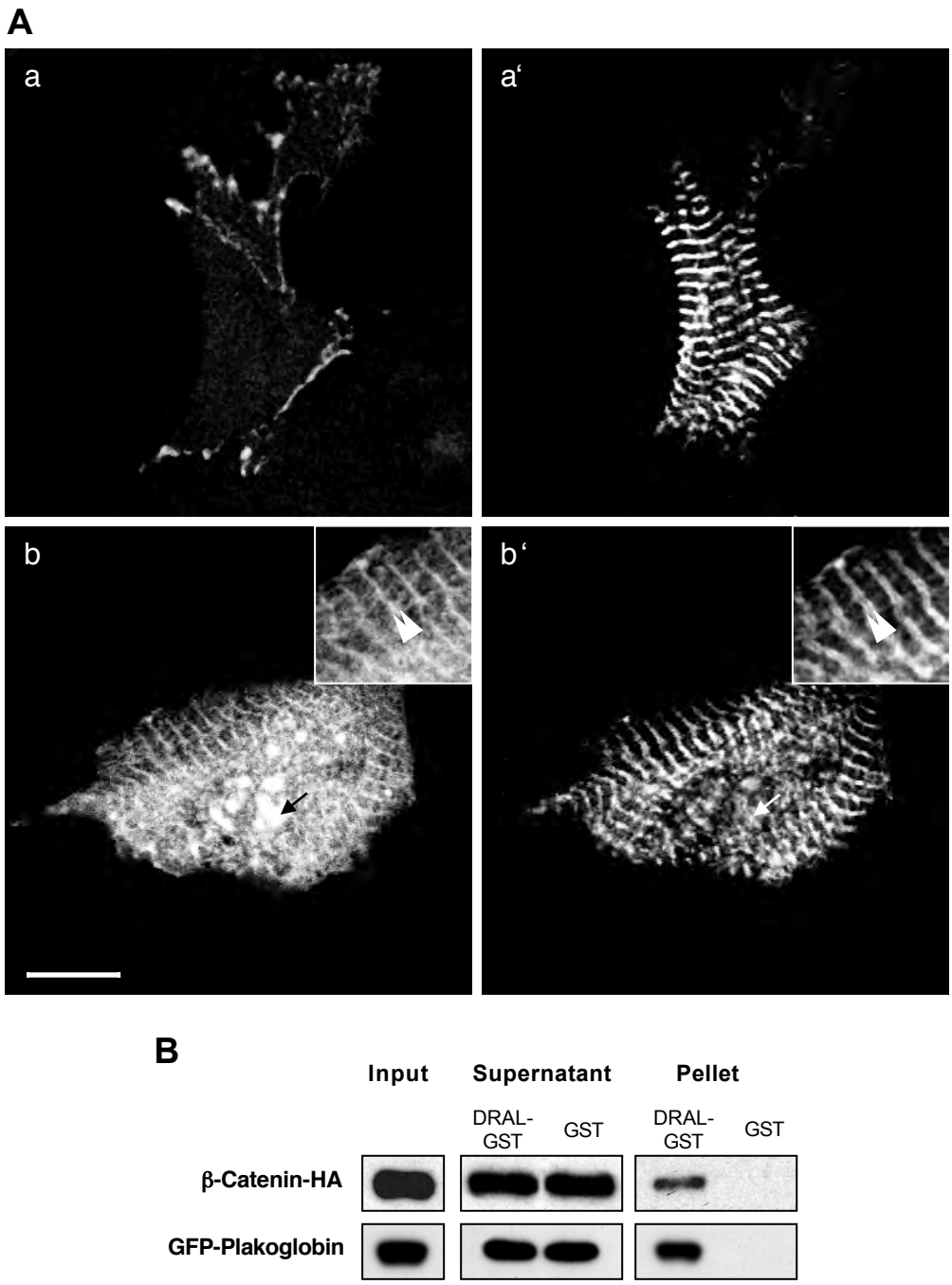

Figure 24. DRAL interacts with members of the catenin family.
A. Cotransfection of neonatal rat cardiomoyctes with GFP-tagged β-catenin (a, b) and FLAG-tagged DRAL (a', b'). The majority of β-catenin localises to the region of the intercalated disc. Although a fraction of β-catenin localises in overexpressing cells to the region of the Z-disc, analysis at high magnification of DRAL localisation revealed no apparent colocalisation of the two proteins in the sarcomere (see arrowheads in inserts). However, a colocalisation of β-catenin with DRAL could sometimes be observed in aggregates in the nucleus (see arrows). Scalebar = 10μm
B. DRAL interacts with β-catenin and plakoglobin in a GST-pulldown experiment. HA-tagged β-catenin and GFP-tagged plakoglobin interact with DRAL-GST, but not with GST alone.

β-catenin dependent expression of a reporter plasmid in a dose dependent manner. In order to study this interaction and to establish a putative role of DRAL as an integrator of different signalling pathways within the sarcomere, we performed cotransfection experiments using epitope tagged constructs of DRAL and β-catenin as well as a GST-pulldown assay. Cotransfection of primary cultures of neonatal rat cardiomyocytes as seen in figure 24 (panel A) showed prominent β-catenin localisation to the region of the intercalated disc and to some extent additional localisation to the Z-disc. Higher resolution of the Z-disc staining of GFP-tagged β-catenin revealed no colocalisation with DRAL. DRAL could be resolved as a doublet flanking the Z-disc, whereas β-catenin localised exclusively to the Z-disc in partially relaxed myofibrils. However, in overexpressing cells, a colocalisation of DRAL and β-catenin was visible in aggregates in the nucleus, potentially indicating an additional nuclear function for DRAL (see figure 24 panel A, b and b').

The biochemical analysis of the interaction of DRAL with β-catenin as well as plakoglobin in a GST-pulldown assay showed a positive result, since the HA-, respectively GFP-tagged constructs were only found in the GST-DRAL, but nor in the GST glutathione sepharose pellet fraction (see figure 24 panel B).

In summary *in vitro* an interaction of DRAL with both catenins, namely β-catenin as well as plakoglobin was biochemically confirmed via GST-pulldown experiments, whereas the *in vivo* localisation of either plakoglobin (data not shown) or of β-catenin showed no obvious interaction of DRAL with both catenins in the cytoplasma and the sarcomeres of neonatal rat cardiomyocytes. However, a partial colocalisation could be observed in the nucleus of β-catenin as well as DRAL overexpressing cells. These results and data from promoter activation experiments of reporter plasmids indicate that despite the pivotal function of DRAL as targeting mechanism for various proteins to the sarcomere, DRAL might serve as an integrator of several cellular signalling pathways, thus, upon change of its subcellular localisation from the sarcomere to the nucleus acting as a corepressor or coactivator for a multitude of transcription factors (Labalette et al., 2004; Wei et al., 2003).

6.2.6.2. Interaction of DRAL with the androgen receptor

Besides the crosstalk of DRAL with the Wnt signalling pathway via direct interaction to β-catenin or plakoglobin, DRAL was also identified as a binding partner for the steroid hormone receptor androgen receptor (AR) (Gobinet et al., 2001; Hsu et al., 2003; Muller et al., 2000; Nessler-Menardi et al., 2000). Most importantly, only activated AR, e.g. by the action of the agonist drug dihydrotestosterone (DHT), was able to interact with DRAL, whereas inactivated AR failed to bind to DRAL (Muller et al., 2000). To investigate the interaction of DRAL with the androgen receptor in more detail, HA-tagged constructs were used in colocalisation experiments using cotransfected cultures of neonatal rat cardiomyocytes. Furthermore, the influence of the AR activation state was studied by exposing the cotransfected cells to the androgen receptor agonist Androstan (5α-Androstan-17β-ol-3-one), to the antagonist Flutamide (2-Methyl-N-[4-nitro-3-(trifluoromethyl)-phenyl]propanamide) as well as in a competition study to both

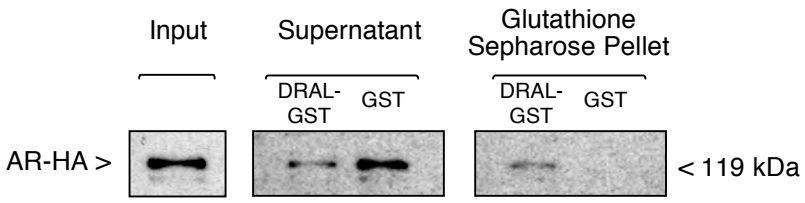

Figure 25. DRAL-GST pulldown assay.
Immunoblot of a DRAL-GST pulldown assay. HA tagged androgen receptor (AR) was detected in an immunoblot using a mRtantiHA antibody and aGoat-anti-Rat conjugated HRPO antibody. HA-tagged AR was only found in the pellet fraction of DRAL-GST, indicating an association of AR with DRAL. GST bound glutathione sepoharose alone did not interact with AR, as seen by the absence of a HA-positive signal in the pellet fraction of GST.

Androstan as well as Flutamide. As shown in figure 26 AR colocalised in the control (no exposure to Androstan or Flutamide) as well as in the Flutamide and the competition experiment (Flutamide and Androstan) to a certain extent with DRAL in sarcomeric structures, whereas the majority was found in a diffuse pattern throughout the cell. The localisation of AR in sarcomeric structures in the control experiment is most likely due to the presence of traces of Testosterone in the fetal calf serum used to supplement the culture before the start of the experiment and therefore might represent a subpopulation of activated AR interacting with DRAL. However, if the androgen receptor is activated by the agonist Androstan, it is exclusively found in the nucleus of transfected cardiomyocytes, indicating that the cloned AR acts like the endogenous receptor. Interestingly, the bulk localisation of DRAL remained unchanged upon exposure to Androstan, suggesting that the binding affinity to the M-band domain is2 as well as to the N2B I-band region of titin is stronger compared with that to AR. The competition of Androstan by an excess of Flutamide leads, depending on the expression level of transfected AR to a nuclear and cytosolic localisation pattern. To further investigate the interaction of DRAL with the AR, a GST-pulldown experiment was established (see figure 25). Only GST-DRAL was capable of interacting with HA-tagged AR, whereas GST alone showed no affinity for the receptor.

In summary, it was shown that AR colocalises in an activation state-dependent manner with DRAL in sarcomeric structures, and that upon excess activation by the agonist Androstan, AR is found exclusively in the nucleus of transfected cardiomyocytes, whereas the bulk population of DRAL remained bound to the sarcomere. The interaction of DRAL with the AR could be positively confirmed by a biochemical GST-pulldown assay.

6.2.6.3. Crosstalk of DRAL with the androgen receptor and the Wnt signalling pathways

Crosstalk with the androgen receptor pathway

The direct interaction of DRAL with several proteins involved in signalling pathways, like the steroid hormone receptor androgen receptor (AR) or the signalling/cytoskeletal protein β-catenin indicate a

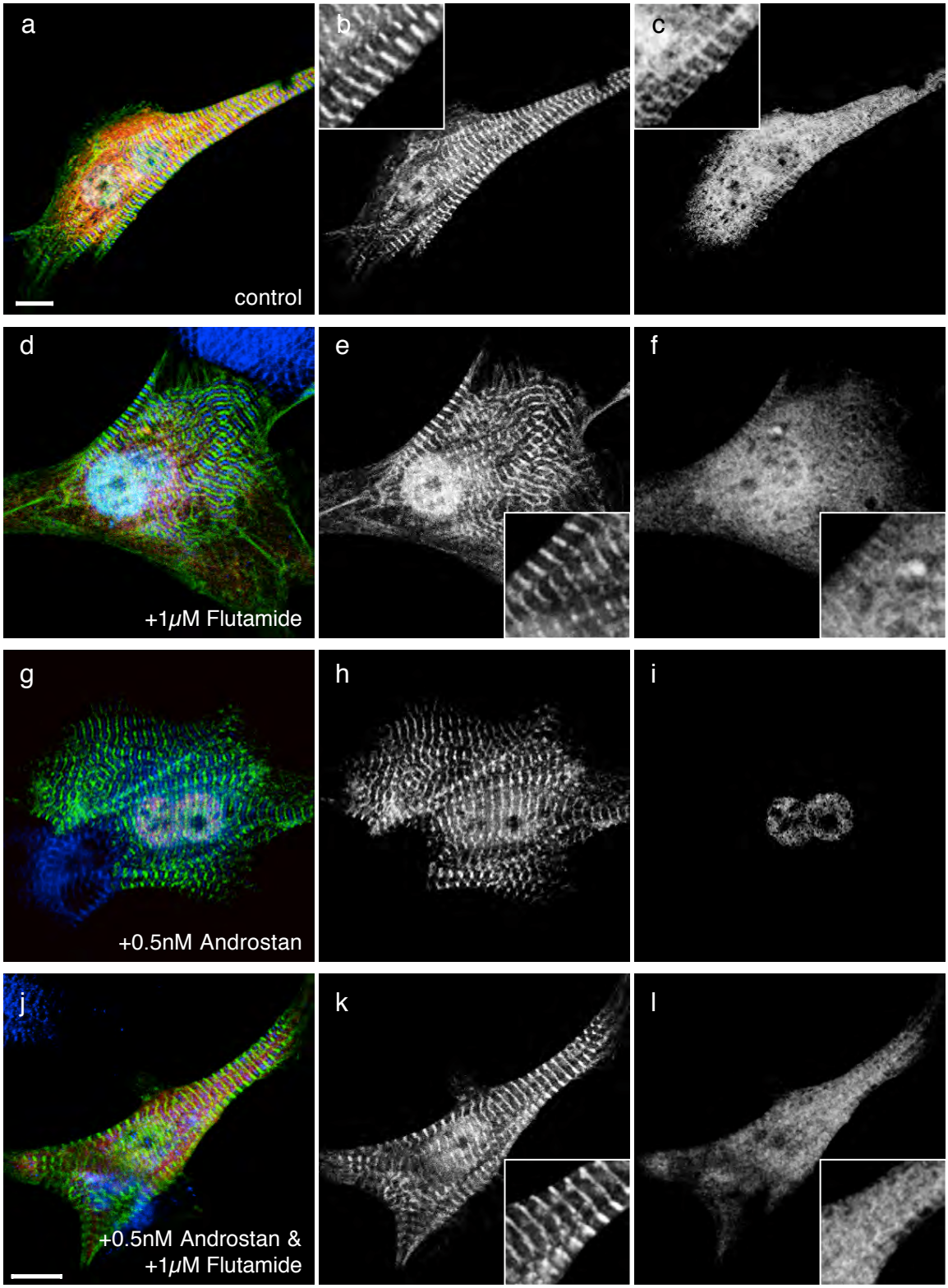

Figure 26. Comparison of DRAL and androgen receptor (AR) subcellular localisation. Neonatal rat cardiomyocytes were cotransfected with GFP-tagged DRAL (b, e, h, k) as well as HA-tagged AR (c, f, i, l) and counterstained with an antibody recognising the M8 epitope of titin (blue in the overlay: a, d, g, j). AR localises in untreated cardiomyocytes as well as in cells exposed to 1μM Flutamide or 1μM Flutamide and 0.5nM Androstan predominantly diffuse. However, a small fraction of AR colocalises with DRAL to the region of the sarcomere. Treatment of cardiomyocytes with 0.5nM Androstan resulted in the recruitment of AR to the nucleus. Scalebar = 10μm.

dual role for DRAL in the cell. DRAL may serve as a sarcomeric and cytoskeletal anchor for a multitude of proteins and in addition as a coactivator or corepressor of transcriptional activity in the nucleus (Gobinet et al., 2001; Hsu et al., 2003; Labalette et al., 2004; Martin et al., 2002; Muller et al., 2000; Nessler-Menardi et al., 2000; Wei et al., 2003). Since most of the investigations involving the activation or repression of transcriptional activity by DRAL used cell lines with no resemblance to muscle cells, we wondered, how DRAL activity might influence androgen receptor signalling and the subsequent cellular response in a myogenic cell. For this study, neonatal mouse cardiomyocytes derived from wildtype as well as from DRAL -/- mice were exposed to either Androstan (agonist) or Flutamide (antagonist) to stimulate the AR mediated signalling pathway. The cellular response was estimated by measuring an increase in cell size, as it was shown that stimulation of the androgen receptor leads to muscle hypertrophy (Hartgens and Kuipers, 2004; Marsh et al., 1998). Figure 27 shows that the exposure of wildtype cells to Androstan leads to no significant hypertrophic response of the cardiomyocytes. Application of the antagonist Flutamide either on its own or in combination with Androstan also showed no differences in the mean cell size. In contrast to wildtype cells, neonatal rat cardiomyocytes derived from DRAL -/- animals displayed a 37% increase in mean cell size compared to wildtype, and thus a general hypertrophic response upon the deletion of the DRAL allele. This hypertrophic phenotype was shown to increase upon application of β-adrenergic stimuli (Kong et al., 2001). In contrast to wildtype cardiomyocytes, DRAL -/- cells displayed with 27% increase in mean cell size a significant hypertrophic response (t=0.975) upon the exposure to 0.5nM Androstan compared to untreated control cells. This effect was almost completely reversed by the additional presence of 1μM Flutamide, indicating that this increase is an exclusive response to the activation of the androgen receptor signalling pathway.

DRAL has always been implicated as a direct coactivator of the androgen receptor (Muller et al., 2000; Wei et al., 2003). However, the observed effect of AR agonists in wildtype vs. DRAL -/- cells resembles more the action of a repressor, since in the presence of DRAL no hypertrophic response could be observed, but in the absence the cells significantly increase their mean cell size. Furthermore, DRAL expression was induced in Androstan treated cells (see figure 27 panel C, lane2), indicating a feedback mechanism in wildtype cells. Figure 26 shows that upon activation of the androgen receptor by Androstan, AR translocates to the nucleus in order to serve its function as transcription factor, whereas the prominent DRAL localisation at the I-band and M-Band of the sarcomere remains unaltered. This indicates that DRAL interaction to the sarcomere is predominant and that a translocation of DRAL to the nucleus is almost negligible. The mechanism of DRAL-mediated repression of the androgen receptor signalling pathway might therefore originate in a scavenger function, anchoring AR via DRAL to the sarcomere, preventing activated AR from translocating into the nucleus of cardiomyocytes and thereby reducing transcriptional activity, since only the activated form of AR interacts with DRAL (Muller et al., 2000).

The excessive activation of steroid receptors like the androgen receptor is usually linked to the development of muscle hypertrophy (Hartgens and Kuipers, 2004). The DRAL mediated repression of the androgen receptor activity might therefore represent a heart-specific protection against the

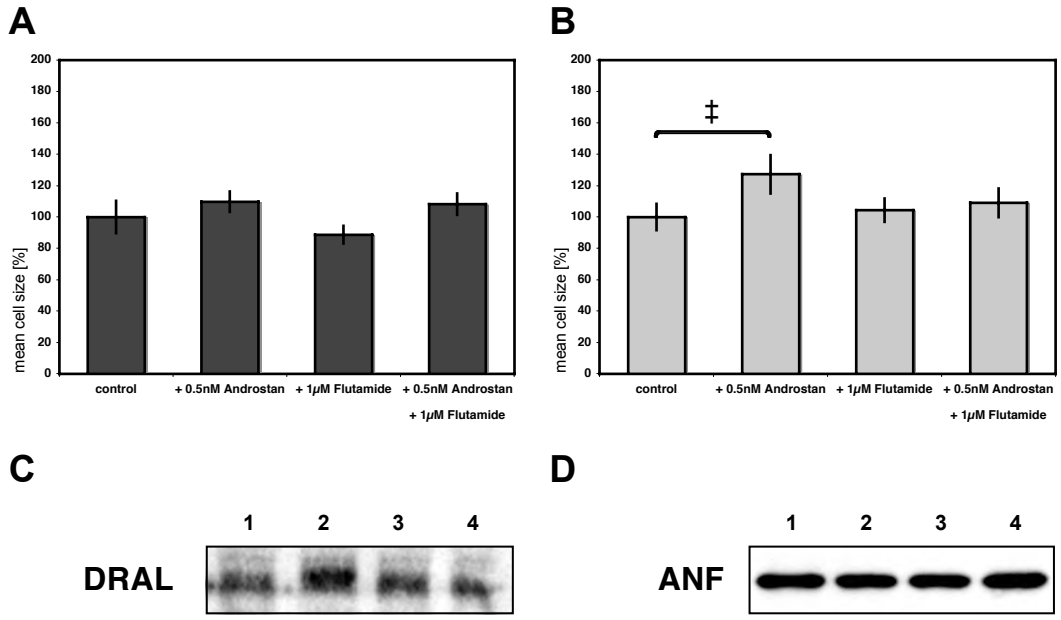

Figure 27. Activation of the androgen receptor (AR) leads to a hypertrophic response in DRAL -/- cardiomyoyctes.

A. Treatment of wildtype neonatal mouse cardiomoyctes with 0.5nM Androstan (AR agonist) or 1μM Flutamide (AR antagonist) or a mixture of both shows no significant changes in mean cell size.

B. Treatment of DRAL -/- neonatal mouse cardiomyoyctes resulted in a significant increase (of about 37%) in the mean cell size of 0.5nM Androstan treated cells, whereas 1μM Flutamide showed no effect on the cell size. Combined treatment of Androstan and Flutamide abolished the Andostan effect, indicating that the increase in cell size was due to the specific activation of the androgen receptor signalling pathway.

C. Wildtype neonatal mouse cardiomyocytes display an increase in DRAL protein levels upon treatment with 0.5nM Androstan (lane 2), whereas Flutamide alone (lane 3) or the combination of Flutamide and Androstan (lane 4) showed no changes in DRAL expression level compared to untreated control cells (lane 1). General protein levels were normalised by Coomassie staining of cell lysates prior to immunoblot analysis (data not shown).

D. The hypertrophic response in DRAL -/- cardiomyocytes to Androstan treatment is not accompanied by an increase in the hypertrophy marker atrial natriuretic factor (ANF) as judged by ANF protein levels of control (lane 1), Androstan (lane 2), Flutamide (lane 3) as well as Androstan and Flutamide treated cells (lane 4). General protein levels were normalised by Coomassie staining of cell lysates prior to immunoblot analysis (data not shown).

development of cardiac hypertrophy, since DRAL expression is highly elevated in the heart, but strongly repressed in skeletal muscle. As seen before, DRAL -/- cardiomyocytes are more prone to develop a hypertrophic reaction in response to steroid treatment by Androstan. An early sign for the development of hypertrophy is the re-expression of fetal isoforms of skeletal and sarcomeric proteins as well as the elevated expression of certain marker genes, like the atrial natriuretic factor ANF (Chien et al., 1991). We questioned therefore, whether the steroid-induced increase in mean cell size in DRAL -/- cardiomyocytes is accompanied by an elevation of the typical hypertrophy marker protein ANF, as demonstrated for another mouse model (Li et al., 2004b). Figure 27 panel D shows that despite the significant increase in cardiomyocyte cell size no upregulation of the hypertrophy marker gene ANF could be detected on the protein level for Androstan treated cells.

Crosstalk with components of the Wnt signalling pathway

Interaction data derived from yeast-two hybrid screens as well as biochemical protein-protein binding experiments indicated that DRAL might play a role in the Wnt signalling pathway via a direct interaction with two of its major components, β-catenin as well as CBP/p300 (Labalette et al., 2004; Wei et al., 2003). The family of the catenin proteins serves a dual role in heart muscle cells. In the cytoskeleton, they are thought to be important for the cytoskeletal integration of the specialised cell-cell contacts of cardiomyocytes, the intercalated disc structures, via anchoring the actin filaments to the cadherin membrane proteins. Catenins serve furthermore, as mediators of cell signals from the membrane to the nucleus of the cell and act as transcriptional coactivators of the TCF/LEF (T cell factor/lymphoid enhancer factor) transcription factor family (Moon et al., 2004).

How DRAL affects the cellular response to the activation of the Wnt signalling pathway and how cardiomyocytes adapt to the ablation of the DRAL allele is the subject of the next set of experiments.

Cellular stress responses are very versatile and range from the alteration of protein levels over a change in the subcellular localisation to increased posttranslational modification of proteins. One of the first signs in cardiomyocytes for increased cellular stress and alterations in the intercalated disc structure is marked by the elevation of the nebulin related LIM protein N-RAP (Ehler et al., 2001). Figure 28 (panel B) shows that N-RAP expression levels are slightly increased in DRAL -/- cardiomyocytes, indicating an increased physiological stress of these heart cells. Since DRAL is interacting with several proteins of the catenin family (see earlier), we questioned whether this increased physiological stress may be accompanied by an increase of the intercalated disc proteins α-catenin, β-catenin and plakoglobin (γ-catenin). As shown in figure 28, all catenins investigated display an elevation in the overall expression level in cultures of DRAL -/- cardiomyocytes compared to wildtype cells (panel C). However, this increase is only prominent in the region of the intercalated disc and not apparent in an elevated nuclear staining of DRAL -/- cardiomyocytes (see figure 28 panel A), suggesting an adaptation at the cytoskeletal level of the cell rather than a major change in the nuclear catenin levels.

The experiments involving the androgen receptor indicated that the mechanism of DRAL mediated repression of the transcriptional co-activation of the AR is most likely due to the strong sarcomeric

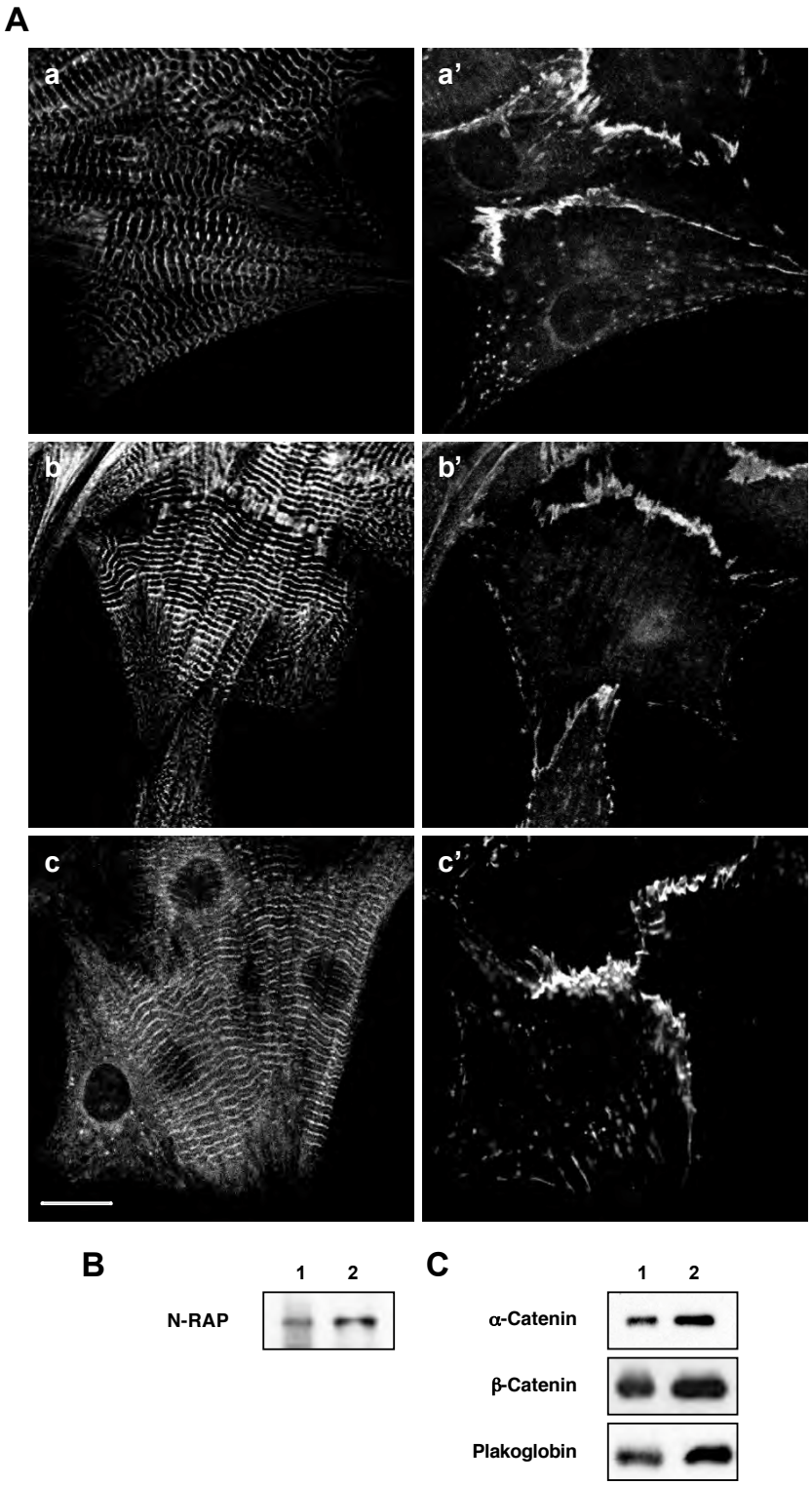

Figure 28. Increased catenin and N-RAP expression in DRAL -/- neonatal mouse cardiomyocytes (NMCs).

A. Comparison of subcellular endogenous α-actinin (a, b) or titin M8 epitope localisation (c) to the localisation of α-catenin (a'), β-catenin (b') and plakoglobin (c'). No obvious changes in the catenin localisation pattern to intercalated disc structures could be observed.

B. DRAL -/- NMCs (lane 2) show an increase in N-RAP expression compared to wildype cells (lane 1).

C. Immunoblot analysis of wildtype (lane 1) as well as DRAL -/- cardiomoycytes (lane 2) show elevated protein levels of all investigated catenin proteins.

General protein levels were normalised by Coomassie staining of cell lysates prior to immunoblot analysis in B and C (data not shown).

anchorage of the DRAL protein and its inability to easily translocate to the nucleus. We investigated therefore, whether the activation of the Wnt signalling pathway may have an influence on the subcellular localisation of DRAL in cultured neonatal cardiomyocytes. A potent activator of the TCF/LEF (T cell factor/lymphoid enhancer factor) transcription via β-catenin is the exposure of cells to LiCl, which mimics the effect of Wnt signalling via inhibition of GSK-3β (Krylova et al., 2002). As shown in figure 29 (panel A) DRAL undergoes a drastic change in its subcellular localisation and shows a strong nuclear accumulation upon treatment of cardiomyocytes with 10mM LiCl, indicating major changes in the functional role of DRAL within these cells. The accumulation of DRAL in the nucleus of cells treated with LiCl strongly resembles the parallel recruitment of β-catenin to the nucleus of these cells (data not shown).

The dramatic changes in the compartmentalisation of DRAL from the sarcomere to the nucleus are accompanied in a general downregulation of DRAL expression, as seen in immunoblots of control as well as LiCl treated whole cell lysates (figure 29 panel B). The parallel elevation of protein levels of β-catenin and Dvl-1 (figure 29 panel B) that are involved in the Wnt signalling pathway indicates further that the downregulation of DRAL might be a direct consequence of a TCF/LEF mediated change in the transcriptional activity in these cells.

Does the activation of the Wnt signalling pathway also lead to morphological changes in the cell size as seen for androgen receptor activation in cardiomyocytes derived from DRAL -/- mice? Again, neonatal mouse cardiomyocytes were assayed for a change in mean cell size and control cells were compared with cultures that were exposed to 10mM LiCl. In contrast to the Androstan treated cells (figure 27 panel B), Lithium chloride treatment does not give rise to a hypertrophic response (figure 29 panel C).

In summary, these results suggest that Wnt activation leads to a strong suppression of DRAL protein levels and to the translocation of DRAL to the nucleus. Although the activation of Wnt resulted in the accumulation of β-catenin in the nucleus as well as in the elevation of Wnt-related expression of signal-proteins like Dvl-1 and β-catenin, no significant changes in the mean cell size could be observed. Recent studies using embryonic stem cell technology and experiments in embryos demonstrated that the activation of the canonical Wnt signalling pathway (via β-catenin) represses heart formation and inhibits a normal cardiac differentiation (Sachinidis et al., 2003). This is finding is in agreement with the reduction of DRAL protein levels, since DRAL can be seen as a marker for differentiated cardiomyocytes. The subcellular translocation of DRAL from the sarcomere to the nucleus indicates however, that there might be an interplay of DRAL and the canonical Wnt signalling pathway via the direct interaction of DRAL with β-catenin and that the fine-tuning of DRAL-mediated changes in the transcriptional activity of TCF/LEF transcription factors is important during embryonic and postnatal heart development. Furthermore, the crosstalk between different signalling pathways such as the Wnt and Androgen receptor pathway (Wei et al., 2003), the interplay between the androgen receptor and the cAMP-responsive element-binding protein (CREB; (Chan and La Thangue, 2001; Labalette et al., 2004)) or the DRAL dependent antagonistic Rho dependent repression of SRF (Muller et al., 2002; Philippar et al., 2004) indicates that DRAL may integrate signals from different

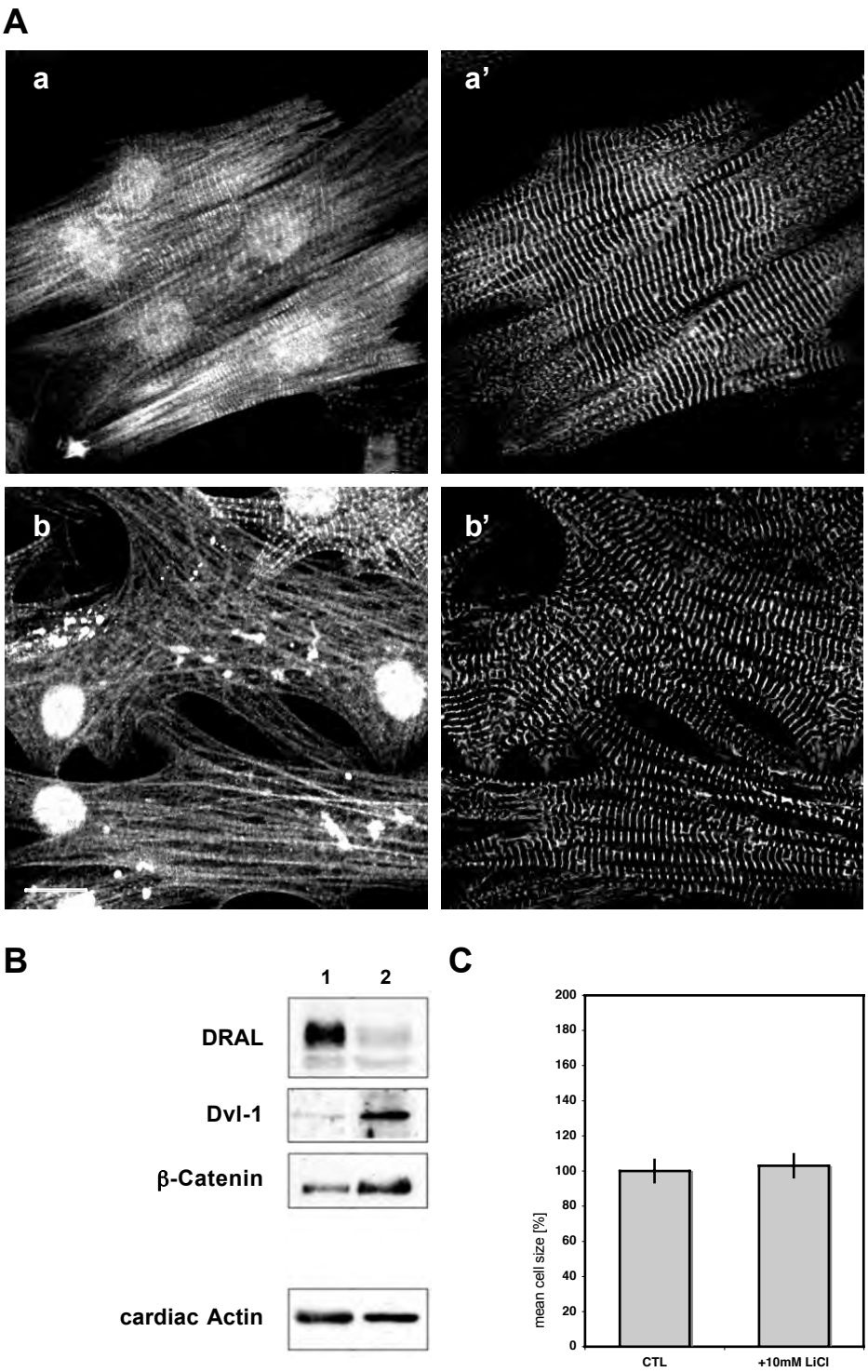

Figure 29. Effect of Wnt-signalling on DRAL localisation and expression level upon treatment of cardiomyocytes with LiCl.

A. Endogenous DRAL compartmentalisation changes from predominantly sarcomeric (a) to nuclear localisation (b) upon treatment of wildtype mouse cardiomyoctes with 10mM LiCl, whereas α-actinin remains associated with the sarcomeric Z-disc. Note that we increased the detector gain in (b) compared to (a) in order to record residual sarcomeric DRAL localisation.The nuclear signal of DRAL in (b) is therefore saturated. Scalebar = 10μm.

B. Immunoblot analysis of untreated wildtype (lane 1) and neonatal mouse cardiomoycytes treated with 10mM LiCl (lane 2) showed elevated expression levels of proteins associated with the Wnt-signalling pathway, such as Dvl-1 as well as β-catenin. DRAL protein levels however, showed a strong suppression upon treatment with 10mM LiCl compared to untreated control cells. Cardiac actin was used as a loading control.

C. No changes were observed in mean cell size of DRAL -/- neonatal mouse cardiomoyctes exposed to 10mM LiCl compared to untreated control cells (CTL).

pathways and, depending on the cellular context and developmental stage, serves as transcriptional co-activator or co-repressor, or as a sarcomeric anchor protein.

6.3. Titin kinase Signalling

The giant protein titin (also known as connectin) is thought to be the central regulator for sarcomeric assembly and maintenance (Tskhovrebova and Trinick, 2003). It offers binding sites for a broad variety of proteins, ranging from structural proteins like α-actinin and actin at the N-terminus, myosin binding protein-C and -H in the sarcomeric A-band to the proteins of the myomesin family and myosin at the C-terminus of the protein, which is located at the M-band of the sarcomere. Its major function during myofibrillogenesis is to integrate all structural components into their correct location forming a functional sarcomere. Hence, it was compared to a blueprint for sarcomere assembly. Mainly composed of structural components like immunoglobulin-like and fibronectin-type III domains, titin contains in its C-terminal part also an autoregulated serine kinase domain (titin kinase, TK; (Mayans et al., 1998)), which was implicated to play a pivotal role during myofibrillar assembly and sarcomeric remodelling. TK can be activated by phosphorylation of a tyrosine residue (Y170; see figure 30 panel A), which unlike other kinases is not located in the activation segment, but in the P+1 loop region of the kinase, indicating an important function in the recognition and binding of putative kinase substrates. Titin kinase activity is furthermore regulated by the conformational change of a regulatory tail fragment (also known as autoinhibitory region of TK) and the modulation via calmodulin, which is thought to interact with the first α helix in the regulatory fragment (αR1; see figure 30 panel A and B; (Amodeo et al., 2001)).

Recently, the protein NBR1 was identified via yeast two-hybrid analysis as a putative interaction partner for the regulatory fragment of titin kinase (data from Prof. M. Gautel). This interaction is thought to occur in a conformation dependent way with the PB1 domain in NBR1 as minimal binding site, thus forming a scaffold for other proteins via direct binding to NBR1 in close proximity to the catalytic core of titin kinase. Besides the interaction of NBR1 to the regulatory tail of TK, NBR1 is also able to form homodimers via its coiled-coil domain. The search for further binding partners of NBR1 via yeast two-hybrid screen indicated a putative interaction of NBR1 with p62/sequestosome 1 (SQSTM1; data from Prof. M. Gautel). This interaction was again mediated by the PB1 domain in both proteins as minimal binding site (see figure 30 panel C). PB1 domains (Phox and Bem1) are composed of approximately 80 amino acids and can be found in a broad variety of cytoplasmic signalling proteins, like PKC-ζ or p62. One characteristic feature of this domain is the capability to form heterodimers via PB1 domain pairing, although not all PB1 domains are able to interact with each other. Highly conserved OPR motifs (also known as PC or AID motifs) are important for the overall association of PB1 domains, whereas flanking sequence motifs are thought to be important for binding specificity (see also Accession number PF00564 in the Pfam database of conserved protein domains: http://pfam.wustl.edu/).

The protein p62 (also known as sequestosome 1) is thought to act as a multivalent scaffolding platform, integrating signals from different kinase signal pathways and subsequently leading to the activation of the transcription factor NFkappaB (Geetha and Wooten, 2002). It contains, besides its N-

Figure 30. Titin kinase signalling.

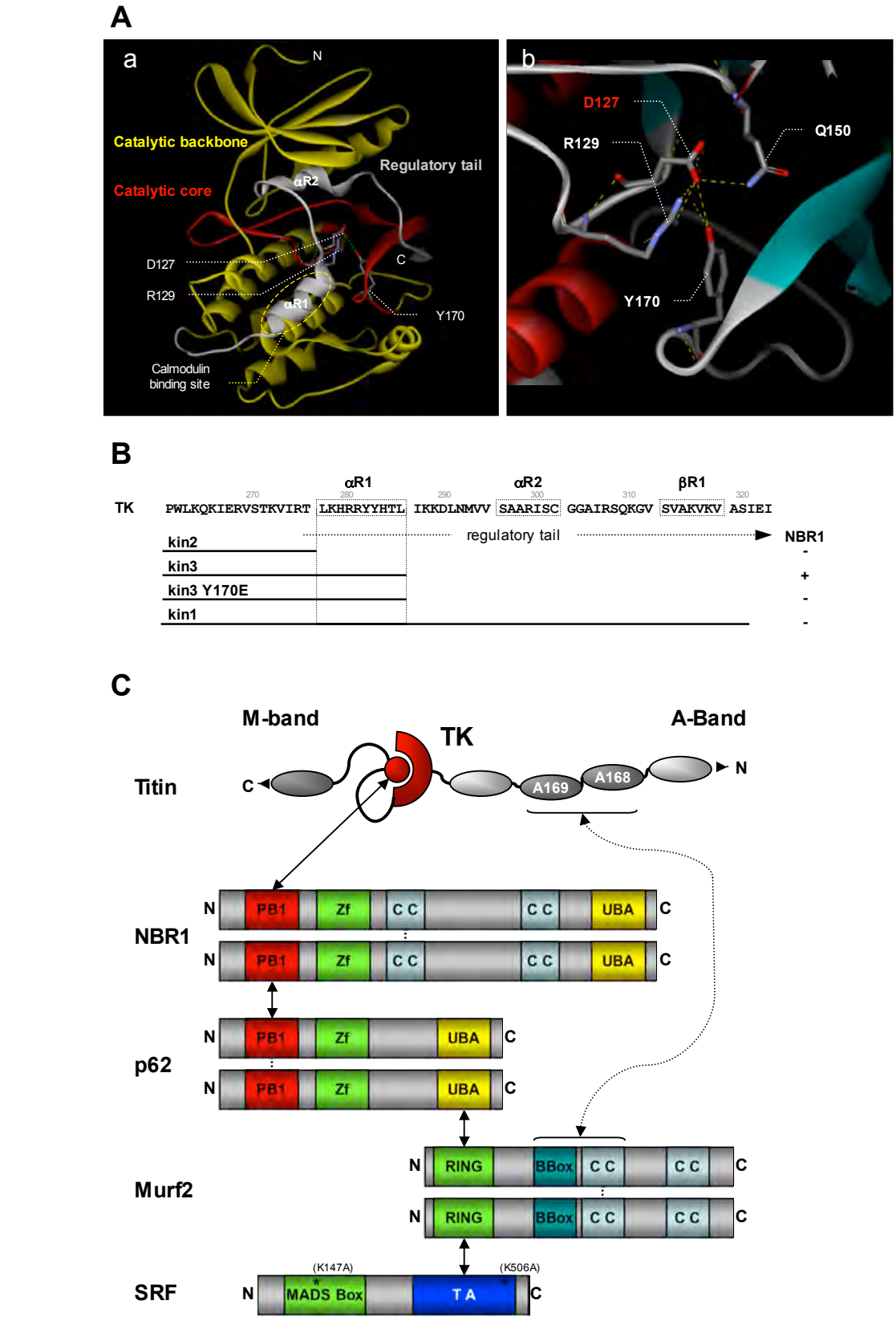

Figure 30. Titin kinase signaling.
A. The crystal structure of titin kinase as determined by (Mayans et al., 1998). The overall structure (a) can be subdivided into a catalytic backbone (in yellow), the catalytic core (in red) and the regulatory tail (in grey). The regulatory tail is composed of two α-helices: αR1, which is thought to be the minimal binding site for calmodulin and α R2. The catalytically important residues D127, R129, Q150 and Y170 can be seen in more detail in (b). The aspartate 127 is thought to be important for the phosphorylation of a serine residue in the designated substrate protein. Via an auto-inhibitory mechanism, D127 is coordinated in its inactive form in a side-chain interaction network with residues R129, Q150 and Y170. Upon phosphorylation of Y170, presumably by Src kinase family members, D127 is released from this interaction network. A second step is necessary for the full activation of titin-kinase: the regulatory tail, blocking the catalytic cleft in the inhibitory form of the kinase has to be positioned away from the catalytic core via an interaction with a modulator protein or via mechanical stretching of the protein.
B. Schematic representation of the titin kinase regulatory tail and influence of titin kinase mutants on the interaction with NBR1. Forced yeast-two hybrid assay with serial truncations and the Y170E mutant of titin kinase suggested that NBR1 binds the semi-opened, non-phosphorylated titin kinase at the αR1 helix of the regulatory tail. This minimal binding site for NBR1 is necessary, but not sufficient, since the interaction of NBR1 with titin kinase is modulated by the phosphorylation state of the kinase. All data from Prof. M. Gautel.
C. Schematic presentation of titin kinase signaling.
The regulatory chain (depicted as a circle) interacts with the PB1 domain of the NBR1 dimer. The homodimerisation of NBR1 is mediated via coiled-coil interactions (dotted line). The other PB1 domain of the NBR1 dimer interacts with the PB1 domain of p62. PB1 domains are known mediators of protein-protein interaction and may trigger the establishment of homo- or heterodimerisation, as seen in the case for the p62 dimer formation (dotted line). The UBA domain of p62 was found to interact with one RING domain of the Murf2 dimer, whose homodimerisation may be mediated by a coiled-coil interaction (dotted line). Interestingly, the B-Box and coiled-domains of Murf1 are known to interact with the A-band Ig-domains A168 and A169 of titin (dotted line). The RING domain of Murf2 was found to mediate the binding of Murf2 to the transactivation domain of the transcription factor SRF. Depicted are also the two putative sumoylation sites within SRF at K147 and K506.
All data from Prof. M. Gautel and Dr. E. Rostkova. Scheme adapted from Prof. M. Gautel.
Abbreviations: Zf = zinc finger domain, CC = coiled-coil domain, UBA = ubiquitin associated domain, PB1 = phox and bem1 domain.

terminal PB1 domain, also a central zinc-finger domain as well as a C-terminal UBA domain. Further screening for protein interaction partners of p62 via yeast two-hybrid identified the muscle protein Murf2 (Muscle Ring Finger protein 2) as putative binding partner of the p62 UBA domain. Although UBA domains (Ubitquitin associated domains) emerged as binding partners for ubiquitin (mono, di-, tri- and tetra-ubiquitin as well as poly-ubiquitin chains), they also bind other proteins as well as mediating the homo- or heterodimerisation of proteins.

Murf2 belongs to a family of muscle-specific proteins (Centner et al., 2001; Pizon et al., 2002; Spencer et al., 2000), which are thought to regulate primary myofibrillogenesis and muscle signalling. Recently, the A-band fibronectin domains A168 and A169, located near the titin kinase domain, were identified as binding partners for the B-Box and coiled-coil motif within Murf1 (see figure 30 panel C; (Centner et al., 2001; McElhinny et al., 2002)), leading to the speculation of a regulatory function of Murf proteins towards the titin kinase. The family of the Murf proteins were further implicated to act as

ubiquitin ligases (E3 enzyme), thereby mediating protein turnover as well as to translocate from the sarcomere to the nucleus under atrophic conditions (Bodine et al., 2001; Pizon et al., 2002). Besides its role in the ubiquitinylation cycle, Murf was also shown to interact with Ubc9 as well Sumo3 (Dai and Liew, 2001; McElhinny et al., 2002), indicating that the family of the Murf proteins may also be connected to the sumoylation pathway (see earlier).

The association of Murf with the Sumo pathway was substantiated, when a bacterial two-hybrid screen using Murf2 as a bait identified the serum response factor (SRF) as a potential interaction partner. SRF is one of the major transcription factors in the cell responsible for the regulation of muscle differentiation (Chai and Tarnawski, 2002; Schneider et al., 1994; Schneider et al., 1992) and has recently been reported to be important in the developmental hypertrophy of skeletal muscles as shown by tissue specific gene deletion in mice (Li et al., 2005).

Figure 30 panel C gives an overview over the proposed signalling pathway by summarising all proteins involved and the interacting minimal binding sites (data from Prof. M. Gautel and Dr. E. Rostkova). The following paragraphs characterise protein interactions in the titin kinase signalling cascade towards the modulation of the transcriptional activity of the serum response factor as well as cellular phenotypes of cardiomyocytes upon stimulation of the signalling pathway and specific mutations of cascade proteins.

6.3.1. Interaction of titin kinase with NBR1

The NBR1 gene (Next to BRCA1) was initially identified as a candidate gene for elevated risk of the development of ovarian cancer. Recent search for interaction partners revealed a multitude of putative binding partners involved in various signalling pathways, like the PKC-ζ interacting protein FEZ1 (fasciculation and elongation protein Zeta-1) as well as the Calcium and Integrin binding protein (CIB), which is associated with Polo-like kinases Fnk/Snk and the Alzheimer related protein Presenilin-2 (Whitehouse et al., 2002). NBR1 was found in a yeast two-hybrid screen to interact with a truncated kinase (kin3) and to require the presence of the first α-helix (αR1) of the regulatory fragment (see figure 30 panel B; data from Prof. M. Gautel). The fragment of the regulatory domain, covering the catalytic core and thereby regulating the accessibility to the catalytic centre is trunctated in this version of the titin kinase, thereby mimicking a semi-activated state of the enzyme. Further deletion (as in kin2) or extension of the regulatory domain (as in kin1) abolishes NBR1 interaction completely (see figure 30 panel B).

In order to become fully enzymatically active, titin kinase has to undergo conformational changes involving the regulatory domain of the enzyme as well as to become phophorylated at tyrosine residue 170 in order release the catalytically important residues D127 and R129 from an inhibitory complex (see figure 30 panel A(b)). This phosphorylation can be mimicked with a mutation of tyrosine to glutamate (Y170E), resulting in a constitutionally active mutant of titin kinase. Testing the constitutionally active kinase Y170E in a forced yeast two-hybrid assay for interaction with NBR1 we noticed a strong abolishment of NBR1 interaction with titin kinase kin3 Y170E as shown in figure 30

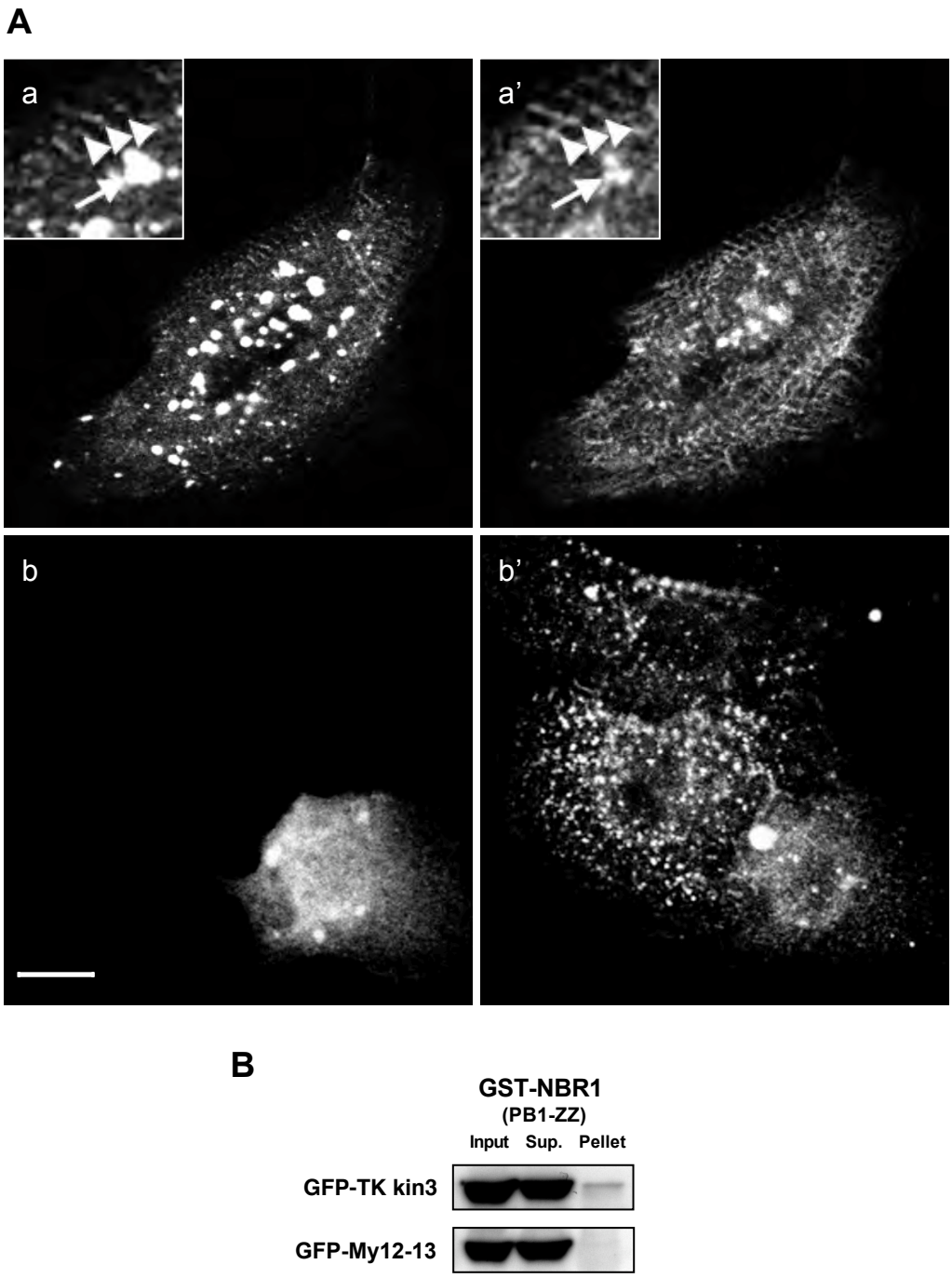

Figure 31. Titin kinase colocalises with NBR1 and p62 in transiently transfected neonatal rat cardiomyoctes.

A. Transiently cotransfection of neonatal rat cardiomoyctes with GFP-tagged NBR1 (a) and T7-tagged titin kinase kin3 (a') results in the strong colocalisation of both proteins into sarcomeric structures (arrowheads in inserts) as well as in vesicular structures in the cytoplasm of the cell (arrow in insets).

Transient transfection of T7-tagged full length titin kinase (b) results in a perturbed endogenous p62 localisation (b') in transfected cells. p62 localisation in untransfected cells display an association p62 to the region of the sarcomeric M-band. Full length titin kinase shows a diffuse and particulate localisation pattern in neonatal rat cardiomyocytes which partly colocalises with the endogenous p62.

Scalebar = 10μm.

B. Co-immunoprecipitation of GST-tagged NBR1 (PB-Zf fragment; see Figure 30) with GFP-tagged titin kinase kin3 or GFP-tagged myomesin domains 12-13 using an antibody specific for the GST-tag. Immunoblot analysis of the Input, Supernatant and Pellet fraction using a GFP-antibody revealed an interaction of NBR1 with titin kinase kin3 but not with GFP-My12-13.

panel B, suggesting that interaction of NBR1 with the α-R1 helix of the regulatory domain is required but not sufficient and that NBR1 may represent a substrate or a regulator of titin kinase activity (all data from Prof. M. Gautel).

Can this putative interaction be confirmed at a cellular level? In order to address this question we established eukaryotic expression constructs of human NBR1 as well as for the truncated version of titin kinase kin3 and transfected neonatal rat cardiomyocytes. As shown in figure 31 both proteins exhibit a strong colocalisation within these cells, in the sarcomere as well as in cytoplasmic vesicles. The localisation of this complex to the sarcomere might result in the interaction of titin kinase with one of its strongest substrates, telethonin.

In summary, NBR1 was found to be a putative substrate or regulator of titin kinase. The protein interacts with the semi-activated state of the kinase with the α-R1 helix of the regulatory domain and the binding is strongly reduced upon phosphorylation of titin kinase, as indicated with experiments using the constitutionally active mutant Y170E of titin kinase. Both proteins display a strong colocalisation in neonatal rat cardiomyocytes upon transfection of tagged eukaryotic expression constructs, indicating a close association of the titin kinase-NBR1 complex *in vivo*. The interaction of NBR1 with proteins involved in other signalling pathways, like the PKCζ signalling and via the Integrin and Calcium binding protein (CIB) indicates further a putative crosstalk of the titin kinase signalling pathway and suggests an integrative function of NBR1 processing signals from a broad variety of pathways.

6.3.2. Titin kinase signalling, p62, Murf2 and beyond

6.3.2.1. Cellular effects of TK on p62 and Murf2

Expanding the signalling of titin kinase and NBR1 we identified in a yeast two-hybrid screen the PB1 domain of p62 as putative interaction partner of the PB1 domain of NBR1. As described earlier, PB1 domains emerged as mediators of protein-protein interactions, enabling the establishment of homo- as well as heterodimers. The flanking regions of the highly conserved OPR motif, which mediates overall PB1 association, are suggested to be responsible for the specificity of the binding. p62 emerged as a scaffolding protein, integrating signals from different signalling pathways and resulting in the activation of the nuclear transcription factor kappaB (NF-κB; (Geetha and Wooten, 2002)).

Can the activation of titin kinase lead to a phenotypical response of p62 localisation at a cellular level? We tested the influence of the constitutive catalytically active titin kinase mutant kin3 Y170E on endogenous p62 localisation within transfected neonatal rat cardiomyocytes (see figure 31 b and b'). Endogenous p62 in untransfected neonatal rat cardiomyocytes is associated to sarcomeric structures as judged by the cross-striated localisation pattern. However, when constitutionally active titin kinase is present within this cell, the sarcomeric localisation of p62 is largely disturbed. In contrast both

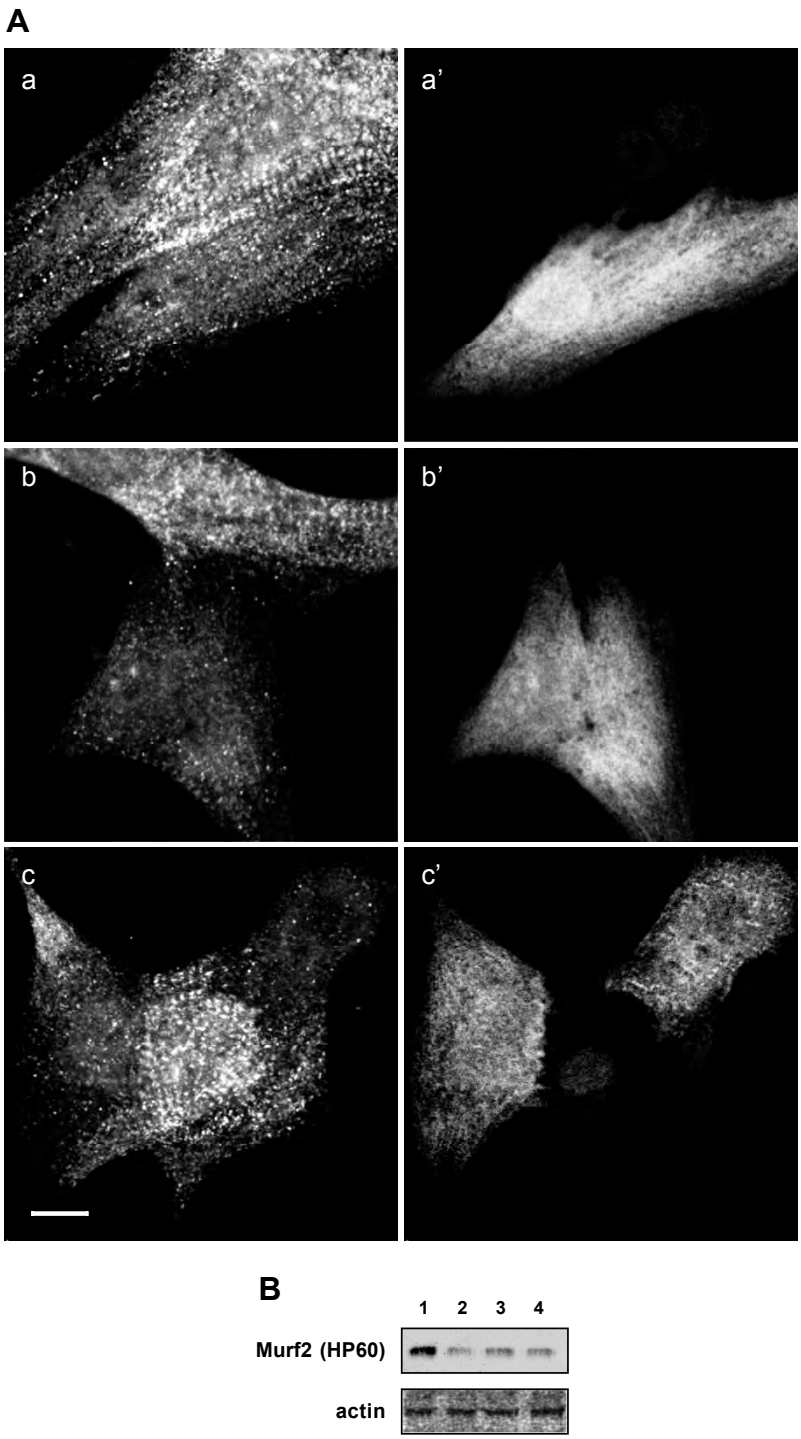

Figure 32. Transfection of wildtype and mutant titin kinase perturbs endogenous Murf2 localisation and expression levels in neonatal rat cardiomyoctes.

A. Confocal pictures of neonatal rat cardiomyocytes transiently transfected with T7-tagged full length wildtype titin kinase (a'), full length Y170E TK (b') as well as wildtype kin3 truncation mutant (c') show a general decrease in endogenous Murf2 staining (a, b, c). Transfected cells show further a decrease in the sarcomeric localisation of Murf2 compared to untransfected control cells, which display a strong association of Murf2 to the region of the sarcomeric M-band. Nuclear background staining in a' and c' is due to the unspecific cross-reaction of the T7 antibody. Scalebar = 10μm.

B. Immunoblot analysis of untransfected neonatal rat cardiomyocytes (lane 1), full length wildtype titin kinase (lane 2), truncation mutant TK-kin3 (lane 3) as well as Y170E titin kinase (full length; lane 4) show a decrease in Murf2 expression (using the Murf2 HP60 antibody; see list of antibodies). Actin staining in the lower panel indicates equal loading of the cell lysates.

proteins colocalise diffusely in the cytoplasm as well in vesicular cytoplasmic structures, indicating a dramatic effect of TK kin3 Y170E on the localisation of p62 and suggesting an interaction of both proteins *in vivo*.

Apart from the dramatic effect of TK kin3 transfection on the p62 localisation we asked, whether a similar cellular phenotype can be observed with Murf2, the subsequent signalling protein in the putative titin kinase signalling cascade. The Murf protein family consists of three different members: Murf1, Murf2 and Murf3. Splice variants as well as tissue specific expression patterns (e.g. the cardiac specific p27 isoform of Murf2) contribute to the variety of this protein family. Murf 2 is via its interaction with the titin immunoglobulin-like domains A168 and A169 closely associated to the sarcomere and was speculated to regulate titin kinase activity. Transfection of titin kinase truncations as well as the constitutionally active Y170E mutant into neonatal rat cardiomyocytes significantly altered Murf2 localisation as well as protein levels (see figure 32). Whereas Murf2 localises putatively via interaction with titin into sarcomeric structures in non-transfected cells, Murf2 exhibits a less sarcomeric and more vesicular localisation in transfected cells (see figure 32 panel A). Furthermore, a significant decrease in the protein levels of Murf2 was observed upon transfection of titin kinase into neonatal rat cardiomyocytes (see figure 32 panel B), suggesting not only an alteration in the subcellular localisation, but also the subsequent degradation of Murf2 or via a feedback mechanism the attenuated expression of the protein, respectively. Interestingly, this alteration in Murf2 localisation and protein level could be achieved regardless of the truncation and activation state of the kinase tested. Another notable difference is seen in the diverse localisation pattern of the different titin kinase constructs. Full-length titin kinase localises mainly diffusely to the cytoplasm and sometimes to the nucleus regardless of the activity state of the enzyme, whereas the semi-active kin3 truncation mutant of titin kinase always showed a more pronounced localisation into sarcomeres (see figure 32 panel A c'). This differential behaviour of wildtype versus kin3 truncation may reflect the interaction of this semi-activated titin kinase with substrates anchored to the sarcomere. Since epitope tagged TK-kin3 proteins locate to the Z-disc of the sarcomere, the Z-disc protein telethonin might, as the major phosphorylation substrate for titin kinase, be responsible for the observed targeting behaviour.

To summarise, the transfection of titin kinase showed dramatic effects on p62 and Murf2 localisation as well as protein levels. This suggests that the interaction data derived from yeast two-hybrid screens, which indicate a signalling cascade ranging from titin kinase to NBR1, from NBR1 to p62 and finally to Murf2 point towards the existence of a huge signalling complex at the region of the sarcomeric M-band (data from Prof. M. Gautel). This signalling complex (or signalsome) can be easily perturbed upon the transfection of eukaryotic expression constructs encoding for the titin kinase, leading to altered subcellular localisations and protein levels of the investigated proteins. The multitude of interaction partners for p62 as well as Murf2 indicate further that the signalsome may also integrate signals from other signalling pathways and expand the variability of sarcomeric signalling via titin kinase.

6.3.2.2. Investigating titin kinase signalling *in vivo*

Recent investigations into the titin kinase activation via computer-simulations indicated the possibility of a tension-induced opening of the enzyme without a complete unfolding of the protein (Grater et al., 2005). The opening of the catalytic core by mechanically unfolding the regulatory domain of the protein suggests a mechano-related activation of titin kinase and indicates a feedback mechanism triggered by muscle activity and mechanical stress. To address the question, whether titin kinase activity can be triggered by the mechanical activity of muscle cells, we mechanically inactivated cardiomyocytes either via excess of potassium chloride in the culture medium, mimicking a cardiac arrest or via other compounds such as BDM or Verapamil (data not shown). Figure 33 gives an overview of the effects observed upon cardiac arrest on the localisation of various proteins identified as members of the titin kinase signalsome complex. Arrested neonatal rat cardiomyocytes develop an atrophic phenotype compared to non-arrested beating control cells, as judged by cell morphology and staining with an antibody recognising myomesin. First, we investigated the localisation of p62 within beating and arrested cardiomyocytes. As seen in figure 33 panel A, p62 displays in beating cardiomyocytes predominantly a sarcomeric localisation. Labelling with the p62 antibody can also be found at the intercalated discs as well as more weakly around the nucleus. Arrested cardiomyocytes however, display a less pronounced sarcomeric localisation, but a more prominent targeting of p62 to perinuclear compartments as well as to intercalated discs. Since p62 shows an altered localisation we questioned, whether Murf2 as a subsequent interaction partner in the putative titin kinase signalling pathway might also be affected by the beating arrest of the cardiomyocytes. Staining of cardiomyocytes with an antibody specific for Murf2 revealed an altered localisation of the protein from a predominant sarcomeric localisation in control cells to a more nuclear associated staining in arrested cardiomyocytes (see figure 33 panel B), indicating that Murf2 seems to shuttle from the sarcomere to the nucleus and serve as an intracellular messenger protein.

The search for putative binding partners of Murf2 revealed that the serum response factor (SRF), along with GATA-4 or MyoD a major transcription factor responsible for the development of muscle cells, might be a downstream target for titin kinase signalling (data from Dr. E. Rostkova and Prof. M. Gautel). Since Murf2 was found to shuttle to the nucleus of the cell, we investigated for changes in SRF localisation and protein levels upon induction of beating arrest in neonatal rat cardiomyocytes. As suggested by its function, endogenous SRF localises in beating control cells primarily to the nucleus of the cell. Mechanically arrested cells however, display a more heterogeneous localisation of SRF, ranging from a mostly nuclear localisation to a predominantly perinuclear aggregate-like localisation (see figure 33 panel C (b)). Analysis of the confocal pictures of arrested cells indicated further a general loss of SRF protein level upon treatment (data not shown). To evaluate the generally lower protein levels of SRF in arrested cardiomyocytes and to distinguish cytoplasmic from nuclear/cytoskeleton bound SRF protein pools, cardiomyocytes were lysed and fractionated via centrifugation in a soluble cytoplasmic and an insoluble pellet fraction. Figure 33 panel D shows that the nuclear pool as well as to a lesser extent the soluble protein fraction of SRF is reduced upon treatment with potassium chloride compared to beating control cells. The general reduction of SRF

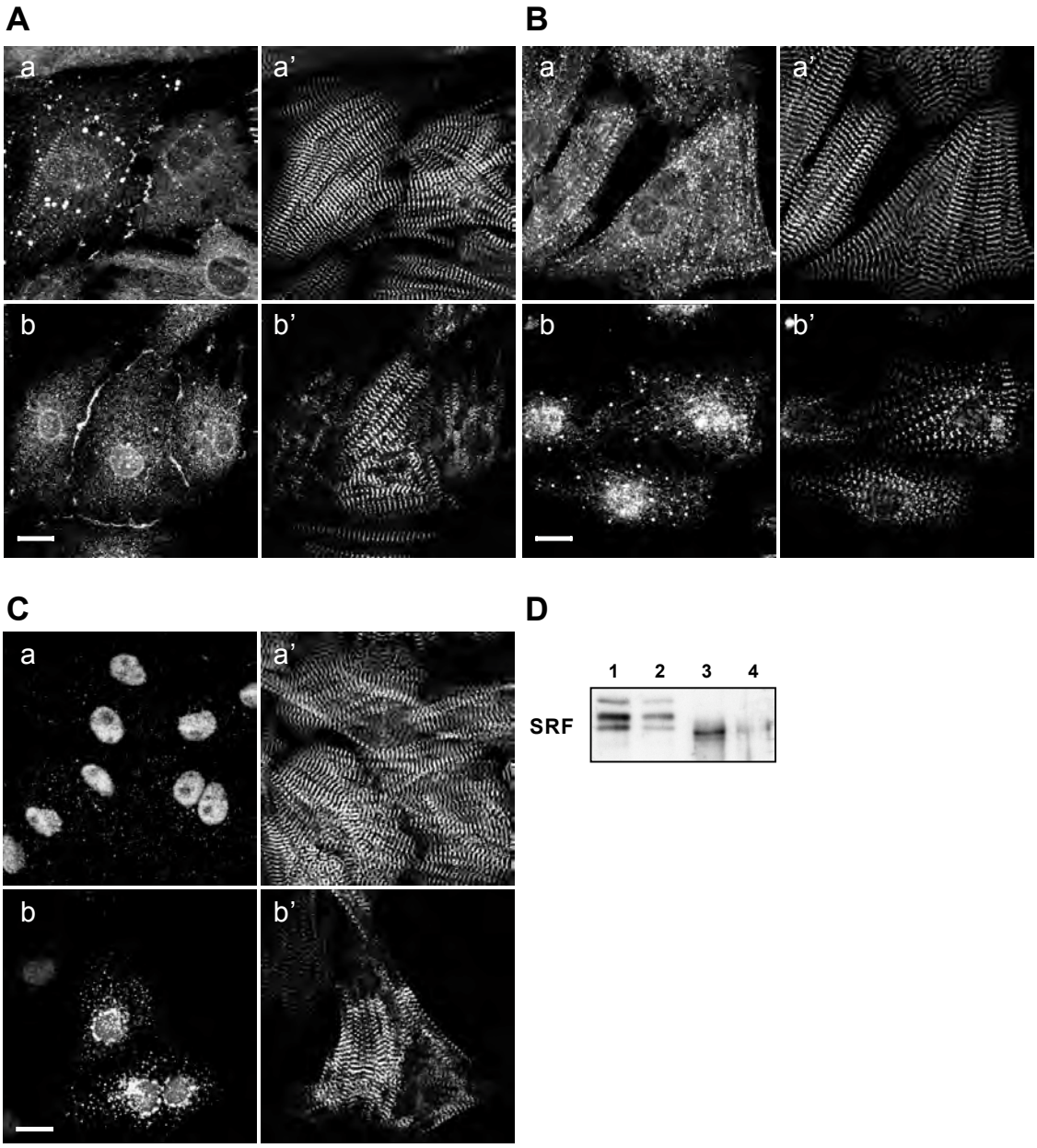

Figure 33. Cardiac arrest in neonatal rat cardiomyocytes induced by Potassium Chloride leads to the translocation of p62, Murf2 and SRF.

A-C. Confocal images of neonatal rat cardiomyocytes incubated for 4-5 days in the presence (b, b') or absence (a, a') of 50mM KCl in the culture medium. A general atrophic phenotype of the treated cells could be observed, as judged by decrease of overall cell size and staining with an antibody against myomesin (a', b') Scalebar = 10μm.

A. Endogenous p62 localisation (a, b) changes in treated cardiomyoctes from predominantly sarcomeric and intercalated disc associated staining to intercalated disc associated and perinuclear localisation of the protein. Note the disappearance of vesicular p62 staining in KCl arrest cells.

B. Murf2 (a, b) translocates from the M-band region of the sarcomere to the nucleus upon exposure of cardiomyocytes to potassium chloride or other inhibitors (data not shown).

C. Nuclear staining of SRF (a, b) in untreated cells is largely abolished in cardiomyocytes exposed to 50mM KCl. SRF localises in treated cells in perinuclear aggregates.

D. Immunoblot analysis of treated (lane 2 & 4) and control cell lysates (lane 1 & 3), fractionated into soluble cytoplasmic supernatant (lane 1 & 2) as well as insoluble nuclear and sarcomeric/cytoskeletal cell-pellet (lane 3 & 4). Staining with an antibody against SRF revealed a decreased protein level of SRF in the soluble as well as in the insoluble fraction of KCL treated cells. The difference in SRF-banding pattern between soluble and insoluble fraction indicates putative post-translational modification of the protein in the cytoplasm of the cell. Protein levels were normalised by Coomassie staining of samples prior to immunoblot analysis (data not shown).

levels and especially the dramatic loss of the nuclear protein fraction upon induced beating arrest of cardiomyocytes and the simultaneous shuttling of Murf2 into the nucleus of the cells suggest that Murf2 may trigger the signal from the titin kinase via an unknown mechanism to SRF.

In summary, we investigated a model system for the mechanically induced (in)activation of the titin kinase signalsome complex. Protein localisation, expression levels and the posttranslational modification of p62 and Murf2 as well as the transcription factor SRF were dramatically altered and the treated cells displayed a morphological phenotype that resembles muscles, which undergo severe atrophy. Especially the dramatically altered Murf2 and SRF localisations indicated that Murf2 might trIger the signal via an unknown mechanism towards SRF, leading to the translocation of SRF from the nucleus to the cytoplasm and subsequently towards its degradation.

6.3.2.3. The serum response factor (SRF)

One major transcription factor important for the development of muscle cells is SRF (serum response factor; (Chai and Tarnawski, 2002; Li et al., 2005; Schneider et al., 1994; Schneider et al., 1992)). SRF was revealed in a bacterial two-hybrid screen as a putative binding partner for the RING domain of Murf2 (pers. communication Prof. M. Gautel and Dr. E. Rostkova). The interaction in SRF is mediated by the C-terminal transactivation domain of the protein, suggesting that Murf might serve as co-activator or co-inhibitor of SRF-mediated gene expression. SRF contains in its N-terminal part a MADS-box, responsible for the dimerisation of the protein and the recognition and binding of SRE (Serum Response Elements) DNA motifs. SRF was recently shown to be modified by the small ubiquitin related modifier (Sumo; see earlier and figure 5 panel A), indicating an altered protein function upon modification by the Sumo pathway (Matsuzaki et al., 2003). SRF is generally localised to the nucleus of the cell (see figure 33 panel C (a) or figure 34 panel A (b)). On treatment of cardiomyocytes with potassium chloride however, the nuclear localisation of SRF was strongly reduced (see earlier). We asked, whether this effect might be correlated to the translocation of Murf2 to the nucleus of the cell upon KCl treatment. Since Murf2 interacts via its RING domain with SRF and proteins harbouring this domain were implicated as E3 enzymes of the SUMO-pathway, we hypothesized that Sumo modification of SRF might be responsible for the observed phenotype.

Figure 34 panel A shows the effect of the overexpression of Sumo1 on the localisation of endogenous SRF in neonatal rat cardiomyocytes. The nuclear localisation as well as the protein level of SRF is reduced in cells over-expressing epitope-tagged Sumo, suggesting that the SRF phenotype in KCl treated cardiomyocytes might be due to the modification of Sumo. Interestingly, this Sumo mediated translocation of SRF from the nucleus to the cytoplasma is not observed in non-muscle cell lines as seen in figure 34 panel B. Whereas cardiomyocytes show the shuttling of SRF from the nucleus to the cytoplasma in cotransfected cells, Cos-1 show a strong colocalisation of both proteins to the nucleus without the occurrence of the cytoplasmic SRF phenotype. This finding suggests that a specific factor might be responsible for the mediation of Sumo to SRF in cardiomyocytes, which is absent in the non-muscle cell line Cos-1.

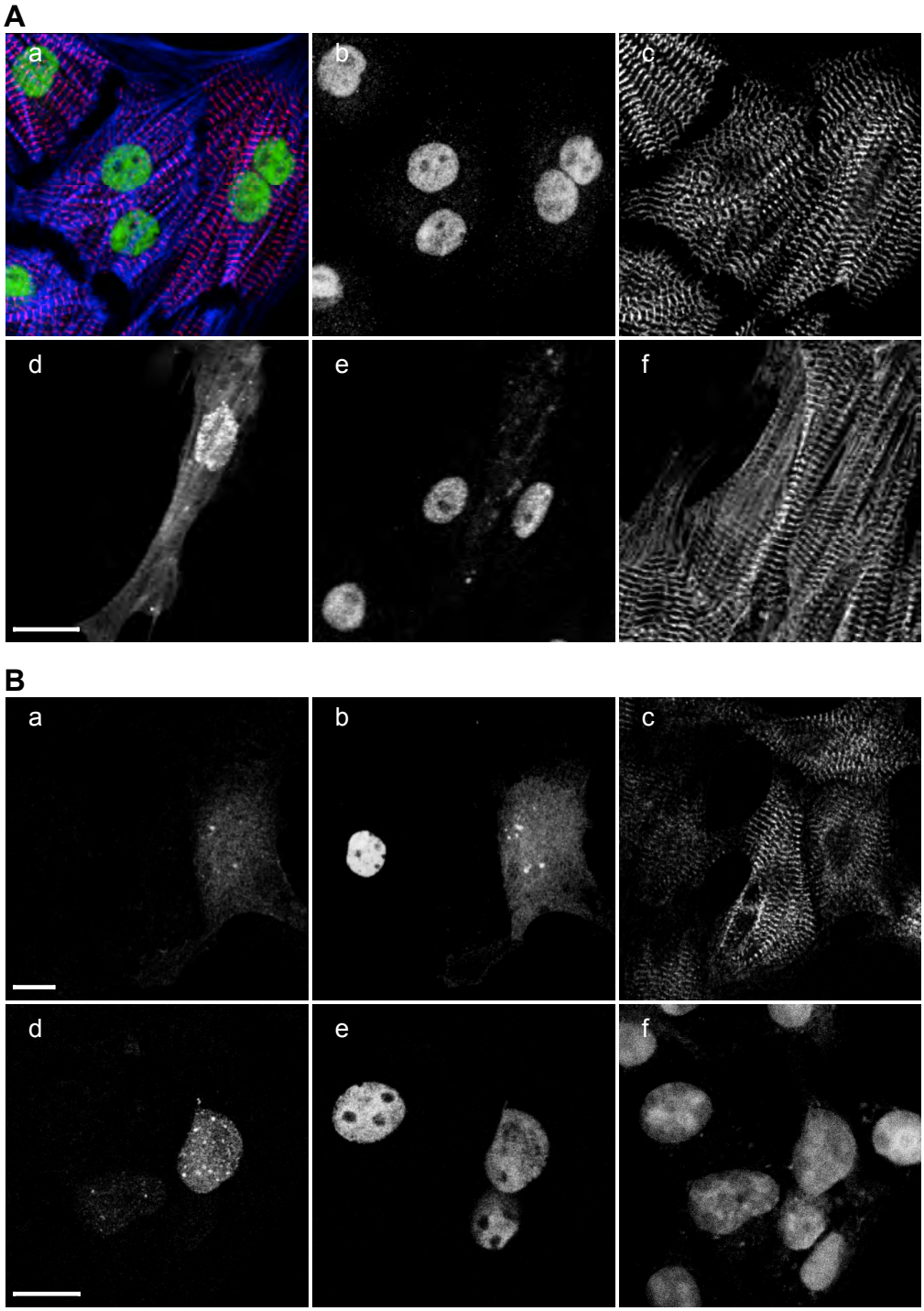

Figure 34. Effect of SRF modification by Sumo-1 in cardiomyocytes and the non-muscle Cos-1 cell line.

A. Effect of endogenous SRF localisation (b, e) in neonatal rat cardiomoycytes upon transient transfection of GFP-tagged Sumo1 (d). SRF localises exclusively to the nucleus of untransfected cardiomyocytes (b, e), whereas transfection of GFP-tagged Sumo1 (d) leads to the nuclear exclusion and degradation of SRF (e; transfected cell). Sarcomeric integrity remains unperturbed as judged by unchanged α-actinin localisation (f). Control cells were counterstained with myomesin (c) as well as fluorescently labelled phalloidin to visualise filamentous actin (a, blue in the overlay).

B. Muscle specific nuclear exclusion of SRF upon transfection of Sumo. Neonatal rat cardiomyocytes (a-c) as well as Cos-1 cells (d-f) were transiently cotransfected with GFP-tagged SRF (b, e) as well as HA-tagged Sumo1 (a, d). Only muscle cells display the nuclear exclusion phenotype of SRF in cotransfected cells, whereas SRF localisation remains unperturbed in Cos-1 cells. Cardiomyocytes were counterstained with myomesin (c), Nuclei of Cos-1 cells were labeled with DRAQ5 (f).

Scalebar = 10μm.

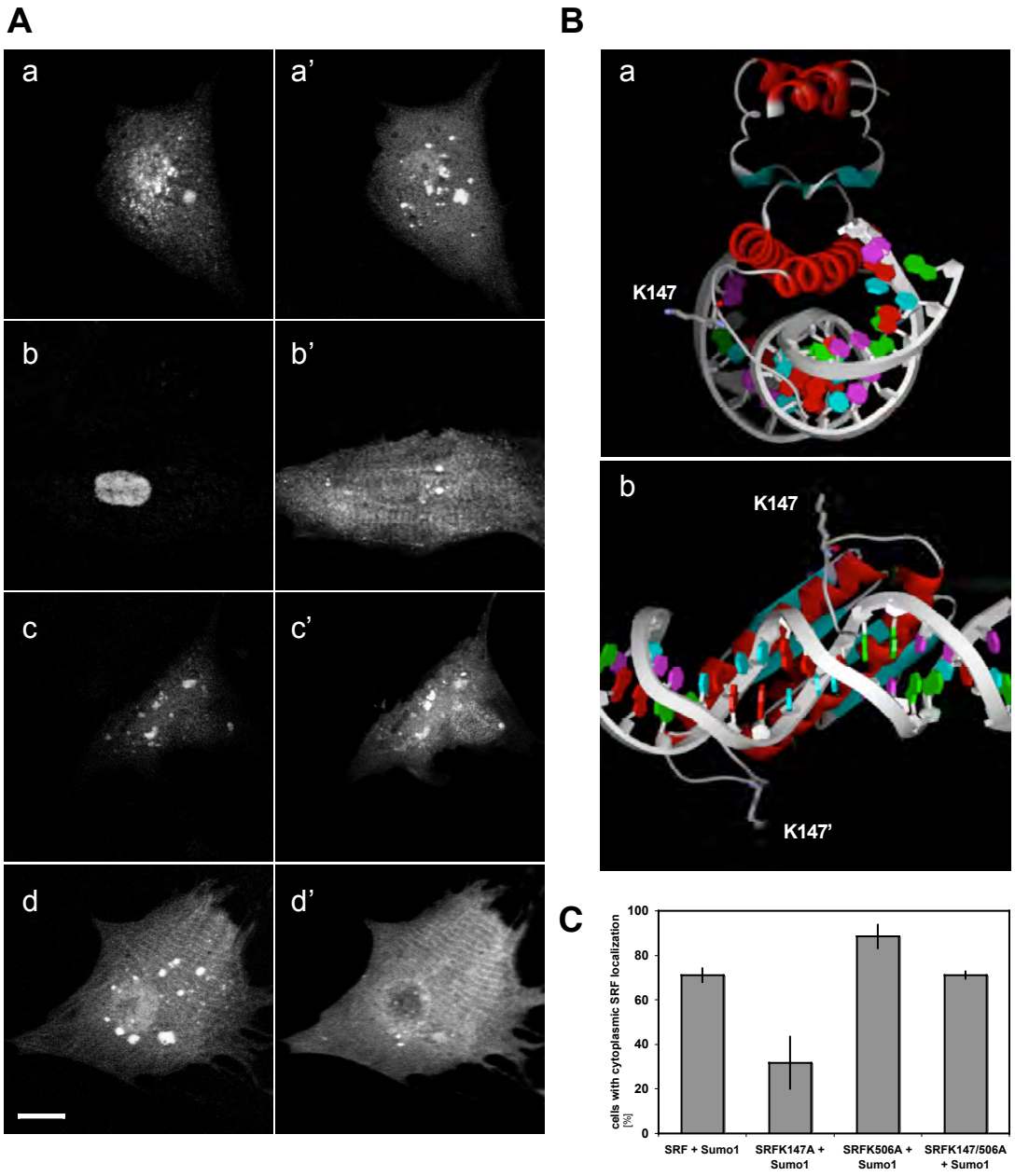

Figure 35. Nuclear exlusion of SRF is mediated by the covalent modification of lysine K147 via the sumoylation-pathway.

A. Transient co-transfection of neonatal rat cardiomoyctes with HA-Sumo1 (a', b', c', d') and GFP-tagged wildtype SRF (a), SRF K147A (b), SRF K506A (c) or SRF K147/506A (d). Only the K147A mutant of SRF showed a persitent nuclear targeting of SRF upon cotransfection with Sumo, whereas the wildtype, the K506A as well as the double mutant (K147A/506A) showed the previously described nuclear exclusion phenotpye of SRF. Scalebar = 10μm.

B. Analysis of the crystal structure of the SRF dimer together with an SRE (serum responsive element; protein database accession number: see text) reveals that the lysine residue K147 is located in the DNA binding site of the MADS-box of SRF. a: frontal view; b: ventral view (rotated 90° upwards in the vertical axis). Crystal data of SRF were from RCSB Protein data bank accession number: 1SRS.

C. Quantification of the cytoplasmic SRF levels (wildtype as well as mutants) upon co-transfection with Sumo1. SRF K147A shows with about 30% a significant decrease in cytoplasmic translocation of SRF compared to around 70% of wildtype and the SRF double mutant as well as 90% of K506A mutant positive cells.

Primary sequence analysis identified two Sumo-motifs (see earlier) within SRF. The first motif is located in the MADS-box of the protein around the lysine residue K147, the second motif is positioned close to the C-terminus of SRF at lysine residue K506. To assess which lysine residue might be a target for Sumo modification of SRF and responsible for the cytoplasmic SRF phenotype in cardiomyocytes, SRF mutants were established, mutating either one of the lysines or both residues. Figure 35 panel A depicts cultures of neonatal rat cardiomyocytes transfected with HA-tagged Sumo1 as well as with either GFP-tagged SRF wildtype, SRF K147A, SRFK506A or the double-mutant SRF K147/506A. Only the K147A mutant of SRF shows a significant difference from the cytoplasmic SRF phenotype, indicating that the Sumo-site responsible for the nuclear exclusion of SRF resides in the MADS-box of the protein. A quantification of the cytoplasmic SRF phenotype upon cotransfection with Sumo revealed that only 30% of cotransfected cells of the SRF K147A mutant showed the nuclear exlusion of SRF compared to around 70% of the wildtype as well as 88% of the SRF K506A mutant. The double mutant SRF K147/506A however, acted indistinguishable from the wildtype, indicating either the presence of a third atypical Sumo site within SRF or of an unknown second mechanism mediating the nuclear exclusion of SRF. Analysis of the available crystal structure of SRF (protein data bank accession numbers: 1SRS or 1K6O) revealed that the modified lysine residue K147A resides directly at the DNA binding site and that upon modification with Sumo, SRF might lose its ability to interact with the DNA (see figure 35 panel B).

In summary, we identified a putative Sumo mediated mechanism, responsible for the nuclear exclusion phenotype observed in KCl treated cardiomyocytes. The modification of SRF is mediated by the lysine residue K147, residing in the DNA binding domain of the protein. Analysis of the tissue specificity of this Sumo mediated SRF phenotype indicated that a muscle-specific factor is required for the catalysation of this modification.

6.3.3. Signalling and structural functions of telethonin

The small muscle-specific protein telethonin (also called T-cap) was originally identified as a binding partner for the first two immunoglobulin-like domains of titin Z1/Z2 (Gregorio et al., 1998; Mues et al., 1998) and was later shown to be a major substrate of the titin kinase (Mayans et al., 1998), suggesting a role of the phosphorylated protein in myofibrillogenesis. Apart from titin, telethonin interacts in its central part (residues 53-81) also with the muscle LIM protein (MLP; (Knoll et al., 2002)) as well as with minK, FATZ (Faulkner et al., 2000; Furukawa et al., 2001) and Ankrd2 (Kojic et al., 2004).

As a preferred substrate for titin kinase in developing skeletal muscle cells, telethonin is phosphorylated at serine residue S157. The close spatial association of telethonin with the kinase domain of titin however, is only apparent in developing myofibrils and telethonin localises later predominantly to the N-terminus of titin at the Z-disc. The following paragraphs investigate the structural functions of the titin kinase substrate telethonin.

6.3.3.1. Sarcomeric targeting of telethonin is mediated by the first 90 residues

The small muscle protein telethonin has been described as Z-disc interacting protein. To assess the functional role of telethonin in the Z-disc, full-length telethonin, the N-terminal 90 residues of telethonin as well as the C-terminal 73 residues of telethonin (amino acid residues 91-163) were transfected into neonatal rat cardiomyocytes (see figure 36). Full-length telethonin localised to the Z-disc and weakly to the M-band of the sarcomere as well as partially to intercalated disc structures in transiently transfected neonatal rat cardiomyocytes (NRCs). Cotransfected epitope-tagged MLP however, a reported binding partner for the central part of telethonin (see earlier), weakly colocalised with telethonin at the region of the Z-disc as well as the intercalated disc, whereas the majority of the muscle LIM protein showed only a diffuse cytoplasmic localisation (see figure 36 panel A (b)).

Next, we sought to identify the sarcomeric targeting domain of telethonin using two deletion mutants coding for amino acid residues 1-90 and 91-163 of the protein. GFP-tagged N-terminal as well as C-terminal telethonin were transiently transfected into neonatal rat cardiomyocytes, and fixed cells were counterstained with antibodies recognising the Z-disc protein α-actinin and the M-band protein myomesin to assess the subcellular localisation of the investigated protein fragments.

As seen in figure 36 (panel B (a-c)) C-terminal telethonin displays a mainly diffuse as well as nuclear localisation. Some protein fractions however, were weakly associated with the Z-disc and the M-band of the sarcomere. In contrast to the C-terminal part, the N-terminus of the protein localises exclusively to the Z-disc of the sarcomere, suggesting a strong interaction of a sarcomeric protein with this part of the protein.

In summary, telethonin displays in transiently transfected cardiomyocytes only a weak association with its reported binding partner MLP. The N-terminal 90 amino acids are sufficient to mediate the Z-disc targeting of the protein. The C-terminus however, containing the serine residue modified by the

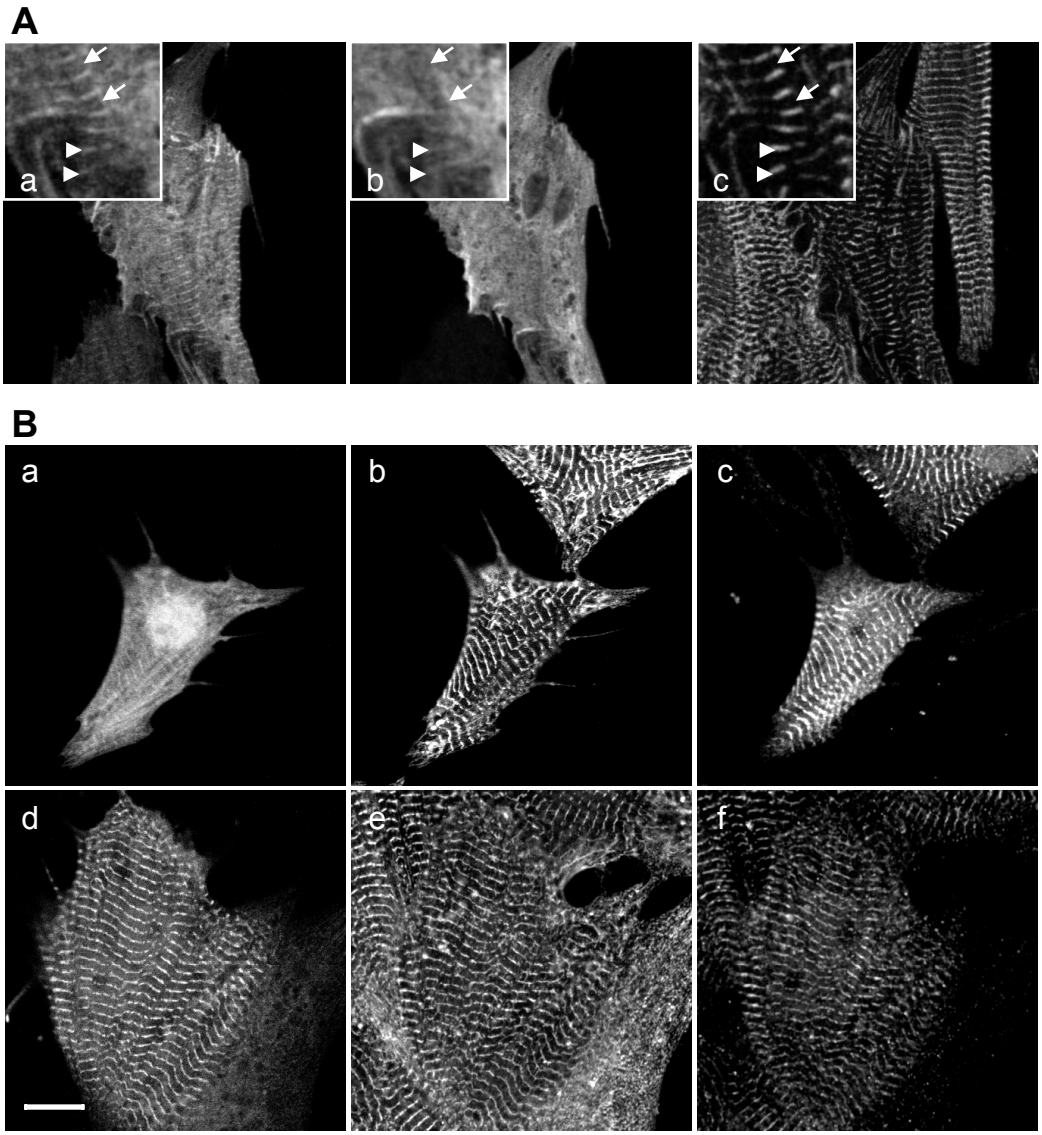

Figure 36. Subcellular localisation of full length as well as truncated telethonin mutants in neonatal rat cardiomoyctes shows that the sarcomeric targeting is mediated by the N-terminal 90 amino acids of the protein.

A. Neonatal rat cardiomoycytes transfected with full length GFP-tagged telethonin (a) and HA-tagged MLP (b) show a colocalisation of both proteins at the region of the sarcomeric Z-disc (arrowheads in inserts). Additionally, a weak association of telethonin to the region of the sarcomeric M-band was observed (arrows in a). Cells were counterstained with α-actinin (c).

B. Localisation analysis of telethonin truncation mutants. GFP-tagged C-terminal telethonin (residues 91-163; a) and N-terminal telethonin (residues 1-90; d) were transfected into neonatal rat cardiomyocytes and the subcellular localisation of the telethonin constructs was compared to α-actinin (b, e) and myomesin (e, f) counterstaining of fixed cells. Whereas N-terminal telethonin localises preferably to the sarcomeric Z-disc, telethonin residues 91-163 are only loosely associated to the Z-disc as well as M-band of the sarcomere and display a pronounced nuclear localisation of the protein.

Scalebar = 10μm.

titin kinase activity displays a predominantly nuclear and diffuse cytoplasmic localisation with a weak association to the Z-disc as well as the M-band of the sarcomere.

6.3.3.2. Biochemical analysis of the titin-telethonin interaction

Telethonin was initially identified as interaction partner of the first two N-terminal immunoglobulin-like domains of titin (Z1Z2; (Gregorio et al., 1998; Mues et al., 1998)). Early experiments in the lab of Prof. Wilmanns indicated that telethonin could be expressed in E.coli only in conjunction with titin Z1Z2 domains, since expression of full-length as well as N-terminal telethonin on its own resulted in the complete or partial aggregation of the protein in inclusion bodies (Zou et al., 2003). These experiments resulted further in a very rough model of the interaction, suggesting that telethonin forms at low concentrations a 1:2 complex with titin Z1Z2 using two antiparallel oriented Z1Z2 domains. This complex seemed further to dimerise at concentrations above 1mg/ml to a higher order of 2:4 for the telethonin:titin Z1Z2 complex.

To investigate the formation of the titin:telethonin complex *in vivo*, we established N- and C-terminally fused split-GFP constructs of titin Z1Z2 domains and cotransfected these constructs together with either HA-tagged full-length telethonin, telethonin residues 1-90 or telethonin residues 91-163 into Cos-1 cells. The reconstitution of intrinsic GFP fluorescence (protein complementation assay; see earlier) should reveal in conjunction with the different telethonin fragments the nature of the titin-Z1Z2 association (antiparallel or parallel) as well as the minimal binding site required for titin:telethonin association.

As shown in figure 37 panel A and B the two titin Z1Z2 molecules associated preferentially with full-length as well as the N-terminal 1-90 residues of telethonin in an antiparallel fashion. Some of the overexpressing Cos-1 cells co-transfected with full-length telethonin and YFP(N)-titin Z1Z2 and YFP(C)-titin Z1Z2 however, showed also the reconstitution of intrinsic GFP fluorescence (see figure 37 panel A (d-f), cell marked with an asterisk). These data in combination with the findings of a higher 2:4 complex formation of telethonin:titin (see earlier) suggests that in overexpressing cells, the threshold for the formation of higher telethonin:titin complexes may be reached. This effect could be only observed with full-length telethonin, indicating that the binding site for the formation of titin:telethonin multimers resides in the C-terminal part of telethonin. Transient transfection experiments of the C-terminal part of telethonin together with the split-GFP constructs for titin Z1Z2 showed no reconstitution of intrinsic GFP fluorescence in either case (data not shown), suggesting that the N-terminal part of telethonin is required for the initial complex formation.

These data could be confirmed in immunoblot-assays of cell lysates of Cos-1 cells co-expressing either HA-tagged full-length telethonin, telethonin N-terminal residues 1-90 or telethonin C-terminal residues 91-163 in combination with split-GFP constructs for titin Z1Z2 domains (YFP(N)-titin Z1Z2 together with YFP(C)-titin Z1Z2 and YFP(N)-titin Z1Z2 together with titin Z1Z2-YFP(C)). Since both halves of reconstituted YFP form a SDS-stable complex during GFP complementation and maturation, the interaction of the two proteins can be visualized by a shift in the molecular weight of the protein detectable in an immunoblot-assay after SDS-PAGE analysis. As seen in figure 37 panel C, this shift

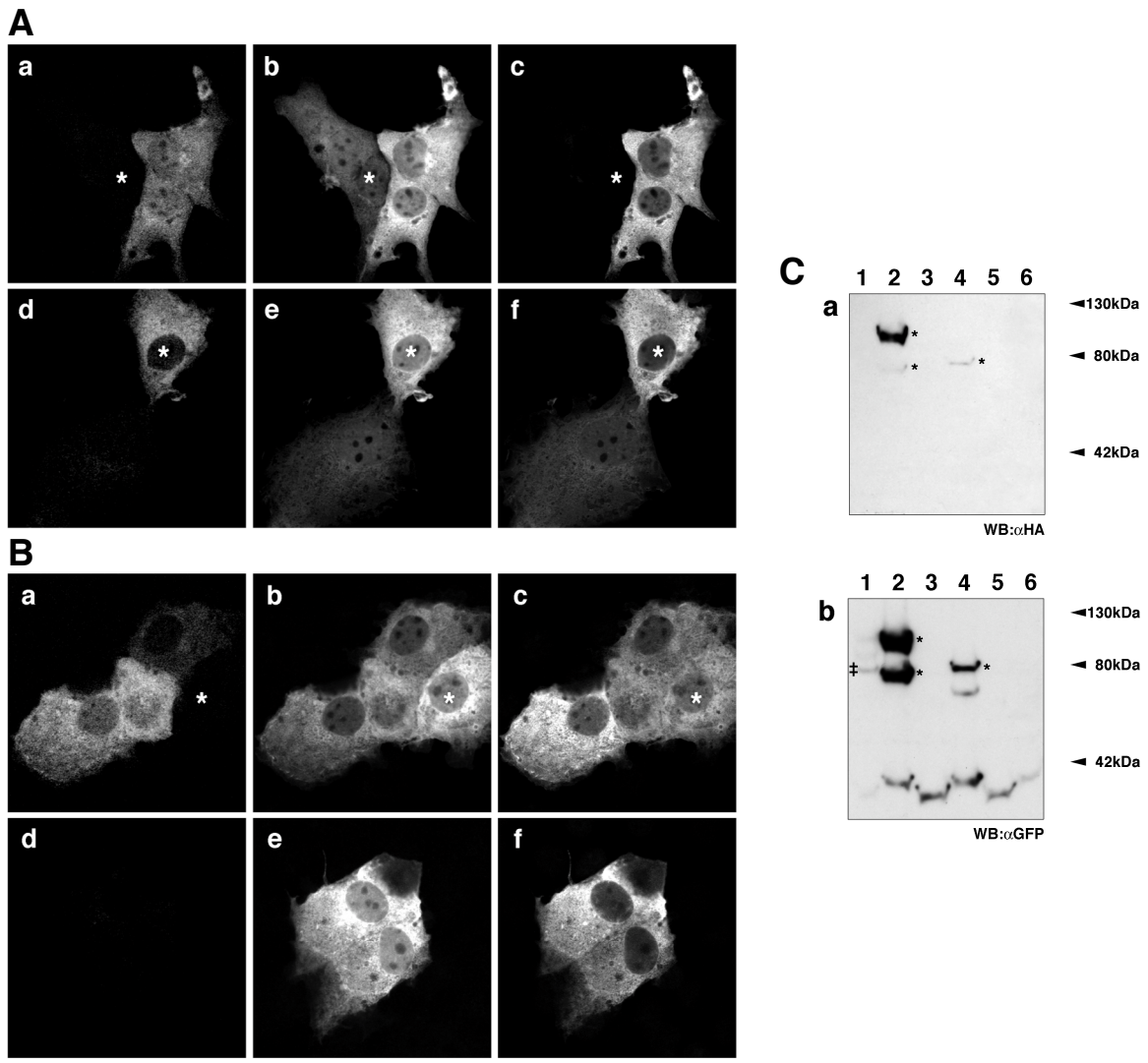

Figure 37. Titin Z1/Z2 and telethonin form a 2:1 complex in vivo with an antiparallel titin Z1/Z2 orientation.

A & B. Characterisation of the titin Z1Z2:telethonin interaction via protein complementation assay using the split-GFP system. Cotransfected cells were detected using a monoclonal GFP-antibody (c, f).

A. The interaction of full length HA-tagged telethonin (b, e) results in a reconstitution of intrinsic GFP-fluorescence (a, d) of cells transfected with YFP(N)-TitinZ1Z2 and TitinZ1Z2-YFP(C) (a-c; reflecting an antiparallel arrangement of the titin Z1Z2 domains) and in some cells co-transfected with YFP(N)-titinZ1Z2 and YFP(C)-titinZ1Z2 (d-f; reflecting a parallel arrangement of the two titin domain-pairs). Asterisk in (a-c) shows a telethonin single-transfected cell, which serves as a bleedthrough control for the intrinsic GFP-fluorescence channel. Asterisk in (d-f) displays a cell with reconstituted intrinsic fluorescence for the parallel titinZ1Z2 domain arrangement.

B. The interaction of N-terminal telethonin residues 1-90 (b, e) results in the reconstitution of intrinsic GFP-fluorescence (a, d) only in cells cotransfected with YFP(N)-titinZ1Z2 and titinZ1Z2-YFP(C) (a-c; titin Z1Z2 domains interact via telethonin in antiparallel fashion) but not in cells cotransfected with YFP(N)-titinZ1Z2 and YFP(C)-titinZ1Z2 (d-f; interaction of titin domains via telethonin in parallel fashion). Asterisk in (a-c) shows a cell positive for only one of the split-GFP constructs, resulting in no detectable signal in the GFP-channel (a).

C. Immunoblot-analysis of co-transfected Cos-1 cells using antibodies recognising the HA-epitope (a) and the GFP-epitope (b). Lysates of Cos-1 cells co-transfected with either HA-tagged full length telethonin (lanes 1 & 2), N-terminal telethonin residues 1-90 (lanes 3 & 4) or C-terminal telethonin residues 91-163 (lanes 5 & 6) as well as the split-GFP pairs YFP(N)-titinZ1Z2 and YFP(C)-titinZ1Z2 (lanes 1, 3, 5; protein complementation of GFP in the parallel case of titin:titin interaction) or the split-GFP pairs YFP(N)-titin Z1Z2 and titinZ1Z2-YFP(C) (lanes 2, 4, 6; protein complementation of GFP in the antiparallel case of titin:titin interaction). Bands marked with asterisks are reactive with the HA as well as with the GFP antibody. Bands marked with a double-cross (‡) indicate also the formation of protein complementation for the parallel titin:titin complex in presence of full length telethonin, indicating the formation of a 2:4 telethonin:titin complex (see text).

in the molecular weight of the YFP-labelled titin Z1Z2 domains is visible only in the antiparallel case of the titin interaction with full-length and N-terminal telethonin (high molecular weight bands in figure 37 panel C (b) lanes 2 and 4), whereas no shift from the monomer state of YFP-labelled titin Z1Z2 proteins occurs in the cells cotransfected with C-terminal telethonin (lanes 5 & 6 of the same figure). Some bands with higher molecular weight than the split-GFP titin Z1Z2 monomers could also be identified for the parallel titin interaction if cotransfected with full-length telethonin (bands marked with a double-cross (‡) in lane 1 of figure 31 panel C (b)), again suggesting the formation of higher complexes by the C-terminal part of full-length telethonin (see earlier).

Interestingly, some of the high molecular weight bands generated by the “cross-linking” of the titinZ1Z2 domains by GFP-maturation are in addition reactive for the HA-antibody, recognising the HA tag in the telethonin fusion proteins (bands marked with an asterisk in figure 37 panel C). This points to the fact that the complete titin:telethonin complex may be still intact during the SDS-PAGE electrophoresis, despite the denaturing effect of the SDS detergent, suggesting a very strong interaction of the two titin Z1Z2 domains with telethonin.

In summary, the data presented indicate a profound role of telethonin in the antiparallel cross-linking of the titin Z1Z2 domains. The minimal binding site sufficient for mediating the interaction of titin with telethonin is situated in the first 90 amino acid residues of the muscle-specific protein telethonin. Data from our *in vivo* experiments as well as from recent publications indicate further that the C-terminus of the protein might be involved in the formation of titin:telethonin multimers. The interaction of titin with telethonin is independent of the interaction with MLP and further not dependent on the S157 phosphorylation site in the C-terminus of telethonin. Telethonin also contains a weaker M-band targeting domain, which resides in the C-terminal 70 residues and might reflect the interaction with the titin kinase domain.

7. Discussion

The sarcomere of striated muscle cells was for a long time a model system for the study of large ordered multi-protein complexes. Its numerous structural components, which have to be spatially and temporally assembled correctly provide further binding sites for a multitude of proteins (Tskhovrebova and Trinick, 2003). Besides their important structural functions, proteins of the sarcomere are further involved in the regulation of metabolic pathways and give feedback or input into various signalling pathways, leading to changes in the global cellular protein expression and the adaption to e.g. mechanical stresses. Recent publications indicate that the sarcomere of muscle cells is not only a static assembly of structural components, but it emerges that a very dynamic interaction network of adaptor and signalling proteins as well as posttranslational modifiers is constantly modifying and remodelling the comparatively long-lived interactions of sarcomeric components like myomesin, myosin, α-actinin or titin.

One of the important structures of cross-striated muscle cells is the sarcomeric M-band. Its major components are the myosin molecules, which form the thick filament, the C-terminus of the giant protein titin (connectin), which is thought to form an antiparallel interaction with the titin C-terminus coming from the other half of the sarcomere as well as the proteins of the myomesin protein family, namely myomesin, M-protein as well as miamesin (myomesin 3). Titin is thought not only to be a major scaffold protein for the sarcomere, but further contains a protein kinase site adjacent to the sarcomeric M-band, suggesting a titin kinase regulated muscle-specific signalling pathway (Mayans et al., 1998). Other known structural components of the M-band comprise of the family of the four and a half LIM domain proteins (FHL), like DRAL or FHL1 (this study, (Lange et al., 2002)) as well as the muscle isoform of creatine kinase (MMCK, (Hornemann et al., 2003)).

The major goal of this study was to gain insight into the complex interplay of protein-protein interactions in the M-band of the sarcomere as well as to investigate the signalling pathways emerging from M-band proteins, such as the titin kinase domain as well as DRAL. Figure 38 summarises known and novel interactions of M-band components, some of them identified and characterised in this dissertation, as well as proteins associated to signalling via titin kinase and the modulation of protein function via DRAL or the sumoylation pathway. References for indicated protein associations in figure 38 are found later in the discussion as well as throughout the results chapter.

7.1. Myomesin interactions

The myomesin protein family consists of three different members: myomesin, M-protein (myomesin 2) as well as miamesin (myomesin 3). During the last few years it was possible to map binding sites for their main structural interaction partners (see figure 39). The N-terminus of M-protein as well as myomesin was implicated to bind to the thick filament protein myosin (Obermann et al., 1996; Obermann et al., 1997; Obermann et al., 1995; Obermann et al., 1998), whereas the central part of both proteins harbours a binding site for MMCK (see Results paragraph and (Hornemann et al., 2003)

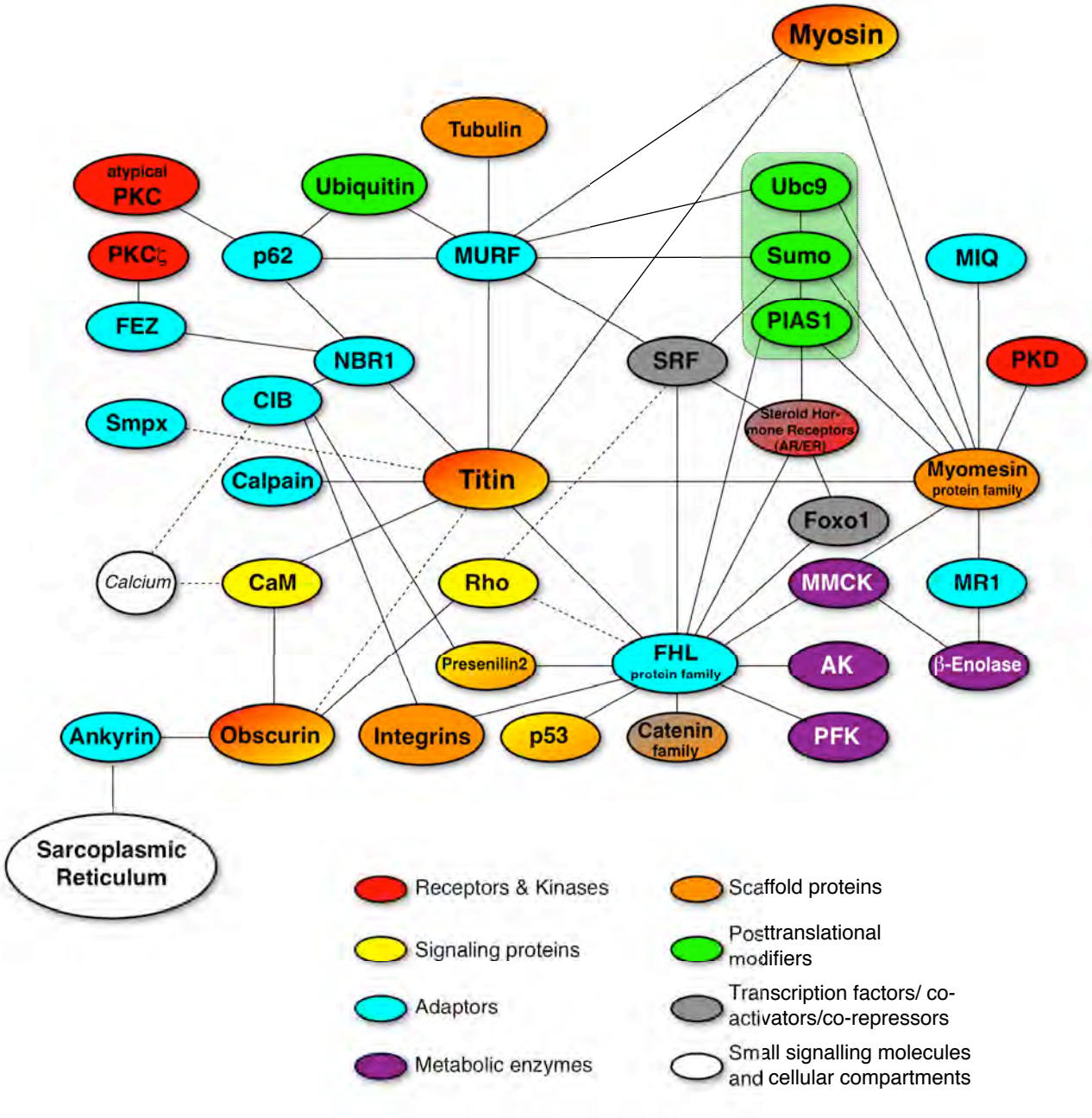

Figure 38. Crosstalk and crosslinks at the sarcomeric M-band.
Schematic representation of protein interactions and protein-protein associations at the sarcomeric M-band forming a complex network of structural, non-structural proteins and signalling molecules. Many proteins have multiple functions, like the structural protein titin, whose kinase domain is situated in the M-band. Many of these interactions provide a feedback into transcriptional pathways, like the androgen receptor pathway, SRF, the Wnt-signaling pathway via the interaction of DRAL with β-catenin or p53 signaling. The localisation of several proteins like obscurin or DRAL display multiple binding sites within the cell, suggesting the presence of a very dynamic network of protein-protein interactions overlying the scaffolding effect of the structural components of the sarcomere. Lines indicate demonstrated protein-protein interactions. Dashed lines indicate putative associations of proteins and small signalling molecules, such as calcium. Proteins of the sumoylation machinery are further enclosed in a green rectangle.
Adapted from Prof. M. Gautel.

Myomesin

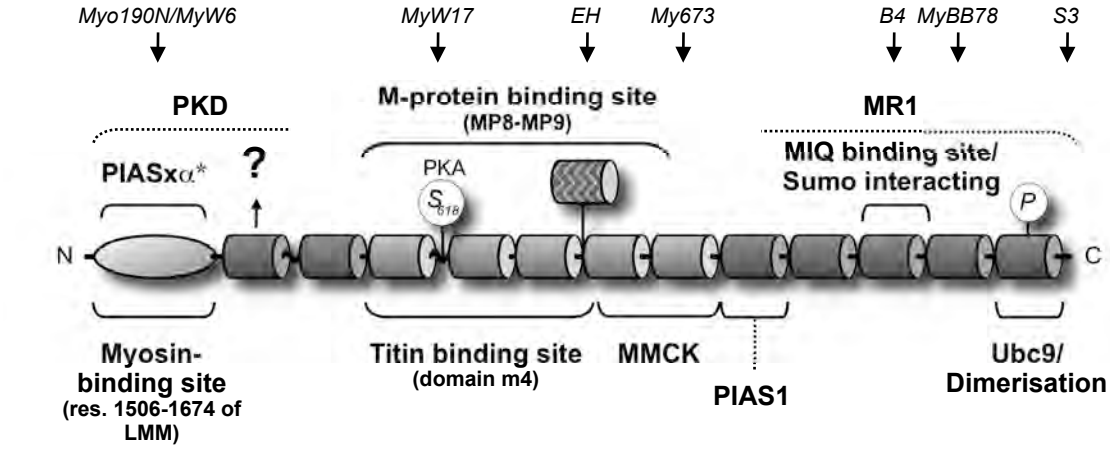

M-protein

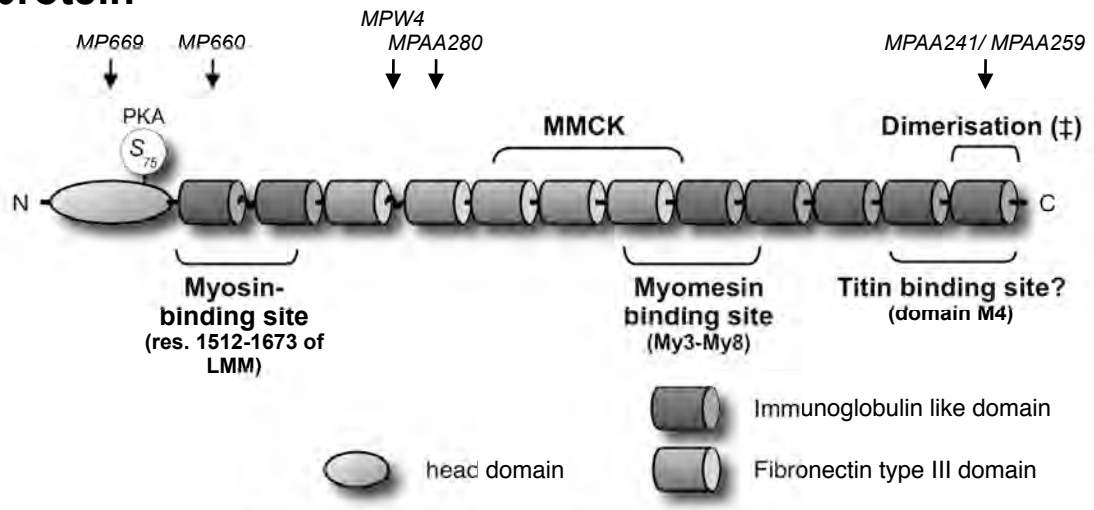

Figure 39. Schematic presentation of known and novel myomesin and M-Protein protein interactions.

Proteins of the myomesin-family harbor binding sites for several structural components of the sarcomere. The N-terminal domains are thought to offer a binding site with myosin (residues 1506-1674 of light meromyosin (LMM) for myomesin and residues 1512-1673 of LMM for M-protein). Myomesin and M-protein contain binding sites for titin domain M4 in the central part of myomesin (fibronectin type III domains 4-6) and at the C-terminus of M-protein (Ig domains 12-13). Myomesin and M-protein are further crosslinked via interactions with each other; domains 3-8 of myomesin interact with domains 7 and 8 in M-protein. The dimerisation of myomesin is mediated by the C-terminal Ig domain of the protein, whereas M-protein may in addition to its dimerisation via domain 13 (‡) form trimers of M-protein dimers, leading to a hexagonal arrangement of the whole M-protein complex (pers. comm. Dr. Nikos Pinotsis, Hamburg). Miamesin, the third member of the myomesin family, highly homologue to M-protein, is also able to form dimers via the conserved binding site in its C-terminal Ig domain (domain 13; data not shown). An unknown binding partner mediates the targeting of myomesin domain 2 to the sarcomere.

The muscle isoform of creatine kinase (MMCK) interacts with myomesin and M-protein, with its binding site situated at the C-terminus of the fibronectin type III domain cluster.

Myomesin interacts further with enzymes of the sumoylation pathway: Ubc9 at the C-terminus of the protein (domain 13), Sumo at domain 11 as well as PIAS1 with domain 9 and PIAS1xα with the N-terminus of the protein (domain 1; asterisk: results Dr. Katrin Hayess, Potsdam).

The interaction of MIQ, an uncharacterised protein with domain 11 of myomesin can be specifically competed by the binding of the B4 antibody. The epitopes and names of different antibodies (in italics) are indicated in the schematic presentations of the two proteins (see also Obermann, Gautel; 1996). Phosphorylation sites in myomesin (S618, domain 13) and M-Protein (S76) are indicated (Obermann, Gautel 1996; Obermann, van der Ven 1998). Not further submapped interaction sites of myomesin with MR1 and PKD are also indicated.

as well as references therein). A binding site for the elastic filament system of the sarcomere, the giant protein titin was mapped in myomesin to domains 4 to 6 (Obermann et al., 1995). Nothing was known about potential interaction partners for the C-terminus of myomesin. Using the yeast two-hybrid screen, we demonstrated that myomesin is able to dimerise via its C-terminal immunoglobulin like domain (domain 13). Since myomesin is thought to be the major structural component of the M-band, the discovery of the antiparallel myomesin dimerisation has major implications on how myomesin might serve its function as a cross-linker of myosin molecules in a web-like structure and the overall structural organisation of the sarcomeric M-band (see below).

The myomesin interaction partners PIAS1, Ubc9 and Sumo identified in the yeast two-hybrid screens indicated the modification of myomesin by the sumoylation pathway (see below). To date, proteins of the myomesin family were only known as substrates for several serine protein kinases, like PKA and PKD (Haworth et al., 2004; Obermann et al., 1997; Obermann et al., 1998). The N-terminal phosphorylation sites in myomesin (S618) and M-protein (S76) were implicated in the modulation of the interaction of both proteins either to titin domain M4 or myosin. A phosphorylation site was also mapped to domain 13 of myomesin, however, identification of the exact serine residue involved in the posttranslational modification of myomesin and the function of the phosphorylation of this domain remains elusive, since the phosphorylation of myomesin at domain 13 had no influence on the dimerisation of the protein (Lange et al., 2005).

Recent publications as well as findings in our yeast two-hybrid screen showed further an interaction of myomesin with several unknown/uncharacterised proteins. The 142 amino acids protein MR1 (myofibrillogenesis regulator 1) was identified in a yeast two-hybrid screen as potential binding partner of myomesin, β-enolase and regulatory myosin light chain (MLC; (Li et al., 2004a)). Interestingly, β-enolase was previously identified as an M-band protein, which interacts with the muscle isoform of creatine kinase (MMCK; (Foucault et al., 1999; Keller et al., 2000)). However, subcellular localisation studies of MR1 in transiently transfected neonatal rat cardiomyocytes using a GFP-tagged construct showed only a marginal binding of the protein at the sarcomeric M-band (data not shown), suggesting a more transient interaction of MR1 with myomesin. MIQ (M-band interacting glutamine-rich protein) however, an uncharacterised protein identified in the yeast two-hybrid screen with myomesin domains 9-13 showed a pronounced colocalisation of GFP-tagged MIQ constructs with the sarcomeric M-band, suggesting a strong interaction of both proteins. This interaction was largely abolished in the presence of myomesin B4 antibody, indicating a competition of MIQ and B4 for the same binding site/epitope within myomesin domain 11. Attempts to clone the missing N-terminal part of the protein using the 5'RACE method failed, possibly due to the unusual presence of highly repetitive sequences within the N-terminal part of the protein. The search for further interaction partners of MIQ suggested only myosin heavy and myosin light chain as putative interaction partners. The function of this protein remains therefore elusive and is even more complicated by the presence of a putative Sumo binding site within myomesin domain 11. The generation of an antibody specific for MIQ might help to reveal some insights into the function of the protein but could possibly be undermined by a low sequence homology of the amino-acid sequence between human, mouse and rat MIQ.

7.1.1. Generation of a three-dimensional M-band model

The major result of the yeast two-hybrid screen searching for novel binding partners of the C-terminal myomesin domains was the finding that myomesin is able to form antiparallel dimers via its last immunoglobulin-like domain. This result has significant impact on the current model of the sarcomeric M-band.

Combining observations from electron micrographs, model interpretations derived from electron density maps as well as biochemical interaction data from the essential structural M-band components with this new result, we were able to generate a new three-dimensional model of the sarcomeric M-band (see figure 40). The major connections between the myosin rods are brought about by myomesin molecules, which bind with their N-termini to myosin and form antiparallel dimers via their last C-terminal domain 13. The central part of myomesin is thought to bind the M4 domain of titin as well as the muscle isoform of creatine kinase (MMCK) and may form the proposed central M-filament structure. It appears that myomesin may function together with the M-band part of titin as the major myosin cross-linking complex and acts as the M-band equivalent of α-actinin in the Z-disc of the sarcomere. Since the exact location and organisation of myosin and titin domains in the M-band are not fully understood, we simplified their appearance in the model by using continuous cylindrical rods and ignoring the fact that e.g. myosin tails interdigitate antiparallelly. Although the myosin binding site for myomesin was mapped to light meromyosin residues 1506 to 1674 and the titin binding site for myomesin is located in domain M4, no information on the three-dimensional organisation on either of these interactions is available.

In our model the thick filaments are cross-connected by a myomesin bridge consisting of two myomesin proteins which interact end-to-end, forming a cross-bridge that contains 24 serially linked Ig-like or Fn type III domains with an overall slack length of about 110nm. Single molecule studies using titin Ig-domains and PEVK as well as N2B fragments indicated that such sequences are highly elastic and generate a restoring force by an entropic chain mechanism (Linke et al., 2002). It is likely that myomesin bridges behave in a similar way in this model (pers. comm. Dr. Irina Agarkova and Roman Schönauer).

The M-band appears in the 3D model as an elastic network with significant capacity for reversible deformation as reflected by the curving of the connecting M-bridges between the thick filaments. Interestingly, the projection of the model in the cross-sectional plane fits the data obtained by analysis of electron micrographs in a satisfactory manner (Crowther and Luther, 1984; Luther and Squire, 1978; Squire, 1981). In our model, the electron dense M4 line is generated by the N-termini of myomesin in conjunction with titin M4. The M4 line is found in all kinds of striated muscles and was early associated with the presence of myomesin. It has been speculated that the general electron density of the M-band may be contributed by MMCK (Strehler et al., 1983). However, MMCK seems not to play an important role in the structure of the sarcomere, since mice deficient for MMCK show no ultrastructural changes in the assembly of the M-band (van Deursen et al., 1993). According to our model, MMCK binding to

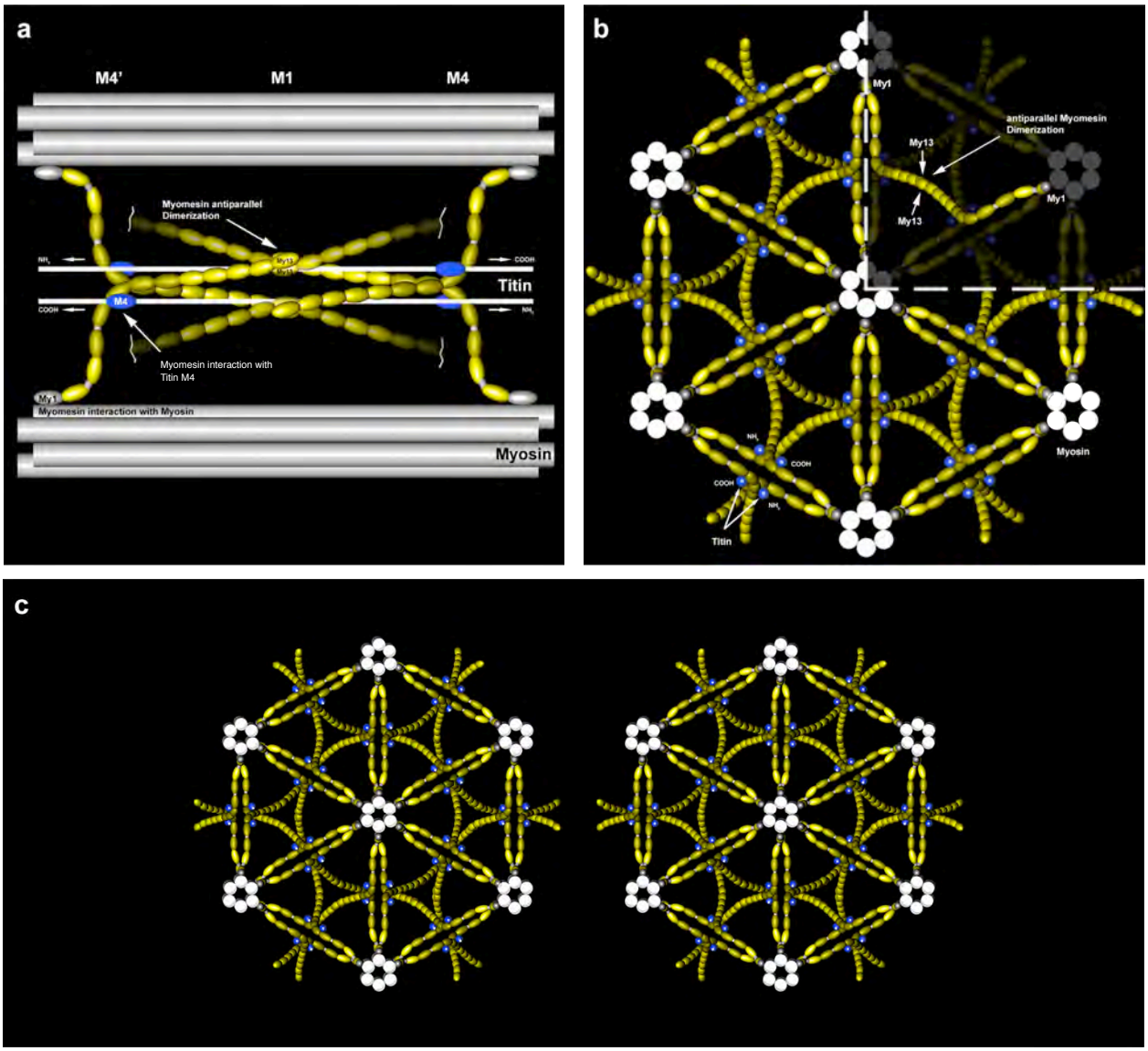

Figure 40. Three dimensional model of the M-band.
Three dimensional model of the sarcomeric M-band based on molecular interactions identified by the myomesin yeast two-hybrid results (see above) and previous publications. Myomesin is depicted in yellow, titin and myosin in gray; immunoglobulin domains in myomesin are presented in lighter shade, fibronectin type III domains in darker shade. Due to the lack of detailed information on the domain arrangement, titin and myosin are respresented only schematically, with the exception of the titin M4 domain (in blue), the binding site for myomesin.
A. Longitudinal view showing two myosin rods, their associated titin strands at this section plane and the connecting myomesin molecules. Antiparallel associated myomesin dimers are indicated.
B. Projection of the molecular interactions between myomesin, titin and myosin in a cross section. The position of a myomesin dimer, crosslinking two neighboring myosin rods is highlighted.
C. Stereo-view of the M-band cross section in B.

domains 7 and 8 of myomesin would occur adjacent to the M4 line of the muscle and in close vicinity to the is2 region of M-band titin, the binding site of DRAL. Another protein interacting with MMCK is M-protein, whose expression is restricted to fast-twitch and cardiac muscles. This tissue specific expression in conjunction with the appearance of the electron dense M1 line in electron micrographs suggests that the source of the electron dense material might be due to M-protein localisation in the middle of the M-band.

Current models of the sarcomeric M-band depict titin as an extended molecule, whose C-termini overlap in the region of the sarcomeric M-band. Due to the lack of data concerning the localisation of titin domains and the presence of several long sequence insertions without any apparent structure it cannot be excluded that titin shows a bent conformation or a loop-like organisation within the M-band.

In conclusion, our model integrates data from biochemical interaction studies, ultrastructural reconstitutions and electron micrographs. Further biochemical studies of M-band proteins, the targeted removal of several M-band components as well as new techniques in the processing of ultrastructural electron micrographic images might shed even more light into the ultrastructure of the M-band.

7.1.2. Myomesin and Sumo

The posttranslational small ubiquitin related modifier (Sumo) is a member of the growing ubiquitin-like protein family. Sumo modification of target proteins regulates general cellular functions. To date a multitude of Sumo-modified proteins has been identified, however, no sarcomeric protein and very few cytoplasmic or membrane proteins like Glut1 and Glut4 were implicated in the posttranslational modification via the sumoylation pathway (Giorgino et al., 2000). In fact, most of the identified target proteins for the sumoylation machinery belong to the group of transcription factors or coactivators/corepressors of transcription, suggesting a pivotal role for the sumoylation of proteins in the regulation of the protein expression.

Two proteins of the sumoylation pathway were identified during the yeast-two hybrid screen for putative interaction partners of myomesin domains 9-13: the Sumo conjugating enzyme Ubc9 (E2 enzyme) as well as the Sumo E3-ligase PIAS1, which interact with domain 13 and 9 of myomesin, respectively. Forced yeast two-hybrid analysis further identified a potential interaction site for Sumo within domain 11 of myomesin. Primary sequence analysis of myomesin identified in conjunction with the alignment of cross-species myomesin sequences, up to nine putative sumoylation sites, which follow the conserved sumoylation motif psi-K-x-D/E (Rodriguez et al., 2001). Only two of these are highly conserved throughout evolution, lysine 1197 in domain 11 as well as lysine residue 1589 located in domain 13 of myomesin (see figure 14 panel A). Mutation of four of these putative sumoylation sites within domains 11 (lysines 1150 and 1197) and 13 (lysines 1589 and 1603) of myomesin however, failed to show a significant change in the SDS-PAGE band-pattern of myomesin after *in vitro* sumoylation of the protein. This suggests that the sumoylation sites within myomesin may not follow the classical sumoylation motif, but belong to a group of uncharacteristic Sumo-sites as also reported for other proteins like the human centromere protein CENP-C fragment (Chung et al., 2004).

Only myomesin domains 2-EH-8 (containing the EH fragment) showed a significantly lower sumoylation efficiency compared to the same domains of myomesin without EH domain. The EH fragment of myomesin is thought to be the domain equivalent of the titin PEVK region, acting as elastic spring element via an intrinsically disordered conformation. A distinct feature of this region is its richness in serine and proline residues (hence the alternative name SP-domain) giving the EH domain the characteristical appearance of a PEST sequence (abbreviavtion of proline, glutamate, serine and threonine rich sequences). PEST sequences have emerged during the last few years as strong proteolytic signals, targeting proteins harbouring these motifs to the ubiquitin mediated proteolysis via the proteasome pathway (Rechsteiner and Rogers, 1996). However, the significantly lower sumoylation efficiency of the EH splice isoform cannot be explained by the presence of typical PEST sequences within the EH domain of myomesin, since sumoylation of proteins containing PEST sequences are thought to increase the stability of the respective protein (Bies et al., 2002). Since there are no data available for the protein turnover of myomesin or EH-myomesin and the influence of the EH fragment on the stability of the protein, one can only speculate about a decreased half-life of the EH-isoform of myomesin.

The heterogenous subcellular localisation of Ubc9, PIAS1 and of the three different Sumo proteins indicates further the multiple functions of the sumoylation machinery within cardiomyocytes. Although PIAS1, Ubc9 and the different Sumo proteins could be found in a cell-stage dependent way at the sarcomeric M-band, no obvious biological function of Sumo modified myomesin could be identified. Immunoblot analysis of various whole muscle extracts showed furthermore no apparent shifts in the molecular weight of endogenous myomesin other than the isoform specific influence of the EH domain, suggesting that only a minute fraction of the protein might be sumoylated at a certain time-point which might be difficult to detect in these assays.

7.2. Dimerisation of M-protein and miamesin (myomesin 3)

The results obtained for domain 13 of myomesin strongly indicated a similar function of M-protein as well as of miamesin domain 13 in the dimerisation of these proteins. Alignment of the protein sequences of myomesin with M-protein as well as miamesin strongly supported this theory, since all proteins display a high degree of identity or homology in the C-terminus of the protein. Forced yeast-two hybrid assays as well as co-immunoprecipitations, however, failed to confirm this hypothesis, since neither of the assays displayed any homodimerisation of M-protein or heterodimerisation of M-protein with myomesin.

The generation of M-protein constructs for X-ray crystallography should shed some light into the apparent differences between myomesin and M-protein. First results on the successful expression and crystalisation of M-protein domains 12-13 carried out by Dr. Nikos Pinotsis indicate that M-protein might indeed interact with itself. The dimerisation of M-protein was additionally confirmed using the split-GFP system, which indicated further that the interaction also occurs in an antiparallel fashion. The

recent discovery of a third member of the myomesin protein family, miamesin, indicated that the dimerisation of myomesin-like proteins via domain 13 might be a distinct feature of all family members. First results investigating the homodimerisation of miamesin domain 13 again utilising the split-GFP system seem to confirm this hypothesis.

How is M-protein as well as miamesin integrated into the three-dimensional M-band? Assuming that the overall minimal binding sites for the different interaction partners of myomesin, M-protein and miamesin are conserved within the protein family, namely an N-terminal interaction site for myosin, a central binding site for titin and a C-terminal dimerisation site, one could speculate that the positioning of M-protein and miamesin within the M-band resembles in great parts that of myomesin. Since M-protein and especially miamesin are poorly biochemically characterised these proteins have to be analysed more thoroughly.

7.3. Structural and signalling functions of DRAL (FHL2)

DRAL (FHL2) emerged during the experiments and in the litreature as a very versatile protein, displaying cell type dependent subcellular localisations and interaction partners. DRAL was characterised as specifically expressed in cardiac muscle. The protein is targeted to two different sites within the sarcomere: the N2B-region of the sarcomeric I-band and to a lesser extent to the M-band of the sarcomere. Using yeast-two hybrid analysis and biochemical interaction methods, two regions within the giant protein titin, namely the unique sequence 3 within the cardiac N2B-region of titin and the insertion sequence 2 of M-band titin, were identified as minimal binding sites, anchoring DRAL to the sarcomere. Intrigued by the similarity of the localisation pattern of DRAL compared with several enzymes of metabolic pathways, e.g. the adenylate kinase and the phosphofructokinase, we have shown that DRAL might mediate the anchorage of these enzymes to the I-band as well the M-band of the sarcomere (see figure 41). Another muscle-specific enzyme, the muscle isoform of creatine kinase was found in a yeast-two hybrid screen to interact with DRAL and members of the myomesin protein family.

Several sarcomeric proteins show a dual-loaclisation within the sarcomere. The muscle-specific protein Calpain-3 (p94) is a titin interacting protein exhibiting a localisation pattern similar to DRAL. It binds to the is7 region of M-band titin and to the I-band of the sarcomere (Kinbara et al., 1997; Sorimachi et al., 1996; Sorimachi et al., 1995). The recently described small muscle protein X chromosome (Smpx or Csl) shows also multiple localisation within the sarcomere (Kemp et al., 2001; Palmer et al., 2001) and is thought to integrate several signalling pathways.

Because of its modular composition (Tskhovrebova and Trinick, 2003), titin serves for many proteins as binding partner, anchoring structural as well as signalling proteins and thus functions as organiser of the sarcomere. Interactions with titin occur via binding to modular domains, like the Ig-like or fibronectin-type III domains or by association to unique sequence insertions. The binding of DRAL to two distinct unique sequence insertions in titin is the first described case of an interaction between a

LIM-only protein and titin. So far, the interaction between LIM proteins like ALP, Cypher 1/ZASP and MLP and the sarcomere have been restricted to the Z-disc protein α-actinin (Faulkner et al., 2000; Flick and Konieczny, 2000; Pomies et al., 1999; Zhou et al., 1999).

The following paragraphs describe in more detail the interaction of DRAL with metabolic enzymes and discuss the role of DRAL in various signalling pathways. In order to investigate the role of DRAL within the developing heart, genetic null-mutants of DRAL were established, but failed to show a drastic phenotype. The last paragraph of this chapter will reflect on the cause of the weak cardiac phenotype of DRAL -/- mouse and address the question of the establishment of a β-catenin/DRAL double knockout.

7.3.1. DRAL interaction with metabolic enzymes

Targeting of metabolic enzymes to the sarcomere has been reported over decades of muscle research (Arnold and Pette, 1970; Dolken et al., 1975; Kraft et al., 2000; Wegmann et al., 1992) and is thought to be important for the provision of energy during muscle contraction (Wallimann and Eppenberger, 1985). The constant dual localisation-pattern of several of these metabolic enzymes at the region of the sarcomeric I-band and the M-band of the muscle suggest a more general mechanism of compartmentalisation of metabolic enzymes, like the DRAL mediated anchorage to the N2B and is2 regions of titin. The I-band association seems further dependent on the buffer conditions used for the sample preparation, since it is primarily observed if bivalent cations chelators as EDTA are omitted (Wegmann et al., 1992). Since our experiments indicate that the function of DRAL as mediator of protein-protein interactions depends on the proper folding of the LIM-domains and the coordination of the Zn^{2+} ions (see figure 23 panel B), it seems very likely that the association of metabolic enzymes is also dependent on a conserved conformation of the LIM domains in DRAL.

DRAL expression was found to be dramatically upregulated after birth. This is similar to results obtained for MMCK (muscle isoform of creatine kinase) expression in developing muscle and might explain the delay in sarcomeric compartmentalisation of this enzyme (Carlsson et al., 1990; Carlsson et al., 1982; Ventura-Clapier et al., 1998).

In summary, DRAL might serve as a general mediator of sarcomeric compartmentalisation for a multitude of proteins. We have shown interactions with several metabolic enzymes, among them MMCK, AK and PFK. Recent publications indicated further binding of DRAL to a multitude of enzymes involved in several metabolic pathways (El Mourabit et al., 2004). Animals that are homozygous null mutants for DRAL seem normal and display no obvious abnormalities in their myofibrils (Chu et al., 2000). However, they seem to be more sensitive to stress situations, such as β-adrenergic stimulation (Kong et al., 2001), which might suggest an impaired ability to cope with abnormal requirements on the cardiac energy metabolism.

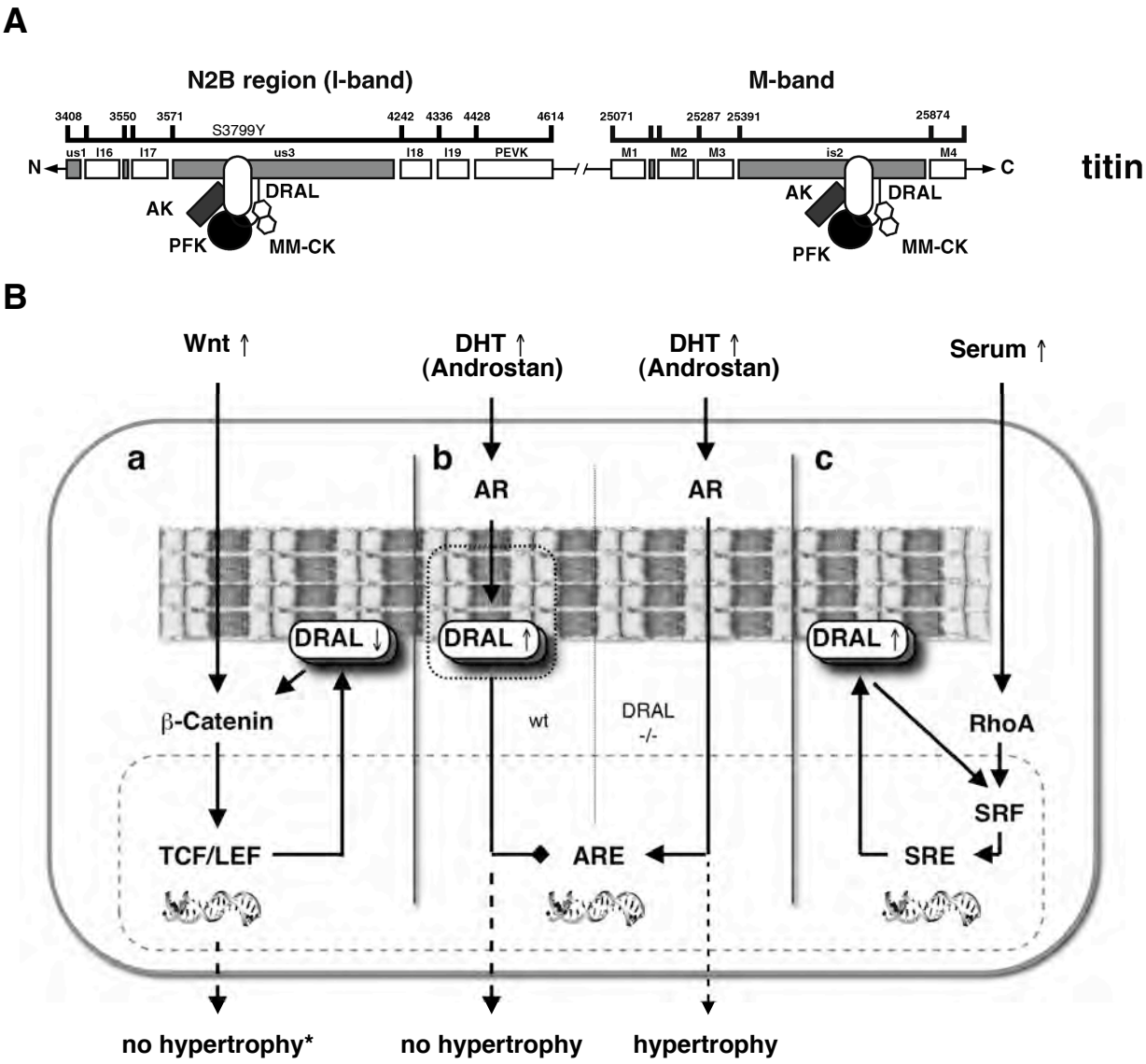

Figure 41. Novel DRAL interactions with the sarcomere and crosstalk of DRAL with various signaling pathways.

A. Schematic representation of DRAL interaction with the N2B and is2 region of titin and associated proteins. DRAL interacts directly with the N2B and is2 regions of cardiac titin and serves as an adaptor protein for the anchorage of metabolic enzymes like the muscle isoform of creatine kinase (MMCK), adenylate kinase (AK) and phosphofructokinase (PFK) to the sarcomere. In addition MMCK is bound to the M-band of the sarcomere via its interaction with proteins of the myomesin family (not shown here). The domain nomenclature and amino acid numbering correspond to that of the human cardiac titin sequence (access number X90568 (Labeit and Kolmerer, 1995)). The position of the newly identified human S3799Y HCM mutation in the N2B region of cardiac Titin (Itoh-Satho et al. 2002) is located within the minimal DRAL binding site and may greatly influence DRAL (or FHL1) mediated binding of metabolic enzymes as well as signalling proteins (e.g. the androgen receptor) to the sarcomere.

B. Known and novel crosstalk of DRAL with the Wnt-1, the androgen receptor and the SRF signalling pathway. a) Activation of Wnt signalling leads to the nuclear accumulation of β-catenin and DRAL and the activation of the TCF/LEF transcription factor family. Subsequently DRAL protein levels are downregulated. However no hypertrophic effect could be observed in DRAL -/- cardiomiocytes (asterisk). b) Activation of the androgen receptor (AR) leads in DRAL-/- cardiomoyctes to the onset of hypertrophy, whereas wildtype cells display no phenotypical signs of increased hypertrophy. Wildtype cells however show elevated DRAL levels upon activation of androgen recptor responsive elements (ARE). The failed activation of ARE in wildtype cardiomyocytes might be due to DRAL mediated anchorage of activated androgen receptor to the sarcomere (dotted rectangle). c) Induction of RhoA signaling by elevated Serum levels leads to the activation of the serum response Factor (SRF). DRAL physically interacts with SRF and enhances its own expression in a positive feedback loop to serum response elements (SRE; (Morlon and Sassone-Corsi, 2003; Phillipar, Schratt, 2004)).

7.3.2. DRAL as signalling modulator

The diversity and multitude of different characterised interaction partners for DRAL and the highly homologous other members of the four and a half LIM-domain protein family suggests important functions for these proteins in the mediation of protein-protein interactions. The interaction partners of DRAL can be subdivided into four large groups: cytoplasmic enzymes, other members of the FHL protein family, proteins of the sarcomere and nuclear associated proteins like proteins of signalling pathways and transcription factors, among them proteins like β-catenin (Wei et al., 2003), CBP/p300 (Labalette et al., 2004), the hormone receptors androgen receptor (Muller et al., 2000) and the oestrogen receptor (Kobayashi et al., 2004) as well as the serum response factor (Philippar et al., 2004). The interaction between DRAL and the latter group of receptors, Co-activators and transcription factors suggests a general function of DRAL as a cell-type specific Co-activator or Co-repressor of transcription, integrating signals and even enabling crosstalk between different signal-pathways. Figure 41 panel B summarises the observed effects of DRAL in the Wnt-1/β-catenin signalling and the androgen receptor pathway.

An interesting feature of DRAL and other members of the FHL protein family is the formation of homo- as well as heterodimers as shown for DRAL and FHL1 (Lange et al., 2002) or for DRAL and FHL3 (Li et al., 2001), which might contribute to the complexity of proteins interacting with either the FHL protein homo- or the heterodimers.

7.3.2.1. DRAL and the Wnt-signalling pathway

Although it was demonstrated that DRAL and members of the catenin protein family physically interact, no obvious colocalisation could be observed in neonatal rat cardiomyocytes, where the majority of e.g. β-catenin is captured in its cytoskeletal role as integral part of the intercalated discs. The induction of the Wnt-1 signalling pathway using LiCl however, showed a dramatic effect on the expression levels and the nuclear localisation patterns of DRAL and β-catenin, suggesting that DRAL in conjunction with cytoplasmic non-phosphorylated β-catenin might modulate Wnt-1-mediated signalling in heart cells. β-catenin and signalling through the canonical Wnt signalling pathway is required for the correct formation of the heart (Lickert et al., 2002) and plays an important role in the endothelial-mesenchymal transdifferentiation (EMT) during heart cushion development (Liebner et al., 2004). The formation of the heart cushion is a prerequisite for the subsequent development of the atrio-ventricular region and the formation of the septum. Besides β-catenin, a number of signalling proteins and transcription factors are involved in the EMT and the subsequent development of heart valves and the septum (for a review see (Armstrong and Bischoff, 2004) and references therein). TGF was reported to play in conjunction with BMP a crucial role for the initiation of the transdifferentiation and was found to induce DRAL expression in a similar transdifferentiation process (Untergasser et al., 2005). Targeted inactivation of the serum response factor (SRF), a recently reported interaction partner of DRAL (Philippar et al., 2004), resulted in a disorganised septum and dilated cardiac chambers in the developing heart, leading to an embryonically lethal cardiac phenotype (Parlakian et

al., 2004). Since it was shown that DRAL expression is detectable rather late on the protein level in embryonic development (between E12.5 and E16.5 in mouse; (Lange et al., 2002)), but DRAL mRNA was already detectable at embryonic day E7.5 within the cardiac crescent and later (E14.5) with the highest expression levels in the ventricular septum (Kong et al., 2001), the concerted action of DRAL and β-catenin as mediators of gene-expression may be limited to a pivotal developmental process in this period, like chamber and ventricular septum formation or the onset of the developmental heart hypertrophy and the closure of the atrial septum (closure of foramen ovale and formation of fossa ovalis) shortly after birth.

An ongoing project investigating the effects of a heart specifc DRAL and β-catenin knockout using a crossbreeding strategy of DRAL knockout mice with mice carrying an inducible β-catenin knockout under the control of an heart-specific promoter using a Cre/Lox-approach, might answer the crosstalk between FHL and the Wnt signalling pathway. Preliminary results indicate an increased occurrence of postnatal lethality as well as an elevated incidence of ventricular septum defects (VSD) at embryonic stage E15.5 of double knockouts, which coincides noticeably with highly elevated DRAL expression in the forming ventricular septum around E14.5 in wildtype animals (see figure 42; for the complete results see Dissertation of A. Hirschy).

7.3.2.2. DRAL and steroid hormone receptors

Apart from β-catenin mediated signalling, DRAL was also implied to play a role in the signalling pathways of several steroid hormone receptors like the androgen receptor (AR) and the oestrogen receptor (Kobayashi et al., 2004; Muller et al., 2000). Steroid hormone receptors emerge as transcription factors that are central to the regulation of transcriptional activity for many genes. Their versatile crosstalk with other signalling pathways and transcription factors or co-activators/co-repressors of transcription, like the serum response factor (Duan et al., 2002; Vlahopoulos et al., 2005), the Forkhead Box class O transcription factors (Foxo1; (Li et al., 2003)) or DRAL as well as interactions with posttranslational modifiers like PIAS1 (Kotaja et al., 2002; Tan et al., 2002) indicate a substantial role for hormonal regulated transcription in cellular signal-response and differentiation. For the heart, hormone receptors are furthermore implicated in the gender-specific difference in life expectancy and vulnerability for the development of cardiovascular diseases (for a review see: (Liu et al., 2003)).

One of the major findings on the impact of DRAL on various signalling pathways was the differential response of wildtype and DRAL -/- cardiomyocytes upon the activation of the androgen receptor pathway by the agonist Androstan. Cardiomyocytes derived from mice that lacked DRAL showed a significant hypertrophic response upon Androstan treatment, whereas wildtype cardiomyocytes were indistinguishable from untreated controls. Since the excessive activation of AR by androgenic stimulation leads to the onset of hypertrophy in cardiomyocytes (Marsh et al., 1998), the elevated protein levels of DRAL in wildtype cardiomyocytes upon treatment with the androgen receptor agonist Androstan may suggest a cellular response to circumvent a hypertrophic response by intercepting the nuclear targeting of AR via DRAL-mediated sarcomeric compartmentalisation. In DRAL -/- cardiomyocytes on the other hand, activated androgen receptor is no longer trapped in the sarcomere,

but instead localises to the nucleus and acts as transcription factor for androgen responsive elements (ARE) leading to a measurable hypertrophic cellular response.

Recent publications indicate that this mechanism of DRAL-regulated compartmentalisation of steroid hormone receptors to the sarcomere might be affected by mutations in the giant protein titin. Several mutations in the N2B as well as the is2 DRAL binding site in titin were associated either with the development of a hypertrophic cardiomyopathy (HCM) or a dilated cardiomyocopathy (DCM) in human case studies (Itoh-Satoh et al., 2002). The only identified mutation in the two different sarcomeric DRAL binding sites which causes familial hypertrophic cardiomyopathy (HCM) is located in the N2B-region of cardiac titin and changes serine 3799 residue to tyrosine. The other two identified mutations located in the N2B and the is2 regions of titin are thought to cause familial dilated cardiomyopathy (DCM). In one of these, the titin N2B binding site for DRAL, glutamine 4053 is mutated to a STOP codon and in the titin is2 binding site for DRAL. Arginine 25618 is changed to glutamine (Matsumoto et al. submitted). First results from these studies using a forced yeast-two hybrid system and β-galactosidase activity assays indicate that at least for the N2B-region of titin a differential interaction strength is observed for DRAL towards the wildtype or the mutated titin N2B-regions. Their interaction intensity might greatly influence the subcellular localisation of DRAL in cardiomyocytes, since the N2B-region was identified as the major interaction site for DRAL in the sarcomere. A stronger interaction of DRAL with N2B, as found for the S3799Y mutation or a weaker interaction as observed for the Q4053STOP mutation might not only affect the DRAL localisation, but also the compartmentalisation of DRAL binding partners, such as steroid hormone receptors or enzymes of the energy metabolism. Results obtained by co-immunoprecipitation experiments, comparing the affinity of DRAL or FHL1 to wildtype as well as the titin N2B S3799Y mutant displayed however, a clear abolishment of the binding of the FHL proteins to the titin mutation (see earlier and figure 21). Future experiments investigating the differential binding affinity of DRAL (or other FHL proteins) to mutated titin isoforms may shed light into a new DRAL associated muscle-specific signalling pathway, which is involved in the onset of several of the identified cardiomyopathies. A comparison between the androgen receptor mediated hypertrophy in DRAL -/- cardiomyocytes as well as the onset of HCM in patients baring the titin N2B S3799Y mutation for example might reveal interesting parallels. Crosstalk of DRAL with other pathways as well as the nuclear functions of DRAL however, might hamper or complicate the analysis of the DRAL modulated signalling pathways.

Since most of the experiments investigating the coactivator or corepressor function of DRAL via Luciferase reporter assay were carried out in non-muscle cells, the influence of DRAL on the subcellular localisation and transcriptional activity of its various transcription factor interaction partners remains elusive for muscle development and maintenance. Furthermore, the crosstalk between several highly interconnected signalling pathways and homo- as well as heterodimerisation among members of the FHL protein family complicates the investigation into the biological functions of DRAL.

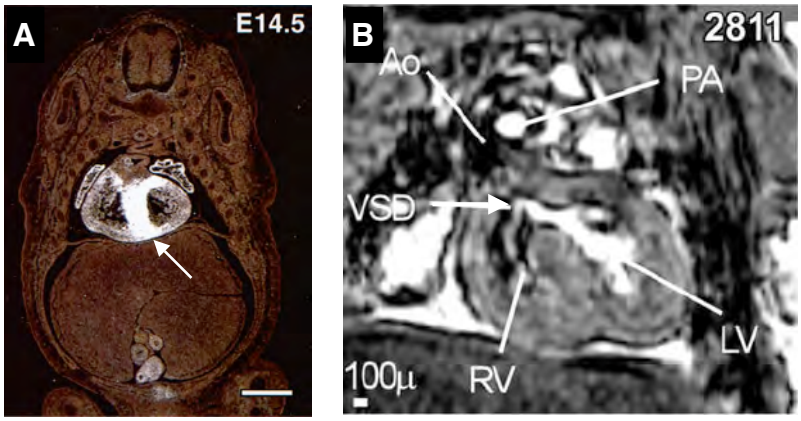

Figure 42. Phenotypic effects of a DRAL and a cardiac specific β-catenin double knockout on the embryonic heart development.
A. In situ hybridisation analysis of DRAL mRNA in mouse at E14.5. The septum primordium displays particularly high levels of DRAL expression during this embryonic stage. Figure adapted from (Kong, Shelton et al. 2001).
B. MRI scan of the heart of β-catenin and DRAL double knockout mice (embryo number 2811) at embryonic stage E15.5 displays a clear ventricular septum defect (VSD). The increased frequency of about 50% for this congenital muscular septum defect in double knockout animals suggests a crosstalk of DRAL with the Wnt signalling pathway in the developmental formation of the septum primordium. Other used abbreviations: Ao - Aorta, PA - pulmonary aorta, RV - right ventricle, LV - left ventricle.
Adapted from Prof. S. Bhattacharya and A. Hirschy.

7.3.3. DRAL knockout

A growing body of evidence indicates that DRAL in conjunction with its various interaction partners may play a crucial role in the cardiac development and maintenance, energy metabolism and cardiac signalling pathways. Attempts to clarify the role of DRAL using genetic knockout models failed to shed light into the functions of this protein. Two different groups reported the generation of null-mutant mice for the DRAL allele (Chu et al., 2000; Kong et al., 2001). No apparent cardiac phenotype was detected: cardiac size and function as well as the expression levels of other members of the FHL protein family remained unchanged (Chu et al., 2000). Only β-adrenergic stimulation induced an cardiac hypertrophy in adult mice, suggesting again a DRAL mediated protective mechanism against the excessive induction of hypertrophic signalling pathways (Kong et al., 2001).

Identical or comparable tissue specific expression pattern among several members of the FHL protein family might account for the absence of a clear cardiac phenotpye. Furthermore, a high level of homology and identical subcellular localisations of several FHL proteins as well as the appearance of heterodimers of FHL proteins indicate a certain level of redundancy in the protein functions of FHL proteins, which may also contribute to the lack of a strong phenotypical response. The broad variety of the interaction partners involved in either signalling or the modulation of gene expression (Kobayashi et al., 2004; Kong et al., 2001; Labalette et al., 2004; McLoughlin et al., 2002; Muller et al., 2000), posttranslational modification of proteins (Li et al., 2002), structural proteins of the sarcomere as well as metabolic enzymes (El Mourabit et al., 2004; Lange et al., 2002) indicate a role for FHL proteins in the integration of signals of different pathways important for the differentiation and maintenance of muscle cells and suggests a more general role of these LIM-only proteins than just as mediators of protein-protein interactions.

7.4. Titin kinase signalling

The giant muscle protein titin (also known as connectin) is an elastic protein and, with about 3 mega Daltons not only the biggest, but also one of the most abundant proteins in vertebrate striated muscle (Au, 2004; Maruyama, 1997; Tskhovrebova and Trinick, 2003). The functions of titin are manifold and are thought to range from the regulation of the sarcomeric assembly, the preservation of the sarcomeric alignment to the maintenance of the sarcomere. Assembled in a modular way from repetitive patterns of immunoglobulin-like and fibronectin-type III domains, its domain architecture is surprisingly simple. An autoregulated serine kinase domain (titin kinase) and several unique sequence insertions however, are found throughout the protein and add to the complexity of the protein structure and functions. The kinase domain of titin was implicated to play an important role in myofibrillar assembly and sarcomeric remodelling (Amodeo et al., 2001; Mayans et al., 1998).

Although calmodulin and the Murf protein family were implied early in the regulation of the titin kinase activity, only one substrate was identified to date, namely the small muscle protein telethonin (also known as T-cap). In order to identify other substrates of titin kinase and to discover downstream targets of the titin kinase signalling pathway, yeast- and bacterial-two hybrid screens were carried out and revealed a complex of proteins, linking titin kinase signalling with one of the major transcription factors in the cell, the Serum Response factor (SRF; see figure 30 C). The titin kinase mediated signalling network further consists of the proteins NBR1 (next to BRCA1), p62 (SQSTM1) and Murf2. Subcellular localisation studies and co-transfection experiments in neonatal rat cardiomyocytes suggested that these proteins might form a protein complex or signalsome with the semi-activated kinase domain of titin. The modulation of titin kinase activity via upstream kinases and modulators like calmodulin (CaM; (Amodeo et al., 2001)) or via mechanical activity (Grater et al., 2005) markedly influences the subcellular localisation of several of these signalsome proteins and resulted ultimately in an altered transcriptional activity via Sumo-mediated nuclear exclusion and subsequent degradation of the serum response factor.

These observations suggest that the kinase domain of titin may act as a central switchboard, combining and integrating the input from several signalling pathways with a mechanical strain sensory function, which may lead to an altered cellular response, like the onset of hypertrophy in its activated or atrophy in its inactivated state. Indeed, a recently identified mutation in the titin kinase domain disrupts this pathway and leads to a hereditary myopathy, underlining the importance of TK mediated signalling for muscle development and maintenance (Xiang et al. unpublished results; pers. comm. M. Gautel).

7.4.1. Structural functions of the titin kinase substrate telethonin

Telethonin (T-cap) emerged as the earliest identified major substrate for the kinase domains of titin (Mayans et al., 1998) and was found to interact and cross-link the two N-terminal immunoglobulin-like

domains of titin (Z1, Z2; (Gregorio et al., 1998; Mues et al., 1998; Zou et al., 2003)). Using dominant-negative approaches in cardiac myocytes, it was suggested by Gregorio and coworkers that telethonin as well as the titin Z1Z2-domains are required for sarcomeric assembly. Telethonin interacts, apart from the titin Ig-domains, with another protein of the sarcomeric Z-disc, the Muscle LIM Protein (MLP) in a non-competitive fashion (Zou et al. unpublished results; pers. comm. M. Wilmanns). Mice that lack MLP show chamber dilation and contractile dysfunction, showing for the first time a muscle disease which is related to a genomic mutation of a component of the Z-disc (Arber et al., 1994; Arber et al., 1997). Telethonin and MLP were further implicated as a mechanical stretch sensor, which was found to be defective and identified as the cause of dilated cardiomyopathy (DCM) in a subset of the European population (Knoll et al., 2002).

Transient transfection of neonatal rat cardiomyocytes using full-length, N-terminal (residues 1-90) or C-terminal telethonin (residues 91-167) showed that the Z-disc targeting domain resides in the N-terminal titin binding domain of the protein, whereas the C-terminus displayed a more ambiguous subcellular localisation. It might be noteworthy that full-length as well as C-terminal telethonin was occasionally found to be weakly associated to the M-band of the sarcomere, the location of the titin kinase domain. Since serine 157, the major titin kinase phosphorylation site in telethonin, is located in the C-terminus of the protein the observed weak M-band localisation might be linked to the posttranslational modification of telethonin via the kinase domain of titin.

The binding of telethonin to the N-terminal Ig-domains of titin is mediated by the first 90 amino-acid residues of the protein and allows the assembly of a hetero-trimeric sandwich-complex, consisting of two antiparallel arranged titin Z1Z2 proteins cross-linked via the telethonin protein ((Zou et al., 2003) and unpublished results Zou and Pinotsis et al., pers. comm. M. Wilmanns). The assembly of this complex was confirmed *in vivo* using the split-GFP-system (see earlier).

The proposed titin-titin cross-linker function of telethonin is somewhat reminiscent of the actin-titin linker function of α-actinin in the Z-disc (Young et al., 1998) or the myosin-titin cross-linker function of myomesin protein family members in the M-band of the sarcomere (this study and (Lange et al., 2005)). Although the telethonin mediated titinZ1Z2 cross-linking function results in a spatially minimised sandwich-type rather than a large rod-type model, several other parallels are evocative: e.g. the antiparallel arrangement as well as the formation of extensive antiparallel β-sheet interactions between the interacting proteins.

The 2:1 stoichiometry of the titinZ1Z2:telethonin complex is in good agreement with electron microscopy data that reveal a two-fold symmetry within the tetragonal Z-disc lattice (Liversage et al., 2001; Luther, 2000; Luther et al., 2003). With a 2:1 ration of titin:actin filaments and spacing considerations caused by the 19.5nm α-actinin intervals and the 28/13 symmetry observed in actin thin filaments as well as the estimated distances between titin Z-disc repeats of about 12nm, the generation of a three-dimensional Z-disc model, including published and novel crystal-structures is possible. Figure 43 displays the crystal-structure of the titin:telethonin sandwich in context with the overall Z-disc structure and explains how an antiparallel titin:titin arrangement may be caused by two titin molecules originating from the same sarcomere, rather than from adjacent sarcomeres.

Figure 43. Structure of the titinZ1Z2:telethonin complex and implications for the three-dimensional structure of the Z-disc.
A. crystal structure of the titinZ1Z2:telethonin protein complex superimposed into the three-dimensional model of the sarcomeric Z-disc. The crystal structure shows clearly the antiparallel arrangement of the Z1Z2 Ig-domains of titin with telethonin as the mediator of the protein-protein interaction and complex-assembly (in a frontal (a) and longitudinal (b) representation). The formation of the complex is mediated by the interaction of antiparallel β-sheets in titin and telethonin. The crystal structure of the complex was solved by the lab of Prof. Wilmanns and has been submitted and deposited in the Protein Data Bank with the accession code 1YA5.
B. Longitudinal view of the Z-disc model. Three actin:titin rods with a 1:2 stoichiometry as well as α-actinin cross-bridges are shown. The titin:telethonin complex is placed at the barbed end of the actin-filaments. The putative titin domain Z3 is depicted as a helical sphere. Two titin molecules run along the helical actin filament and mediate the binding to α-actinin in the region of the Z-repeats (ZR). For reasons of clarity, the helical actin-filament structure was transparently masked behind a cylinder. Apart from titin, telethonin, α-actinin and actin, only nebulin is shown in the model, providing an N-terminal actin-cap.
C. Axial view of the assembled three-dimensional Z-disc model. The position of the titin:telethonin complex within the tetragonal lattice of the sarcomeric Z-disc is more obvious in this view.

Figure 43. Structure of the titinZ1Z2:telethonin complex and the structure of the Z-disc.

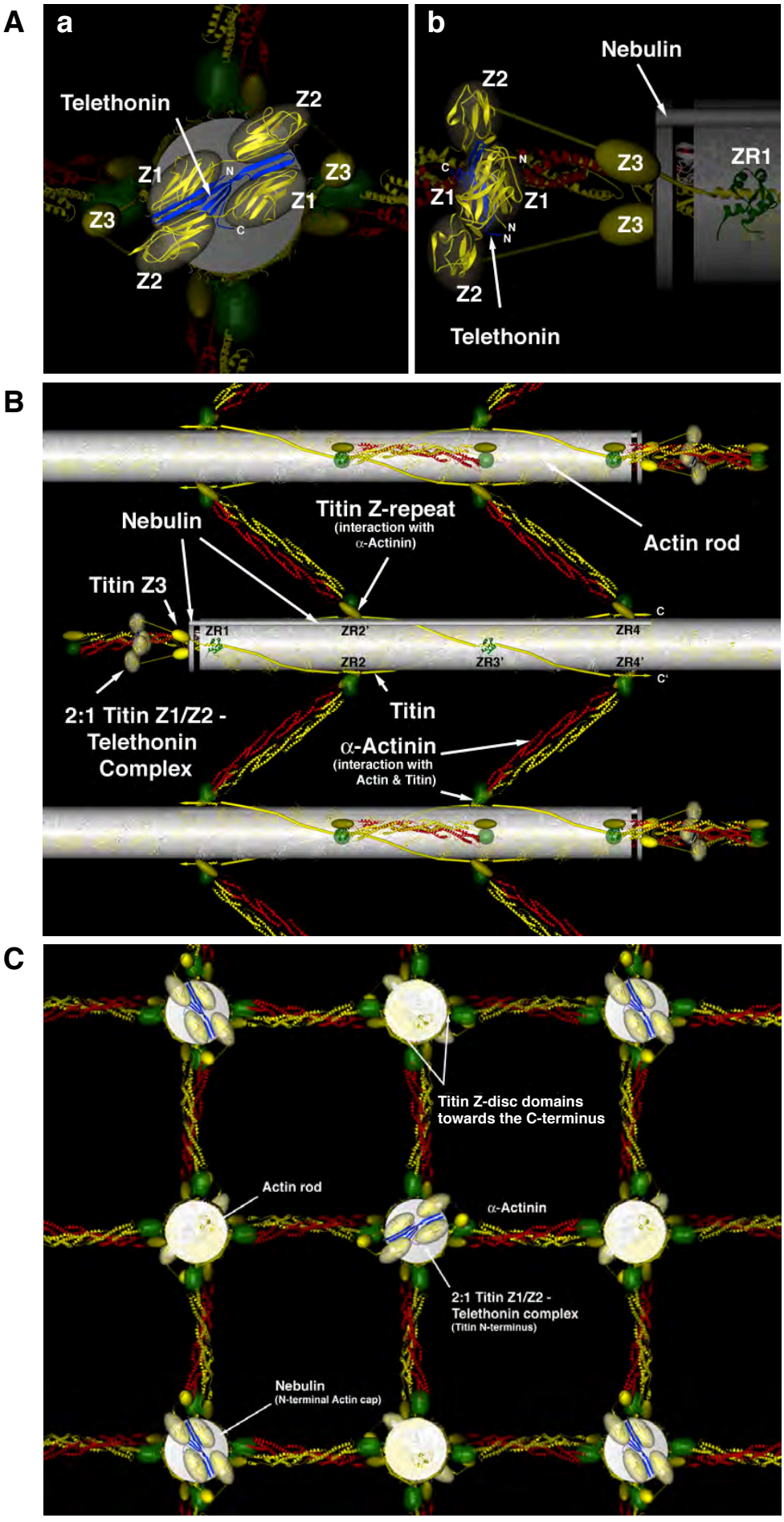

8. Materials and Methods

8.1. General methods in molecular biology

8.1.1. PCR

PCR reactions were carried out in a total volume of 25µl or 50µl with the following components: 100pg-1ng template DNA, 1x Taq polymerase buffer or 1x Pfu polymerase buffer (containing $MgCl_2$), 1µM of each primer (forward and reverse), 0.2mM dNTP mixture, 2units Taq (Sigma), Pfu (Stratagene) or Phusion polymerase (Finnzymes). Reactions were covered with mineral oil and run on an Eppendorf mastercycler gradient (Eppendorf scientific inc., New York, USA) using primer specific cycle conditions.

8.1.2. RT-PCR

RT-PCR reactions were carried out using the Qiagen OneStep RT-PCR kit, in a total volume of about 25µl with the following components: 1x Qiagen OneStep RT-PCR buffer,1x Q-solution, 400µM dNTP mix, 0.6µM of each primer, 1x enzyme mix (containing the reverse transcriptase as well as a HotstarTaq polymerase), RNAse and DNAse free water in the appropriate volume and 1pg to 2µg template RNA. Reactions were overlayed with mineral oil and run on an Eppendorf mastercycler gradient (see earlier) using primer specific conditions.

8.1.3. Isolation of plasmid DNA

Plasmid DNA was isolated using the NucleoSpin Plasmid kit (Macherey-Nagel GmbH & Co. KG, Düren, Germany). Isolated clones from bacterial plates were grown in 4ml LB-medium supplemented with the appropriate antibiotic on a shaking platform over night at 37°C.

After centrifugation at 3500rpm, bacterial pellets were suspended in 250µl buffer A1 by vortexing. Lysis of cells was induced after adding 250µl buffer A2 (alkaline lysis) and incubation for 5 minutes at room temperature. Lysed cells were incubated with buffer A3 (acidic precipitation buffer) and centrifuged for 10 minutes at 13000rpm in a tabletop centrifuge to precipitate cell debris and genomic DNA. The supernatant was loaded on the gel-affinity-column and centrifuged for 1 minute at 13000rpm in a tabletop centrifuge. The bound DNA was washed once with 600µl buffer A4 (centrifugation for 1min. at 13000rpm) and after a final centrifugation step of 2 minutes at 13000rpm to remove residual ethanolic washing buffer eluted into a clean eppendorf tube with 50µl AE buffer by centrifugation for 1 minute.

8.1.4. Plasmid digests

For preparative digests, 3-5µg plasmid DNA were digested with 10-30U of enzyme in the appropriate 1x or 2x restriction buffer for 3 hours. Alternatively, DNA was digested with 1-10U enzyme over night. A list of enzymes that can be used in over night digestions can be found in the New England Biolabs catalogue. When required, digestion mixes were supplemented with 1x bovine serum albumine (BSA, supplied by enzyme manufacturer). Enzymes were derived from Roche (Rotkreuz, Switzerland), Angewandte Biotechnologie Systeme (AGS, Axon Lab, Wallisellen, Switzerland), New England Biolabs (NEB, Bioconcept, Allschwil, Switzerland), MBI Fermentas (Fermentas, MBI, Basel, Switzerland) and Promega (Promega, www.promega.com).

8.1.5. Isolation of DNA-fragments from Agarose gels

Digests were run on a preparative 1% or 2% agarose gel in 0.5x Tris-borate EDTA (TBE) buffer (Ausubel et al. 1987). Bands were visualized by ethidium bromide fluorescence by a long-range ultraviolet light source, excised with a clean scalpel and purified using the Nucleospin extract kit (Macherey-Nagel GmbH & Co. KG, Düren, Germany) according to the manufacturer's specifications. Yield and purity of the isolated fragments were judged by running isolated fragments on a 0.8-2% agarose gel and comparing the fluorescence intensity with a standard 1kb DNA ladder (purchased from Eurogenetic, Seraing, Belgium).

8.1.6. Ligation of DNA fragments

DNA fragments were quantified on agarose gels as described earlier and the amount of insert DNA needed for a given amount of vector DNA was calculated using the following equation:

$$amount_{insert}[ng] = \frac{amount_{vector}[ng] \cdot size_{insert}[kb]}{size_{vector}[kb]} \cdot \left[ratio \frac{insert}{vector} \right]$$

Ligations were carried out in a total volume of 10µl using 20-50ng of vector and insert: vector ratios of 3:1, 1:1 and 1:3. As a control, vector without insert was ligated. For ligations involving compatible overhangs, the incubation was carried out either at a temperature of 25°C for 2 hours or at 16°C over night. For blunt ligations, incubations were always done over night at 16°C. Vector DNA, insert DNA, 1x T4 ligation buffer (containing 10mM ATP) and 0.5-1µl T4 DNA ligase (NEB or Promega) were mixed and incubated as described above. In general 5µl or 1µl of reaction mixture were used for transformation of chemically or electrocompetent cells, respectively.

8.1.7. Transformation of chemical competent cells

For the propagation of plasmid DNA *E. coli* from the strains XL-1 blue or BL-21 star (DL3; Invitrogen, Bsel, Switzerland) were used. Two protocols were used for transformation of chemically competent cells:

Protocol 1 (TSS method): XL-1 blue cells were thawed on ice and divided into 100µl aliquots. Subsequently, 5µl of ligation mix or 1-10ng of supercoiled plasmid were added and cells were incubated on ice for 5 minutes. 300µl of SOC-medium were added and the cells were incubated on a shaker platform for 45 minutes to 1 hour (depending on antibiotic resistance). 50-200µl were spread on bacterial plates with the appropriate antibiotic and incubated over night at 37°C.

Protocol 2 (Inoue method): XL-1 blue cells were thawed on ice and divided into 100µl aliquots. Subsequently, 5µl of ligation mix or 1-10ng of supercoiled plasmid were added and cells were incubated for 30 minutes on ice, heat-shocked at 42°C for 90 seconds, incubated on ice for 3 additional minutes. 300µl SOC medium was added and subsequent steps were carried out as for protocol 1.

8.1.8. Preparation of chemical competent cells

XL-1 blue or BL-21 (DL3) cells star from a glycerol stock were transferred to 4ml LB medium containing tetracycline and incubated over night on a shaker in the dark at 37°C. The over night culture was transferred to 500ml Psi broth medium and grown at 37°C with aeration to a density of OD_{550} = 0.48. The suspension was incubated for 15 minutes on ice and cells were afterwards centrifuged for 5 minutes at 3-5000 x g. The supernatant was discarded and cells were resuspended in 200ml (0.4 volumes) of TfbI buffer and incubated for another 15 minutes on ice. Cells were centrifuged with the same parameters again and the cell pellet was resuspended in 20ml (0.04 volumes) of TfbII buffer, incubated on ice for another 15 minutes and either used immediately or aliquoted into 200-400µl aliquots, snap frozen in liquid nitrogen and stored at –80°C for later use.

8.1.9. Transformation of electro-competent cells

For electroporation, XL-1 blue were used. Cells were thawed on ice, 40µl aliquots were transferred to ice-cold clean electroporation cuvettes (0.2mm gap width, BTX, Axon Lab), 1µl of ligation mix was added and incubated on ice for 30 minutes. Cells were electroporated in a BTX electroporator model ECM 600 at 1.5kV, 2.5 kV/resistance, 129 Ohm. Directly after the electroporation step, 1ml of SOC medium was added into the cuvette, mixed and transferred to a Falcon tube. Cells were incubated at 37°C for one hour with shaking and 200µl aliquots were spread out on plates supplied with the appropriate antibiotic.

8.1.10. Preparation of electro-competent cells

XL-1 blue cells from a glycerol stock were transferred to 4ml LB medium containing tetracycline and incubated over night in the dark at 37°C on a shaker. 1 litre of LB-medium or alternatively 1 litre YENB medium was inoculated with the pre-culture and grown to an OD_{600} = 1. The cell suspension was poured into precooled centrifuge flasks, chilled on ice for 30 minutes and centrifuged at 4°C for 10 minutes at 4000g. The cells were washed once with 1 litre of ice-cold dd-water and after another centrifugation step resuspended in a total volume of 400ml with ice-cold 10% glycerol, split into 50 ml Falcon tubes and centrifuged again for 7 minutes at 4000g. The supernatant was carefully removed and each pellet was resuspended in 100 to 200μl 10% glycerol by vortexing. Aliquots of about 50μl were pipetted into precooled eppendorf tubes, snap frozen in liquid nitrogen and stored at –80°C for further use.

8.1.11. Protein expression in eColi and purification

BL-21 star cells were transformed with bacterial expression plasmids using the TSS method, streaked out on bacterial LB plates supplemented with Ampicillin and grown over night at 37°C. 5 colonies were picked, inoculated in 5 ml LB medium with Ampicillin and grown over night at 37°C on a shaker. The over night pre-culture was subsequently diluted to 500ml LB medium and grown at 37°C and increased aeration on a shaker to an OD_{600} = 1. The expression was started by IPTG induction (final concentration of 0.2μM) and the medium was supplemented with 50μM $ZnSO_4$. After 30 minutes, cells were centrifuged at 4000g for 15 minutes and resuspended in 1/25 volume of ice-cold STE-Lysis buffer and chilled on ice. To induce lysis, Lysozyme was added to a final concentration of 0.5mg/ml and cells were incubated for 30 minutes on ice on a shaking platform. Cell lysate was sonicated 3 times for 10 seconds at an output of 6 and a duty cycle of 50 using a Bransons Sonifier 250 with a small tip. Sonicated lysate was centrifuged at 15000g for 20 minutes in a cooled ultracentrifuge and supernatant was transferred to a clean Falcon tube. An appropriate volume of Glutathione Sepharose (about 500μl; Pharmacia Biotech, Uppsala, Sweden) was washed once with modified STE-buffer and resuspended in half of the original volume with modified STE buffer. The washed beads were added to the cell lysate and incubated for 30 minutes on a shaker platform at 4°C. Glutathione Sepharose beads were pelleted for 5 minutes with 2500rpm, resuspended in ice-cold modified STE buffer using half of the original volume of the Glutathione Sepharose and stored for further use on ice.

Correct expression and purity of the GST fusion protein was monitored using SDS-PAGE.

8.1.12. GST-pulldown

For pulldown assays, defined amounts of GST-fusion protein loaded beads or beads with GST alone were washed once in IP buffer and incubated for 2 to 3 hours on ice with precleared lysates from Cos-1 cells expressing the respective binding partners or controls normalized for protein content. Following incubation, the complexes were pelleted by centrifugation in a tabletop centrifuge with

2500rpm at 4°C, washed three times in ice cold IP buffer and resuspended 1:1 in SDS-PAGE sample buffer, boiled for 2 minutes and separated by SDS-PAGE analysis followed by immunoblotting.

8.1.13. Co-immunoprecipitation

For co-immunoprecipitation assays plasmids encoding the two putative interaction partners or controls were cotransfected into Cos-1 cells. Cells were harvested 24-48 hours later and lysed in IP-Lysis buffer. After preclearing by incubation with Protein G Plus / Protein A agarose (Oncogene) diluted in IP-buffer, the lysates were incubated with primary antibody at 4°C for 2 hours to overnight. Then Protein G Plus / Protein A agarose was added and incubated for 1 to 3 hours at 4°C. Following several washes with IP-buffer, the beads and supernatants were processed for SDS-PAGE and immunoblotting (see below).

8.1.14. SDS-Page and immunoblotting

Protein samples were mixed with SDS sample buffer in a ratio of 1:1, denatured for 2 minutes at 100°C and stored until further use at –20°C.

SDS-PAGE was performed on either 12.5% or on linear gradient gels of 6-20% or 8-22% Acrylamid concentration (according to (Laemmli, 1970; Matsudaira and Burgess, 1978)).

Separated proteins were either immediately visualized by Coomassie blue staining or blotted onto nitrocellulose membranes (Hybond-C extra, Amersham; Protran, Schleicher & Schuell) over night using 60mA and a wet-blot transfer unit (Biorad). Reversible staining with Ponceau-Red (Serva) was performed on membranes to estimate the loading of the samples to normalized protein content. Blocking of unspecific binding sites was carried out in 5% non fat dry milk powder (Migros, Switzerland; Sainsbury, UK) in Low Salt, containing 10mM HEPES pH7.4, 154mM NaCl, 0.1% Tween-20 for 30 minutes to 1 hour. Incubations with primary and secondary antibodies (diluted in 5% milk powder in Low Salt) were performed for 1 hour at room temperature. Alternatively, incubation with the primary antibody was carried out over night at 4°C. Washing steps, 3 times for 5 minutes, with either Low salt with 5% milk-powder after the primary or Low Salt only after the secondary antibody followed the incubation (see table 1 and 2 for antibodies; note that primary antibody dilution for immunoblots were 10 fold increased). Detection of immunocomplexes was performed with a super-signal solution containing 1% Luminol, 1% Iodophenol and 50mM Tris pH 7.5 for chemiluminescence by peroxidase catalisation.

8.1.15. DNA sequencing

Sequencing reactions were done using the ABI PRISM™ BigDye Terminator Cycle Sequencing Reaction Kit (PE Applied Biosystems). Approximately 200ng template was used per sequencing reaction. 3µl of 5x sequencing buffer, 0.3µl primer (10pmol/µl) and 2µl termination ready reaction

(TRR) mix were added to the DNA and the mixture was diluted with dd-water to a total volume of 20µl. The thermocycler was run according to the following program: denaturation for 10 seconds at 96°C, annealing for 10 seconds at 50°C and elongation for 4 minutes at 60°C, with a cycle number of 25. The amplified DNA was purified on a Sephadex G-50 column: 750µl of G-50 slurry (prepared by dissolving G-50 matrix and water overnight, followed by autoclaving) was transferred to small spin columns and centrifuged for 2 minutes at 13000g. 4µl of the purified DNA was mixed with 20µl of Template Suppression Reagent. The mixture was incubated for 2 minutes at 95°C, mixed, centrifuged shortly and loaded into an ABI PRISM capillary sequencer. Sequences were analysed using the EditView (PE Applied Biosystems) and SeqMan program (DNASTAR Inc., Madison, USA).

8.1.16. Yeast two-hybrid screen and forced yeast two-hybrid assay

All DNA fragments used for yeast two-hybrid screen and forced yeast two-hybrid analysis were amplified using PCR and cloned into the pLexA- (bait plasmid) or into the pAct2-plasmid (prey plasmid) and used to transform the yeast strain L40 (Stenmark et al., 1995; Vojtek et al., 1993). Correct expression of the LexA fusion protein was tested by immunoblotting yeast extracts with a LexA antibody (Santa Cruz Biotechnology). For a screen, after co-transformation with an adult human cardiac cDNA library in pAct2 or pGad10 (Clontech) the yeast transformants were assayed for growth on selection plates (see earlier) and for β-galactosidase activity. Library plasmids from positive clones were isolated and sequenced. To confirm interactions and search for minimal binding sites in a forced yeast two-hybrid assay, bait and prey plasmids were co-transformed and assayed as described above and elsewhere (see Results paragraph).

For detailed information on methods and protocols refer to the yeast protocols handbook (accession number: PT3024-1) available on the Clontech homepage (www.clontech.com).

8.1.17. X-ray crystallography

Crystals of proteins were grown using the hanging drop vapor diffusion method by mixing equal volumes of about 15 mg/ml protein solution and mother liquid containing 5% [w/v] PEG 8000 and 100 mM sodium citrate buffer (pH 4.45). Prior to data collection, the crystals were immersed into a solution containing 20% [v/v] MPD, 7.5% [w/v] PEG 35000, 100 mM sodium citrate buffer (pH 4.45), and 250 mM (NH4)2SO4, and then cooled in liquid N2. A multiple wavelength anomalous dispersion (MAD) experiment using the SeMet version of the protein complex was carried out on the tuneable beamline BW6 (MPG-ASMB/DESY, Hamburg).

The selenium positions were determined and refined using the peak data set of the MAD data with the CNS v1.1 program suite. Model building was carried out with the program O (www.bioxray.dk/~mok/o-files.html). At the early stages of refinement, molecular dynamics based on maximum-likelihood algorithms was carried out using CNS. Solvent molecules were added by using

the ARP/warp program package. For detailed information refer to Dr. Nikos Pinotsis and Prof. Matthias Wilmanns.

8.1.18. Northern blot analysis

Total human heart RNA was purchased from Stratagene. RNA of mouse hearts was prepared using Trizol (Gibco) according to the manufacturer. RNA amounts were equalised via photo-spectrometry and prepared for analysis on an RNA-gel by mixing the sample with RNA sample buffer. The samples were run on a 1% denaturing agarose-MOPS gel at 70-80V for approximately 3 hours and subsequently blotted over night onto a nylon membrane (Hybond-N, Pharmacia). The transferred RNA was fixed and cross-linked via UV (Jencons PLS) and incubation at 80°C for 1 hour.

Following prehybridisation with hybridisation solution for 1-4 hours at 42°C, the blots were incubated over night at 42°C with hybridisation solution containing ^{32}P radioactively labelled probes (prepared with and according to the Ready-to Go kit from Amersham). After successive washing steps with increased stringency using 2xSSC, 2xSSC and 0.1% SDS and 0.1xSSC and 0.1%SDS at room temperature or 65°C, the wet membranes were wrapped into Saran-film and exposed to Xray-films (Fuji-film XR) at -80°C using an intensifying screen.

For further details refer to the Hybond manual (Amersham) as well as to current protocols in molecular biology (Ausubel, 1988).

8.2. General methods in cell culture and immunofluorescence

8.2.1. Cryosectioning

Freshly dissected mouse hearts were snap frozen in isopentane in liquid nitrogen and stored at –80°C until sectioning. 10μm thick sections were generated on a Microm HM 560 cryostat with a cutting temperature of –22 to –18°C. Sections were mounted on gelatine coated slides, dried for 1 hour at room temperature and stored at –20°C until further processing.

8.2.2. Isolation and culture of neonatal rat cardiomyocytes (NRCs)

Newborn mouse and rat hearts were dissected, digested with collagenase (Worthington Biochemical Corp., Freehold, NY, USA) and pancreatin (Gibco Lab., Grand Island, NY, USA) and cultured as described (Komiyama et al., 1996; Sen et al., 1988). Alternatively a commercially available cardiomyocyte isolation system was used (Worthington Biochemical Corporation) and cells were prepared according to the provided protocol. Cells were plated onto fibronectin- or collagen-coated dishes (10μg/ml fibronectin) with a density of $0.4x10^6$ cells per 35 mm dish in plating medium. For live observations, cells were plated on laminin-coated glass-bottom culture dishes (MatTek Corp.,

Ashland, MA, USA). After 1day, the medium was either replaced by maintenance medium directly or after the transfection procedure (see below).

8.2.3. Transfection of NRCs

Two hours before transfection the cells were changed to transfection medium. Transfections were carried out using the Escort III transfection reagent from Sigma. 1μg-2μg supercoiled plasmid DNA as well as 4μl-6μl Escort III were diluted into 100μl OptiMEM (or DMEM) in separate siliconised tubes and mixed by pipetting, respectively. The DNA and Escort III transfection reagent were mixed and incubated at room temperature for at least 5 minutes allowing the DNA-Lipid complex to be formed. Cells were washed twice with OptiMEM or DMEM. The DNA-Lipid complex was added to 0.8ml maintenance medium without antibiotics and pipetted onto washed cells. Cell cultures were incubated for 6 to 10 hours at 37°C, 5%CO_2 and subsequently the medium was replaced with normal maintenance medium.

For experiments involving the use of media supplements like Androstan, Flutamide, LiCl or KCl, cells were kept for 1 day in maintenance medium, washed twice with PBS and transferred into maintenance medium supplemented with the appropriate amount of the chemical, but without serum and phenylephrine, and cultured for another 2 to 4 days.

8.2.4. Culture and transfection of Cos-1 cells

Cultivation of Cos-1 cells (Gluzman, 1981) was carried out in Cos culture medium.

Transfection of Cos-1 cells was performed using electroporation with a BTX electroporator model ECM 600 or chemically using the liposomal transfection reagent Escort IV (Sigma). For electroporation cells were grown in 10cm dishes to near confluence, trypsinised and mixed with Cos culture medium to inhibit trypsin activity, centrifuged at 140g and washed twice using a 1000μl pipette for resuspension in 10 ml 1x PBS. Cells were resuspended in 1x PBS to a density of $2x10^6$ cells / 150μl. Electroporation was carried out using sterile BTX electroporation cuvettes with a gap width of 4mm. 10μg of supercoiled plasmid DNA was transferred to the electroporation cuvette and 150μl cell suspension ($2x10^6$ cells) was added and incubated for 5 minutes on ice. Electroporation was carried out at Resistance/capacitance settings of 300V, 125μF and 72 Ohm. After the electroporation procedure, the cells were taken up in 200μl warm Cos culture medium and plated into 10cm dishes. For liposomal transfection of Cos-1 cells using Escort IV, the protocol for the transfection of NRCs was used (see earlier). Medium was changed after one day and cells were lysed after one or two additional days of cell growth.

8.2.5. Preparation of Cos-1 extracts

Lysis of transfected Cos-1 cells (see earlier) was carried out in lysis buffer containing 0.5% NP-40. Cell cultures were washed once with ice cold 1x PBS and 0.1 – 1ml lysis buffer was applied onto the culture dish. After incubation of 5 minutes, cells were scraped off on ice and the lysate was transferred to a clean eppendorf tube and incubated for 10 minutes on a shaking platform at 4°C. For further solubilization of protein complexes, samples were sonicated in an ice waterbath (ELMA sonicator, Transsonic Digitals, Singen, Germany) at maximum settings for 10 minutes. Removal of cell debris and insoluble complexes was done in a centrifugation step in a tabletop centrifuge with 5000rpm at 4°C. The supernatant was transferred to a clean eppendorf tube and stored for further use at 4°C. SDS samples were prepared for immunoblotting as described earlier and protein levels of exogenous fusion proteins were normalized using immuno-chemiluminescence intensity.

8.2.6. Immunofluorescence

For the *in situ* and *in vitro* stainings with antibodies against cytoskeletal and sarcomeric proteins as well as for detection of exogenously expressed tagged fusion proteins, the sections, resp. cells were fixed with 4% paraformaldehyde (PFA) in phosphate-buffered saline (1x PBS) for 10 minutes at room temperature. Samples were permeabilized with 0.2% Triton X-100 in PBS for 10 minutes and subsequently blocked for at least 30 minutes in 5% normal pre-immune goat serum in Tris buffered saline (TBS; resp. Gold buffer, GB) at room temperature. Alternatively, specimen were fixed after washing with PBS with ice cold methanol for 5 minutes at –20°C and before blocking with 5% pre-immune goat serum in TBS once washed for 5 minutes in PBS at room temperature. Further steps are equal for both preparation procedures.

Primary and secondary antibody were diluted in 1% BSA/TBS. The primary antibody incubation was carried out over night at 4°C or for 1 hour at room temperature. The incubation with the secondary antibody was performed for 1 hour at room temperature. Samples were washed thrice with PBS for 5 minutes after incubation of primary and secondary antibodies. A list of used antibodies and fluorescent reagents is presented in table 2a and 2b.

Specimen were mounted in Lisbeth's embedding medium and covered with coverslips for confocal laser scanning microscopy.

8.2.7. Laser Scanning Microscopy and image processing

Images of immunofluorescent labelled specimen were acquired by confocal laser scanning microscopy on an inverted Leica Confocal Laser Scanning Microscope (inverted Microscope DM IRB/E) and the Leica TCS-NT program using an Argon-Krypton mixed gas laser resp. a combination of Argon-Helium-Neon lasers or a Zeiss LSM510 Meta system equipped with an Argon-laser, Helium-Neon-lasers and a UV-diode. The images were recorded using a Leica PL APO 100x/1.4 oil, PL APO 63x/1.4 oil immersion, a PL APO 40x/1.4 oil objective or a PLAN Apochromat 63x/1.4 oil objective.

Further image processing was done on a Silicon Graphics Indy or O2 (Irix 6.5) using the image processing software Imaris (version 2 or 3; Bitplane AG Zürich, Switzerland) as well as Selima as image database (Bitplane, (Messerli et al., 1993)) and Adobe Photoshop (CS) for image collection and fine sampling.

8.2.8. FRET experiments

For experiments involving the fluorescence energy transfer method (FRET) two different approaches were employed: the sensitised emission method as well as the acceptor photobleaching technique (Berney and Danuser, 2003). For sensitised emission the individual channels were first imaged sequentially; subsequently only the CFP signal was excited and any signal in the YFP channel was recorded. Single transfections of CFP and YFP fusion proteins, respectively as well as cotransfections of CFP and YFP alone resultet in no signal in the FRET channel (negative control), while a fusion protein of CFP and YFP produced a FRET signal (positive control). In the case of the acceptor photobleaching method, first single channels were recorded, then a small area in a cell was bleached in the YFP channel and the signal in the CFP channel was again recorded. Quantification was performed by calculating the received (CFP) signal in the bleached area and subtracting it against the background measured in an unbleached area. Image processing was done using Adobe Photoshop (CS) and NIH-Image or ImageJ (www.rbs.info.nih.gov/ij).

8.3. Used antibodies and fluorescently labelled chemicals for immunofluorescence

Table 11. Used primary antibodies and fluorescent reagents.

Antibody dilutions for immunofluorescence. Note that antibody dilutions for immunoblots were 10 fold increased

Protein	Antibody clone	Dilution / Conc.	Company
total F-Actin	Alexa-488 labelled Phalloidin Alexa-546 labelled Phalloidin Alexa-633 labelled Phalloidin	1:50 1:50 1:50	Molecular probes, Switzerland
α–sarc. Actinin	monoclonal mouse anti α–Actinin (sarcomeric., EA53)	1:500	Sigma
α–sm Actin	monoclonal mouse anti α–smooth muscle Actin (clone 1A4)	1:100	Sigma
ANF	polyclonal rabbit anti atrial natriuretic factor	1:50	Zymed, CH
Pan-Cadherin	polyclonal rabbit anti Cadherin	1:100	Sigma
α–Catenin	polyclonal rabbit anti α–Catenin	1:250	Sigma
β–Catenin	polyclonal rabbit anti β–Catenin	1:200	Sigma
Plakoglobin (γ-Catenin)	monoclonal mouse anti Plakoglobin	1:100	Transduction Lab.
Desmoplakin	polyclonal rabbit anti Desmoplakin	1:200	Serotec
DRAL	polyclonal rabbit anti DRAL	1:100	generous gift of Dr. B. Schäfer
Dvl-1	polyclonal rabbit anti Dishevelled	1:50	generous gift of Dr. P. Salinas
FLAG epitope	monoclonal mouse anti FLAG M2	1:100	Sigma
GFP	monoclonal mouse anti GFP	1:100	Roche
HA epitope	monoclonal rat anti HA monoclonal mouse anti HA	1:100 1:100	Roche
β-1D-Integrin	polyclonal rabbit anti β-1D-Integrin	1:50	generous gift of Dr. G. Tarone
Myomesin	monoclonal mouse anti Myomesin (B4)	1:50	raised in our laboratory [Grove et al.1984]
sarc MHC	monoclonal mouse sarcomeric Myosin heavy chain (A4.1025)	1:5	generous gift of Dr. S.M. Hughes
MLCK	polyclonal sheep anti myosin light chain kinase	1:500	generous gift of Prof. M.C. Schaub
N-RAP	polyclonal rabbit anti N-RAP (nebulin related anchorage protein)	1:100	generous gift of Dr. R. Horowits
nucleus	DRAQ5	1:50	Biostatus, UK
nucleus	DAPI	1:100	Sigma
nucleus	H-33342		Hoechst (Sigma)
Phosphofructokinase	polyclonal rabbit anti phosphofructokinase	1:100	generous gift of Dr. M. Bähler
Spectrin	polyclonal rabbit anti Spectrin	1:200	Biogenesis

Titin	polyclonal rabbit anti Titin (M-band epitope) m8	1:50	generous gift of Dr. M. Gautel
Titin	monoclonal mouse anti Titin clone 9D10 (PEVK I-band epitope) IgM	1:3	Developmental Studies Hybridoma Bank, Iowa, USA
Titin	polyclonal chicken anti Titin N2A	1:50	generous gift of Dr. C. Gregorio
Titin	monoclonal mouse anti Titin N2B (I19 epitope)	1:1	generous gift of Dr. M. Gautel
Titin	monoclonal mouse anti Titin T12 (Z-disk epitope)	1:100	generous gift of Dr. D.O. Fürst
Vinculin	monoclonal mouse anti Vinculin (clone hVin-1)	1:20	Sigma

Table 12. Used secondary antibodies.

Antibody dilutions for immunofluorescence are shown.

Protein	Conjugate	Dilution / Conc.	Company
goat anti rabbit Ig	FITC	1:100	Cappel, Organon, Teknika AG, CH
goat anti mouse Ig	FITC	1:100	Cappel, Organon, Teknika AG, CH
goat anti mouse IgM (μ-chain specific)	FITC	1:100	Sigma
horse anti mouse (no cross-reaction with rat)	FITC	1:50	Vector
donkey anti chicken IgY	FITC	1:100	The Binding Site Ltd., Birmingham, UK
goat anti rat	Cy2	1:100	Jackson (distributed by Milan)
donkey anti rat Ig (no cross reaction with mouse)	Cy2	1:100	Jackson (distributed by Milan)
polyclonal goat anti mouse Ig (H+L)	Cy3	1:500	Jackson (distributed by Milan)
polyclonal goat anti rabbit Ig (H+L)	Cy3	1:1000	Jackson (distributed by Milan)
polyclonal goat anti mouse IgG (γ-chain specific)	Cy3	1:200	Jackson (distributed by Milan)
donkey anti rat Ig (no cross-reaction with mouse)	Cy3	1:100	Jackson (distributed by Milan)
donkey anti sheep Ig	Cy3	1:50	Jackson (distributed by Milan)
donkey anti mouse IgM	Cy5	1:100	Jackson (distributed by Milan)
goat anti mouse Ig	Cy5	1:100	Jackson (distributed by Milan)
donkey anti mouse Ig (no cross-reaction rat)	Cy5	1:100	Jackson (distributed by Milan)
goat anti rabbit	Cy5	1:100	Jackson (distributed by Milan)

8.4. Used peroxidase conjugated antibodies

Table 13. List of used horseradish peroxidase coupled antibodies.

Dilutions of conjugated antibodies for immunoblotting are shown.

Protein	Conjugate	Dilution / Conc.	Company
polyclonal rabbit anti mouse Ig+M	Horse radish peroxidase	1:1000	DAKO, CH
polyclonal goat anti rabbit Ig (H+L)	Horse radish peroxidase	1:1000	Calbiochem, CH
polyclonal rabbit anti rat	Horse radish peroxidase	1:1000	DAKO, CH

8.5. Used media, solutions and buffers

8.5.1. Isolation of plasmid DNA

S1 buffer
50mM Tris/Cl
10mM EDTA
pH 8
RNAse A

S2 buffer
200mM NaOH
1% SDS

S3 buffer
2.8M KAc
60 % Acetic acid

N2 buffer
100mM Tris
15 % Ethanol
900mM KCl
pH 7.4 (66% H_3PO_4)

N3 buffer
100mM Tris
15% Ethanol
1.15M KCl
pH 7.4 (66% H_3PO_4)

N5 buffer
100mM Tris
15% Ethanol
1M KCl
pH 7.4 (66% H_3PO_4)

8.5.2. DNA

0.5x TE

5mM TRIS-HCl
0.5mM EDTA
pH 7.5

0.5x TBE (for 10 litres)

54g Trizma base
27.5g boric acid
4.6g EDTA

Loading buffer I

0.02% bromphenol blue
0.004% Xylene cyanole FF
13.3% w/w sucrose

Ethidium bromide stock (1:25000)
10mg/ml ethidium bromide

8.5.3. Bacteria

Psi broth (per litre)
5g bacto yeast extract
20g bacto tryptone
5g magnesium sulfate
ph 7.6 with potassium hydroxide

TfbI
30mM potassium acetate
100mM rubidium chloride
10mM calcium chloride
50mM manganese chloride
15% v/v glycerol
pH 5.8 with diluted acetic acid

TfbII
10mM MOPS
75mM calcium chloride
10mM rubidium chloride
15% v/v glycerol
pH 6.5 with diluted NaOH

LB medium (for 5 litres)
25g bacto yeast extract
50g bacto-tryptone
50g sodium chloride
0.2ml 5M sodium chloride

LB-agar
7.5g bacto agar
per 500ml LB medium

SOC medium (for 2 litres)
40g bacto tryptone
10g yeast extract
1g sodium chloride
20ml 250mM potassium chloride
pH 7.0 with NaOH

40ml 1M glucose
(add after autoclaving)

Ampicillin stock (1:1000)
50mg/ml Ampicillin

Tetracycline stock (1:1000)
10mg/ml in 70% EtOH

Kanamycin stock (1:1000)
30mg/ml Kanamycin

Karbenicillin stock (1:1000)
50mg/ml Karbenicillin

bacterial glycerol stock
300µl 50% glycerol
750µl bacteria in LB

STE-Lysis buffer
see GST-pulldown

8.5.4. Cell culture

PBS (10x stock solution)
1.5M sodium chloride
65mM Na_2HPO_4 x $2H_2O$
27mM potassium chloride
15mM KH_2PO_4
pH 7.2-7.4

SD medium
26mg soybean trypsin inhibitor
2mg bovine pancreas DNAse
150mg BSA
dissolve in 50ml DMEM,
incubate 15min at room temperature
filtrate sterile

Cos lysis buffer
100mM KCl
10mM HEPES pH 7.9
5mM $MgSO_4$
1mM DTT
0.2mM EGTA
50μM $ZnSO_4$
1.5% Triton X-100
1x Protease Inhibitor complete
EDTA free (Roche)

Plating medium
67% Dulbecco's MEM (Amimed AG)
17% Medium M199
10% horse serum (Gibco)
5% fetal calf serum
4mM glutamine
1% Penicillin/Streptomycin
(Amimed)

NRC Maintenance medium
20% Medium M199
75% DBSS-K
4% Horse serum
4mM glutamine
1% Penicillin/Streptomycin
0.1mM Phenylephrine

DBSS-K
6.8g/l sodium chloride
0.14mM NaH_2PO_4
0.2mM calcium chloride
0.2mM $MgSO_4$ x 7 H_2O
1mM Dextrose
2.7mM $NaHCO_3$

Cos culture medium
89% Dulbecco's MEM high glucose
10% fetal calf serum
1% Penicillin/Streptomycin
4mM glutamine

NRC Transfection medium
20% Medium M199
75% DBSS-K
4% Horse serum
4mM glutamine

8.5.5. Northern blot

10x MOPS
0.2M 3-[N-Morpholino] propane
-sulphonic acid
0.5M Na-acetate pH7.0
0.01M Na_2EDTA

20xSSC
3M NaCl
0.3M Na_3citrate

Loading buffer
1x MOPS
18.5% Formaldehyde
50% Formamide
4% Ficoll 400
0.02% bromphenol blue
0.1% Ethidium bromide

Hybridisation solution
1.5x SSPE
7% SDS
10% PEG 8000
100μg/ml sheared salmon sperm
DNA
250μg/ml Heparin

20x SSPE
3.6M NaCl
0.2M Sodium phosphate
0.02M EDTA pH7.7

8.5.6. GST-pulldown assay & co-immunoprecipitation

STE-Lysis buffer
100mM KCl
10mM HEPES pH 7.9
50μM $ZnSO_4$
1% Triton X-100
1mM DTT
0.5mg/ml Lysozyme

modified STE buffer
100mM KCl
10mM HEPES pH 7.9
50μM $ZnSO_4$

Wash buffer
100mM KCl
10mM HEPES pH 7.9
5mM $MgSO_4$
0.2mM EGTA
50μM $ZnSO_4$
0.5% NP-40
1mM DTT
1x Protease Inhibitor complete
EDTA free (Roche)

IP-Lysis buffer
150mM NaCl
10mM Tris-HCl pH7.9
1mM DTT
0.25% NP-40
1x Protease Inhibitor complete
EDTA free (Roche)

IP-buffer
150mM NaCl
10mM Tris-HCl pH7.9
1mM DTT
1x Protease Inhibitor complete
EDTA free (Roche)

8.5.7. Immunofluorscence and specimen preparation

Gelatine coated slides
1% gelatine
0.1% potassium chromosulfate
(dissolve in water at 50-60°C)

clean slides if necessary with
10% HCl in EtOH / methanol

Tris buffered saline (Gold buffer)
20mM Trizma base
155mM NaCl
2mM EGTA
2mM $MgCl_2$
pH 7.5

Lisbeth's embedding medium
15ml 0.1M Tris pH 9.5
35ml glycerol
2.5g n-propyl gallate

4% PFA in PBS (100ml)
4g PFA
7.5μl 10N NaOH
heat to 65°C and stir until dissolved
filter

PBS
see cell culture

Relaxation buffer (2x stock)
7mM EGTA
20mM Imidazole
1mM magnesium chloride
14.5mM phosphocreatine
4mM Mg ATP
100mM potassium chloride
pH 7.0 with potassium hydroxyde
add 0.1% Saponin before use

8.5.8. SDS-PAGE and immunoblotting

SDS sample buffer ("blue wonder"; modified after Laemmli 1970; Ehler et al. 1999)
3.7M Urea
134.6mM Tris
5.4% SDS
2.3% NP-40
4.45% β-mercaptoethanol
4% glycerol
6mg/100ml bromophenolblue
pH 6.8

Lower buffer (for 0.5 litre)
1.5M Trizma base (91g)
0.4% SDS (2g)
62.5ml 1N HCl
pH 8.8

Upper buffer (for 0.5 litre)
0.5M Trizma base (30.3g)
0.4% SDS (2g)
48ml 1N HCl
pH6.8

Low salt (for 1 litre)
0.9% w/w sodium chloride
10mM Trizma base pH 7.4
0.1% Tween-20

Blotting buffer (1 litre)
3g Trizma base
14.5g glycine
0.1g SDS
200ml methanol

Coomassie blue
50% methanol
10% acetic acid
0.2% Coomassie R-250
(filter)

enhanced chemoluminescence solution
7.5ml water
1ml Luminol stock
1ml Iodophenol stock
0.5ml 1M Tris pH 7.5

add in the dark shortly before use
5µl 30% H_2O_2

Luminol 10x stock (10ml)
25mM Luminol (50mg)
dissolve in H_2O

Iodophenol 10x stock (10ml)
5nM Iodophenol (11mg)
dissolve in DMSO

Stripping buffer
62.5mM Tris pH 6.7
2% SDS
100mM β-mercaptoethanol

incubate 30 minutes at 50°C and wash twice with low salt for 10 minutes

Running buffer 10 x stock (1 litre)
30g Trizma base
144g glycine
10g SDS

8.6. Used Vectors

8.6.1. Eukaryotic expression vectors

8.6.1.1. Fluorescent protein vectors

All used pECFP, pEGFP and pEYFP vectors were constructed and sold from Clontech (BD Bioscience; www.clontech.com).

For the generation of the split-GFP vectors, the N-terminal 172 amino acids of CFP, GFP or YFP and the C-terminal part (residues 156-239) of CFP, GFP or YFP (Fang and Kerppola, 2004) were subcloned into the pEGFP-C1 or -N1 vector backbone via PCR using appropriate primers and restriction enzymes (see Primer section). The correct sequences were confirmed via sequencing.

8.6.1.2. HA-tagged vectors

The HA-vectors pHA-C1, pHA-N1 and pHA-N3 were constructed using the pEGFP vector backbone and linker-ligation. The nomenclature refers to the pEGFP-vector reading frame.

8.6.1.3. pcDNA vectors

All used pcDNA vectors were from Invitrogen (www.invitrogen.com).

8.6.1.4. pCMV vectors

The pCMV-vectors were derived from pCMV5 (QBiogene) and modified for further use by the group of Prof. Mathias Gautel.

8.6.2. Bacterial expression vectors

8.6.2.1. pGex-vectors

pGex-3X and pGex-2TK were constructed and sold by Pharmacia. The pGex-C1 vector with a multiple cloning site compatible to the pEGFP-C1 was constructed using linker ligation (see primer section).

8.6.2.2. pET vectors

pETev-6His for the expression of the His-tagged protein fusions was derived from the lab of Prof. Mathias Gautel.

8.7. Used primers

	mouse Adenylate kinase		mouse androgen receptor
AK.fwd	gaagatctaccATGGAAGAGAAGCTGAAGAAGGCC	AR.fwd	gaagatctATGGAGGTGCAGTTAGGGCTGGGA
AK.rev	ccgctcgagCTTCAGGGAGTCAAGATAGGTGCA	AR.rev	ccgctcgagCTGTGTGTGGAAATAGATGGGCTTG
	mouse phophofructokinase		human presenilin2
PFK.fwd	gaagatctaccATGACCCATGAAGAGCATCATGC	hPS2.fwd	gaagatctaccATGCTCACATTCATGGCCTCTGAC
PFK.rev	ccgctcgagGACGGCGGCTTCTCCAGACCGT	hPS2.rev	ccgctcgagGATGTAGAGCTGATGGGAGG
	human titin kinase		mouse Csl / Smpx
hTK.fwd	cggCTCGAGccaccATGAACTATGATGAAGAGG	Smpx.fwd	gaagatctaccATGTCGAAGCAGCCAATTTCCAAC
hTK.rev	cccAAGCTTaatttcaatggatgcc	Smpx.rev	ccgctcgagCTGTTCACCTTTGGGGACAAATTTC
	human titin N2B		human Murf2
N2B.fwd	gaagatctATGGAAGGCACTGGCCCAATTTTCATCAAAGAA	hMurf2.fwd	gaAGATCTgccaccATGAGCGCATCTCTGAATTAC
N2B.rev	ccgctcgagCACTGTCACAGTTAGTGTGGCTGTACAGCT	hMurf2.rev	ccccccgggcTTCATTTAGGGAGTTCAACCAGG
N2BS3799Y.fwd	tacATTTTGGAGCAAGACAAGCTC	hMurf2_XhoI.fwd	ccgCTCGAGccaccATGAGCGCATCTCTGAATTAC
N2BS3799Y.rev	GAGCTTGTCTTGCTCCAAAATgtaTTGCAATTCCTGAGCTCCCAAAG		
	human titin Z1Z2		mouse Myomesin
hTitinZ1Z2.fwd	ccgCTCGAGccaccATGACAACTCAAGCACCGAC	mMy9.fwd	cgGGATCCgccaccATGCCTGTTGTGGCTGAAAC
hTitinZ1Z2.rev	cgggatccTCTTCACCTTGAACCAGTAATTCAG	mMy9.rev	ccgctcgagccCTTGTGCTCCTGGCTGAGGGC
		mMy10.fwd	cgGGATCCgccaccATGAAACGTCTGCTTGCCCTC
	human Myomesin	mMy10.rev	ccgctcgagccTTGCTTCCTGATCCATTCTTGTCG
hMy2_ass.fwd	GCATTGCTCCATAGCAGGCTGGCCAG	mMy11.fwd	ccgCTCGAGccaccatgGGAGACGTTTATAAG
hMy2_ass.rev	CTGGCCAGCCTGCTATGGAGCAATGC	mMy11.rev	ccgctcgagccAGACAACGCTATCTTCTTGC
hMy9_NheI.fwd	gctagcATGGTGGCAGAGACCCGTCCA	mMy12.fwd	ccgCTCGAGccaccatgGCCTTCCAAGACTTGATG
hMy9.fwd	ccgCTCGAgccaccATGGTGGCAGAGACCCGTCCA	mMy12.rev	cccAAGCTTGAGACCACCTAACACCCG
hMy13_BamHI.rev	cgggatcctaCTTGGCCTTCTTGCCACC	mMy12_XhoI.rev	ccgctcgagccGAGACCACCTAACACCCG
hMy13.rev	cgggatcCTTGGCCTTCTTGCCACC	mMy13.fwd	ccgCTCGAGccaccatgCAAGCATTTGATGAGGCC
hMy_ass.fwd	GTGGCAGAGACCCGTCCAGG	mMy13.rev	cccAAGcttggacttctggttgccc
hMy_ass.rev	CCTGGACGGGTCTCTGCCAC		

	human Myomesin		mouse Myomesin
hMy2.fwd	gGAATTCgccaccATGCTGAATGAAG ACCATC	mMy11_ K1150A.fwd	gccAAGAAGGAGACTCATATTG
hMy8.rev	ccgctcgagctTCCTGGACGGGTCTCT GCCACAAC	mMy11_ K1150A.rev	CACACAATATGAGTCTCCTTggcAAT ATTTGCCACCTTGCATTTC
hMyK1589R.fwd	agaAACGAGAAGCCACTGACCTC		
hMyK1589R.rev	GAGGTCAGTGGCTTCTCGTTtctCAG CCAGGACACCTCAGGGG	mMy11_ K1159A.fwd	gccGATGAGAGGGAGATATCAG
hMyK1603R.fwd	aggTTTGAGGCCGGGAAAACCGC	mMy11_ K1159A.rev	CACTGATATCTCCCTCTCATCggcG TACCACACAATATGAGTCTC
hMyK1603R.rev	GCGGTTTTCCCGGCCTCAAAcctGA GaCTGCAGTGGTCGTCAG	mMy11_ K1197A.fwd	gccGATGACCGAGGAAAAGATAAG
hMy12_pETev.fwd	gccAAGGAGACTCATATTGTGTG	mMy11_ K1197A.rev	CTTATCTTTTCCTCGGTCATCggcCA GGATAACTTCATAAATCC
hMy13_pETev.fwd	ccgctcgagTGGACAAGCATACGATGA GG		
hMy13_pETev.rev	cgacgcgtTCACTTGGCCTTCTTGCCA CC		linker
hMyR116P.fwd	cccGCCCGGGTGTTGGGAGGTC	gfp2c2n1.fwd	agtACCGGTcgccaccATGGTGAGCAA GGGCGAG
hMyR116P.rev	GACCTCCCAACACCCGGGCgggATT TTTCTCGGCAATGGCAG	gfp2c2n1.rev	gatcCGGCCGgaCTTGTACAGCTCGT CCATGC
hMyD1580K.fwd	aagGTGGTCACCATCCAGGAGGG	pGex_ GFP-MCS.fwd	gatctgctagcAGATCTCGAGCTCAAGC TTCGAATTCTGCAGTCGACGGTAC CGCGGGCCCGGGATCCACCGGAT CTAGATAA
hMyD1580K.rev	CCCTCCTGGATGGTGACCACcttTG GGAGACCTCCCAACACCC	pGex_ GFP-MCS.rev	aattTTATCTAGATCCGGTGGATCCC GGGCCCGCGGTACCGTCGACTGC AGAATTCGAAGCTTGAGCTCGAGA TCTgctagca
hMyK1588D.fwd	gacGCCCTTAATCTCACTTGCAAC	C12C2.fwd	gatcggAGATCTCGAGCTCA
hMyK1588D.rev	GTTGCAAGTGAGATTAAGGGCgtcC CCCTCCTGGATGGTGAC	C12C2.rev	agctTGAGCTCGAGATCTcc
	human NBR1		human Telethonin
hNBR1.fwd	gaAGATCTgccaccatggaaccacaggttact c	hTel.fwd	cggCTCGAGccaccATGGCTACCTCA GAGC
hNBR1.rev	tccgCTCGAGtgatagcgttggctgtaccag	hTel.rev	cccAAGCTTgcctctctgtgcttcctg
	human SRF		split-GFP
hSRF.fwd	ccgctcgagccaccatgttaccgacccaagctg	GFP_N.fwd	CGCTACCGGTCGCCACCATGGTGA GC
hSRF.rev	ggaattccttcactcttggtgctgtgg	GFP_N.rev	agatctcgatccgccGATGTTGTGGCGGA TCTTGA
hSRFK147A.fwd	CATGCCatggagttcatcgacaacaagctg	GFP_C.fwd	aaaccggtcgccaccATGGACAAGCAGA AGAACGG
hSRFK147A.rev	CATGccatGGCgatcttcacgcggccccgg	GFP_C.rev	tctgaCGGCCGacttGTACAGCTCGTC CATGCC
			human Ubc9
		hUbe21.fwd	agagatctgccaccATGTCGGGGATCGC CCTCAG
		hUbe21.rev	ggaattcgTGAGGGCGCAAACTTCTTG GC

	Sequencing
T3.fwd	aattaaccctcactaaaggg
T7Term.rev	gctagttattgctcagcgg
Sp6.rev	ATTTAGGTGACACTATAG
pEGFPend.fwd	agaccccaacgagaagcg
Sv40.rev	CATTCATTTTATGTTTCAG
pGex.fwd	TTGCAGGGCTGGCAAGCCACG
pGex.rev	gggagctgcatgtgtcagagg
pAct2.fwd	TATAACGCGTTTGGAATCACTACAGGG
pAct2.rev	AAATTGAGATGGTGCACGATGCAC

	human PIAS1
hPias1.fwd	gaAGATCTaccATGGCGGACAGTGCGGAAC
hPias1.rev	gGAATTCgGTCCAATGAAATAATGTCTGG
hPias1dC.rev	gGAATTCgCGGTGCCCAAGTGCCATCCT
hPias1dN.fwd	gaAGATCTaccATGTCTGCCAAGAGGACCTG

	mouse Sumo
mSumo1.fwd	cggCTCGAGccaccATGTCTGACCAGGAGGC
mSumo1.rev	cccAAGCTTAACCGTCGAGTGACCCCCC
mSumo1dC.rev	cccAAGCTTctaCGTTTGTTCCTGATAAAC
mSumo2.fwd	cggCTCGAGccaccATGGCCGACGAGAAACC
mSumo2.rev	cccAAGCTTgtagacacctccagtctgc
mSumo3.fwd	cggCTCGAGccaccATGTCGGAAGAGAAGCC
mSumo3.rev	cccAAGCTTatagcacaggtcaggacaac
mSumo3_pET.fwd	ccgCTCGAGTGAAGAGAAGCCCAAG
mSumo3_pET.rev	cgacgcgtctaTCCTCCTGTCTGCTGCTGG

	human MIQ
5'Race_1.rev	GTGGGTCTGCTCCCAACCCTGTTCCC
5'Race_2.rev	GTTCCCAAGCCCGTTCCTGAGCCCC
5'Race_3.rev	CCTGAGCCCCTTTCTGGGTCTGCCTC
5'Race_dT.fwd	ggaattctcgaggatccACCGGTgcggccgcAAGCTTttttttttttttttttt
5'Race_A1.fwd	ggaattctcgaggatccACCGG
5'Race_A2.fwd	aggatccACCGGTgcggccgcAAGC
probe21.fwd	AGAGGCAGACCCAGAAAGG
probe21.rev	CCTCAGGCTTGGGCTCAGTTG
probe39.fwd	GGACCCAGGGACACAGT
probe39.rev	TCTGAACCTCTCCTTGAAC

9. References

Agarkova, I., D. Auerbach, E. Ehler, and J.C. Perriard. 2000. A novel marker for vertebrate embryonic heart, the EH-myomesin isoform. *J Biol Chem*. 275:10256-64.

Agarkova, I., R. Schoenauer, E. Ehler, L. Carlsson, E. Carlsson, L.E. Thornell, and J.C. Perriard. 2004. The molecular composition of the sarcomeric M-band correlates with muscle fiber type. *Eur J Cell Biol*. 83:193-204.

Amodeo, P., M.A. Castiglione Morelli, G. Strazzullo, P. Fucile, M. Gautel, and A. Motta. 2001. Kinase recognition by calmodulin: modeling the interaction with the autoinhibitory region of human cardiac titin kinase. *J Mol Biol*. 306:81-95.

Arber, S., G. Halder, and P. Caroni. 1994. Muscle LIM protein, a novel essential regulator of myogenesis, promotes myogenic differentiation. *Cell*. 79:221-31.

Arber, S., J.J. Hunter, J. Ross, Jr., M. Hongo, G. Sansig, J. Borg, J.C. Perriard, K.R. Chien, and P. Caroni. 1997. MLP-deficient mice exhibit a disruption of cardiac cytoarchitectural organization, dilated cardiomyopathy, and heart failure. *Cell*. 88:393-403.

Armstrong, E.J., and J. Bischoff. 2004. Heart valve development: endothelial cell signaling and differentiation. *Circ Res*. 95:459-70.

Arnold, H., and D. Pette. 1970. Binding of aldolase and triosephosphate dehydrogenase to F-actin and modification of catalytic properties of aldolase. *Eur J Biochem*. 15:360-6.

Arrio-Dupont, M., G. Foucault, M. Vacher, A. Douhou, and S. Cribier. 1997. Mobility of creatine phosphokinase and beta-enolase in cultured muscle cells. *Biophys J*. 73:2667-73.

Au, Y. 2004. The muscle ultrastructure: a structural perspective of the sarcomere. *Cell Mol Life Sci*. 61:3016-33.

Auerbach, D., S. Bantle, S. Keller, V. Hinderling, M. Leu, E. Ehler, and J.C. Perriard. 1999. Different domains of the M-band protein myomesin are involved in myosin binding and M-band targeting. *Mol Biol Cell*. 10:1297-308.

Auerbach, D., B. Rothen-Ruthishauser, S. Bantle, M. Leu, E. Ehler, D. Helfman, and J.C. Perriard. 1997. Molecular mechanisms of myofibril assembly in heart. *Cell Struct Funct*. 22:139-46.

Ausubel, F.M. 1988. Current protocols in molecular biology. Wiley, New York. Loseblattsammlung pp.

Bantle, S., S. Keller, I. Haussmann, D. Auerbach, E. Perriard, S. Muhlebach, and J.C. Perriard. 1996. Tissue-specific isoforms of chicken myomesin are generated by alternative splicing. *J Biol Chem*. 271:19042-52.

Bennett, P.M., D.O. Furst, and M. Gautel. 1999. The C-protein (myosin binding protein C) family: regulators of contraction and sarcomere formation? *Rev Physiol Biochem Pharmacol*. 138:203-34.

Berney, C., and G. Danuser. 2003. FRET or no FRET: a quantitative comparison. *Biophys J*. 84:3992-4010.

Bies, J., J. Markus, and L. Wolff. 2002. Covalent attachment of the SUMO-1 protein to the negative regulatory domain of the c-Myb transcription factor modifies its stability and transactivation capacity. *J Biol Chem*. 277:8999-9009.

Bisig, D., P. Weber, L. Vaughan, K.H. Winterhalter, and K. Piontek. 1999. Purification, crystallization and preliminary crystallographic studies of a two fibronectin type-III domain segment from chicken tenascin encompassing the heparin- and contactin-binding regions. *Acta Crystallogr D Biol Crystallogr*. 55:1069-73.

Bodine, S.C., E. Latres, S. Baumhueter, V.K. Lai, L. Nunez, B.A. Clarke, W.T. Poueymirou, F.J. Panaro, E. Na, K. Dharmarajan, Z.Q. Pan, D.M. Valenzuela, T.M. DeChiara, T.N. Stitt, G.D. Yancopoulos, and D.J. Glass. 2001. Identification of ubiquitin ligases required for skeletal muscle atrophy. *Science*. 294:1704-8.

Bonne, G., L. Carrier, J. Bercovici, C. Cruaud, P. Richard, B. Hainque, M. Gautel, S. Labeit, M. James, J. Beckmann, and et al. 1995. Cardiac myosin binding protein-C gene splice acceptor site mutation is associated with familial hypertrophic cardiomyopathy. *Nat Genet*. 11:438-40.

Carlsson, E., B.K. Grove, T. Wallimann, H.M. Eppenberger, and L.E. Thornell. 1990. Myofibrillar M-band proteins in rat skeletal muscles during development. *Histochemistry*. 95:27-35.

Carlsson, E., U. Kjorell, L.E. Thornell, A. Lambertsson, and E. Strehler. 1982. Differentiation of the myofibrils and the intermediate filament system during postnatal development of the rat heart. *Eur J Cell Biol*. 27:62-73.

Centner, T., J. Yano, E. Kimura, A.S. McElhinny, K. Pelin, C.C. Witt, M.L. Bang, K. Trombitas, H. Granzier, C.C. Gregorio, H. Sorimachi, and S. Labeit. 2001. Identification of muscle specific ring finger proteins as potential regulators of the titin kinase domain. *J Mol Biol*. 306:717-26.

Chai, J., and A.S. Tarnawski. 2002. Serum response factor: discovery, biochemistry, biological roles and implications for tissue injury healing. *J Physiol Pharmacol*. 53:147-57.

Chan, H.M., and N.B. La Thangue. 2001. p300/CBP proteins: HATs for transcriptional bridges and scaffolds. *J Cell Sci*. 114:2363-73.

Chan, K.K., S.K. Tsui, S.M. Lee, S.C. Luk, C.C. Liew, K.P. Fung, M.M. Waye, and C.Y. Lee. 1998. Molecular cloning and characterization of FHL2, a novel LIM domain protein preferentially expressed in human heart. *Gene*. 210:345-50.

Chien, K.R., K.U. Knowlton, H. Zhu, and S. Chien. 1991. Regulation of cardiac gene expression during myocardial growth and hypertrophy: molecular studies of an adaptive physiologic response. *Faseb J*. 5:3037-46.

Chu, P.H., W.M. Bardwell, Y. Gu, J. Ross, Jr., and J. Chen. 2000. FHL2 (SLIM3) is not essential for cardiac development and function. *Mol Cell Biol*. 20:7460-2.

Chung, T.L., H.H. Hsiao, Y.Y. Yeh, H.L. Shia, Y.L. Chen, P.H. Liang, A.H. Wang, K.H. Khoo, and S. Shoei-Lung Li. 2004. In vitro modification of human centromere protein CENP-C fragments by small ubiquitin-like modifier (SUMO) protein: definitive identification of the modification sites by tandem mass spectrometry analysis of the isopeptides. *J Biol Chem*. 279:39653-62.

Cooke, R. 2004. The sliding filament model: 1972-2004. *J Gen Physiol*. 123:643-56.

Crowther, R.A., and P.K. Luther. 1984. Three-dimensional reconstruction from a single oblique section of fish muscle M-band. *Nature*. 307:569-70.

Dai, K.S., and C.C. Liew. 2001. A novel human striated muscle RING zinc finger protein, SMRZ, interacts with SMT3b via its RING domain. *J Biol Chem*. 276:23992-9.

De Strooper, B., and W. Annaert. 2001. Where Notch and Wnt signaling meet. The presenilin hub. *J Cell Biol*. 152:F17-20.

Dolken, G., E. Leisner, and D. Pette. 1975. Immunofluorescent localization of glycogenolytic and glycolytic enzyme proteins and of malate dehydrogenase isozymes in cross-striated skeletal muscle and heart of the rabbit. *Histochemistry*. 43:113-21.

Duan, R., W. Xie, X. Li, A. McDougal, and S. Safe. 2002. Estrogen regulation of c-fos gene expression through phosphatidylinositol-3-kinase-dependent activation of serum response factor in MCF-7 breast cancer cells. *Biochem Biophys Res Commun*. 294:384-94.

Duval, D., G. Duval, C. Kedinger, O. Poch, and H. Boeuf. 2003. The 'PINIT' motif, of a newly identified conserved domain of the PIAS protein family, is essential for nuclear retention of PIAS3L. *FEBS Lett*. 554:111-8.

Ehler, E., R. Horowits, C. Zuppinger, R.L. Price, E. Perriard, M. Leu, P. Caroni, M. Sussman, H.M. Eppenberger, and J.C. Perriard. 2001. Alterations at the intercalated disk associated with the absence of muscle LIM protein. *J Cell Biol*. 153:763-72.

Ehler, E., B.M. Rothen, S.P. Hammerle, M. Komiyama, and J.C. Perriard. 1999. Myofibrillogenesis in the developing chicken heart: assembly of Z-disk, M-line and the thick filaments. *J Cell Sci*. 112 (Pt 10):1529-39.

El Mourabit, H., S. Muller, L. Tunggal, M. Paulsson, and M. Aumailley. 2004. Analysis of the adaptor function of the LIM domain-containing protein FHL2 using an affinity chromatography approach. *J Cell Biochem*. 92:612-25.

Fang, D., and T.K. Kerppola. 2004. Ubiquitin-mediated fluorescence complementation reveals that Jun ubiquitinated by Itch/AIP4 is localized to lysosomes. *Proc Natl Acad Sci U S A*. 101:14782-7.

Faulkner, G., G. Lanfranchi, and G. Valle. 2001. Telethonin and other new proteins of the Z-disc of skeletal muscle. *IUBMB Life*. 51:275-82.

Faulkner, G., A. Pallavicini, A. Comelli, M. Salamon, G. Bortoletto, C. Ievolella, S. Trevisan, S. Kojic, F. Dalla Vecchia, P. Laveder, G. Valle, and G. Lanfranchi. 2000. FATZ, a filamin-, actinin-, and telethonin-binding protein of the Z-disc of skeletal muscle. *J Biol Chem*. 275:41234-42.

Faulkner, G., A. Pallavicini, E. Formentin, A. Comelli, C. Ievolella, S. Trevisan, G. Bortoletto, P. Scannapieco, M. Salamon, V. Mouly, G. Valle, and G. Lanfranchi. 1999. ZASP: a new Z-band alternatively spliced PDZ-motif protein. *J Cell Biol*. 146:465-75.

Fields, S., and O. Song. 1989. A novel genetic system to detect protein-protein interactions. *Nature*. 340:245-6.

Fimia, G.M., D. De Cesare, and P. Sassone-Corsi. 2000. A family of LIM-only transcriptional coactivators: tissue-specific expression and selective activation of CREB and CREM. *Mol Cell Biol*. 20:8613-22.

Finn, B.E., and S. Forsen. 1995. The evolving model of calmodulin structure, function and activation. *Structure*. 3:7-11.

Flick, M.J., and S.F. Konieczny. 2000. The muscle regulatory and structural protein MLP is a cytoskeletal binding partner of betaI-spectrin. *J Cell Sci*. 113 (Pt 9):1553-64.
Foucault, G., M. Vacher, T. Merkulova, A. Keller, and M. Arrio-Dupont. 1999. Presence of enolase in the M-band of skeletal muscle and possible indirect interaction with the cytosolic muscle isoform of creatine kinase. *Biochem J*. 338 (Pt 1):115-21.
Freiburg, A., and M. Gautel. 1996. A molecular map of the interactions between titin and myosin-binding protein C. Implications for sarcomeric assembly in familial hypertrophic cardiomyopathy. *Eur J Biochem*. 235:317-23.
Furukawa, T., Y. Ono, H. Tsuchiya, Y. Katayama, M.L. Bang, D. Labeit, S. Labeit, N. Inagaki, and C.C. Gregorio. 2001. Specific interaction of the potassium channel beta-subunit minK with the sarcomeric protein T-cap suggests a T-tubule-myofibril linking system. *J Mol Biol*. 313:775-84.
Garvey, S.M., C. Rajan, A.P. Lerner, W.N. Frankel, and G.A. Cox. 2002. The muscular dystrophy with myositis (mdm) mouse mutation disrupts a skeletal muscle-specific domain of titin. *Genomics*. 79:146-9.
Geetha, T., and M.W. Wooten. 2002. Structure and functional properties of the ubiquitin binding protein p62. *FEBS Lett*. 512:19-24.
Gehmlich, K., C. Geier, K.J. Osterziel, P.F. Van der Ven, and D.O. Furst. 2004. Decreased interactions of mutant muscle LIM protein (MLP) with N-RAP and alpha-actinin and their implication for hypertrophic cardiomyopathy. *Cell Tissue Res*. 317:129-36.
Geier, C., A. Perrot, C. Ozcelik, P. Binner, D. Counsell, K. Hoffmann, B. Pilz, Y. Martiniak, K. Gehmlich, P.F. van der Ven, D.O. Furst, A. Vornwald, E. von Hodenberg, P. Nurnberg, T. Scheffold, R. Dietz, and K.J. Osterziel. 2003. Mutations in the human muscle LIM protein gene in families with hypertrophic cardiomyopathy. *Circulation*. 107:1390-5.
Gerull, B., M. Gramlich, J. Atherton, M. McNabb, K. Trombitas, S. Sasse-Klaassen, J.G. Seidman, C. Seidman, H. Granzier, S. Labeit, M. Frenneaux, and L. Thierfelder. 2002. Mutations of TTN, encoding the giant muscle filament titin, cause familial dilated cardiomyopathy. *Nat Genet*. 30:201-4.
Giorgino, F., O. de Robertis, L. Laviola, C. Montrone, S. Perrini, K.C. McCowen, and R.J. Smith. 2000. The sentrin-conjugating enzyme mUbc9 interacts with GLUT4 and GLUT1 glucose transporters and regulates transporter levels in skeletal muscle cells. *Proc Natl Acad Sci U S A*. 97:1125-30.
Gluzman, Y. 1981. SV40-transformed simian cells support the replication of early SV40 mutants. *Cell*. 23:175-82.
Gobinet, J., G. Auzou, J.C. Nicolas, C. Sultan, and S. Jalaguier. 2001. Characterization of the interaction between androgen receptor and a new transcriptional inhibitor, SHP. *Biochemistry*. 40:15369-77.
Grater, F., J. Shen, H. Jiang, M. Gautel, and H. Grubmuller. 2005. Mechanically induced titin kinase activation studied by force-probe molecular dynamics simulations. *Biophys J*. 88:790-804.
Gregorio, C.C., K. Trombitas, T. Centner, B. Kolmerer, G. Stier, K. Kunke, K. Suzuki, F. Obermayr, B. Herrmann, H. Granzier, H. Sorimachi, and S. Labeit. 1998. The NH2 terminus of titin spans the Z-disc: its interaction with a novel 19-kD ligand (T-cap) is required for sarcomeric integrity. *J Cell Biol*. 143:1013-27.
Guo, D., M. Li, Y. Zhang, P. Yang, S. Eckenrode, D. Hopkins, W. Zheng, S. Purohit, R.H. Podolsky, A. Muir, J. Wang, Z. Dong, T. Brusko, M. Atkinson, P. Pozzilli, A. Zeidler, L.J. Raffel, C.O. Jacob, Y. Park, M. Serrano-Rios, M.T. Larrad, Z. Zhang, H.J. Garchon, J.F. Bach, J.I. Rotter, J.X. She, and C.Y. Wang. 2004. A functional variant of SUMO4, a new I kappa B alpha modifier, is associated with type 1 diabetes. *Nat Genet*. 36:837-41.
Gutierrez-Cruz, G., A.H. Van Heerden, and K. Wang. 2001. Modular motif, structural folds and affinity profiles of the PEVK segment of human fetal skeletal muscle titin. *J Biol Chem*. 276:7442-9.
Hackman, P., A. Vihola, H. Haravuori, S. Marchand, J. Sarparanta, J. De Seze, S. Labeit, C. Witt, L. Peltonen, I. Richard, and B. Udd. 2002. Tibial muscular dystrophy is a titinopathy caused by mutations in TTN, the gene encoding the giant skeletal-muscle protein titin. *Am J Hum Genet*. 71:492-500.
Hartgens, F., and H. Kuipers. 2004. Effects of androgenic-anabolic steroids in athletes. *Sports Med*. 34:513-54.
Haworth, R.S., F. Cuello, T.J. Herron, G. Franzen, J.C. Kentish, M. Gautel, and M. Avkiran. 2004. Protein kinase D is a novel mediator of cardiac troponin I phosphorylation and regulates myofilament function. *Circ Res*. 95:1091-9.
Hayashi, T., T. Arimura, M. Itoh-Satoh, K. Ueda, S. Hohda, N. Inagaki, M. Takahashi, H. Hori, M. Yasunami, H. Nishi, Y. Koga, H. Nakamura, M. Matsuzaki, B.Y. Choi, S.W. Bae, C.W. You, K.H. Han, J.E. Park, R. Knoll, M. Hoshijima, K.R. Chien, and A. Kimura. 2004. Tcap gene mutations in hypertrophic cardiomyopathy and dilated cardiomyopathy. *J Am Coll Cardiol*. 44:2192-201.
Hein, S., and J. Schaper. 2002. Weakness of a giant: mutations of the sarcomeric protein titin. *Trends Mol Med*. 8:311-3.

Hornemann, T., S. Kempa, M. Himmel, K. Hayess, D.O. Furst, and T. Wallimann. 2003. Muscle-type creatine kinase interacts with central domains of the M-band proteins myomesin and M-protein. *J Mol Biol*. 332:877-87.

Hsu, C.L., Y.L. Chen, S. Yeh, H.J. Ting, Y.C. Hu, H. Lin, X. Wang, and C. Chang. 2003. The use of phage display technique for the isolation of androgen receptor interacting peptides with (F/W)XXL(F/W) and FXXLY new signature motifs. *J Biol Chem*. 278:23691-8.

Itoh-Satoh, M., T. Hayashi, H. Nishi, Y. Koga, T. Arimura, T. Koyanagi, M. Takahashi, S. Hohda, K. Ueda, T. Nouchi, M. Hiroe, F. Marumo, T. Imaizumi, M. Yasunami, and A. Kimura. 2002. Titin mutations as the molecular basis for dilated cardiomyopathy. *Biochem Biophys Res Commun*. 291:385-93.

Kadrmas, J.L., and M.C. Beckerle. 2004. The LIM domain: from the cytoskeleton to the nucleus. *Nat Rev Mol Cell Biol*. 5:920-31.

Kang, S.I., W.J. Chang, S.G. Cho, and I.Y. Kim. 2003. Modification of promyelocytic leukemia zinc finger protein (PLZF) by SUMO-1 conjugation regulates its transcriptional repressor activity. *J Biol Chem*. 278:51479-83.

Kawasaki, T., T. Kitsukawa, Y. Bekku, Y. Matsuda, M. Sanbo, T. Yagi, and H. Fujisawa. 1999. A requirement for neuropilin-1 in embryonic vessel formation. *Development*. 126:4895-902.

Keller, A., J. Demeurie, T. Merkulova, G. Geraud, C. Cywiner-Golenzer, M. Lucas, and F.P. Chatelet. 2000. Fibre-type distribution and subcellular localisation of alpha and beta enolase in mouse striated muscle. *Biol Cell*. 92:527-35.

Kemp, T.J., T.J. Sadusky, M. Simon, R. Brown, M. Eastwood, D.A. Sassoon, and G.R. Coulton. 2001. Identification of a novel stretch-responsive skeletal muscle gene (Smpx). *Genomics*. 72:260-71.

Kenny, P.A., E.M. Liston, and D.G. Higgins. 1999. Molecular evolution of immunoglobulin and fibronectin domains in titin and related muscle proteins. *Gene*. 232:11-23.

Kim, K.I., S.H. Baek, and C.H. Chung. 2002. Versatile protein tag, SUMO: its enzymology and biological function. *J Cell Physiol*. 191:257-68.

Kinbara, K., H. Sorimachi, S. Ishiura, and K. Suzuki. 1997. Muscle-specific calpain, p94, interacts with the extreme C-terminal region of connectin, a unique region flanked by two immunoglobulin C2 motifs. *Arch Biochem Biophys*. 342:99-107.

Klaavuniemi, T., A. Kelloniemi, and J. Ylanne. 2004. The ZASP-like motif in actinin-associated LIM protein is required for interaction with the alpha-actinin rod and for targeting to the muscle Z-line. *J Biol Chem*. 279:26402-10.

Knoll, R., M. Hoshijima, H.M. Hoffman, V. Person, I. Lorenzen-Schmidt, M.L. Bang, T. Hayashi, N. Shiga, H. Yasukawa, W. Schaper, W. McKenna, M. Yokoyama, N.J. Schork, J.H. Omens, A.D. McCulloch, A. Kimura, C.C. Gregorio, W. Poller, J. Schaper, H.P. Schultheiss, and K.R. Chien. 2002. The cardiac mechanical stretch sensor machinery involves a Z disc complex that is defective in a subset of human dilated cardiomyopathy. *Cell*. 111:943-55.

Knudsen, K.A., A.P. Soler, K.R. Johnson, and M.J. Wheelock. 1995. Interaction of alpha-actinin with the cadherin/catenin cell-cell adhesion complex via alpha-catenin. *J Cell Biol*. 130:67-77.

Kobayashi, S., H. Shibata, K. Yokota, N. Suda, A. Murai, I. Kurihara, I. Saito, and T. Saruta. 2004. FHL2, UBC9, and PIAS1 are novel estrogen receptor alpha-interacting proteins. *Endocr Res*. 30:617-21.

Kojic, S., E. Medeot, E. Guccione, H. Krmac, I. Zara, V. Martinelli, G. Valle, and G. Faulkner. 2004. The Ankrd2 protein, a link between the sarcomere and the nucleus in skeletal muscle. *J Mol Biol*. 339:313-25.

Komiyama, M., T. Soldati, P. von Arx, and J.C. Perriard. 1996. The intracompartmental sorting of myosin alkali light chain isoproteins reflects the sequence of developmental expression as determined by double epitope-tagging competition. *J Cell Sci*. 109 (Pt 8):2089-99.

Kong, Y., J.M. Shelton, B. Rothermel, X. Li, J.A. Richardson, R. Bassel-Duby, and R.S. Williams. 2001. Cardiac-specific LIM protein FHL2 modifies the hypertrophic response to beta-adrenergic stimulation. *Circulation*. 103:2731-8.

Kotaja, N., U. Karvonen, O.A. Janne, and J.J. Palvimo. 2002. PIAS proteins modulate transcription factors by functioning as SUMO-1 ligases. *Mol Cell Biol*. 22:5222-34.

Kraft, T., T. Hornemann, M. Stolz, V. Nier, and T. Wallimann. 2000. Coupling of creatine kinase to glycolytic enzymes at the sarcomeric I-band of skeletal muscle: a biochemical study in situ. *J Muscle Res Cell Motil*. 21:691-703.

Kruger, N.J., and D.T. Dennis. 1985. A source of apparent pyrophosphate:fructose 6-phosphate phosphotransferase activity in rabbit muscle phosphofructokinase. *Biochem Biophys Res Commun*. 126:320-6.

Krylova, O., J. Herreros, K.E. Cleverley, E. Ehler, J.P. Henriquez, S.M. Hughes, and P.C. Salinas. 2002. WNT-3, expressed by motoneurons, regulates terminal arborization of neurotrophin-3-responsive spinal sensory neurons. *Neuron*. 35:1043-56.

Kulke, M., S. Fujita-Becker, E. Rostkova, C. Neagoe, D. Labeit, D.J. Manstein, M. Gautel, and W.A. Linke. 2001. Interaction between PEVK-titin and actin filaments: origin of a viscous force component in cardiac myofibrils. *Circ Res*. 89:874-81.

Labalette, C., C.A. Renard, C. Neuveut, M.A. Buendia, and Y. Wei. 2004. Interaction and functional cooperation between the LIM protein FHL2, CBP/p300, and beta-catenin. *Mol Cell Biol*. 24:10689-702.

Labeit, S., and B. Kolmerer. 1995. Titins: giant proteins in charge of muscle ultrastructure and elasticity. *Science*. 270:293-6.

Laemmli, U.K. 1970. Cleavage of structural proteins during the assembly of the head of bacteriophage T4. *Nature*. 227:680-5.

Lange, S., D. Auerbach, P. McLoughlin, E. Perriard, B.W. Schafer, J.C. Perriard, and E. Ehler. 2002. Subcellular targeting of metabolic enzymes to titin in heart muscle may be mediated by DRAL/FHL-2. *J Cell Sci*. 115:4925-36.

Lange, S., M. Himmel, D. Auerbach, I. Agarkova, K. Hayess, D.O. Furst, J.C. Perriard, and E. Ehler. 2005. Dimerisation of myomesin: implications for the structure of the sarcomeric M-band. *J Mol Biol*. 345:289-98.

Leger, J.P., F.M. Smith, and R.W. Currie. 2000. Confocal microscopic localization of constitutive and heat shock-induced proteins HSP70 and HSP27 in the rat heart. *Circulation*. 102:1703-9.

Letunic, I., R.R. Copley, S. Schmidt, F.D. Ciccarelli, T. Doerks, J. Schultz, C.P. Ponting, and P. Bork. 2004. SMART 4.0: towards genomic data integration. *Nucleic Acids Res*. 32 Database issue:D142-4.

Li, H.Y., E.K. Ng, S.M. Lee, M. Kotaka, S.K. Tsui, C.Y. Lee, K.P. Fung, and M.M. Waye. 2001. Protein-protein interaction of FHL3 with FHL2 and visualization of their interaction by green fluorescent proteins (GFP) two-fusion fluorescence resonance energy transfer (FRET). *J Cell Biochem*. 80:293-303.

Li, P., H. Lee, S. Guo, T.G. Unterman, G. Jenster, and W. Bai. 2003. AKT-independent protection of prostate cancer cells from apoptosis mediated through complex formation between the androgen receptor and FKHR. *Mol Cell Biol*. 23:104-18.

Li, R., J.S. Wang, Q. Sun, J. Wang, X. Yang, H.Y. Huang, P. Zhou, and H. Han. 2002. [Screening and detecting of proteins interaction with KyoT]. *Yi Chuan Xue Bao*. 29:175-80.

Li, S., M.P. Czubryt, J. McAnally, R. Bassel-Duby, J.A. Richardson, F.F. Wiebel, A. Nordheim, and E.N. Olson. 2005. Requirement for serum response factor for skeletal muscle growth and maturation revealed by tissue-specific gene deletion in mice. *Proc Natl Acad Sci U S A*.

Li, T.B., X.H. Liu, S. Feng, Y. Hu, W.X. Yang, Y. Han, Y.G. Wang, and L.M. Gong. 2004a. Characterization of MR-1, a novel myofibrillogenesis regulator in human muscle. *Acta Biochim Biophys Sin (Shanghai)*. 36:412-8.

Li, Y., I. Kishimoto, Y. Saito, M. Harada, K. Kuwahara, T. Izumi, I. Hamanaka, N. Takahashi, R. Kawakami, K. Tanimoto, Y. Nakagawa, M. Nakanishi, Y. Adachi, D.L. Garbers, A. Fukamizu, and K. Nakao. 2004b. Androgen contributes to gender-related cardiac hypertrophy and fibrosis in mice lacking the gene encoding guanylyl cyclase-A. *Endocrinology*. 145:951-8.

Liao, J., Y. Fu, and K. Shuai. 2000. Distinct roles of the NH2- and COOH-terminal domains of the protein inhibitor of activated signal transducer and activator of transcription (STAT) 1 (PIAS1) in cytokine-induced PIAS1-Stat1 interaction. *Proc Natl Acad Sci U S A*. 97:5267-72.

Lickert, H., S. Kutsch, B. Kanzler, Y. Tamai, M.M. Taketo, and R. Kemler. 2002. Formation of multiple hearts in mice following deletion of beta-catenin in the embryonic endoderm. *Dev Cell*. 3:171-81.

Liebner, S., A. Cattelino, R. Gallini, N. Rudini, M. Iurlaro, S. Piccolo, and E. Dejana. 2004. Beta-catenin is required for endothelial-mesenchymal transformation during heart cushion development in the mouse. *J Cell Biol*. 166:359-67.

Lin, R.J., T. Sternsdorf, M. Tini, and R.M. Evans. 2001. Transcriptional regulation in acute promyelocytic leukemia. *Oncogene*. 20:7204-15.

Linke, W.A., M. Kulke, H. Li, S. Fujita-Becker, C. Neagoe, D.J. Manstein, M. Gautel, and J.M. Fernandez. 2002. PEVK domain of titin: an entropic spring with actin-binding properties. *J Struct Biol*. 137:194-205.

Lisowsky, T., P.L. Polosa, A. Sagliano, M. Roberti, M.N. Gadaleta, and P. Cantatore. 1999. Identification of human GC-box-binding zinc finger protein, a new Kruppel-like zinc finger protein, by the yeast one-hybrid screening with a GC-rich target sequence. *FEBS Lett*. 453:369-74.

Liu, P.Y., A.K. Death, and D.J. Handelsman. 2003. Androgens and cardiovascular disease. *Endocr Rev*. 24:313-40.

Liversage, A.D., D. Holmes, P.J. Knight, L. Tskhovrebova, and J. Trinick. 2001. Titin and the sarcomere symmetry paradox. *J Mol Biol*. 305:401-9.

Louis, H.A., J.D. Pino, K.L. Schmeichel, P. Pomies, and M.C. Beckerle. 1997. Comparison of three members of the cysteine-rich protein family reveals functional conservation and divergent patterns of gene expression. *J Biol Chem*. 272:27484-91.
Luders, J., G. Pyrowolakis, and S. Jentsch. 2003. The ubiquitin-like protein HUB1 forms SDS-resistant complexes with cellular proteins in the absence of ATP. *EMBO Rep*. 4:1169-74.
Luther, P., and J. Squire. 1978. Three-dimensional structure of the vertebrate muscle M-region. *J Mol Biol*. 125:313-24.
Luther, P.K. 2000. Three-dimensional structure of a vertebrate muscle Z-band: implications for titin and alpha-actinin binding. *J Struct Biol*. 129:1-16.
Luther, P.K., and R.A. Crowther. 1984. Three-dimensional reconstruction from tilted sections of fish muscle M-band. *Nature*. 307:566-8.
Luther, P.K., R. Padron, S. Ritter, R. Craig, and J.M. Squire. 2003. Heterogeneity of Z-band structure within a single muscle sarcomere: implications for sarcomere assembly. *J Mol Biol*. 332:161-9.
Ma, K., and K. Wang. 2002. Interaction of nebulin SH3 domain with titin PEVK and myopalladin: implications for the signaling and assembly role of titin and nebulin. *FEBS Lett*. 532:273-8.
Marchler-Bauer, A., and S.H. Bryant. 2004. CD-Search: protein domain annotations on the fly. *Nucleic Acids Res*. 32:W327-31.
Marsh, J.D., M.H. Lehmann, R.H. Ritchie, J.K. Gwathmey, G.E. Green, and R.J. Schiebinger. 1998. Androgen receptors mediate hypertrophy in cardiac myocytes. *Circulation*. 98:256-61.
Martin, B., R. Schneider, S. Janetzky, Z. Waibler, P. Pandur, M. Kuhl, J. Behrens, K. von der Mark, A. Starzinski-Powitz, and V. Wixler. 2002. The LIM-only protein FHL2 interacts with beta-catenin and promotes differentiation of mouse myoblasts. *J Cell Biol*. 159:113-22.
Maruyama, K. 1997. Connectin/titin, giant elastic protein of muscle. *Faseb J*. 11:341-5.
Matsudaira, P.T., and D.R. Burgess. 1978. SDS microslab linear gradient polyacrylamide gel electrophoresis. *Anal Biochem*. 87:386-96.
Matsuzaki, K., T. Minami, M. Tojo, Y. Honda, Y. Uchimura, H. Saitoh, H. Yasuda, S. Nagahiro, H. Saya, and M. Nakao. 2003. Serum response factor is modulated by the SUMO-1 conjugation system. *Biochem Biophys Res Commun*. 306:32-8.
Mayans, O., P.F. van der Ven, M. Wilm, A. Mues, P. Young, D.O. Furst, M. Wilmanns, and M. Gautel. 1998. Structural basis for activation of the titin kinase domain during myofibrillogenesis. *Nature*. 395:863-9.
McConnell, M.J., N. Chevallier, W. Berkofsky-Fessler, J.M. Giltnane, R.B. Malani, L.M. Staudt, and J.D. Licht. 2003. Growth suppression by acute promyelocytic leukemia-associated protein PLZF is mediated by repression of c-myc expression. *Mol Cell Biol*. 23:9375-88.
McElhinny, A.S., K. Kakinuma, H. Sorimachi, S. Labeit, and C.C. Gregorio. 2002. Muscle-specific RING finger-1 interacts with titin to regulate sarcomeric M-line and thick filament structure and may have nuclear functions via its interaction with glucocorticoid modulatory element binding protein-1. *J Cell Biol*. 157:125-36.
McLoughlin, P., E. Ehler, G. Carlile, J.D. Licht, and B.W. Schafer. 2002. The LIM-only protein DRAL/FHL2 interacts with and is a corepressor for the promyelocytic leukemia zinc finger protein. *J Biol Chem*. 277:37045-53.
Melandri, R., G. Re, C. Lanzarini, C. Rapezzi, O. Leone, I. Zele, and G. Rocchi. 1996. Myocardial damage and rhabdomyolysis associated with prolonged hypoxic coma following opiate overdose. *J Toxicol Clin Toxicol*. 34:199-203.
Melchior, F. 2000. SUMO--nonclassical ubiquitin. *Annu Rev Cell Dev Biol*. 16:591-626.
Messerli, J.M., H.T. van der Voort, E. Rungger-Brandle, and J.C. Perriard. 1993. Three-dimensional visualization of multi-channel volume data: the amSFP algorithm. *Cytometry*. 14:725-35.
Miller, J.H. 1972. Experiments in Molecular Genetics. Cold Spring Harbor Laboratory.
Miller, J.H. 1992. A Short Course in Bacterial Genetics. Cold Spring Harbor Laboratory Press.
Miller, J.R., and R.T. Moon. 1996. Signal transduction through beta-catenin and specification of cell fate during embryogenesis. *Genes Dev*. 10:2527-39.
Miller, M.K., M.L. Bang, C.C. Witt, D. Labeit, C. Trombitas, K. Watanabe, H. Granzier, A.S. McElhinny, C.C. Gregorio, and S. Labeit. 2003. The muscle ankyrin repeat proteins: CARP, ankrd2/Arpp and DARP as a family of titin filament-based stress response molecules. *J Mol Biol*. 333:951-64.
Minty, A., X. Dumont, M. Kaghad, and D. Caput. 2000. Covalent modification of p73alpha by SUMO-1. Two-hybrid screening with p73 identifies novel SUMO-1-interacting proteins and a SUMO-1 interaction motif. *J Biol Chem*. 275:36316-23.
Mistry, A.C., A. Kato, Y.H. Tran, S. Honda, T. Tsukada, Y. Takei, and S. Hirose. 2004. FHL5, a novel actin-binding protein, is highly expressed in eel gill pillar cells and responds to wall tension. *Am J Physiol Regul Integr Comp Physiol*. 287:R1141-54.
Mohapatra, B., S. Jimenez, J.H. Lin, K.R. Bowles, K.J. Coveler, J.G. Marx, M.A. Chrisco, R.T. Murphy, P.R. Lurie, R.J. Schwartz, P.M. Elliott, M. Vatta, W. McKenna, J.A. Towbin, and N.E. Bowles. 2003.

Mutations in the muscle LIM protein and alpha-actinin-2 genes in dilated cardiomyopathy and endocardial fibroelastosis. *Mol Genet Metab*. 80:207-15.
Moolman-Smook, J., E. Flashman, W. de Lange, Z. Li, V. Corfield, C. Redwood, and H. Watkins. 2002. Identification of novel interactions between domains of Myosin binding protein-C that are modulated by hypertrophic cardiomyopathy missense mutations. *Circ Res*. 91:704-11.
Moon, R.T., A.D. Kohn, G.V. De Ferrari, and A. Kaykas. 2004. WNT and beta-catenin signalling: diseases and therapies. *Nat Rev Genet*. 5:691-701.
Moreira, E.S., T.J. Wiltshire, G. Faulkner, A. Nilforoushan, M. Vainzof, O.T. Suzuki, G. Valle, R. Reeves, M. Zatz, M.R. Passos-Bueno, and D.E. Jenne. 2000. Limb-girdle muscular dystrophy type 2G is caused by mutations in the gene encoding the sarcomeric protein telethonin. *Nat Genet*. 24:163-6.
Morgan, M.J., and A.J. Madgwick. 1996. Slim defines a novel family of LIM-proteins expressed in skeletal muscle. *Biochem Biophys Res Commun*. 225:632-8.
Mues, A., P.F. van der Ven, P. Young, D.O. Furst, and M. Gautel. 1998. Two immunoglobulin-like domains of the Z-disc portion of titin interact in a conformation-dependent way with telethonin. *FEBS Lett*. 428:111-4.
Muller, J.M., U. Isele, E. Metzger, A. Rempel, M. Moser, A. Pscherer, T. Breyer, C. Holubarsch, R. Buettner, and R. Schule. 2000. FHL2, a novel tissue-specific coactivator of the androgen receptor. *Embo J*. 19:359-69.
Muller, J.M., E. Metzger, H. Greschik, A.K. Bosserhoff, L. Mercep, R. Buettner, and R. Schule. 2002. The transcriptional coactivator FHL2 transmits Rho signals from the cell membrane into the nucleus. *Embo J*. 21:736-48.
Nessler-Menardi, C., I. Jotova, Z. Culig, I.E. Eder, T. Putz, G. Bartsch, and H. Klocker. 2000. Expression of androgen receptor coregulatory proteins in prostate cancer and stromal-cell culture models. *Prostate*. 45:124-31.
Nieset, J.E., A.R. Redfield, F. Jin, K.A. Knudsen, K.R. Johnson, and M.J. Wheelock. 1997. Characterization of the interactions of alpha-catenin with alpha-actinin and beta-catenin/plakoglobin. *J Cell Sci*. 110 (Pt 8):1013-22.
Obermann, W.M., M. Gautel, F. Steiner, P.F. van der Ven, K. Weber, and D.O. Furst. 1996. The structure of the sarcomeric M band: localization of defined domains of myomesin, M-protein, and the 250-kD carboxy-terminal region of titin by immunoelectron microscopy. *J Cell Biol*. 134:1441-53.
Obermann, W.M., M. Gautel, K. Weber, and D.O. Furst. 1997. Molecular structure of the sarcomeric M band: mapping of titin and myosin binding domains in myomesin and the identification of a potential regulatory phosphorylation site in myomesin. *Embo J*. 16:211-20.
Obermann, W.M., U. Plessmann, K. Weber, and D.O. Furst. 1995. Purification and biochemical characterization of myomesin, a myosin-binding and titin-binding protein, from bovine skeletal muscle. *Eur J Biochem*. 233:110-5.
Obermann, W.M., P.F. van der Ven, F. Steiner, K. Weber, and D.O. Furst. 1998. Mapping of a myosin-binding domain and a regulatory phosphorylation site in M-protein, a structural protein of the sarcomeric M band. *Mol Biol Cell*. 9:829-40.
Ordahl, C.P., G.L. Evans, T.A. Cooper, G. Kunz, and J.C. Perriard. 1984. Complete cDNA-derived amino acid sequence of chick muscle creatine kinase. *J Biol Chem*. 259:15224-7.
Palmer, S., N. Groves, A. Schindeler, T. Yeoh, C. Biben, C.C. Wang, D.B. Sparrow, L. Barnett, N.A. Jenkins, N.G. Copeland, F. Koentgen, T. Mohun, and R.P. Harvey. 2001. The small muscle-specific protein Csl modifies cell shape and promotes myocyte fusion in an insulin-like growth factor 1-dependent manner. *J Cell Biol*. 153:985-98.
Parlakian, A., D. Tuil, G. Hamard, G. Tavernier, D. Hentzen, J.P. Concordet, D. Paulin, Z. Li, and D. Daegelen. 2004. Targeted inactivation of serum response factor in the developing heart results in myocardial defects and embryonic lethality. *Mol Cell Biol*. 24:5281-9.
Pena, J., E. Luque, C. Aranda, I. Jimena, and R. Vaamonde. 1993. Experimental heroin-induced myopathy: ultrastructural observations. *J Submicrosc Cytol Pathol*. 25:279-84.
Philippar, U., G. Schratt, C. Dieterich, J.M. Muller, P. Galgoczy, F.B. Engel, M.T. Keating, F. Gertler, R. Schule, M. Vingron, and A. Nordheim. 2004. The SRF target gene Fhl2 antagonizes RhoA/MAL-dependent activation of SRF. *Mol Cell*. 16:867-80.
Pindel, E.V., N.Y. Kedishvili, T.L. Abraham, M.R. Brzezinski, J. Zhang, R.A. Dean, and W.F. Bosron. 1997. Purification and cloning of a broad substrate specificity human liver carboxylesterase that catalyzes the hydrolysis of cocaine and heroin. *J Biol Chem*. 272:14769-75.
Pizon, V., A. Iakovenko, P.F. Van Der Ven, R. Kelly, C. Fatu, D.O. Furst, E. Karsenti, and M. Gautel. 2002. Transient association of titin and myosin with microtubules in nascent myofibrils directed by the MURF2 RING-finger protein. *J Cell Sci*. 115:4469-82.

Pomies, P., T. Macalma, and M.C. Beckerle. 1999. Purification and characterization of an alpha-actinin-binding PDZ-LIM protein that is up-regulated during muscle differentiation. *J Biol Chem*. 274:29242-50.
Poukka, H., P. Aarnisalo, U. Karvonen, J.J. Palvimo, and O.A. Janne. 1999. Ubc9 interacts with the androgen receptor and activates receptor-dependent transcription. *J Biol Chem*. 274:19441-6.
Rechsteiner, M., and S.W. Rogers. 1996. PEST sequences and regulation by proteolysis. *Trends Biochem Sci*. 21:267-71.
Rodriguez, M.S., C. Dargemont, and R.T. Hay. 2001. SUMO-1 conjugation in vivo requires both a consensus modification motif and nuclear targeting. *J Biol Chem*. 276:12654-9.
Sachdev, S., M.K. Raychowdhury, and S. Sarkar. 2003. Human fast skeletal myosin light chain 2 cDNA: isolation, tissue specific expression of the single copy gene, comparative sequence analysis of isoforms and evolutionary relationships. *DNA Seq*. 14:339-50.
Sachinidis, A., B.K. Fleischmann, E. Kolossov, M. Wartenberg, H. Sauer, and J. Hescheler. 2003. Cardiac specific differentiation of mouse embryonic stem cells. *Cardiovasc Res*. 58:278-91.
Salzberg, S.L. 1998. Computational methods in molecular biology. Elsevier, Amsterdam. 371 pp.
Scavello, G.S., Jr., P.C. Paluru, J. Zhou, P.S. White, E.F. Rappaport, and T.L. Young. 2005. Genomic structure and organization of the high grade Myopia-2 locus (MYP2) critical region: mutation screening of 9 positional candidate genes. *Mol Vis*. 11:97-110.
Schafer, B.W., and J.C. Perriard. 1988. Intracellular targeting of isoproteins in muscle cytoarchitecture. *J Cell Biol*. 106:1161-70.
Schiaffino, S., and C. Reggiani. 1996. Molecular diversity of myofibrillar proteins: gene regulation and functional significance. *Physiol Rev*. 76:371-423.
Schmeichel, K.L., and M.C. Beckerle. 1994. The LIM domain is a modular protein-binding interface. *Cell*. 79:211-9.
Schmidt, D., and S. Muller. 2003. PIAS/SUMO: new partners in transcriptional regulation. *Cell Mol Life Sci*. 60:2561-74.
Schneider, M.D., L.A. Kirshenbaum, T. Brand, and W.R. MacLellan. 1994. Control of cardiac gene transcription by fibroblast growth factors. *Mol Reprod Dev*. 39:112-7.
Schneider, M.D., W.R. McLellan, F.M. Black, and T.G. Parker. 1992. Growth factors, growth factor response elements, and the cardiac phenotype. *Basic Res Cardiol*. 87 Suppl 2:33-48.
Scholl, F.A., P. McLoughlin, E. Ehler, C. de Giovanni, and B.W. Schafer. 2000. DRAL is a p53-responsive gene whose four and a half LIM domain protein product induces apoptosis. *J Cell Biol*. 151:495-506.
Schultz, J., F. Milpetz, P. Bork, and C.P. Ponting. 1998. SMART, a simple modular architecture research tool: identification of signaling domains. *Proc Natl Acad Sci U S A*. 95:5857-64.
Sen, A., P. Dunnmon, S.A. Henderson, R.D. Gerard, and K.R. Chien. 1988. Terminally differentiated neonatal rat myocardial cells proliferate and maintain specific differentiated functions following expression of SV40 large T antigen. *J Biol Chem*. 263:19132-6.
Sorimachi, H., S. Kimura, K. Kinbara, J. Kazama, M. Takahashi, H. Yajima, S. Ishiura, N. Sasagawa, I. Nonaka, H. Sugita, K. Maruyama, and K. Suzuki. 1996. Structure and physiological functions of ubiquitous and tissue-specific calpain species. Muscle-specific calpain, p94, interacts with connectin/titin. *Adv Biophys*. 33:101-22.
Sorimachi, H., K. Kinbara, S. Kimura, M. Takahashi, S. Ishiura, N. Sasagawa, N. Sorimachi, H. Shimada, K. Tagawa, K. Maruyama, and et al. 1995. Muscle-specific calpain, p94, responsible for limb girdle muscular dystrophy type 2A, associates with connectin through IS2, a p94-specific sequence. *J Biol Chem*. 270:31158-62.
Spencer, J.A., S. Eliazer, R.L. Ilaria, Jr., J.A. Richardson, and E.N. Olson. 2000. Regulation of microtubule dynamics and myogenic differentiation by MURF, a striated muscle RING-finger protein. *J Cell Biol*. 150:771-84.
Squire, J. 1981. The Structural basis of muscular contraction. Plenum Press, New York. XVII, 698 pp.
Steiner, F., K. Weber, and D.O. Furst. 1999. M band proteins myomesin and skelemin are encoded by the same gene: analysis of its organization and expression. *Genomics*. 56:78-89.
Stenmark, H., G. Vitale, O. Ullrich, and M. Zerial. 1995. Rabaptin-5 is a direct effector of the small GTPase Rab5 in endocytic membrane fusion. *Cell*. 83:423-32.
Stolz, M., and T. Wallimann. 1998. Myofibrillar interaction of cytosolic creatine kinase (CK) isoenzymes: allocation of N-terminal binding epitope in MM-CK and BB-CK. *J Cell Sci*. 111 (Pt 9):1207-16.
Strehler, E.E., E. Carlsson, H.M. Eppenberger, and L.E. Thornell. 1983. Ultrastructural localization of M-band proteins in chicken breast muscle as revealed by combined immunocytochemistry and ultramicrotomy. *J Mol Biol*. 166:141-58.
Takahashi, Y., E.A. Toh, and Y. Kikuchi. 2003. Comparative analysis of yeast PIAS-type SUMO ligases in vivo and in vitro. *J Biochem (Tokyo)*. 133:415-22.

Tan, J.A., S.H. Hall, K.G. Hamil, G. Grossman, P. Petrusz, and F.S. French. 2002. Protein inhibitors of activated STAT resemble scaffold attachment factors and function as interacting nuclear receptor coregulators. *J Biol Chem*. 277:16993-7001.

Taniguchi, Y., T. Furukawa, T. Tun, H. Han, and T. Honjo. 1998. LIM protein KyoT2 negatively regulates transcription by association with the RBP-J DNA-binding protein. *Mol Cell Biol*. 18:644-54.

Towbin, J.A., and N.E. Bowles. 2000. Genetic abnormalities responsible for dilated cardiomyopathy. *Curr Cardiol Rep*. 2:475-80.

Trask, R.V., and J.J. Billadello. 1990. Tissue-specific distribution and developmental regulation of M and B creatine kinase mRNAs. *Biochim Biophys Acta*. 1049:182-8.

Tskhovrebova, L., and J. Trinick. 2003. Titin: properties and family relationships. *Nat Rev Mol Cell Biol*. 4:679-89.

Untergasser, G., R. Gander, C. Lilg, G. Lepperdinger, E. Plas, and P. Berger. 2005. Profiling molecular targets of TGF-beta1 in prostate fibroblast-to-myofibroblast transdifferentiation. *Mech Ageing Dev*. 126:59-69.

van Deursen, J., A. Heerschap, F. Oerlemans, W. Ruitenbeek, P. Jap, H. ter Laak, and B. Wieringa. 1993. Skeletal muscles of mice deficient in muscle creatine kinase lack burst activity. *Cell*. 74:621-31.

Vandekerckhove, J., and K. Weber. 1984. Chordate muscle actins differ distinctly from invertebrate muscle actins. The evolution of the different vertebrate muscle actins. *J Mol Biol*. 179:391-413.

Varriano-Marston, E., C. Franzini-Armstrong, and J.C. Haselgrove. 1984. The structure and disposition of crossbridges in deep-etched fish muscle. *J Muscle Res Cell Motil*. 5:363-86.

Ventura-Clapier, R., A. Kuznetsov, V. Veksler, E. Boehm, and K. Anflous. 1998. Functional coupling of creatine kinases in muscles: species and tissue specificity. *Mol Cell Biochem*. 184:231-47.

Vlahopoulos, S., W.E. Zimmer, G. Jenster, N.S. Belaguli, S.P. Balk, A.O. Brinkmann, R.B. Lanz, V.C. Zoumpourlis, and R.J. Schwartz. 2005. Recruitment of the androgen receptor via serum response factor facilitates expression of a myogenic gene. *J Biol Chem*.

Vojtek, A.B., S.M. Hollenberg, and J.A. Cooper. 1993. Mammalian Ras interacts directly with the serine/threonine kinase Raf. *Cell*. 74:205-14.

Wallimann, T., and H.M. Eppenberger. 1985. Localization and function of M-line-bound creatine kinase. M-band model and creatine phosphate shuttle. *Cell Muscle Motil*. 6:239-85.

Wallimann, T., M. Wyss, D. Brdiczka, K. Nicolay, and H.M. Eppenberger. 1992. Intracellular compartmentation, structure and function of creatine kinase isoenzymes in tissues with high and fluctuating energy demands: the 'phosphocreatine circuit' for cellular energy homeostasis. *Biochem J*. 281 (Pt 1):21-40.

Walzel, B., O. Speer, E. Boehm, S. Kristiansen, S. Chan, K. Clarke, J.P. Magyar, E.A. Richter, and T. Wallimann. 2002a. New creatine transporter assay and identification of distinct creatine transporter isoforms in muscle. *Am J Physiol Endocrinol Metab*. 283:E390-401.

Walzel, B., O. Speer, E. Zanolla, O. Eriksson, P. Bernardi, and T. Wallimann. 2002b. Novel mitochondrial creatine transport activity. Implications for intracellular creatine compartments and bioenergetics. *J Biol Chem*. 277:37503-11.

Wegmann, G., E. Zanolla, H.M. Eppenberger, and T. Wallimann. 1992. In situ compartmentation of creatine kinase in intact sarcomeric muscle: the acto-myosin overlap zone as a molecular sieve. *J Muscle Res Cell Motil*. 13:420-35.

Wei, Y., C.A. Renard, C. Labalette, Y. Wu, L. Levy, C. Neuveut, X. Prieur, M. Flajolet, S. Prigent, and M.A. Buendia. 2003. Identification of the LIM protein FHL2 as a coactivator of beta-catenin. *J Biol Chem*. 278:5188-94.

Wheater, P.R., H.G. Burkitt, B. Young, J.W. Heath, and P.J. Deakin. 1996. Wheater's functional histology a text and colour atlas. Churchill Livingstone, Edinburgh etc. 407 pp.

Whitehouse, C., J. Chambers, K. Howe, M. Cobourne, P. Sharpe, and E. Solomon. 2002. NBR1 interacts with fasciculation and elongation protein zeta-1 (FEZ1) and calcium and integrin binding protein (CIB) and shows developmentally restricted expression in the neural tube. *Eur J Biochem*. 269:538-45.

Xia, H., S.T. Winokur, W.L. Kuo, M.R. Altherr, and D.S. Bredt. 1997. Actinin-associated LIM protein: identification of a domain interaction between PDZ and spectrin-like repeat motifs. *J Cell Biol*. 139:507-15.

Xu, X., S.E. Meiler, T.P. Zhong, M. Mohideen, D.A. Crossley, W.W. Burggren, and M.C. Fishman. 2002. Cardiomyopathy in zebrafish due to mutation in an alternatively spliced exon of titin. *Nat Genet*. 30:205-9.

Yamada, Y., N. Takakura, H. Yasue, H. Ogawa, H. Fujisawa, and T. Suda. 2001. Exogenous clustered neuropilin 1 enhances vasculogenesis and angiogenesis. *Blood*. 97:1671-8.

Yamasaki, R., M. Berri, Y. Wu, K. Trombitas, M. McNabb, M.S. Kellermayer, C. Witt, D. Labeit, S. Labeit, M. Greaser, and H. Granzier. 2001. Titin-actin interaction in mouse myocardium: passive tension modulation and its regulation by calcium/S100A1. *Biophys J*. 81:2297-313.

Young, P., C. Ferguson, S. Banuelos, and M. Gautel. 1998. Molecular structure of the sarcomeric Z-disk: two types of titin interactions lead to an asymmetrical sorting of alpha-actinin. *Embo J*. 17:1614-24.

Zhou, Q., P. Ruiz-Lozano, M.E. Martone, and J. Chen. 1999. Cypher, a striated muscle-restricted PDZ and LIM domain-containing protein, binds to alpha-actinin-2 and protein kinase C. *J Biol Chem*. 274:19807-13.

Zou, P., M. Gautel, A. Geerlof, M. Wilmanns, M.H. Koch, and D.I. Svergun. 2003. Solution scattering suggests cross-linking function of telethonin in the complex with titin. *J Biol Chem*. 278:2636-44.

10. Acknowledgements

In memory of Ilse Lange.

This dissertation is dedicated to my family, for their continuous support and help.

I would like to thank all friends and colleges who have contributed to this work. I am very grateful to my two supervisors, Jean-Claude Perriard and Mathias Gautel for the opportunity of working in two labs and for their endless and generous support.

A very special and big thanks goes to Elisabeth Ehler for all the help, knowledge and scientific as well as non-scientific advises over the years and for “proofreading this masterpiece at 00:05 a.m. on a Saturday” morning without falling asleep.

I thank all members of the two groups for providing a stimulating research atmosphere. The scientific help of Daniel Auerbach and Irina Agarkova as well as the stimulating discussions with Christine “Tini” Munding are especially acknowledged. Elena “Lena” Rostkova, Atsushi “San” Fukuzawa as well as Birgit “Beergut” Brandmeier are also acknowledged for providing a fruitful atmosphere in the lab.

Last, but not least, I would like to thank my collaborators in Hamburg, especially Mathias Wilmanns and Nikos Pinotsis for stimulating input into my scientific work.

11. Curriculum Vitae

11.1. Personal data

Name:	Stephan Lange
Date of birth:	28.10.1975
Place of birth:	Berlin, Germany
Citizenship:	German
Permanent address:	Bernulfstr. 17 12524 Berlin Germany

11.2. Scientific education

University entrance qualification: Alexander von Humboldt Gymnasium
Berlin, Germany
Abitur, 02.05.1995

University studies:

1995-2001
Humboldt University Berlin, Germany
Oct. 1999 – Jul. 2000
International exchange student (ERASMUS studentship)
Eidgenössische Technische Hochschule (ETH) Zürich
Zürich, Switzerland
Dec. 2000 – Sep. 2001
External diploma thesis, ETH Zürich
Zürich, Switzerland

2001-2002
Research fellow in the Institute of Plant Sciences,
Group of Prof. Apel
Zürich, Switzerland

2001-2005
PhD student, group of Prof. Perriard and Prof. Gautel
Institute of Cell Biology, ETH Zürich, Switzerland
The Randall Division of Cell and Molecular Biophysics and
Cardiovascular Division, King's College London
London, United Kingdom

11.3. List of publications

- Subcellular targeting of metabolic enzymes to titin in heart muscle may be mediated by DRAL/FHL-2.
  Lange S., Auerbach D., McLoughlin P., Perriard E., Schafer B. W., Perriard J. C., Ehler E. **2002**. *Journal of Cell Science*. 115(24). 4925-36.
- M-band: a safeguard for sarcomere stability?
  Agarkova I., Ehler E., Lange S., Schoenauer R., Perriard J. C. **2003**. *Journal of Muscle Research and Cell Motility*. 24(2-3). 191-203.
- Dimerisation of myomesin: implications for the structure of the sarcomeric M-band.
  Lange S., Himmel M., Auerbach D., Agarkova I., Hayess K., Furst D. O., Perriard J. C., Ehler E. **2005**. *Journal of Molecular Biology*. 345(2). 289-98.
- The sarcomeric M-band during development and disease.
  Lange S., Agarkova I., Perriard J.C., Ehler E. **2005**. *submitted*.
- From A to Z and Back? Sarcomeric proteins on the move.
  Lange S., Ehler E., Gautel M. **2005**. *submitted*.
- A titin kinase signaling complex controls muscle gene expression and protein turnover.
  Lange S., Xiang F., Yakovenko A., Vihola A., Hackman P., Rostkova E., Kristensen K., Brandmeier B., Franzen G., Hedberg B., Gunnarsson L.G., Hughes S.M., Marchand S., Sejersen T., Richard I., Edström L., Ehler E., Udd B., Gautel M. **2005**. *submitted*.

11.4. List of talks and presentations

- Measurement of the intraliposomal pH-changes by Bacteriorhodopsin using Quantitative Laser Scanning Microscopy.
  Lange S., Galius V., Fiedler S. **2000**. *238. WE Heraeus-Seminar : Nanobionics – from Molecules to Application*. Marburg, Germany. Poster.
- The targeting mechanism of the four-and-a half LIM domain protein DRAL (FHL-2) into the sarcomere.
  Lange S., Auerbach D., Perriard J. C., Ehler E. **2001**. *7th Novartis Cardiovascular Biology and Clinical Implications Meeting*. Interlaken, Switzerland. Talk.
- DRAL: a four and a half LIM domain protein mediates metabolic enzyme compartmentation in the sarcomere.
  Lange S., Auerbach D., McLoughlin P., Perriard E., Schafer B. W., Perriard J. C., Ehler E. **2002**. *USGEB meeting*. Lugano, Switzerland. Poster.
- Crosslinking of the thick filaments in the M-band: a novel role for Myomesin.
  Lange S., Auerbach D., Perriard J. C., Ehler E. **2002**. *8th Novartis Cardiovascular Biology and Clinical Implications Meeting*. Villars, Switzerland. Poster.

- Crosslinking of the thick filaments in the M-band: a novel role for Myomesin.
  Lange S., Auerbach D., Perriard J. C., Ehler E. **2003**. *USGEB meeting*. Davos, Switzerland. Poster.
- New molecules involved in physiological hypertrophy in mouse heart?
  Keller G., Lange S., Leu M., Ehler E., Perriard J.C. **2003**. *USGEB meeting*. Davos, Switzerland. Poster.
- Myomesin interactions: generation of a new M-band model.
  Lange S., Auerbach D., Gautel M., Perriard J. C., Ehler E. **2003**. *London Muscle Conference*. London, United Kingdom. Poster.
- Crosslinking of the thick filaments in the M-band: a novel role for Myomesin.
  Lange S., Auerbach D., Perriard J. C., Ehler E. **2003**. *CardioAscona Meeting*. Ascona, Switzerland. Poster.
- Crosstalks and Crosslinks in the sarcomeric M-band.
  Lange S., Himmel M., Auerbach D., Agarkova I., Hayess K., Furst D. O., Perriard J. C., Ehler E. **2004**. *ETH Zürich D-BIOL Meeting*. Davos, Switzerland. Poster.
- Sarcomeric signalling pathways: from the titin kinase to the M-band and beyond.
  Lange S., Yakovenko A., Rostkova E., Brandmeier B., Kristensen J., Ehler E., Gautel M. **2004**. *CAMKIN Meeting*. Athens, Greece. Talk.